Apport de la modélisation semi-mécanistique dans l'étude pharmacocinétique/pharmacodynamique des antibiotiques seuls et en combinaison dans la lutte contre les bactéries résistantes

Vincent Aranzana-Climent

THESE

Pour l'obtention du Grade de

DOCTEUR DE L'UNIVERSITE DE POITIERS

(Faculté Médecine et Pharmacie)
(Diplôme National - Arrêté du 25 mai 2016)

Ecole Doctorale « *Sciences Biologiques & Santé* »
Secteur de Recherche : Pharmacologie et sciences du médicament

Présentée par :

Vincent Aranzana-Climent

****

Apport de la modélisation semi-mécanistique dans l'étude pharmacocinétique/pharmacodynamique des antibiotiques seuls et en combinaison dans la lutte contre les bactéries résistantes.

****

Directeurs de Thèse :
Dr Nicolas Grégoire
Dr Julien Buyck

****

Soutenue le 4 Octobre 2019

devant la Commission d'Examen

****

JURY

Dr Aude Ferran, *Ecole Nationale Vétérinaire de Toulouse*	Rapporteur
Dr Jérémie Guedj, *Université Paris Diderot*	Rapporteur
Pr Lena Friberg, *Université d'Uppsala*	Examinateur
Pr Sebastian Wicha, *Université d'Hambourg*	Examinateur
Pr William Couet, *Université de Poitiers*	Examinateur
Dr Nicolas Grégoire, *Université de Poitiers*	Directeur de thèse
Dr Julien Buyck, *Université de Poitiers*	Directeur de thèse

I. Remerciements

Au Dr Aude Ferran et au Dr Jérémy Guedj pour avoir accepté d'être rapporteurs de ce travail. Sincères remerciements.

To Pr Lena Friberg for accepting to be part of this jury, but also for the internship four years ago and for the helpful discussions we had during the CO-ACTION project. Tack så mycket !

To Pr Sebastian Wicha for accepting to be part of this jury, and for the discussions about the GPDI and about modelling in general. Tausend dank!

Au Pr William Couet qui après mon premier stage (il y a déjà 6 ans !) a tapé à suivre pour que je puisse poursuivre ma formation en Suède et aux Pays-Bas. Puis qui m'a fait revenir en défense afin de préparer la combinaison qui m'enverra (j'espère) en terre promise. Si vous n'aviez pas mis les ingrédients j'aurais probablement fini hors-jeu, soyez assurés de toute ma gratitude.

Au Dr Julien Buyck, qui a accepté de co-encadrer cette thèse avec un thésard qui n'avait pas fait une seule expérience de microbiologie de sa vie avant la thèse. Merci pour ta patience, tes conseils, ta bonne humeur et pour ta cave à bières ! Dans l'espoir de continuer à travailler ensemble.

Au Dr Nicolas Grégoire, qui a co-encadré cette thèse, mais aussi tous les stages qui ont précédé. Je ne sais comment tu as pu me supporter aussi longtemps, tout en continuant de répondre à mes questions même après la quinzième interruption de la journée. Ce que je sais en revanche c'est que je n'en serais pas là sans toi. Merci infiniment et j'espère que l'on pourra continuer à collaborer.

Je tiens à remercier tous les membres de l'U1070 que j'ai pu côtoyer au cours de cette thèse et des stages qui l'ont précédé :

A Emma, merci d'avoir supporté ces très longues journées dans le L2, et plus difficile de m'avoir supporté, malgré des débuts difficiles. On n'aura pas fait ça pour rien !

A Grace et Isabelle, merci pour les longues journées à Prebios, ces longues heures avec des résultats pas toujours à la hauteur de nos efforts.

A Alexia, partenaire de galère à bord du navire *hollow fibre artisanal*, pour y avoir passé beaucoup de temps malgré les cours à préparer.

To Shachi, for letting a novice like me model your data, it was a pleasure to work with you on this " " "rapidly growing" " " bacteria.

Au Pr Sandrine Marchand, pour tes conseils et le temps passé sur les protocoles d'expérimentation, sois assurée de toute ma reconnaissance.

A Patrice, Helene, Christophe et Julian merci pour les dosages, les re-dosages- les changements de méthode, les matrices compliquées....

A Muriel et Agnès (Tic et Taz on me dit dans l'oreillette), pour les commandes mais surtout l'ambiance !

To Bruna, for bringing your humor and no nonsense approach to research in our lab, it was a pleasure to meet you.

A Karin, la seule Suédoise du Loir et Cher à Chantal qui est parti chercher le Cantal qu'elle avait oublié à Angers.

A Laure, Blandine, Kévin, Damien, Rana, Hari, François, Jean-Phillippe ; Sophie et Etienne ainsi qu'à tous les membres de l'U1070 au CHU.

A tous les copains de Poitiers ou presque, Adélie, Alexis, Romain, Anaïs et Obélia, merci pour les PLB, les vacances à Lacanau, les jeux, le gâteau à la noix de coco et plein d'autres…

A tous les copains Charentais ou presque, Laurent (33700 code postal inoubliable), Julie (Burger Quizz à 2h30 du matin, meilleure idée !), Mimi (Je travaille mais je serais là pour le PLB !), P-E a.k.a. Mr le premier ministre, Camille Devys (tu veux des vis ?!), Diane (Sacré premier de l'an !), Thomas (Pour les contrepèteries et les opéras), Fanny (Pour les tests de Suèdois dès que je parle d'Uppsala).

To Ile and Katie, who are more than just theatre buddies, thank you for those great moments spent together. Thanks to all the Thisbe members that I had the chance to play along with, these moments away from science were truly appreciated!

To Ricardo and Danielle for the boardgame evenings and good moments shared, obrigado!

A Simon, même s'il est difficile de se voir aussi souvent qu'avant, sache que ton amitié m'est précieuse.

A mes parents et à mon frère qui m'ont toujours soutenu et me soutiennent encore dans tout ce que j'entreprends, merci infiniment.

A mon Dragon pour ton amour tout simplement.

Table des matières

II. Liste des publications

1. Pre-clinical pharmacokinetic and pharmacodynamic data to support cefoxitin nebulization for the treatment of Mycobacterium abscessus. Shachi Mehta*, **Vincent Aranzana-Climent***, Blandine Rammaert, Nicolas Grégoire, Sandrine Marchand, William Couet, Julien M Buyck. Antimicrobial Agents and Chemotherapy, 2019
2. Clinical Pharmacokinetics and Pharmacodynamics of Colistin. Nicolas Grégoire, **Vincent Aranzana-Climent**, Sophie Magréault, Sandrine Marchand, William Couet. Clinical Pharmacokinetics 2017
3. In Vitro Activity of Polymyxin B Alone and in Combination Against Colistin-Resistant Acinetobacter Baumannii. **Vincent Aranzana-Climent**, Alexia Chauzy, Nicolas Grégoire, Sandrine Marchand, William Couet, Julien M. Buyck. In manuscript
4. Semi-mechanistic PK-PD modelling of combined polymyxin B and minocycline against a polymyxin-resistant strain of *Acinetobacter baumannii*. **Vincent Aranzana-Climent**, Julien M. Buyck, Younes Smani, Jerónimo Pachón-Diaz, Sandrine Marchand, William Couet, Nicolas Grégoire. Submitted to Clinical Microbiology and Infection.

III. Liste des communications

1. Use of a semi-mechanistic PK-PD model to quantify the combination effect of polymyxin B and minocycline against polymyxin-resistant *Acinetobacter baumannii*. Vincent Aranzana-Climent, Julien Buyck, Lena Friberg, Younes Smani, Jeronimo Pachon-Diaz, Emma Marquizeau, William Couet, Nicolas Gregoire, International Society of Anti-Infective Pharmacology (ISAP) Young Investigator Sesssion, Présentation Orale
2. Use of a semi-mechanistic PK-PD model to quantify the combination effect of polymyxin B and minocycline against polymyxin-resistant *Acinetobacter baumannii*. **Vincent Aranzana-Climent**, Julien Buyck, Lena Friberg, Younes Smani, Jeronimo Pachon-Diaz, Emma Marquizeau, William Couet, Nicolas Gregoire, 29th European Congress of Clinical Microbiology and Infectious Diseases (ECCMID), poster P2110
3. A PK/PD type modelling approach to support time-kill data interpretation of cefoxitin for the treatment of *Mycobacterium abscessus* – Shachi Metha, **Vincent Aranzana-Climent**, Nicolas Grégoire, Sandrine Marchand, Julien Buyck, William Couet
4. *In vitro* activity of polymyxin B alone and in combination against colistin-resistant *Acinetobacter baumannii*. **Vincent Aranzana-Climent**, Alexia Chauzy, Nicolas Gregoire, Sandrine Marchand, William Couet, Julien Buyck, 29th European Congress of Clinical Microbiology and Infectious Diseases (ECCMID), poster P2797
5. Use of a semi-mechanistic PK-PD model to quantify the combination effect of polymyxin B and minocycline against polymyxin-resistant *Acinetobacter baumannii*, **Vincent Aranzana-Climent**, Julien M. Buyck, Lena E. Friberg, Younes Smani, Jerónimo Pachón-Diaz, Emma Marquizeau, William Couet, Nicolas Grégoire, Population Approach Group in Europe (PAGE) Meeting 2019, Poster I-15

IV. Liste des abréviations

AUC : *Area Under the Curve* – Aire sous la courbe

CDC : Centers for Disease Control and prevention

CLSI : *Clinical and Laboratory Standards Institute*

C_{max} : Concentration maximale

CMI : Concentration Minimale Inhibitrice

CMS : *Colistimethate Sodium* - méthanesulfonate de colistine sodique

ECDC : European Centers for Disease Control and Prevention

EUCAST : *European Comittee on Antimicrobial Susceptibility Testing*

FICI : *Fractionnal Inhibitory Concentration Index*

JAC : *Journal of Antimicrobial Chemotherapy*

JPIAMR : *Joint Program Initiative on Antimicrobial Resistance*

ND-AB : *Neglected and Disused Antibiotics* - antibiotiques oubliés et non utilisés (ND-AB)

OMS : Organisation Mondiale de la Santé

PD : Pharmacodynamie

PK : Pharmacocinétique

PK/PD : Pharmacocinétique/Pharmacodynamie

$T_{>MIC}$: Temps au-dessus de la CMI

UFC : Unité Formant Colonie

G7 : Groupe des sept

G20 : Groupe des 20

WGS : *Whole genome sequencing* – Séquençage de génome entier

V. Liste des figures

VI. Liste des tableaux

VII. Généralités : PK/PD des antibiotiques

L'antibiorésistance est la propriété d'une bactérie d'être résistante à un/des antibiotique(s). Elle peut être innée ou acquise [1]. Les bactéries résistantes posent un important problème de santé publique, en 2009 l'ECDC (European Centers for Disease Control and Prevention) a estimé que l'antibiorésistance était responsable de 25000 morts et d'1.5 milliards d'€ de coûts directs et indirects par an au sein de l'Union Européenne [2]. En 2013, la CDC américaine (Centers for Disease Control and prevention) a estimé que l'antibiorésistance était responsable de 23000 morts par an ainsi que de 55 milliards de $ en coûts directs et en perte de productivité aux Etats-Unis [3]. Si aucune mesure n'était prise, le rapport O'Neill de 2014 [4] prévoyait que les bactéries multirésistantes seraient responsables de 10 millions de mort par an soit plus de morts que le cancer d'ici 2050. L'Organisation Mondiale de la Santé (OMS) a désigné la lutte contre les bactéries multirésistantes comme une des priorités majeures des politiques de santé mondiales [5]. Le causes de l'émergence de cette antibiorésistance sont multiples mais Depuis les années 80, le nombre de molécules mises sur le marché diminue (Figure 1) et les résistances aux nouveaux antibiotiques apparaissent très vite après la mise sur le marché [6] d'où l'importance d'optimiser les molécules actuellement à notre disposition et/ou de les utiliser en combinaison.

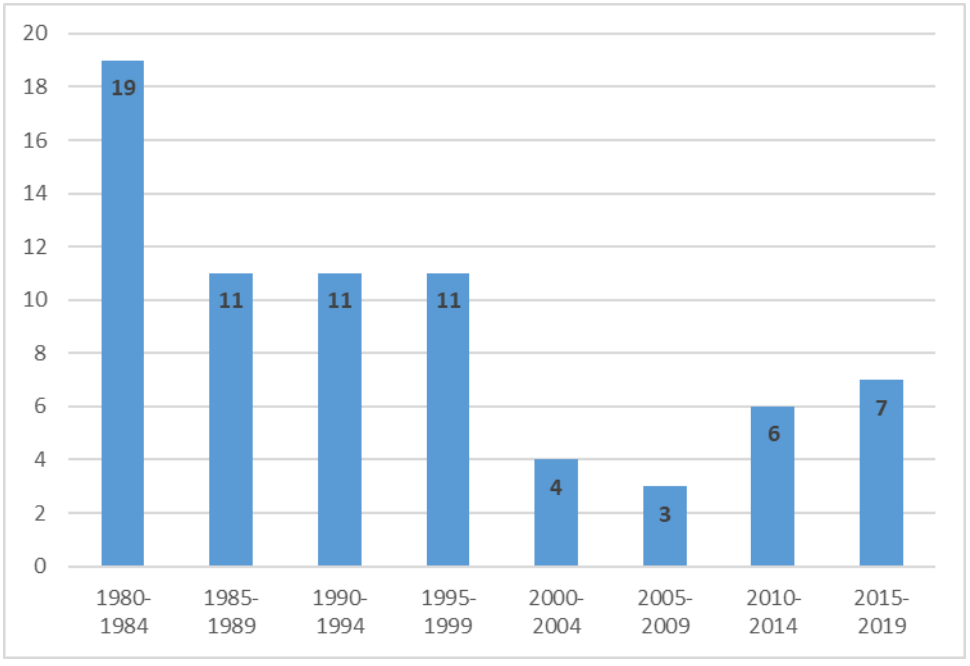

Figure 1. Nombre d'antibiotiques systémiques approuvés par la FDA depuis 1980 (d'après[6] complété pour la tranche 2015-2019[7])

Parmi les molécules à notre disposition, d'anciennes molécules telles que les polymyxines connaissent une résurgence car peu utilisées entre les années 1970 et 2000 elles ont conservé une efficacité contre les bactéries multirésistantes. Cependant, ayant été mises sur le marché dans les années 50, elles n'ont pas suivi

un processus de développement aussi rigoureux que les molécules récentes, et de nouvelles études sont nécessaires [8]. D'autre part, les antibiotiques utilisés en combinaison étant en général autorisés séparément, leur activité combinée n'est pas étudiée avant la mise sur le marché et des études supplémentaires sont donc nécessaires.

C'est ici tout l'intérêt des études de pharmacocinétique/pharmacodynamie des antibiotiques pour optimiser leur efficacité, prévenir les résistances et donc prolonger la durée de vie de ces antibiotiques déjà à notre disposition.

La pharmacocinétique (PK) est l'étude de l'évolution des concentrations d'un médicament au cours du temps après son administration. La pharmacodynamie (PD) est l'étude de la relation entre un effet pharmacologique et la concentration en antibiotique. La PK/PD est la combinaison de ces deux sciences qui nous permet in fine de suivre l'effet de la molécule en fonction du temps (Figure 2).

De multiples approches ont été développées pour étudier la PK/PD des antibiotiques utilisés seuls ou en combinaison, l'objet de cette partie est d'en proposer un résumé.

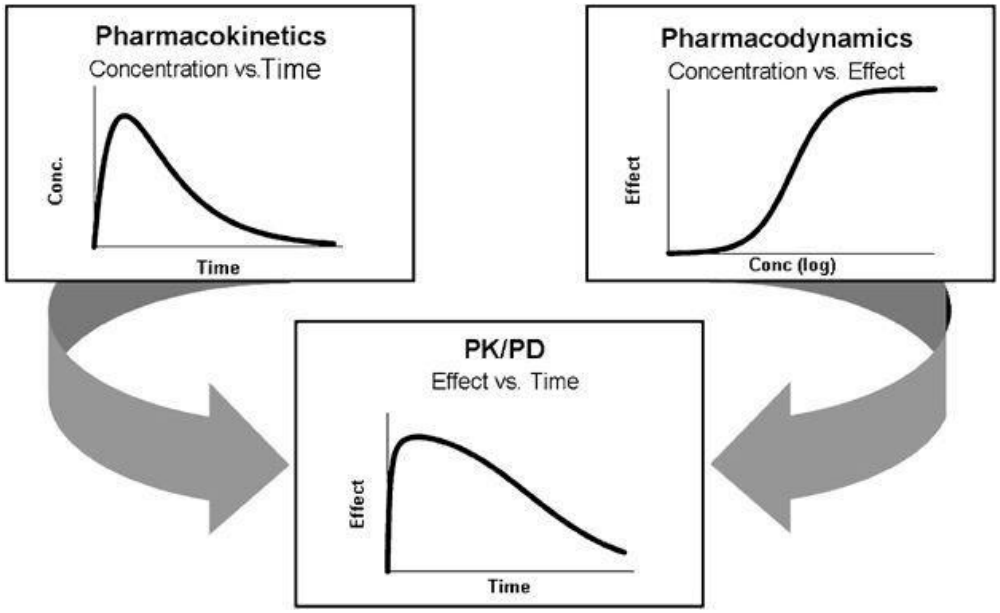

Figure 2. Schéma représentant ce que sont la PK, la PD et leur association. (D'après [9])

VII.A. Antibiotiques utilisés seuls

VII.A.1. Concentration minimale inhibitrice

La détermination de la concentration minimale inhibitrice (CMI) est une des méthodes les plus répandues d'évaluation de l'activité d'un antibiotique sur une bactérie. Elle doit sa popularité à sa simplicité de réalisation et d'interprétation qui permet sa réalisation dans un contexte aussi bien académique que de

routine hospitalière. Plusieurs protocoles existent pour déterminer cette concentration, le plus répandu est dit de « microdilution en bouillon». Les organismes de consensus EUCAST et CLSI ont standardisé cette procédure avec des différences mineures entre les protocoles[10,11]. Typiquement il est préparé un inoculum de bactéries provenant d'une culture sur gélose, dans du bouillon de culture ajusté à une densité d'environ 5 * 10^5 UFC/mL et mis au contact d'une gamme de concentrations d'antibiotiques souvent préparée par dilution sérielle au demi. La préparation est incubée à une température et pendant une durée dépendant du type de bactérie étudié, généralement 16 à 24h à 35°C. A la fin de la période d'incubation la pousse des bactéries est évaluée visuellement ou par spectrophotométrie et la CMI est définie comme étant la concentration minimale inhibant complètement la pousse visible des bactéries.[10]

En pratique, une fois la valeur de CMI obtenue elle est comparée à des valeurs de références pour l'antibiotique et l'espèce qui sont données par deux organismes de consensus (EUCAST[12] et CLSI[13]) permettant de classer l'isolat étudié comme sensible ou résistant à l'antibiotique (ou de sensibilité intermédiaire dans certains cas).

La CMI présente plusieurs problèmes. Tout d'abord, l'activité d'un antibiotique est réduite à sa capacité à maintenir la densité de la bactérie étudiée sous un seuil de détection à un temps donné, c'est-à-dire qu'un antibiotique induisant un déclin initial du nombre de bactéries suivi d'une repousse aura une CMI identique à celle d'un antibiotique n'ayant aucun effet sur les bactéries. Le même raisonnement peut être tenu pour un antibiotique tuant tous les bactéries vis-à-vis d'un antibiotique maintenant la densité juste en dessous du seuil de détection.

De plus, lorsqu'ensuite l'on compare les valeurs de CMI obtenues aux valeurs de référence, et que l'on classe les bactéries en sensibles et résistantes, on confond les bactéries ayant une CMI très faible (supposées très sensibles à l'antibiotique) et celles ayant une CMI juste en dessous de la valeur de référence, idem pour les bactéries classées comme résistantes. Or, souvent la CMI est vue comme un seuil à atteindre afin d'obtenir un effet de l'antibiotique que ce soit *in vitro* ou *in vivo*.

Les valeurs potentielles de CMI sont limitées aux concentrations testées, aussi il est communément admis que les valeurs de CMI sont précises à 1 dilution près[14], donc quand les concentrations testées suivent une suite géométrique de raison 2 la CMI est peu précise et peut varier d'un facteur 4.

Aussi, la détermination de la CMI suppose que l'antibiotique testé est à concentration constante pendant la durée d'incubation *i.e.* que l'antibiotique est stable dans les conditions d'étude. Ce qui n'est pas toujours le cas comme montré dans l'article 1. Dans ce cas l'interprétation de la CMI semble difficile.

En résumé, la CMI est un index facile à déterminer et utile mais qui apporte une information incomplète car basé sur une mesure à un instant donné, peu précis et difficile à interpréter dans le cas de molécules instables

ou en présence de phénomènes de décroissance puis de repousse bactérienne. Il est donc insuffisant pour l'étude détaillée de la PD d'un antibiotique.

VII.A.2. Index PK/PD

La mesure de référence pour l'évaluation de la PK/PD des antibiotiques est depuis une trentaine d'année l'approche de détermination des index PK/PD. Ces index combinent un marqueur d'exposition PK, le C_{max}, l'AUC ou $T_{>MIC}$, et un marqueur pharmacodynamique, la CMI. L'objectif est de déterminer une valeur cible de ces index qui soit prédictive de l'efficacité de l'antibiotique en clinique.

La détermination de la relation entre un index PK/PD et l'effet de la molécule implique que l'on puisse étudier différent schémas posologiques afin d'obtenir différentes valeurs d'AUC, de $T_{>MIC}$ et de C_{max}. Actuellement sa détermination est faite partir d'expériences où la PK est dynamique, soit *in vitro* à partir d'expériences d'*hollow fibre* ou d'expérience *in vivo,* les expériences chez la souris formant l'essentiel de la littérature sur les index PK/PD. Mais une étude de Khan et al. [15] a montré qu'il était possible de coupler un modèle de la PK humaine d'un antibiotique à un modèle PD développé à partir de données issus d'études de bactéricidie à concentration constante d'antibiotique afin de déterminer l'index PK/PD le plus prédictif de l'efficacité.

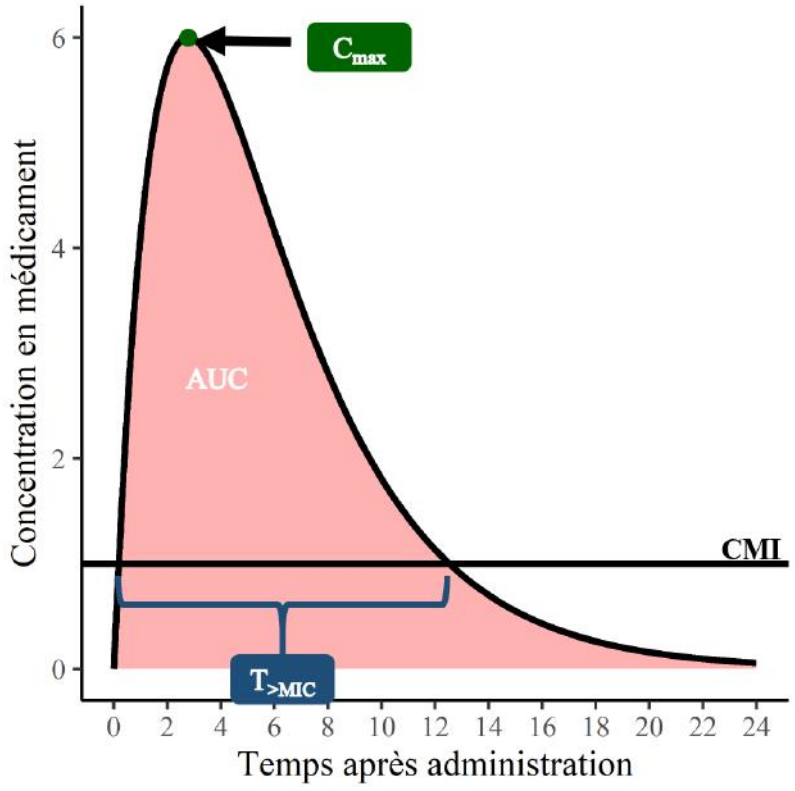

Figure 3. Index PK/PD. CMI est la concentration minimale inhibitrice, C_{max} est la concentration maximale obtenue après une administration, $T_{>MIC}$ est la durée pendant laquelle la concentration est supérieure à la CMI, AUC est l'aire sous la courbe des concentrations en fonction du temps.

Cette approche consiste à relier une mesure d'effet à l'un des trois index PK/PD illustrés par la figure 3, *f*AUC/MIC, *f*C_{max}/MIC et *f*$T_{>MIC}$ où AUC (*area under the curve*) est l'aire sous la courbe PK montrant la variation de la concentration en antibiotique en fonction du temps. C_{max} est la concentration maximale en antibiotique observée et $T_{>MIC}$ est la fraction du temps où la concentration en antibiotique est au-dessus de la CMI. Le préfixe *f* (*free*) signifie que l'on s'intéresse aux concentrations libres d'antibiotique. En absence de plus de précisions, il est supposé que l'AUC et le $T_{>MIC}$ sont calculés sur 24 heures et à l'état stable PK [16].

Pour chaque paire antibiotique-bactérie étudiée, l'index PK/PD étant le plus prédictif de l'efficacité est déterminé en reportant sur un graphique une mesure d'effet (classiquement le nombre de CFU/mL 24 heures après l'infection) en fonction de chaque index PK/PD, pour chacun des index, on opère une régression avec un modèle de type E_{max} sigmoïde (Equation 1) reliant l'effet et l'index PK/PD. La régression ayant le plus grand coefficient de corrélation permet de déterminer le meilleur index PK/PD prédictif de l'efficacité. Un exemple de cette démarche est illustré par la figure 5.

$$Effet = E_0 - \frac{E_{max} \times IndexPKPD^{\gamma}}{EIndex_{50}^{\gamma} + IndexPKPD^{\gamma}} \qquad \text{Equation 1}$$

Où E_0 est la valeur de la variable d'effet en absence de traitement, E_{max} est l'effet maximum dû à l'antibiotique, IndexPKPD est la valeur de l'index PK/PD étudié, $EIndex_{50}$ est la valeur de l'index PKPD induisant 50% d'E_{max} et γ est le coefficient de sigmoïdicité.

Premièrement ces index, étant dépendants de la CMI partagent ses défauts. L'imprécision de la mesure de la CMI se répercute sur les index, ainsi que l'incapacité à différencier les bactéries complètement résistantes de celles qui sont d'abord sensibles puis repoussent.

Le choix d'un de ces index comme valeur cible pour optimiser un schéma posologique n'est pas anodin puisqu'il entrainera des recommandations très différentes. Comme illustré par la figure 4, si l'on cherche à maximiser fCmax/MIC seule importe la dose administrée, pas la fréquence de ré-administration dans ce schéma on recommandera plus facilement 4g/8h que 1g/2h. Si l'on cherche à optimiser $fT_{>MIC}$ on peut être amené à recommander des schémas posologiques avec une fréquence élevée de ré-administration, qui sont les plus à même de maintenir la concentration au-dessus de la CMI pendant un intervalle de temps long, dans ce cas on recommanderait plutôt 1g/2h que 4g/8h. *f*AUC/MIC combine en quelque sorte les deux autres index, pour une pharmacocinétique linéaire 1g/2h ou 4g/8h produira la même *f*AUC/MIC.

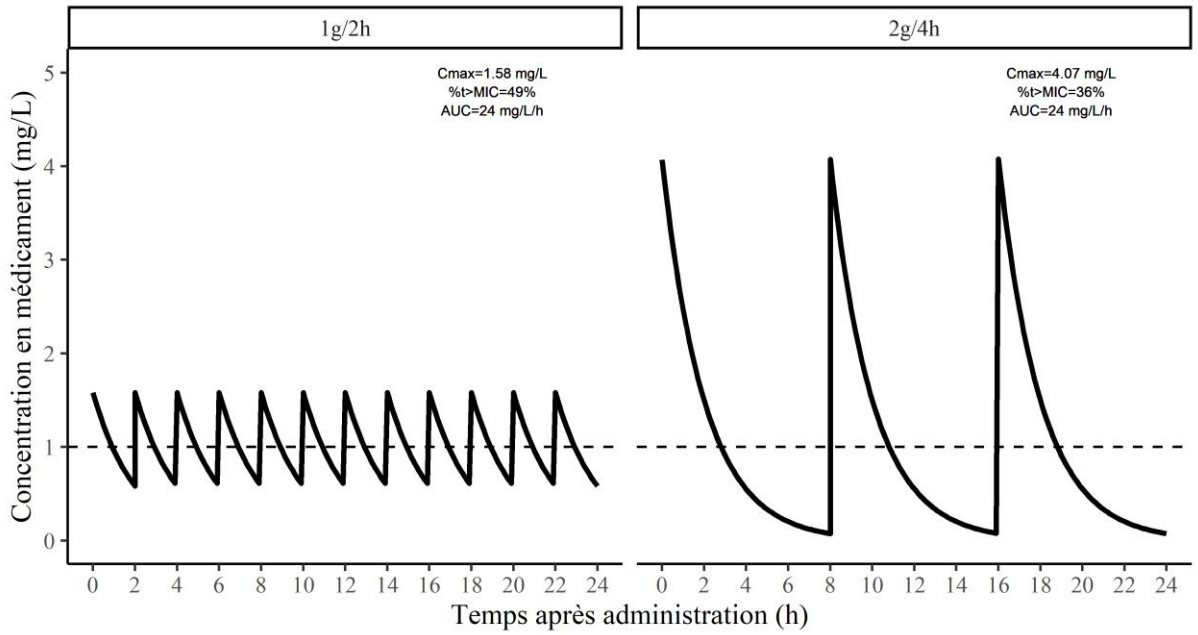

Figure 4. Simulations de concentrations attendues à l'état stable pour un antibiotique injecté par bolus intraveineux suivant une pharmacocinétique linéaire d'ordre 1. Le panneau de gauche représente les concentrations attendues après administration d'1g toutes les 2 h, le panneau de droite représente les concentrations attendues après injection de 2g toutes les 4h.

Une autre faiblesse de ces index vient de la difficulté à choisir un seul index pour une molécule donnée. Le tableau 1 présente les index PK/PD qui ont été sélectionnés pour plusieurs grandes classes d'antibiotiques.

En fonction des molécules, des bactéries voire même des modèles d'étude (*e.g.* modèle murin ou *in vitro*) l'index sélectionné varie. Par exemple l'index le plus corrélé à l'efficacité de la dalbavancine contre *Staphylococcus aureus* était l'AUC/MIC alors que contre *Streptococcus pneumoniae* c'était la C_{max}/MIC[17].

Tableau 1. Index PK/PD corrélés à l'efficacité pour différentes classes d'antibiotiques (d'après [18])

Classe d'antibiotique	**Index corrélé à l'efficacité**	**Références**
Beta-lactamines	fT>MIC	[19]
Aminoglycosides	fCmax/MIC ou fAUC/MIC	[20–22]
Fluoroquinolones	fCmax/MIC ou fAUC/MIC	[23–26]
Oxazolidinone (linezolide)	fT>MIC ou fAUC/MIC	[27,28]
Tetracyclines and glycylcycline	fT>MIC ou fAUC/MIC	[29–31]
Macrolides, ketolides et azalides	fCmax/MIC ou fT>MIC ou fAUC/MIC	[32–38]
Glycopeptides	fCmax/MIC ou fT>MIC ou fAUC/MIC	[17,39–42]

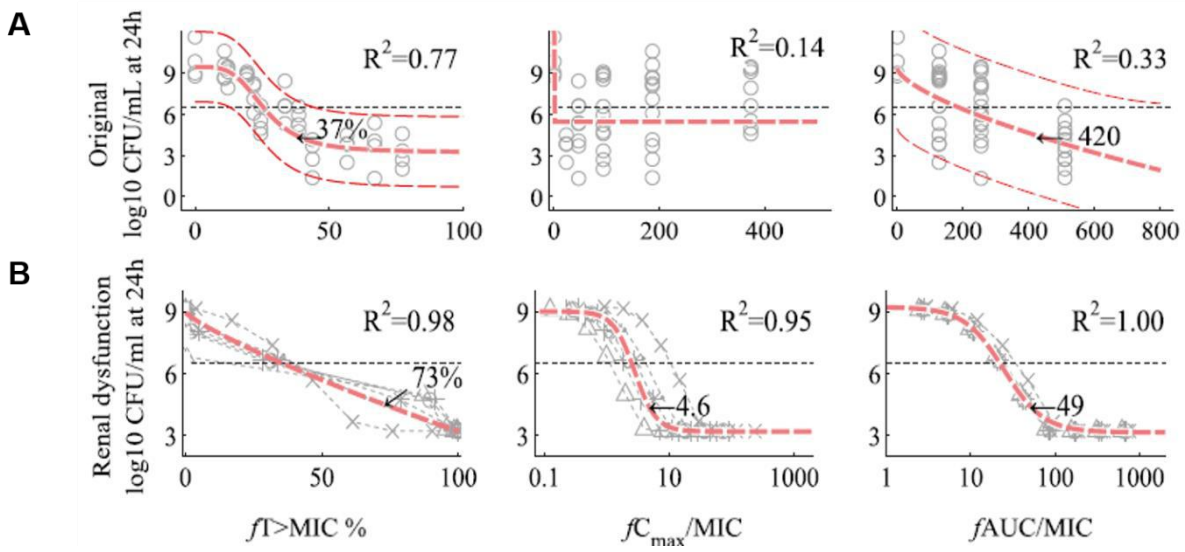

*Figure 5. Corrélation entre index PK/PD (en abscisse) et densité bactérienne à 24h (en ordonnée). Les données ont été obtenues **A**. à partir d'expériences d'un modèle PK/PD décrivant l'activité du méropénème contre Pseudomonas aeruginosa ATCC27853 dans un modèle d'infection de la souris **B.** à partir de simulations obtenues grâce à un modèle PK du méropénème chez les patients adultes[43], avec une diminution de la clairance rénale, et le modèle PK/PD décrivant l'activité du méropénème contre Pseudomonas aeruginosa ATCC27853 dans un modèle d'infection de la souris (d'après [44])*

VII.A.3. Modélisation mathématique

Les méthodes d'analyse de la PK/PD d'antibiotiques par modélisation mathématique semi-mécanistique se sont développées afin de pouvoir palier les défauts de la CMI et des index PK/PD. Et permettent d'analyser des données longitudinales (*e.g.* UFC en fonction du temps), la CMI et les index PK/PD étant des outils inadaptés pour ce type de données.

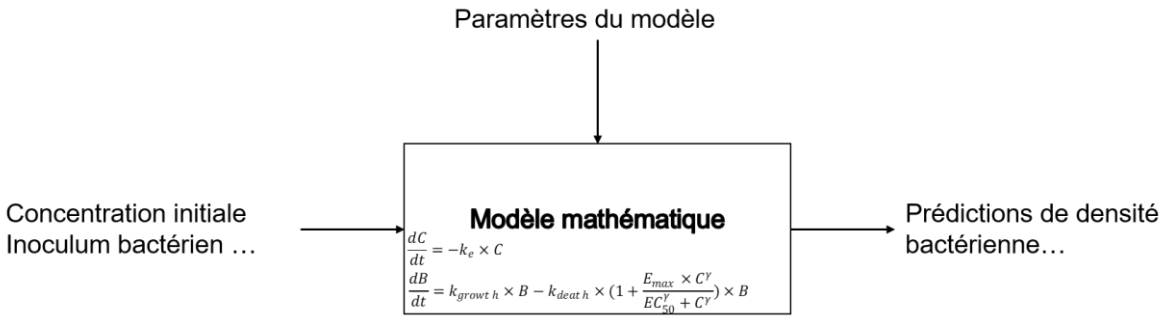

Figure 6. Représentation schématique de la modélisation mathématique

La modélisation mathématique (illustrée en figure 6) consiste à développer un modèle mathématique, constitué d'équations qui vont permettre de lier les données expérimentales connues d'avance (*e.g.* concentration initiale en antibiotique, inoculum bactérien initial…) à des prédictions de variables d'intérêt mesurées (*e.g.* concentration en antibiotique et/ou densité bactérienne au cours de l'expérience). A l'intérieur des équations ce lien est réalisé par des variables appelées paramètres du modèle, dont les valeurs seront estimées à partir de logiciels d'estimation grâce auxquels il est possible de trouver pour un modèle donné les valeurs de paramètres minimisant l'écart entre les prédictions et les mesures. Les modèles sont dit semi-mécanistiques quand les équations utilisées intègrent des informations provenant de nos connaissances du système étudié (*e.g.* mécanismes d'action de la molécule étudiée, connaissance du cycle de vie de la bactérie).

Les modèles PK/PD utilisés se découpent en plusieurs sous modèles interconnectés

VII.3.a. Modèle pharmacocinétique

Tout d'abord il faut modéliser les variations en concentrations d'antibiotiques. Dans certaines expériences elles ne varient pas (*kill-curve* statiques avec une molécule stable), mais il arrive que les molécules utilisées soient instables auquel cas la dégradation de l'antibiotique peut par exemple, être prise en compte par un modèle de dégradation de premier ordre (Equation 2)

$\frac{dC}{dt} = -k_e \times C$ Equation 2

Une pharmacocinétique mono, bi- ou tri-compartimentale peut être simulée *in vitro* en utilisant des dispositifs dit de « modèle pharmacocinétique *in vitro* » ou d'*hollow fibre*.

Modèle de croissance bactérienne

Un modèle simple de croissance bactérienne a été proposé par Jusko *et al.* [45] où les bactéries sont considérées comme un ensemble homogène (B) qui se multiplient à une fréquence k_{growth} et meurent de façon naturelle à une fréquence k_{death} en suivant l'équation 3.

$$\frac{dB}{dt} = k_{growth} \times B - k_{death} \times B \qquad \text{Equation 3}$$

Cette équation permet de décrire l'évolution de la densité bactérienne lors de la phase de croissance exponentielle en absence d'antibiotique.

Des modifications ont été proposées afin de rendre compte du plateau bactérien qui est observé *in vitro* et *in vivo*. Campion *et al.*[46] ont proposé d'utiliser une fonction logistique suivant l'équation 4.

$$\frac{dB}{dt} = (k_{growth} - k_{death}) \times (1 - \frac{B}{B_{max}}) \times B \qquad \text{Equation 4}$$

Où B_{max} représente la densité bactérienne maximale du système étudié.

Une autre possibilité est de modéliser la croissance par une équation saturable de type Emax comme proposé par Meagher et al[47] suivant l'équation 5 :

$$\frac{dB}{dt} = \frac{VG_{max} \times B}{B_m + B} - k_{death} \times B \qquad \text{Equation 5}$$

Où VG_{max} est la fréquence maximale de réplication des bactéries et B_m la densité bactérienne pour laquelle cette fréquence est 50% de VG_{max}.

Une troisième possibilité, avancée par Nielsen *et al* [48], basée sur les travaux de Balaban *et al.* [49] est de considérer que la phase de plateau observée est due à un changement métabolique des bactéries, qui, à des fortes densités passent en phase de repos. Les équations 6 et 7 décrivent ce modèle :

$$\frac{dG}{dt} = k_{growth} \times G - k_{death} \times G - (k_{growth} - k_{death}) \times (\frac{G+R}{B_{max}}) \times G \qquad \text{Equation 6}$$

$$\frac{dR}{dt} = -k_{death} \times R + (k_{growth} - k_{death}) \times (\frac{G+R}{B_{max}}) \times G \qquad \text{Equation 7}$$

Où G sont les bactéries en phase de croissance (*Growing*) et R sont les bactéries en phase de repos (*Resting*). Le choix du modèle est souvent empirique et dépend grandement de la richesse des données disponibles. Le modèle logistique permet en général de décrire les données de façon adéquate mais le modèle incluant des

bactéries en phase de repos insensibles à l'antibiotique permet de décrire un effet inoculum (*i.e.* une efficacité réduite de l'antibiotique lorsque l'inoculum initial augmente).

VII.3.b. Modèles d'effets

Le modèle reliant la concentration en antibiotique et l'effet est le plus souvent un effet de type E_{max} sigmoïde, tel que décrit dans l'équation 8.

$$Effet = \frac{E_{max} \times C^{\gamma}}{EC_{50}^{\gamma} + C^{\gamma}} \qquad \text{Equation 8}$$

Où E_{max} est l'effet maximal, C la concentration en antibiotique, EC_{50} la concentration en antibiotique provoquant 50% de l'E_{max} et γ la constante de sigmoïdicité. Cette équation peut se simplifier en E_{max} non sigmoïde ($\gamma = 1$), en modèle puissance ($C^{\gamma} <<< EC50^{\gamma}$) ou en modèle linéaire ($\gamma = 1$ et $C <<< EC_{50}$). Là encore le choix de modèle d'effet est empirique et l'on choisira généralement l'équation permettant la meilleure adéquation entre les prédictions du modèle et les données.

En fonction des connaissances vis-à-vis du mécanisme d'action de l'antibiotique étudié, le modèle d'effet de l'antibiotique peut s'intégrer de différentes manières au modèle de croissance bactérienne :

$$\frac{dB}{dt} = k_{growth} \times \left(1 - \frac{E_{max} \times C^{\gamma}}{EC_{50}^{\gamma} + C^{\gamma}}\right) \times B - k_{death} \times B \qquad \text{Equation 9}$$

$$\frac{dB}{dt} = k_{growth} \times B - k_{death} \times \left(1 + \frac{E_{max} \times C^{\gamma}}{EC_{50}^{\gamma} + C^{\gamma}}\right) \times B \qquad \text{Equation 10}$$

$$\frac{dB}{dt} = k_{growth} \times B - k_{death} \times B - \frac{E_{max} \times C^{\gamma}}{EC_{50}^{\gamma} + C^{\gamma}} \times B \qquad \text{Equation 11}$$

Si l'on suppose que l'antibiotique ralentit la croissance bactérienne, on choisira l'équation 9. Si au contraire nous considérons que l'antibiotique tue la bactérie, on pourra choisir l'équation 10 ou l'équation 11. Le paramètre E_{max} s'interprète différemment en fonction des paramétrisations. Dans l'équation 9 il doit s'interpréter comme un pourcentage maximal de réduction de la vitesse de pousse, dans l'équation 10 E_{max} est un pourcentage maximal d'augmentation de la vitesse de mort bactérienne. Dans l'équation 11 E_{max} est une constante de vitesse de mort, de même unité que k_{growth} et k_{death}.

VII.3.c. Modèles de résistance

Les modèles de résistance bactérienne aux antibiotiques peuvent se décomposer en 2 grandes catégories. Les modèles de sous-populations et les modèles d'adaptation.

VII.A.c.i. Modèles de sous-populations

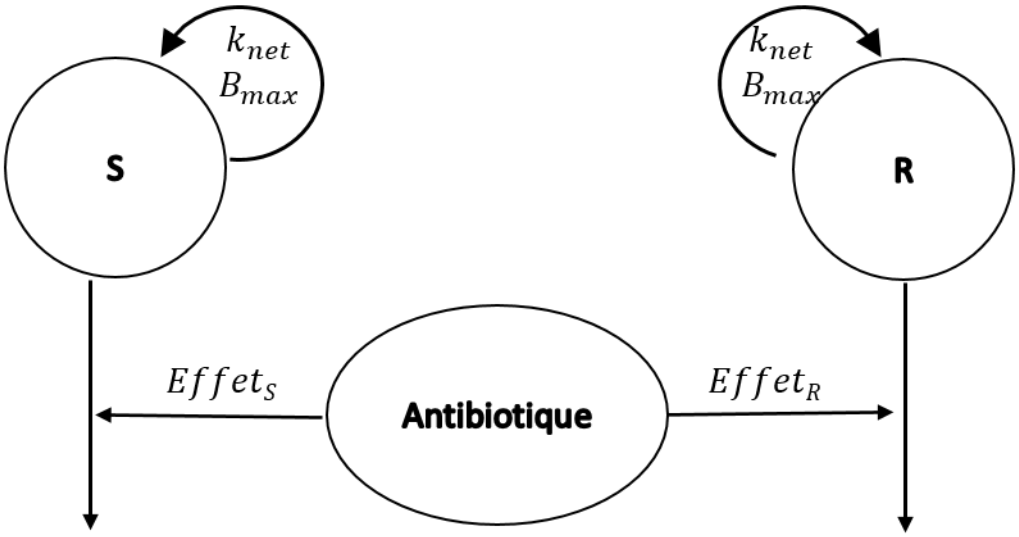

Figure 7. Exemple de modèle de sous populations. S représente la densité bactérienne des bactéries sensibles, R représente la densité bactérienne des bactéries résistantes, k_{net} représente la constante de vitesse de croissance apparente des bactéries, B_{max} est la capacité maximale du système, $Effet_S$ et $Effet_R$ sont les constantes de vitesse d'effet de l'antibiotique sur les bactéries sensibles ou résistantes respectivement.

Dans ces modèles on considère notre population bactérienne comme un ensemble de 2 ou plus sous populations ayant des sensibilités différentes à l'antibiotique. La plupart du temps on considère que les diverses sous-populations existent au début de l'expérience et la proportion de chacune est estimée lors de la modélisation [50]. Dans certains travaux, il a été considéré que ces sous-populations résistantes peuvent apparaître lors de l'expérience avec une constante de mutation estimée par le modèle [51]. Elles sont souvent considérées stables mais une constante de réversion peut aussi être estimée [52].

La différence de sensibilité peut se manifester comme une modification de l'EC_{50} dans le cas où le même effet maximal est atteignable en augmentant les concentrations en antibiotiques par rapport aux bactéries sensibles. Si de fortes doses ne permettent pas d'atteindre l'E_{max} initial, alors la résistance est modélisée comme une modification de l'E_{max}.

VII.A.c.ii. Modèles d'adaptation

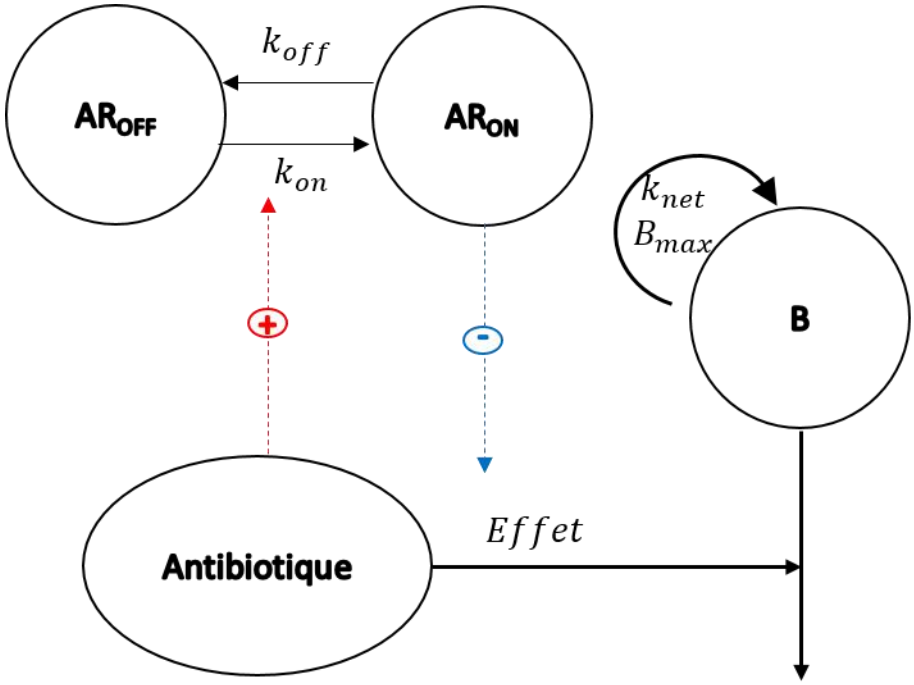

Figure 8. Exemple de modèle d'adaptation. B représente la densité bactérienne, ARoff et ARon sont des compartiments virtuels représentant la proportion de bactéries non adaptées ou adaptées respectivement, knet représente la constante de vitesse de croissance apparente des bactéries, B_{max} est la capacité maximale du système, Effet est le constante de vitesse d'effet de l'antibiotique sur les bactéries, k_{on} est la constante de vitesse de passage de l'état non adapté à l'état adapté, k_{off} est la constante de vitesse de passage de l'état adapté à l'état non adapté. La flèche rouge indique que la concentration en antibiotique augmente la vitesse de passage de l'état non adapté à l'état adapté, la flèche bleue indique que la quantité AR_{on} diminue la constante d'effet de l'antibiotique.

Une autre possibilité, est de considérer la population bactérienne comme homogène, initialement complètement sensible à l'antibiotique, mais capable de développer une résistance une fois mise en contact avec ce dernier. Une approche développée par Tam *et al.* [53] propose de modéliser l'adaptation des bactéries comme une augmentation de l'EC_{50} en la multipliant par un facteur alpha donné par l'équation 12 :

$$\alpha = 1 + \beta \times (1 - e^{-C_t \times t \times \tau}) \quad \text{Equation 12}$$

Où β est le pourcentage maximal d'adaptation, C_t la concentration en antibiotique, t le temps écoulé depuis le début de l'expérience, et τ la constante de vitesse d'adaptation.

Une approche développée par Mohammed *et al.* [54] propose de considérer les proportions de bactéries adaptées et non adaptées comme des compartiments du modèle, par exemple:

$$\frac{dAR_{on}}{dt} = k_{on} \times AR_{off} - k_{off} \times AR_{on} \quad \text{Equation 13}$$

$\frac{dAR_{off}}{dt} = k_{off} \times AR_{on} - k_{on} \times AR_{off}$ Equation 14

$E_A = E_{A,0} \times (1 - AR_{on})$ Equation 15

Où AR_{on} et AR_{off} représentent la proportion de bactéries adaptées et non adaptées respectivement, k_{on} et k_{off} représentent la constante de vitesse de passage des bactéries de l'état non adapté à l'état adapté et vice-versa respectivement, E_A est l'effet de la molécule A modifié par l'adaptation et $E_{A,0}$ est l'effet de la molécule A en absence d'adaptation.

Cette approche à l'avantage de rendre plus facile l'implémentation d'une réversion de l'adaptation (en ajoutant une constante de réversion aux équations différentielles des compartiments concernés) ainsi que le test de différentes fonctions reliant la vitesse d'adaptation et la concentration en antibiotique.

Les deux approches (sous-population et adaptation) sont en général capables, d'un point de vue statistique, de décrire les données aussi bien l'une que l'autre. Mais si les données disponibles pour la modélisation ne sont que des comptes de bactéries totales, sans distinctions des potentielles sous-populations, une étude de Jacobs *et al.* [55] montre que lors du développement du modèle, les critères statistiques d'évaluation nous amèneront à choisir le modèle de sous populations la plupart du temps. Cette étude met l'accent sur le fait que le choix du modèle de résistance ne peut être purement basé sur des critères statistiques mais doit se baser sur des expériences mécanistiques, comme le comptage des sous populations de bactéries résistantes, la détermination de la fréquence de bactéries résistantes au début de l'expérience, le séquençage des bactéries ou l'étude de leur expression génique.

L'approche d'analyse des données par modélisation mathématique a l'avantage de prendre en compte l'évolution de l'effet de l'antibiotique au cours du temps et ne pâtit donc pas des mêmes problèmes que la CMI ou les index PK/PD.

Cependant une contrainte associée avec l'utilisation de ces méthodes est qu'il faut des données plus riches et donc plus coûteuses à obtenir que pour la CMI ou les index PK/PD, puisqu'il faut un suivi des concentrations et de l'effet de l'antibiotique au cours du temps. Aussi il faut prendre en compte le temps de développement du modèle qui est plus long que la simple analyse par index PK/PD.

Une fois développé, le modèle mathématique peut être utilisé pour faire des simulations d'effet attendu dans des conditions non testées (utilisation d'un autre schéma posologique, d'un autre inoculum bactérien…) ce qui permet de prédire les schémas posologiques efficaces mieux qu'avec l'utilisation des index PK/PD.

VII.B. Antibiotiques combinés

Face aux dangers de l'antibiorésistance et compte tenu du faible nombre de nouveaux antibiotiques, l'association d'antibiotiques est de plus en plus utilisée à l'hôpital. En effet, 25 à 50% des patients souffrant de bactériémie, d'infection du site opératoire ou de pneumonie, ainsi que plus de 50% des patients présentant un choc septique dans un service de réanimation reçoivent une combinaison d'antibiotiques [56]. Ces combinaisons sont souvent choisies de manière empirique, et leur intérêt clinique reste débattu [56–59]. Cependant, les méta-analyses qui ne montrent pas de supériorité de la combinaison vis-à-vis de la monothérapie se limitent aux traitement par des β-lactamines à large spectre et la combinaison peut conserver un intérêt dans le traitement des infections sévères à bactéries Gram-négatives pour lesquelles il y a pénurie de traitements [60].

Il y a donc un intérêt à étudier la pharmacodynamie des combinaisons d'antibiotiques afin d'optimiser leur utilisation.

Lors de l'étude des combinaisons, l'objectif premier est de déterminer quelles combinaisons d'antibiotiques sont intéressantes. Les combinaisons intéressantes sont les combinaisons dites synergiques, la synergie est un terme très général voulant dire « travaillant ensemble » et son opposé l'antagonisme signifie « travaillant contre » [61]. Cette notion de synergie, a fait l'objet de nombreuses revues et publications [61–63]. En partant de ces définitions très générales plusieurs paradigmes de synergie ont vu le jour.

Le plus simple de ces paradigmes et celui du *highest single agent* [64] (littéralement : agent le plus actif) aussi appelé *cooperative effect synergy* [63] (littéralement : synergie par effet coopératif), il est illustré par la figure 9. Dans ce contexte, une combinaison de molécules sera dite synergique si l'effet de la combinaison des deux molécules à des concentrations données est plus important que l'effet de la molécule seule la plus efficace à cette même concentration. En termes mathématiques soit *a* la concentration de la molécule $\mathcal{A}$ et *b* la concentration de la molécule $\mathcal{B}$, *E(a)* et *E(b)* l'effet observé après administration de la molécule $\mathcal{A}$ ou $\mathcal{B}$ aux concentrations *a* ou *b* respectivement, une combinaison sera synergique si *E(a+b)* l'effet de la combinaison à ces concentrations est supérieur à l'effet de la molécule la plus efficace en monothérapie.

$\mathcal{A}+\mathcal{B}$ est synergique si $E(a+b) > max(E(a), E(b))$

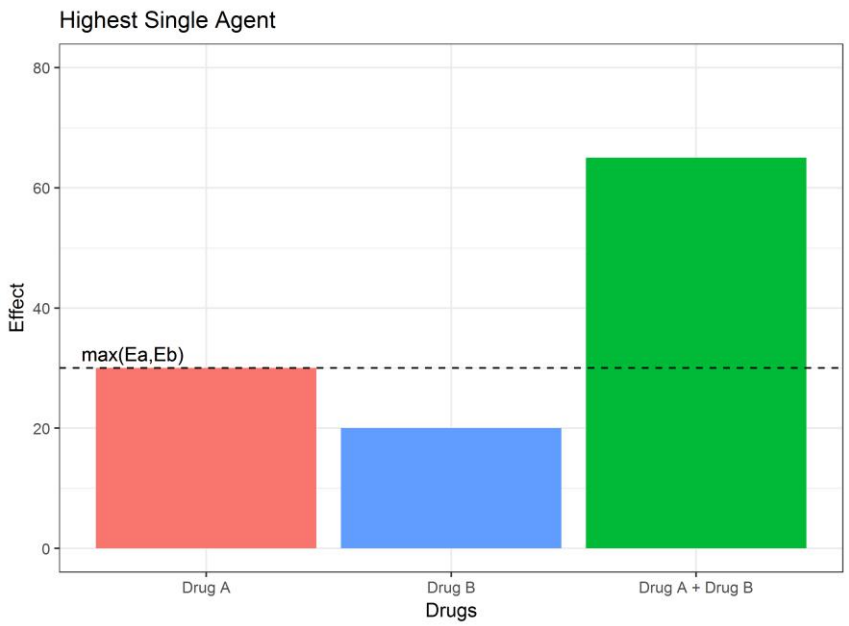

Figure 9. Représentation graphique de la synergie selon le paradigme du highest single agent. La droite en pointillés représente l'effet de la molécule la plus active (Drug A). La combinaison (Drug A + Drug B) est synergique car l'effet produit est plus grand que l'effet de la molécule la plus active (Drug A) (d'après [64])

Ici l'effet de la combinaison est comparé à l'effet maximum des monothérapies, mais d'autres paradigmes ont utilisé d'autre références. Pour les plus populaires de ces paradigmes, l'additivité de Loewe [65] et l'indépendance de Bliss [66], le point de référence est l'effet attendu de la combinaison des deux molécules combinées, en faisant différentes hypothèses en fonction du modèle choisi, mais dans ces deux modèles la synergie est donc définie ainsi :

$\mathcal{A}$ + $\mathcal{B}$ est synergique si $E(a+b)_{observé} > E(a+b)_{attendu}$

Ces deux paradigmes vont être maintenant détaillés.

VII.B.1. Additivité de Loewe

Dans le contexte de l'additivité de Loewe on va chercher quelle quantité ou concentration de chaque molécule produit le même effet quantitatif que l'autre afin de pouvoir construire une prédiction de l'effet combiné des deux molécules dans l'hypothèse d'une absence d'interaction, appelé additivité [64] . L'additivité de Loewe repose sur deux principes, le principe d'équivalence des concentrations selon lequel pour tout effet produit par une concentration a de la molécule $\mathcal{A}$ il existe une concentration b_a de la molécule $\mathcal{B}$ qui produira le même effet. Cette hypothèse implique que les deux molécules données seules produisent le même effet maximal, sinon une fois atteint l'effet maximal le plus faible on ne pourrait plus trouver de concentration de la molécule la moins efficace produisant un effet plus grand. L'autre principe est le principe

de « fausse » (*sham* en anglais) combinaison qui dicte que l'on peut produire l'effet de la combinaison en combinant l'un de ses composants avec lui-même, mathématiquement si deux molécules sont additives :

$E(a+b) = E_A(a+a_b) = E_B(b_a+b) = E_{AB}$ Equation 16

Avec $E_A(a+a_b)$ l'effet de la molécule $\mathcal{A}$ donnée seule à la concentration $a+a_b$ étant identique à l'effet $E_B(b_a+b)$ produit par la molécule $\mathcal{B}$ donnée seule à la concentration b_a+b, étant identique à la combinaison des deux molécules données aux concentrations a de $\mathcal{A}$ + b de $\mathcal{B}$.

Soit A la concentration de $\mathcal{A}$ donnée seule produisant l'effet de la combinaison aux concentrations a+b, E_{AB}. B la concentration de $\mathcal{B}$ donnée seule produisant l'effet de la combinaison aux concentrations a+b, E_{AB}. Si l'on fait l'hypothèse que pour tout effet de la combinaison E_{AB} il y a proportionnalité entre les concentrations A et B produisant le dit effet, on peut écrire ce ratio R = A/B.

En appliquant le principe d'équivalence des concentrations on peut écrire :

$a+a_b = A$ Equation 17

En effet, la concentration A peut être vue comme une combinaison de la molécule $\mathcal{A}$ à une concentration a avec elle-même à une concentration a_b qui produirait un effet équivalent à une concentration b de la molécule $\mathcal{B}$. En partant de l'hypothèse de ratio constant de concentrations pour produire le même effet, cette équation peut donc s'écrire ainsi :

$a + a_b = A \leftrightarrow a + b \times R = A$ Equation 18

Et elle peut être développée de façon à obtenir l'équation emblématique de l'additivité de Loewe :

$$a + a_b = A \leftrightarrow a + b \times R = A \leftrightarrow a + b \times \frac{A}{B} = A \leftrightarrow \frac{a}{A} + \frac{b}{B} = 1$$ Equation 19

Cette équation est populaire car très facile d'utilisation, elle définit les conditions dans lesquelles les molécules $\mathcal{A}$ et $\mathcal{B}$ testées seront considérées comme additives. Pour un effet donné, il suffit donc de déterminer les concentrations de chacun des produits donnés seuls qui produisent cet effet (A et B) ainsi que les concentrations qui permettent d'observer cet effet en combinaison (a et b), s'en suit le calcul de l'index de combinaison (CI) défini grâce à l'équation 20 ci-dessous.

$$CI = \frac{a}{A} + \frac{b}{B}$$ Equation 20

Si celui-ci est = 1 la combinaison est dite additive, elle produit l'effet escompté dans les conditions de Loewe, si CI >1 la combinaison est dite antagoniste et si CI <1 la combinaison est dite synergique.

Un autre outil né de cette équation est une représentation graphique appelée isobologramme [61]. Elle consiste à tracer un graphique avec pour coordonnées les concentrations en $\mathcal{A}$ et en $\mathcal{B}$ nécessaires pour atteindre un effet donné et de tracer une droite d'équation b = B - a * R représentant les concentrations nécessaires pour obtenir l'effet si la combinaison était additive. On peut ensuite sur ce graphique représenter par des points les combinaisons de concentrations a + b permettant d'obtenir le niveau d'effet considéré, si les points sont sous la droite d'additivité, la combinaison sera dite synergique, ou antagoniste si les points sont au-dessus de cette ligne. Une représentation graphique tirée de [64] :

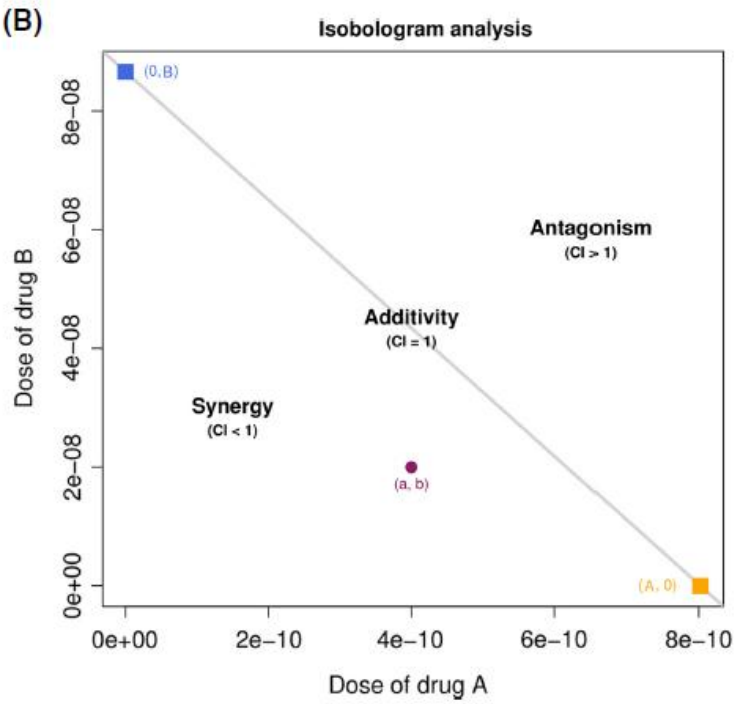

Figure 10. Isobologramme. Pour un effet donné (par exemple 50% de l'effet maximal) sont représentées les concentrations de $\mathcal{A}$ nécessaires pour l'obtenir (en abscisse) et les concentrations de $\mathcal{B}$ nécessaires pour l'obtenir (en ordonnée). Une ligne de non interaction (ici appelée « Additivity ») est tracée en reliant les points représentant les concentrations d'antibiotiques seuls produisant l'effet (les carrés bleus et jaunes) puis pour un point est placé pour la combinaison de concentrations testée (le point violet). Celui-ci se trouvant sous la droite de non interaction, la combinaison est considérée synergique (d'après [64])

Les équations de l'additivité de Loewe et les outils en découlant (CI et isobologrammes) ont été étendus aux situations où le ratio de concentrations nécessaires pour produire l'effet n'était pas constant, et où l'effet maximal des deux molécules était différent [67–69].

Exemple numérique illustrant l'additivité de Loewe

Soit deux molécules $\mathcal{A}$ et $\mathcal{B}$, dont les effets suivent un modèle E_{max} sigmoïde avec pour paramètres :

$E_{max,A} = E_{max,\,B} = 1$; $EC_{50,A}$= 0.1 mg/L et $EC_{50,B}$ = 1 mg/L ; $\gamma = 0.5$

Soient a et b les concentrations de $\mathcal{A}$ et $\mathcal{B}$ utilisées en combinaison. A la concentration de $\mathcal{A}$ qui a le même effet seul que les concentrations a et b associées.

$E(A) = E(a + b)$ Equation 21

Soit a_b la concentration de $\mathcal{A}$ qui a le même effet que b. D'après les hypothèse d'additivité de Loewe on a, et si on calcule R, le ratio de concentrations de a et b donnant le même effet, à partir du ratio des EC_{50} on a :

$$A = a + a_b = a + b\frac{EC_{50a}}{EC_{50b}} = EC_{50a}\left(\frac{a}{EC_{50a}} + \frac{b}{EC_{50b}}\right) \qquad \text{Equation 22}$$

On peut alors calculer l'effet de la concentration A de $\mathcal{A}$ correspondant à l'effet de a+b en association comme :

$$E(a+b) = E_A(A) = \frac{E_{maxA} \times EC_{50a}^{\gamma}\left(\frac{a}{EC_{50a}} + \frac{b}{EC_{50b}}\right)^{\gamma}}{EC_{50a}^{\gamma} + EC_{50a}^{\gamma}\left(\frac{a}{EC_{50a}} + \frac{b}{EC_{50b}}\right)^{\gamma}} \qquad \text{Equation 23}$$

Soit
$$E(a+b) = \frac{E_{maxA} \times \left(\frac{a}{EC_{50a}} + \frac{b}{EC_{50b}}\right)^{\gamma}}{1 + \left(\frac{a}{EC_{50a}} + \frac{b}{EC_{50b}}\right)^{\gamma}} \qquad \text{Equation 24}$$

Par exemple pour a=0.1 mg/L et b=1 mg/L (les 2 valeurs d'EC_{50}) on a

$$E(a+b) = \frac{1 \times \left(\frac{0.1}{0.1} + \frac{1}{1}\right)^{0.5}}{1 + \left(\frac{0.1}{0.1} + \frac{1}{1}\right)^{0.5}} \approx 59\% \quad \text{Equation 25}$$

Si on prend a=0.1 mg/L et b=0.1 mg/L on a E(a+b) = 0.51

La figure 11 donne une représentation graphique de l'effet attendu de la combinaison par rapport aux effets des molécules données seules. Pour simplifier la représentation les concentrations a et b utilisées en combinaisons sont identiques.

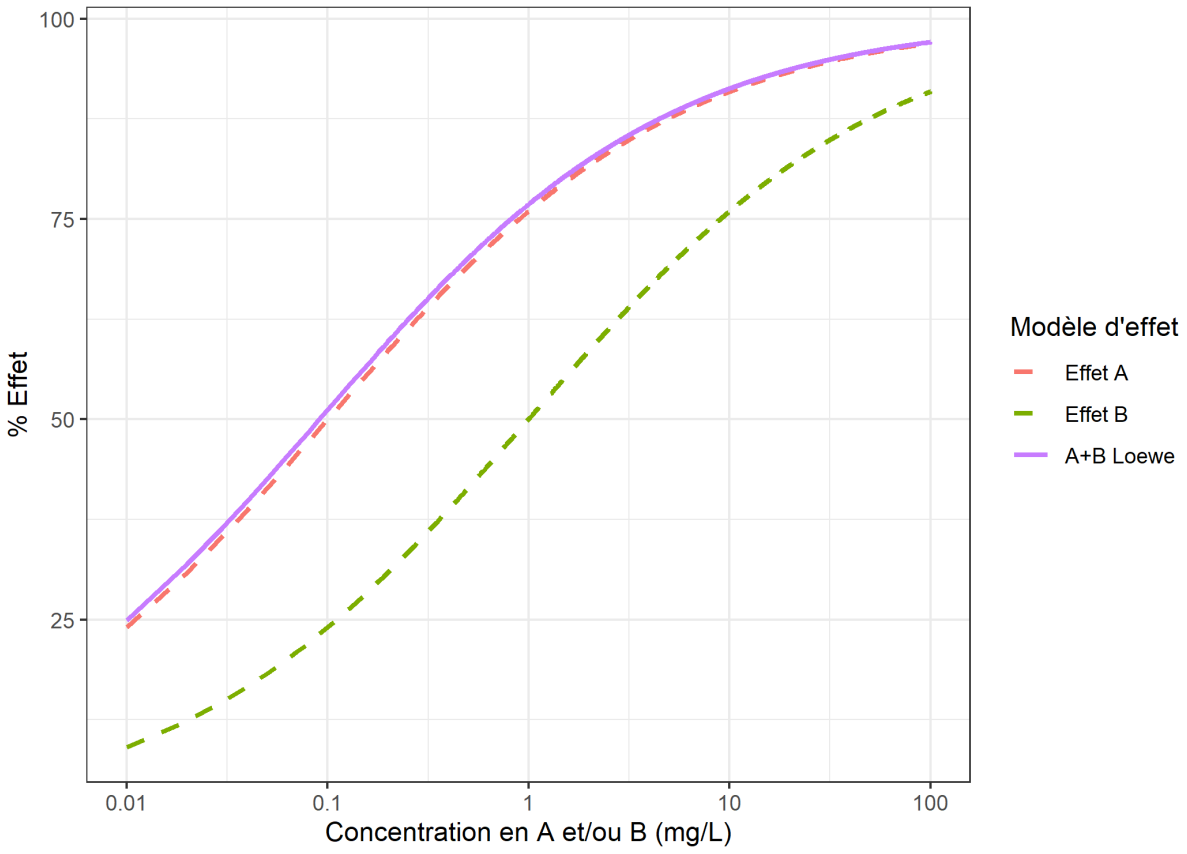

Figure 11. Représentation graphique de l'effet attendu de la combinaison des molécules $\mathcal{A}$ et $\mathcal{B}$ sous l'hypothèse de l'additivité de Loewe. .

VII.B.2. Indépendance de Bliss

L'autre méthode pour établir une prédiction de l'effet attendu de la combinaison de deux molécules combinées est appelée l'indépendance de Bliss [66]. Dans ce paradigme on fait l'hypothèses que les deux molécules utilisées agissent sur des sites d'action indépendants. L'équation donnant l'effet attendu d'une combinaison additive, tirée des statistiques est la suivante :

$$E(a+b)_{attendu} = E(a) + E(b) - E(a) \times E(b) \qquad \text{Equation 26}$$

Où E(a+b) est l'effet de la combinaison aux concentrations a + b, E(a) est l'effet de la molécule $\mathcal{A}$ à la concentration a et E(b) est l'effet de la molécule $\mathcal{B}$ à la concentration b. Pour que cette équation soit applicable il faut que les effets soient exprimés en fraction de l'effet maximal, allant de 0 à 1. Il faut donc

normaliser les effets sur l'effet maximal. Si les deux molécules ont des effets maximum différents, il faut normaliser les effets sur l'effet maximal le plus élevé.

Comme pour l'additivité de Loewe, il est possible de calculer un CI dont la formule est la suivante :

$$CI = \frac{E(a)+E(b)-E(a)\times E(b)}{E(a+b)_{observé}} \qquad \text{Equation 27}$$

Son interprétation est identique au CI calculé sous l'additivité de Loewe, à savoir CI<1 signifie synergie et CI>1 signifie antagonisme. En revanche il n'existe pas de représentation graphique spécifique à l'indépendance de Bliss équivalente aux isobologrammes de Loewe.

C'est en se plaçant dans l'un de ces deux paradigmes que les résultats d'expériences étudiant la PK/PD des combinaisons d'antibiotiques seront analysées.

Exemple numérique illustrant l'additivité de Bliss

Si l'on reprend les deux molécules $\mathcal{A}$ et $\mathcal{B}$ utilisées dans l'exemple illustrant l'additivité de Bliss ayant les mêmes relations concentration-effet et les mêmes paramètres, à savoir :

$E_{max,A} = E_{max,B} = 1$; $EC_{50,A} = 0.1$ mg/L et $EC_{50,B} = 1$ mg/L ; $\gamma = 0.5$

Si la combinaison des deux molécules est considérée comme additive en partant des hypothèses de Bliss, l'effet attendu de la combinaison est donné par l'équation 19, rappelée ici :

$$E(a+b)_{attendu} = E(a) + E(b) - E(a)\times E(b) \qquad \text{Equation 28}$$

Où E(a+b) est l'effet de la combinaison aux concentrations a + b, E(a) est l'effet de la molécule $\mathcal{A}$ à la concentration a et E(b) est l'effet de la molécule $\mathcal{B}$ à la concentration B.

Par exemple pour a=0.1 mg/L et b=1 mg/L (les 2 valeurs d'EC_{50}) on a

$$E(a+b) = \frac{E_{maxA}\times a^{\gamma}}{EC_{50A}^{\gamma}+a^{\gamma}} + \frac{E_{maxB}\times b^{\gamma}}{EC_{50B}^{\gamma}+b^{\gamma}} - \frac{E_{maxA}\times a^{\gamma}}{EC_{50A}^{\gamma}+a^{\gamma}} \times \frac{E_{maxB}\times b^{\gamma}}{EC_{50B}^{\gamma}+b^{\gamma}} \qquad \text{Equation 29}$$

$$E(a+b) = \frac{1\times 0.1^{0.5}}{0.1^{0.5}+0.1^{0.5}} + \frac{1\times 1^{0.5}}{1^{0.5}+1^{0.5}} - \frac{1\times 0.1^{0.5}}{0.1^{0.5}+0.1^{0.5}} \times \frac{1\times 1^{0.5}}{1^{0.5}+1^{0.5}} = 0.75 \qquad \text{Equation 30}$$

A noter que dans ce cas puisque $E_{max,A} = E_{max,B} = 1$, il n'est pas nécessaire de normaliser par E_{max}.

De même si a=0.1 mg/L et b=0.1 mg/L on a E(a+b) = 0.62

La figure 12 donne une représentation graphique de l'effet attendu de la combinaison par rapport aux effets des molécules données seules. Pour simplifier la représentation les concentrations a et b utilisées en combinaisons sont identiques.

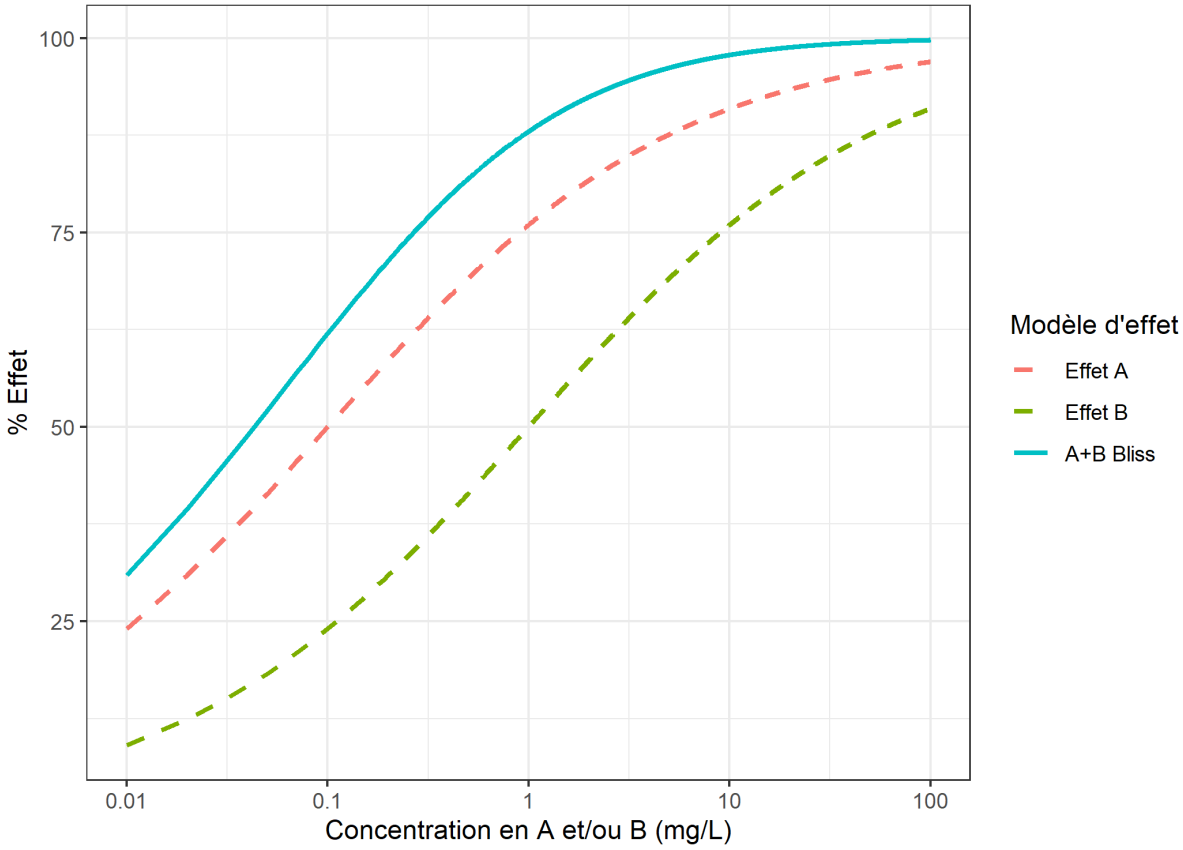

Figure 12. Représentation graphique de l'effet attendu de la combinaison des molécules $\mathcal{A}$ et $\mathcal{B}$ sous l'hypothèse de l'indépendance de Bliss. .

Comparaison des exemples d'application de Loewe et Bliss

Si l'on reprend nos deux molécules A et B et que l'on calcule l'effet attendu pour des concentrations a et b égales aux EC_{50} des molécules administrées seules, en supposant toujours que la combinaison est additive selon les critères de Loewe et de Bliss, on constate une différence d'effet attendu. En effet :

Hypothèse de Loewe : $E(a+b) = \frac{1\times\left(\frac{EC_{50,A}}{EC_{50,A}}+\frac{EC_{50,B}}{EC_{50,B}}\right)}{1+\left(\frac{EC_{50,A}}{EC_{50,A}}+\frac{EC_{50,B}}{EC_{50,B}}\right)} = \frac{2}{3} \approx 59\%$ Equation 31

Hypothèse de Bliss : $E(a+b) = 0.5 + 0.5 - 0.5 \times 0.5 = 75\%$ Equation 32

La figure 13 présente graphiquement ces différences d'effet attendu :

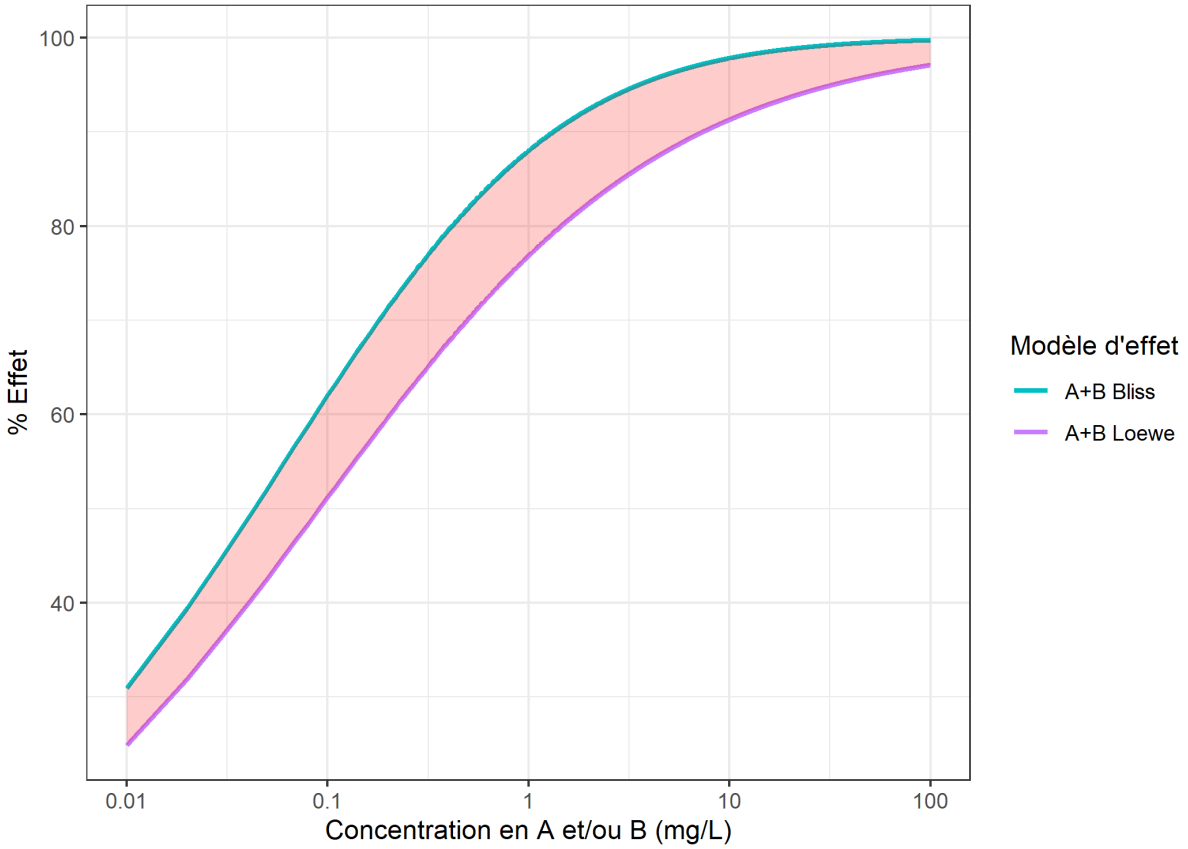

Figure 13. Représentation graphique de la différence des effets attendus de la combinaison des molécules $\mathcal{A}$ et $\mathcal{B}$ en fonction l'hypothèse d'interaction posée. La zone rouge représente les valeurs d'effet pour lesquelles on conclurait à un antagonisme selon l'indépendance de Bliss mais à une synergie selon l'additivité de Loewe.

La zone rouge pâle, met en évidence les valeurs d'effet observés pour lesquelles on conclurait à un antagonisme (effet plus faible qu'attendu en cas d'additivité) si l'on suivait les hypothèses de Bliss alors que l'on conclurait à un une synergie (effet plus fort qu'attendu en cas d'additivité) si l'on suivait les hypothèses de Loewe.

Cette dépendance de l'interprétation des résultats sur le paradigme utilisé a déjà été discutée par Rao et al.[70]

VII.B.3. Checkerboards

L'expérience de base d'étude de la PK/PD de combinaisons d'antibiotiques est l'expérience dite de « checkerboard » (damier en anglais). C'est l'extension de la détermination de la CMI aux combinaisons d'antibiotiques. Ce plan expérimental permet de tester une importante gamme de concentrations d'antibiotiques en combinaison en peu de temps. Il consiste à préparer dans une plaque 96 puits des dilutions sérielles des deux antibiotiques un en colonne et l'autre en lignes (*cf.* figure 11), puis d'ajouter une densité

bactérienne connue de bactéries. Cette plaque est ensuite incubée à une température et pendant une durée dépendant de la bactérie (*i.e.* 20h à 37°C pour *Acinetobacter baumannii*) puis la croissance est évaluée optiquement.

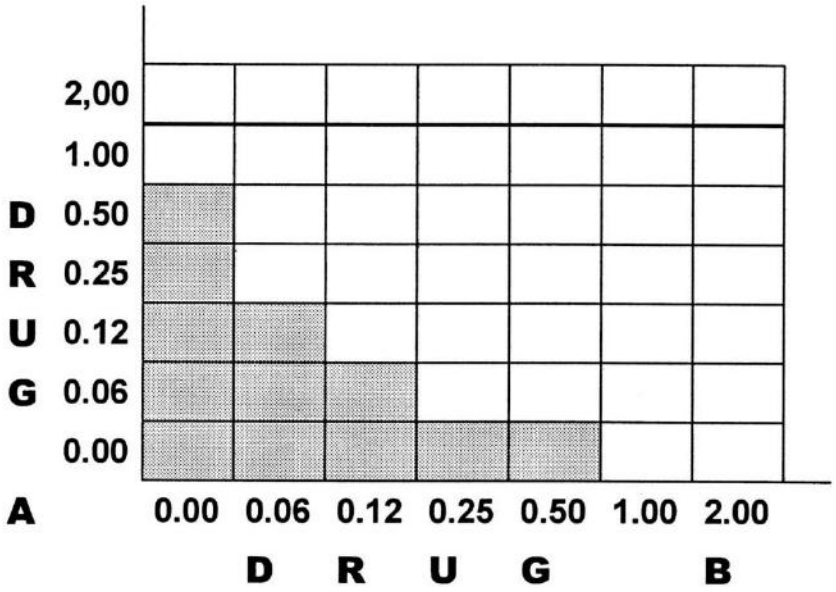

Figure 14. Exemple de plaque de checkerboard. La plus forte concentration en molécule A est préparée dans la première ligne (en haut) puis diluée au demi jusqu'à l'avant dernière ligne, la dernière ligne permet la détermination de la CMI de la molécule B. Le même procédé est effectué pour la molécule B mais en partant de la dernière colonne (à droite). Les zones grises représentent les puits pour lesquelles une pousse des bactéries est observée.(d'après [71])

Pour chaque puits pour lequel la pousse bactérienne est inhibée on peut calculer le Fractional Inhibition Concentration Index (FICI) en suivant la formule suivante :

$$FICI = \frac{a}{MIC_A} + \frac{b}{MIC_B} \quad \text{Equation 33}$$

Le FICI n'est autre que le CI dérivé des équations de Loewe. Une fois le FICI calculé pour tous les puits où la pousse est inhibée il est en général reporté le FICI le plus bas observé sur la plaque[72]. Ce $FICI_{min}$ est ensuite interprété en suivant la règle suivante définie par le journal JAC [73]: $FICI_{min} <= 0.5$: combinaison synergique, $FICI_{min} > 4$ combinaison antagoniste, $0.5 < FICI_{min} <= 4$: pas d'interaction. Certains auteurs[74], dans un souci d'avoir une mesure plus représentative de l'effet observé sur toute la plaque 96 puits considèrent un FICI moyen ($FICI_{mean}$) qui s'obtient en faisant la moyenne des FICI calculés à partir des puits à l'interface de la ligne pousse/inhibition de pousse. L'interprétation du $FICI_{mean}$ est la même que celle du $FICI_{min}$.

La technique des checkerboards se reposant sur des dilutions sérielles de raison 2, et sur une lecture optique partage les mêmes problèmes que la CMI vis-à-vis de l'imprécision des mesures. Ceci se traduit par une variabilité dans les résultats observés par Rand *et al.* [75], qui recommande de faire au moins 5 réplicats

dont 80% donnent le même résultat vis-à-vis de la synergie étudiée afin de pouvoir conclure en utilisant cette technique.

VII.B.4. Index PK/PD en combinaison

De multiples approches ont été proposées pour étendre les index PK/PD aux combinaisons d'antibiotiques. Par exemple il a été fait la somme des AUC/MIC des antibiotiques seuls afin d'obtenir un index de la combinaison [76,77].

Mouton *et al.*[76] ont utilisé une combinaison linéaire des index prédicteurs de l'effet en monothérapie. Par exemple pour l'étude de l'efficacité de la combinaison de la ticarcilline avec la tobramycine dans un modèle d'infection murin de la cuisse, un modèle linéaire combinant T>0.25*MIC pour la ticarcilline et Log(AUC) pour la tobramycine (voir Equation 34) s'est avéré prédictif de l'efficacité de la combinaison.

$$CFU/g(t = 24h) = \beta_1 \times (T > 0.25 * MIC) + \beta_2 \times log(AUC) \qquad \text{Equation 34}$$

Den Hollander *et al.* [78] ont proposé de nouveaux index PK/PD spécifiques aux combinaisons. L'approche est similaire aux index PK/PD utilisés pour les monothérapies, tout d'abord, pour chacun des antibiotiques une CMI en combinaison (MIC_{combi}) est déterminée en utilisant la technique des E-tests (Figure 12).

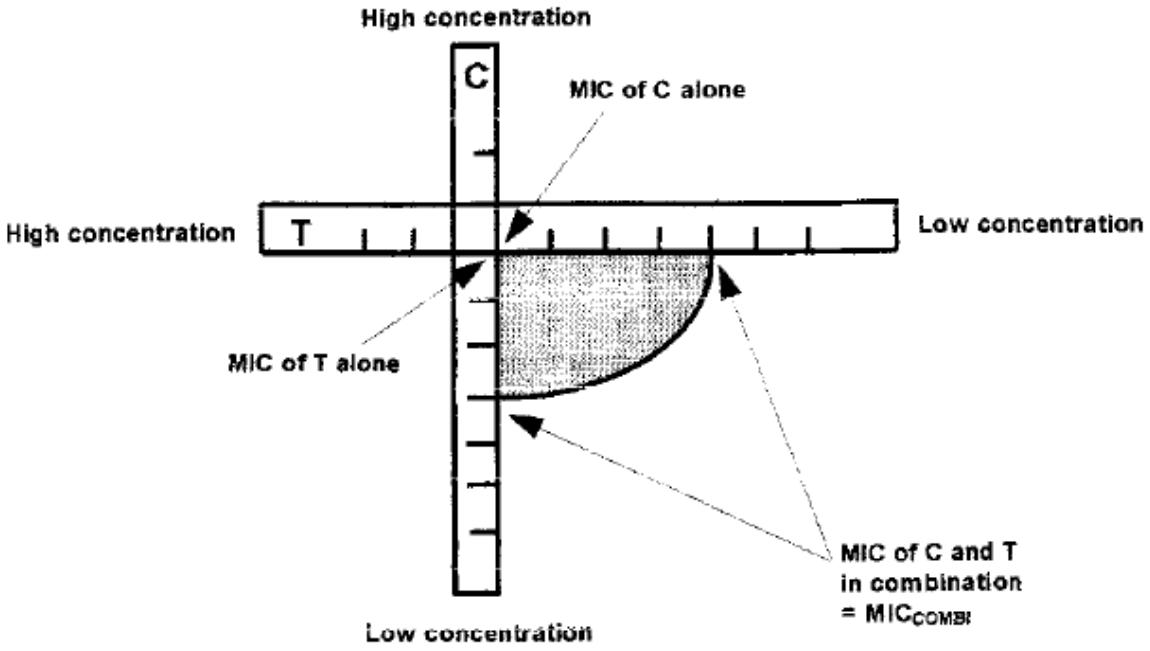

Figure 15. Détermination des CMI en combinaison par la méthode des E-tests. Les bandelettes contenant les antibiotiques T et C sont placées orthogonalement, sur une gélose inoculée avec la bactérie à tester. Les limites de la zone d'inhibition vont permettre de déterminer les CMI en combinaison (d'après [78])

Aussi, des *checkerboards* ont été réalisés afin de déterminer pour chaque combinaison le FICI. Enfin les concentrations en antibiotique ont été utilisées pour calculer un FIC_{combi} tout au long de l'expérience (Equation 35) :

$$FIC_{combi}(t) = \frac{C_A(t)}{MIC_A} + \frac{C_B(t)}{MIC_B} \qquad \text{Equation 35}$$

Quatre index PK/PD ont été construits : le logarithme décimal de l'aire sous la courbe $FIC_{combi}(t)$ ($\log_{10}$ AUC_{FIC}) ; le logarithme décimal du FIC_{combi} maximal ($C_{MAX\text{-}FIC}$) ; le pourcentage du temps pendant lequel les concentrations des antibiotiques sont supérieures à la CMI en combinaison (%T>MIC_{COMBI}), et le pourcentage du temps pendant lequel le FIC_{combi} est supérieur au FICI (%T>FICI). La corrélation entre ces index et la différence entre la densité bactérienne à 24h et au début de l'expérience est ensuite examinée.

Cependant ces approches partagent les même défauts que les index PK/PD pour antibiotiques seuls, avec un niveau de complexité supplémentaire, rendant la détermination de schémas posologiques optimaux difficile[79].

VII.B.5. Modélisation des combinaisons

Les modèles semi-mécanistiques développés pour l'analyse de l'effet des antibiotiques donnés seuls peuvent être étendus aux combinaisons, par modification des fonctions régissant l'effet sur les bactéries. Afin de

pouvoir définir une équation régissant l'effet combiné des deux molécules il s'agit tout d'abord de se mettre dans l'un des paradigmes cités précédemment.

Greco *et al.*[80] ont proposé en 1990 une équation basée sur l'additivité de Loewe, permettant de relier les concentrations en 1-β-D-Arabinofuranosylcytosine, en cisplatine et la densité en cellules tumorales observées. Cette équation a été ensuite généralisée[62] pour une application à tout type d'effets, notamment pour les combinaisons d'antibiotiques :

$$1 = \frac{D_1}{IC_{50,1} \times \left(\frac{E}{E_{max}-E}\right)^{\frac{1}{m_1}}} + \frac{D_2}{IC_{50,2} \times \left(\frac{E}{E_{max}-E}\right)^{\frac{1}{m_2}}} + \frac{\alpha \times D_1 \times D_2}{IC_{50,1} \times IC_{50,2} \times \left(\frac{E}{E_{max}-E}\right)^{\frac{1}{2\times m_1}+\frac{1}{2\times m_2}}} \qquad \text{Equation 36}$$

Où D_i est la dose de l'antibiotique i, $IC_{50,i}$ est la dose de i qu'il faut pour observer la moitié de l'effet maximal E_{max}, m_i est une puissance représentant la sigmoïdicité de la courbe concentration-effet de l'antibiotique i, et αest une facteur représentant le niveau de synergie (α=0 : pas d'interaction, α<0 antagonisme, α>0 synergie). Cette équation (ou une simplification de celle-ci) a été utilisée dans deux modèles PK/PD étudiant les antibiotiques[51,81]

Plus récemment, une approche dérivée de l'indépendance de Bliss a été utilisée par Wicha *et al.*[82] pour l'étude de la combinaison du méropénème et de la vancomycine contre *Staphylococcus aureus*. Nous ne discutons ici que de l'effet sur les bactéries en phase de croissance (GRO dans la publication) et l'expression de l'effet du méropénème est simplifiée. L'effet des molécules prises seules est exprimé comme une réduction de la constante de vitesse de duplication des bactéries (k_{doub}) et peut être exprimé ainsi :

$$k_{doub} = k_{doub,0} \times E_{MER} \qquad \text{Equation 37}$$

$$k_{doub} = k_{doub,0} \times E_{VAN} \qquad \text{Equation 38}$$

Avec $k_{doub,0}$la constante de vitesse de duplication des bactéries en absence d'antibiotique, E_{MER} et E_{VAN} la réduction relative de k_{doub} en présence de méropénème ou de vancomycine, respectivement.

L'effet combiné des molécules est exprimé comme la multiplication des effets en monothérapie :

$$E_{combiné} = E_1 \times E_2 \qquad \text{Equation 39}$$

Et k_{doub} s'exprime ainsi : $k_{doub} = k_{doub,0} \times E_{combiné}$ Equation 40

Une autre approche, plus simple, est d'additionner les effets observés en monothérapie pour obtenir l'effet de la combinaison et ce, pour chaque sous population :

$$E_{AB,i} = E_{A,i} + E_{B,i} \qquad \text{Equation 41}$$

Cette approche simple a été appliquée dans de multiples articles[83–85].

Cette approche a été modifiée en faisant l'hypothèse que l'un ou l'autre (voire les deux) des antibiotiques modifiait l'effet de l'antibiotique qui lui était associé. Cette interaction entre les antibiotiques associés a pu être modélisée comme une modification de l'E_{max} de l'autre antibiotique [86,87] ou comme une modification de l'EC_{50} de l'autre antibiotique [84,88,89].

Une équation empirique a été développée par Mohamed *et al.*[90] :

$$E_{AB} = E_A \times \left(1 + \frac{E_B}{E_A + E_B}\right)^{Int} + E_B \times \left(1 + \frac{E_A}{E_A + E_B}\right)^{Int} \quad \text{Equation 42}$$

Dans cette équation Int est un paramètre représentant l'interaction entre les deux molécules, si Int=0 l'équation se réduit en l'équation xx d'addition des effets. Si Int < 0 les molécules sont dites antagonistes et si Int >0 les molécules sont dites synergiques.

L'approche la plus récente, proposée par Wicha *et al.*[91] appelée *General PharmacoDynamic Interaction model* (GPDI model) a été développée. Cette approche, est compatible avec l'additivité des effets (Equation 41), l'indépendance de Bliss (Equation 26) ainsi que l'additivité de Loewe (Equation 23). Cette approche repose sur une modification de l'expression des effets en monothérapie de telle façon à ce que l'un des paramètres (E_{max}, EC_{50}) soit fonction de la concentration de l'autre antibiotique, par exemple :

$$E_A = \frac{E_{max,A} \times C_A^{H_A}}{\left(EC_{50,A} \times \left(1 + \frac{INT_{AB} \times C_B^{H_{INT,AB}}}{EC_{50,INT,AB}^{H_{INT,AB}} + C_B^{H_{INT,AB}}}\right)\right)^{H_A} + C_A^{H_A}} \quad \text{Equation 43}$$

$$E_B = \frac{E_{max,B} \times C_B^{H_B}}{\left(EC_{50,B} \times \left(1 + \frac{INT_{BA} \times C_A^{H_{INT,BA}}}{EC_{50,INT,BA}^{H_{INT,BA}} + C_A^{H_{INT,BA}}}\right)\right)^{H_B} + C_B^{H_B}} \quad \text{Equation 44}$$

Où INT_{AB} est le paramètre d'interaction de B sur A, si $INT_{AB} = 0$ pas d'interaction de B sur A, si $INT_{AB} > 0$ B augmente l'EC_{50} de A donc antagonisme, si $INT_{AB} < 0$ B diminue l'EC_{50} de A donc synergie. $EC_{50,INT,AB}$ est la concentration en B nécessaire pour observer 50% de l'interaction maximale INT_{AB}, et $H_{INT,AB}$ est un facteur de sigmoïdicité. Dans leur travail Wicha *et al.* appliquent cette approche à des données de 200 combinaisons (paires d'antibiotiques) chez *Saccharomyces cerevisiae* et notent que seulement 11% des interactions observées sont bidirectionnelles, montrant de ce fait l'intérêt d'une approche pouvant identifier les interactions monodirectionnelles.

VIII. Objectif de la thèse

Dans le contexte actuel où il est important d'optimiser les antibiotiques à notre disposition et de rationaliser l'utilisation des combinaisons d'antibiotiques, l'objectif général de cette thèse est de montrer l'apport de la modélisation semi-mécanistique dans l'étude PK/PD des antibiotiques donnés seuls et en combinaison et dans la lutte contre les bactéries résistantes.

Pour y parvenir deux études seront présentés :

1. Une étude de la PK/PD de la céfoxitine contre une souche de *Mycobacterium abscessus*. Dans une première partie, il a été montré que l'administration de la céfoxitine par nébulisation permet d'obtenir des concentrations pulmonaires 1000 fois plus importantes qu'après une administration intraveineuse, faisant de la céfoxitine un bon candidat à la nébulisation. Dans la seconde partie un modèle PK/PD semi-mécanistique a été développé à partir de données *in vitro*, ce qui permet d'identifier la relation concentration-effet pour deux sous-populations bactériennes tout en tenant compte de la dégradation de la molécule.

2. Une étude de la PK/PD de l'association polymyxine B et minocycline contre une souche d'*Acinetobacter baumannii* résistante à la polymyxine B. Cette étude *in vitro* comprend des données de bactéricidie avec suivi de la densité de bactéries résistantes à la polymyxine B, enrichies d'expériences complémentaires servant à préciser les caractéristiques de cette sous-population résistante. Ces données ont toutes été analysées par modélisation PK/PD semi-mécanistique, ce qui a notamment permis de quantifier l'importance de l'interaction entre les deux molécules et de formuler des hypothèses sur les mécanismes de cette interaction.

IX. Mycobacterium abscessus

IX.A. Mycobactéries à croissance rapide

Les mycobactéries sont divisées en deux groupes principaux, le complexe *Mycobacterium tuberculosis* d'une part, et les bactéries non tuberculiniques d'une autre part. Parmi ces dernières, le complexe *Mycobacterium abscessus* fait partie des mycobactéries dites à croissance rapide. On parle de complexe car trois sous-espèces ont été identifiées, *M. abscessus* subsp. *abscessus*, *M. abscessus* subsp. *massiliense* et *M. abscessus* subsp. *bolletii*. Les deux sous-espèces majeures, *abscessus* et *massiliense* diffèrent vis-à-vis du gène *erm(41)* responsable d'une résistance intrinsèque aux macrolides chez la sous-espèce *abscessus* alors que *massiliense* y est sensible [92]. La sous-espèce *abscessus* et la sous-espèce *massiliense* sont retrouvés en proportion similaires dans les échantillons cliniques [93] tandis que la sous espèce *bolletii* est rarement isolée [94].

La prévalence de ces infections est à géographie variable. A cause de difficultés d'identification, les études épidémiologiques font parfois référence aux infections dues au complexe *M. abscessus/chelonae*, par exemple, aux USA il a été montré que ce complexe était responsable de moins d'une infection pulmonaire par 100 000 habitants [95]. En revanche en Asie du Sud-Est la prévalence est plus importante, atteignant par exemple 1.7 cas pour 100 000 habitants à Taiwan [96].Cette infection rare est responsable d'infections des tissus mous, de la peau et d'infections pulmonaires chez les patients immunodéprimés, notamment ceux atteints de la mucoviscidose [97–99] et est associée à un mauvais pronostic avec une mortalité à l'hôpital de 15.7% [100]. Le traitement standard dans les infections à *M. abscessus* est la clarithromycine associée à un aminoside (e.g. amikacine) et une β-lactamine (e.g. céfoxitine ou imipénème). Cependant, *M. abscessus* est capable d'exprimer de nombreux gènes de résistance et a été qualifié de « cauchemar pour antibiotique »[99], *e.g.* 80% des souches sont résistantes à la clarithromycine, ce qui associé au mauvais pronostic justifie la nécessité de nouvelles études sur le traitement de ces infections, notamment l'étude de combinaisons. La céfoxitine et l'amikacine sont les deux molécules ayant montré la meilleure efficacité *in vitro* contre *M. abscessus*[101–103]. Dans l'article 1 nous avons évalué l'efficacité *in vitro* de la céfoxitine contre *M. abscessus*, il convient donc de présenter cette molécule d'abord.

IX.B. Cefoxitine

La céfoxitine est une céphamycine semi-synthétique dont la formule chimique est donnée par la figure 16.

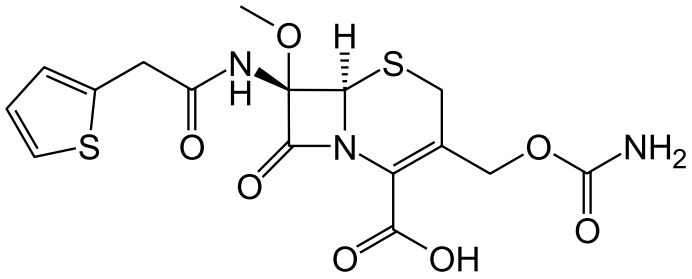

Figure 16. Formule chimique de la céfoxitine (d'après [104])

IX.B.1. Mécanisme d'action

La céfoxitine inhibe la synthèse du peptidoglycane en se liant aux D,D-transpeptidases aussi appelée protéines liant les pénicillines, enzymes permettant la finalisation du peptidoglycane bactérien. Chez les mycobactéries cette étape est principalement due aux L,D-transpeptidases et il a été montré que la cefoxitine se liait aussi à ces enzymes[105]

IX.B.2. Spectre antibactérien et indications

La cefoxitine présente un large spectre antibactérien qui comprend des bactéries Gram + (Streptocoques et staphylocoques), des bactéries Gram – (*Escherichia coli*, *Proteus mirabilis*, *Klebsiella pneumoniae*) certaines bactéries anaérobies ainsi que certaines mycobactéries non tuberculeuses telles que *M. abscessus*. En clinique, cette molécule est indiquée en antibioprophylaxie chirurgicale et dans le traitement des infections dues à *M. abscesssus*, *M. fortuitum* et *M. chelonae*[106].

IX.B.3. Mécanismes de résistance

La céfoxitine est insensible à la majorité des bêta-lactamases y compris celles de spectre étendu[107]. Cependant elle reste susceptible aux bêta-lactamases de la famille AmpC, et est même un inducteur de leur production[108], ce qui se traduit notamment par un antagonisme lorsque la molécule est associée avec une bêta-lactamine susceptible d'être dégradée par AmpC[109].

IX.C. Article 1: Pre-clinical pharmacokinetic and pharmacodynamic data to support cefoxitin nebulization for the treatment of Mycobacterium abscessus.

AMERICAN SOCIETY FOR MICROBIOLOGY | Antimicrobial Agents and Chemotherapy®

PHARMACOLOGY

Preclinical Pharmacokinetic and Pharmacodynamic Data To Support Cefoxitin Nebulization for the Treatment of *Mycobacterium abscessus*

Shachi Mehta,[a,b] Vincent Aranzana-Climent,[a,b] Blandine Rammaert,[a,b,d] Nicolas Grégoire,[a,b] Sandrine Marchand,[a,b,c] William Couet,[a,b,c] Julien M. Buyck[a,b]

[a]Inserm U1070, Pôle Biologie Santé, Poitiers, France
[b]UFR Médecine-Pharmacie, Université de Poitiers, Poitiers, France
[c]Service de Toxicologie-Pharmacocinétique, CHU Poitiers, Poitiers, France
[d]Service de Maladies Infectieuses, CHU Poitiers, Poitiers, France

ABSTRACT *Mycobacterium abscessus* is responsible for difficult-to-treat chronic pulmonary infections in humans. Current regimens, including parenteral administrations of cefoxitin (FOX) in combination with amikacin and clarithromycin, raise compliance problems and are frequently associated with high failure and development of resistance. Aerosol delivery of FOX could be an interesting alternative. FOX was administered to healthy rats by intravenous bolus or intratracheal nebulization, and concentrations were determined in plasma and epithelial lining fluid (ELF) by liquid chromatography-tandem mass spectrometry. After intrapulmonary administration, the FOX area under the curve within ELF was 1,147 times higher than that in plasma, indicating that this route of administration offers a biopharmaceutical advantage over intravenous administration. FOX antimicrobial activity was investigated using time-kill curves combined with a pharmacokinetic/pharmacodynamic (PK/PD) type modeling approach in order to account for its *in vitro* instability that precludes precise determination of MIC. Time-kill data were adequately described by a model including *in vitro* degradation, a sensitive (S) and a resistant (R) bacteria subpopulation, logistic growth, and a maximal inhibition-type growth inhibition effect of FOX. Median inhibitory concentrations were estimated at 16.2 and 252 mg/liter for the S and R subpopulations, respectively. These findings suggest that parenteral FOX dosing regimens used in patients for the treatment of *M. abscessus* are not sufficient to reduce the bacterial burden and that FOX nebulization offers a potential advantage that needs to be further investigated.

KEYWORDS *Mycobacterium abscessus*, cefoxitin, nebulization, pharmacokinetics-pharmacodynamics

Mycobacterium abscessus is the most frequent rapidly growing mycobacteria in human pathology (1). This emerging pathogen is mainly responsible for chronic pulmonary infections in patients with cystic fibrosis (1) and is considered a "new antibiotic nightmare" because of its intrinsic resistance to a broad range of antibiotics, including classical antituberculous agents such as ethambutol, pyrazinamide, and isoniazid (2). Presently there is no reliable antibiotic treatment to cure *M. abscessus* pulmonary infections (2–4). In fact, treatment for pulmonary infections caused by *M. abscessus* is not well standardized yet (4, 5). It consists of intravenous (i.v.) administration of amikacin (AMK) and cefoxitin (FOX) in combination with oral administration of clarithromycin (CLR) for several months (4). Unfortunately, this treatment is associated

Citation Mehta S, Aranzana-Climent V, Rammaert B, Grégoire N, Marchand S, Couet W, Buyck JM. 2019. Preclinical pharmacokinetic and pharmacodynamic data to support cefoxitin nebulization for the treatment of *Mycobacterium abscessus*. Antimicrob Agents Chemother 63:e02651-18. https://doi.org/10.1128/AAC.02651-18.

Address correspondence to William Couet, william.couet@univ-poitiers.fr.

Shachi Mehta and Vincent Aranzana-Climent contributed equally to this work.

Received 20 December 2018
Returned for modification 26 March 2019
Accepted 27 April 2019
Accepted manuscript posted online 6 May 2019
Published 24 June 2019

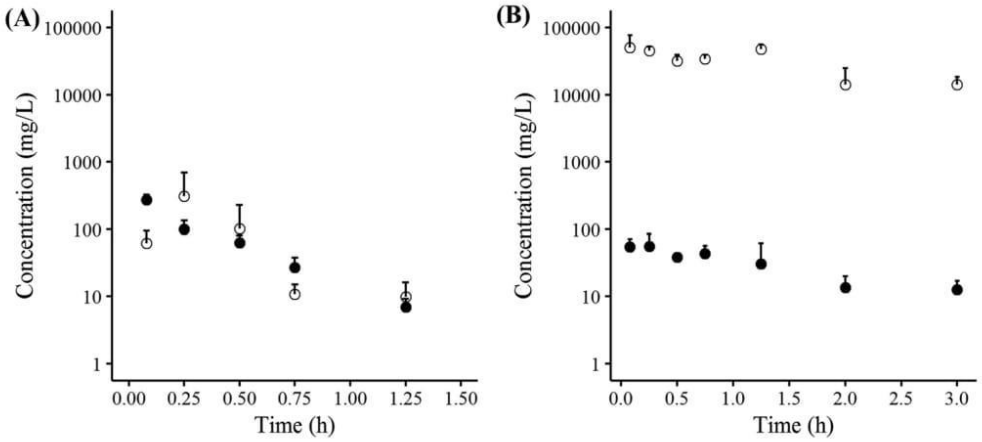

FIG 1 Observed mean concentration ± SD versus time profiles of FOX following i.v. (A) and NEB (B) treatment. Closed symbols correspond to the total plasma concentrations, and open symbols represent ELF concentrations.

with high failure rates, showing infection relapse or death (6). Furthermore, long-term treatments, from several months to a year, with parenterally administered antibiotics are not only challenging and relatively costly but also responsible for low compliance (4). In this context, alternative routes of administration, such as aerosol delivery, should be considered. Nebulization (NEB) is more convenient than i.v. administration and results in higher lung concentrations, and higher efficacy, along with limited systemic side effects, may be achieved (7).

A recent series of well-controlled experiments in healthy rats have shown that antibiotics, such as fluoroquinolones (8), with high membrane permeability are rapidly absorbed after NEB, whereas compounds with much lower membrane permeability, such as colistin (CST) (9), aztreonam (ATM) (10), tobramycin (TOB) (11), gentamicin (GEN), and AMK (12), are slowly absorbed after NEB, leading to high sustained local concentrations, and much higher pulmonary epithelial lining fluid (ELF) concentrations of GEN after NEB than i.v. administration have recently been reported in critically ill patients (13). A simple rule to be considered is that antibiotics that cannot be administered orally, because of poor oral bioavailability due to limited membrane permeability, are, for that same reason, the best candidates for aerosol delivery to treat pulmonary infections. Interestingly, FOX and AMK are rather hydrophilic and are not substantially absorbed after oral administration because of their limited membrane permeability. All of these parameters make FOX as well as AMK good candidates for NEB (12). However, if FOX and AMK present similarities in terms of pharmacokinetics (PK), including low volume of distribution and mostly renal elimination, they do not share similarities in terms of pharmacodynamics (PD). Aminoglycosides, including AMK, are considered to be concentration dependent, whereas β-lactam antibiotics such as FOX are usually supposed to exhibit time-dependent activity (14). Moreover, characterization of FOX activity against *M. abscessus* is made difficult due to its rapid degradation (15, 16) and has been reported only on rare occasions (17–19). Therefore, the objective of this study was first to compare the intrapulmonary PK of FOX after NEB and i.v. administration to healthy rats and then to characterize its *in vitro* PD against a selected strain of *M. abscessus*.

RESULTS

Pharmacokinetics in healthy rats. FOX concentration-time profiles after i.v. administration and NEB are presented in Fig. 1. After i.v. administration, FOX concentrations were almost superimposed in plasma and ELF except at early times due to distribution within ELF. Accordingly, FOX exposure in ELF and plasma was comparable (mean areas under unbound concentration-time curve from time zero to infinity in plasma [$AUC_{u,plasma}$] and ELF [$AUC_{u,ELF}$] of 107 h·μg/ml and 103 h·μg/ml, respectively),

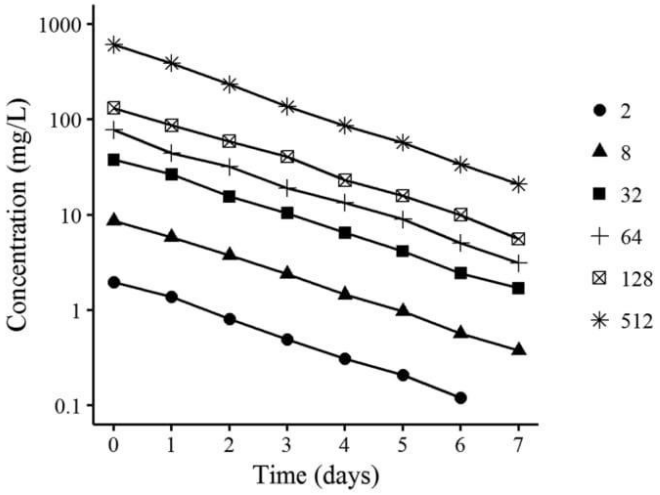

FIG 2 Observed concentration versus time profiles of FOX in 7H9 broth. Initial concentrations of FOX are in mg/liter and indicated by different symbols.

corresponding to a ratio of 1.04. Estimated elimination half-lives in ELF ($t_{1/2}$ = 0.19 h) and plasma ($t_{1/2}$ = 0.23 h) were also virtually identical. After NEB, FOX concentrations were much higher within ELF than in plasma, with $AUC_{u,ELF}$ of 119,289 h·μg/ml and $AUC_{u,plasma}$ of 104 h·μg/ml, corresponding to a ratio of 1,147. Noticeably, $AUC_{u,plasma}$ was identical after NEB and i.v. administration, but the $AUC_{u,ELF}$ was 1,113-fold higher after NEB than after i.v. administration. Again, ELF and plasma concentrations decreased approximately in parallel with time after NEB (Fig. 1), with corresponding half-lives estimated at 1.54 h and 1.23 h, respectively, which is at least 6 times longer than that after i.v. administration.

***In vitro* FOX degradation.** FOX degradation followed first-order kinetics with a half-life estimated at 1.5 days (Fig. 2).

***In vitro* pharmacodynamics. (i) Time-kill kinetics assay.** The first series of time-kill experiments showed no effect for initial FOX concentrations equal to or lower than 16 mg/liter. An initial CFU decay followed by regrowth was observed at day 2 for initial concentrations equal to 32 mg/liter and at day 6 for initial concentrations equal to 64 mg/liter. A decay without regrowth over 8 days was observed for initial concentrations above 128 mg/liter (Fig. 3A). The second series of time-kill kinetics showed that a CFU decay followed by a regrowth occurs for initial FOX concentrations between 12

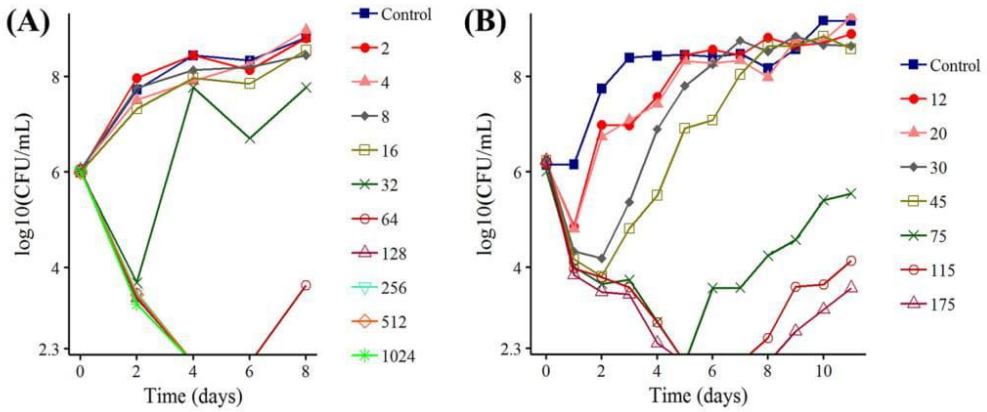

FIG 3 Representative results of FOX time-kill curves against *M. abscessus* CIP 104536 strain. Initial concentrations of FOX are in mg/liter and indicated by different symbols. The ordinate shows the change in the number of CFU (log_{10} scale) per ml of broth. The limit of quantification was 200 CFU/ml (2.3 in log_{10}). (A) First series of experiments. (B) Second series of experiments.

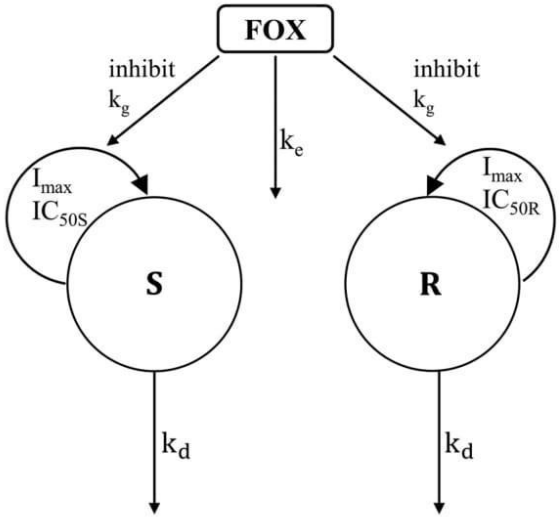

FIG 4 Schematic diagram of the final PK/PD type model. Bacteria multiplied with a first-order rate constant (K_g) in the susceptible (S) and resistant (R) bacterial compartment, and all bacteria had natural death rates (K_d). The cefoxitin compartment (FOX), with a first-order elimination rate (ke), was driving to the bacterial growth inhibition following an I_{max} model.

and 175 mg/liter and that time to regrowth increased with the initial FOX concentrations (Fig. 3B).

(ii) Time-kill modeling. Initially the first series of time-kill kinetics experiments was analyzed using a growth inhibition I_{max} (maximal inhibition) model, with Hill coefficient, with a single homogenous population of bacteria (see the supplemental material). After pooling the two time-kill data sets, a growth inhibition I_{max} model with two subpopulations (Fig. 4), susceptible (S) and resistant (R), best described the experimental data. Visual predictive checks (VPCs) with observed and simulated CFU, with 80% prediction interval, show that model predictions fit the experimental data well, except at a 45-mg/liter initial FOX concentration (Fig. 5). Pharmacodynamics (PD) parameter estimates are presented in Table 1. Noticeably, the difference in susceptibilities of the two bacterial subpopulations is reflected by a 50% inhibitory concentration for the resistant subpopulation (IC_{50R}) 15-fold higher than the IC_{50} for the susceptible subpopulation (IC_{50S}).

(iii) Simulations of CFU versus time profiles without FOX degradation. According to simulations, FOX has no effect on both the S and R subpopulations at a concentration equal to 10 mg/liter and an effect on the S subpopulation only at concentrations equal to 20, 100, or 200 mg/liter (Fig. 6). FOX has no effect on the R subpopulation at concentrations of 20 and 100 mg/liter but has an effect followed by regrowth at a concentration of 200 mg/liter. Complete bacterial killing is expected at 300 mg/liter.

DISCUSSION

The initial PK part of this study has clearly demonstrated a major effect of the route of administration on FOX concentrations within ELF. The targeting advantage (TA) provided by NEB, corresponding to the ratio of $AUC_{u,ELF}$ after NEB versus after i.v. administration and reflecting the relative increased FOX exposure within ELF after NEB, was close to a thousand (TA of 1,113). This high TA is consistent with values previously reported under similar experimental conditions: 242, 2,673, 874, and 162 for TOB (11), ATM (10), AMK, and GEN (12), which are all antibiotics with low membrane permeability precluding oral administration. By comparison, for ciprofloxacin (CIP) and moxifloxacin (MXF), two fluoroquinolone antibiotics with high membrane permeability allowing oral administration, the ratio of $AUC_{u,ELF}$ after NEB versus that after i.v. administration were close to unity (TA of 1.2 for CIP and TA of 0.95 for MXF) (8), suggesting limited, if any,

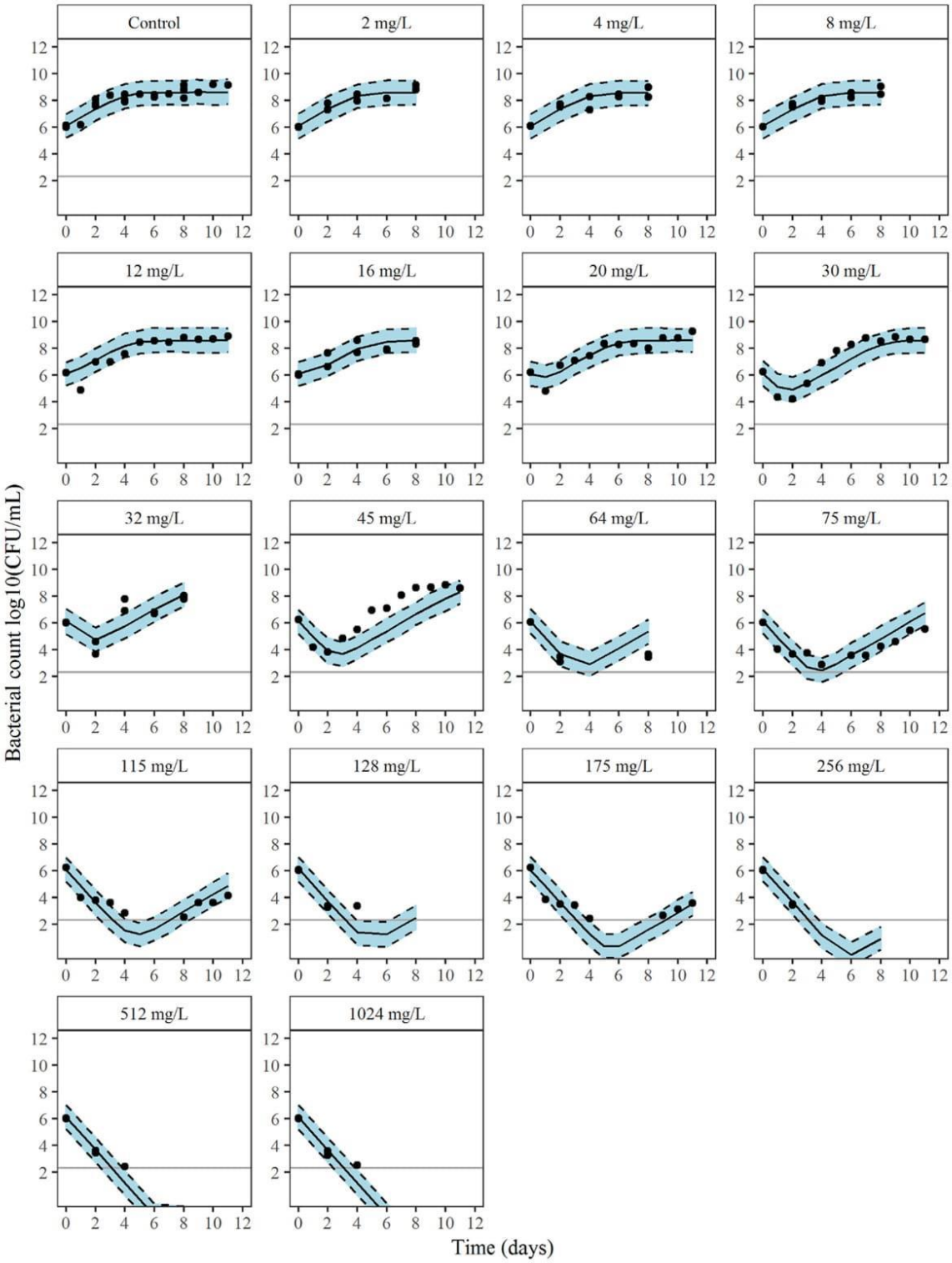

FIG 5 Visual predictive checks (VPCs) for the final PK/PD type model of FOX against *M. abscessus* CIP 104536 with observed bacterial counts (circles), medians (black continuous line), and 80% prediction intervals (black dotted line) of simulated data. Plots include growth control and experimental data by time-kill kinetics. The indicated concentrations are the initial FOX concentrations. The line shows the limit of quantification (200 CFU/ml).

biopharmaceutical advantage of NEB. However, TA values determined in rats after intratracheal administration with the Penn-Century microsprayer cannot be directly extrapolated to humans. Indeed, using this mode of administration, virtually 100% of the dose is absorbed and systemically bioavailable, leading to comparable plasma AUCs

TABLE 1 PD parameter estimations, derived from the growth inhibition model fitted to time-kill kinetics assay

Parameter	Explanation	Estimation (% RSE[a])
LGINOC (log_{10}CFU/ml)	Initial bacterial density	6.1 (1)
K_g (day^{-1})	Bacterial growth rate constant	4.3 (6)
B_{max} (log_{10}CFU/ml)	Bacterial count in stationary phase	9.05 (1)
K_d (day^{-1})	Bacterial death rate constant	2.83 (7)
I_{max}	Maximum fractional reduction of growth by FOX	1 (fixed)
IC_{50S} (mg/liter)	FOX concentration that results in 50% of I_{max} for susceptible subpopulation	16.2 (11)
IC_{50R} (mg/liter)	FOX concentration that results in 50% of I_{max} for resistant subpopulation	252 (20)
K_e (day^{-1})	Degradation rate constant for FOX followed by first-order process	0.438 (fixed)
MUTF	Mutation frequency of bacteria	−9.66 (6)
γ	Hill factor for growth inhibition due to drug activity	4.8 (39)

[a]RSE, relative standard errors.

independent of the route of administration (8–12). This characteristic, which was confirmed in the present study ($AUC_{u,plasma}$ of 103 h·μg/ml after i.v. and 104 h·μg/ml after NEB treatment), does not reflect the clinical setting, with only a small fraction of the dose being absorbed after aerosolization. This can be illustrated by comparing results obtained after nebulization of GEN in rats (12) and patients (13). Comparison of $AUC_{u,plasma}$ values in patients indicates that GEN systemic exposure was close to 5% after NEB compared with i.v. administration.

The PD of FOX, and in particular the potential advantage provided by NEB, not in terms of increased exposure at the infection site but rather in terms of antimicrobial efficacy, was investigated during the second part of this study. Our time-kill results are consistent with those obtained during previous studies over this relatively limited period of time (18, 19). FOX is supposed to be a time-dependent antibiotic, and accordingly it is recommended to maintain concentrations higher than the MIC with no need for high peak concentrations. However, characterization of *in vitro* FOX activity against mycobacterium species is made difficult for two different reasons. Although *M.*

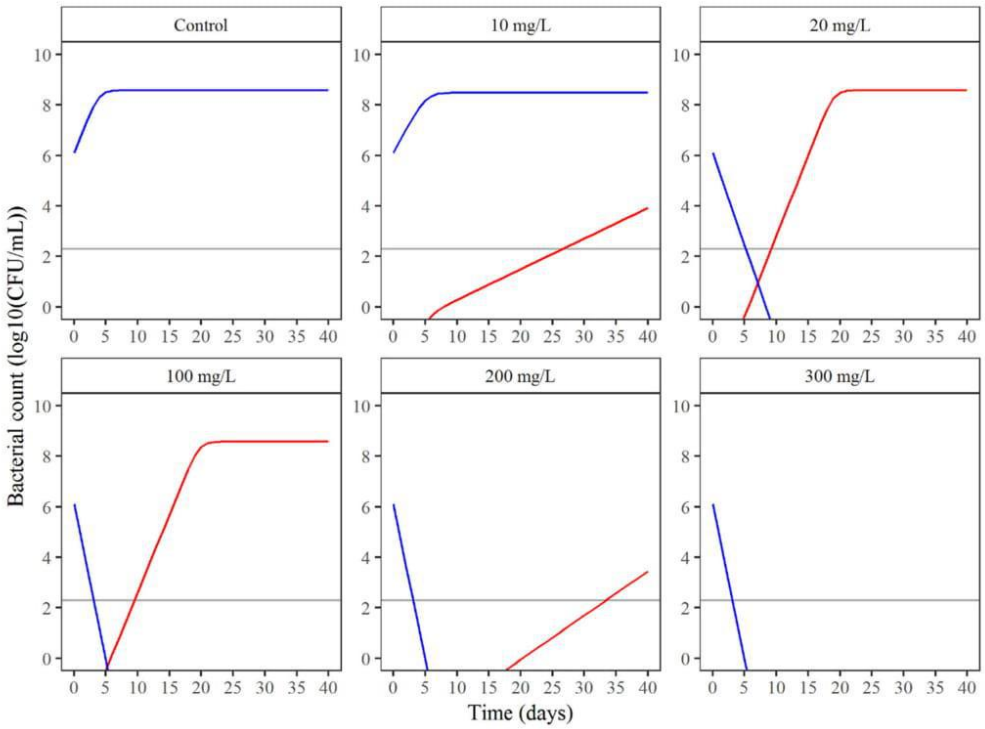

FIG 6 Simulations of CFU counts versus time at several FOX concentrations without considering FOX degradation, using the final PK/PD type model (2 subpopulations) of FOX against *M. abscessus* CIP 104536. Red lines represent the amount of resistant bacteria, and blue lines represent the amount of susceptible bacteria. Horizontal lines show the limit of quantification (200 CFU/ml).

abscessus is considered to be a rapidly growing mycobacterial species, compared with other mycobacteria, such as *M. tuberculosis*, experiments take longer with mycobacterium species than with other bacteria. As an example, MIC determination is conducted over 3 days for *M. abscessus* compared with 1 day for most bacteria. In addition, FOX is degraded within 7H9 broth with an elimination half-life close to 1.5 days, meaning that after 3 days, FOX concentration within the liquid medium would only be 25% of the initial concentration. Actually, FOX degradation within liquid medium was initially documented by Oberholtzer and Brenner (20) and then identified as a real problem for MIC determination by Rominski et al. (15). In fact, when an apparent MIC is reported at 8 mg/liter, it should be noted that this corresponds to the initial FOX concentration, which, after 3 days, or 2 half-lives, should be down to 2 mg/liter. Therefore, the intermediate FOX concentration at 4 mg/liter would better reflect the "true" MIC. In order to take into account this degradation, especially for interpretation of time-kill kinetics experiments conducted over time periods longer than a week, a PK/PD type modeling approach was used. The fact that FOX concentrations decay with time due to *in vitro* first-order degradation was taken into account just as if this was due to *in vivo* elimination. However, the *in vitro* degradation variability was negligible, and the degradation half-life was set at 1.5 days for the PK/PD type modeling, conducted in two separate steps.

Initially, time-kill experiments were conducted at 11 different initial concentrations, from 2 to 1,024 mg/liter, corresponding to multiple values of the apparent MIC, as commonly done (here we used 0.25 to 128 times the MIC), plus a control (Fig. 3). There was virtually no effect at initial concentrations equal to or lower than 16 mg/liter. When the initial concentration was equal to 32 mg/liter, an initial decay of CFU was observed, followed by regrowth after 2 days. For initial concentrations equal to or higher than 64 mg/liter, a CFU decay was observed with no regrowth after 2 days. The question was to determine whether regrowth observed at the intermediate FOX concentration could be explained by its degradation, starting from 32 mg/liter and dropping down to 16 mg/liter and 8 mg/liter after 1.5 and 3 days, respectively. A PK/PD type model was used to answer this question. With this type of model, it can be considered that the antibiotic acts by inhibiting bacterial growth (bacteriostatic effect) or by stimulating bacterial kill (bactericidal effect). Since, according to Lavollay et al. (17) and Greendyke and Byrd (21), FOX is supposed to possess bacteriostatic activity against *M. abscessus*, a growth inhibition PD model was selected with a single homogenous bacterial population. This model provided reasonably good data fitting (see the supplemental material), but noticeably, using the same strain (CIP 104536), Ferro et al. have identified a FOX-resistant subpopulation, preexistent at time zero (22), suggesting that the PK/PD model with a single homogenous bacterial population is not appropriate. However, our initial data set, with regrowth observed at only one FOX concentration, was probably not sufficiently informative to support the superiority of two subpopulations (S and R) versus one population PD model. Therefore, we decided to initiate a second series of time-kill experiments with more intermediate initial FOX concentrations, i.e., susceptible enough to provide initial CFU decay followed by regrowth. Noticeably, according to the one-population model, regrowth should always start at the same FOX concentration (the nadir). Therefore, time to nadir should increase with the initial FOX concentration, more precisely by 1.5 days, corresponding to FOX degradation half-life, each time the initial concentration is increased by twofold. The effect of initial FOX concentration on time to nadir would not be the same in the presence of one and two subpopulations. The supplementary intermediate FOX concentrations used for this second time-kill set of experiments (12, 20, 30, 45, 75, 115, and 175 mg/liter), the frequency of CFU determinations (every day instead of every 2 days), and the experiment duration (increased from 8 to 11 days) were selected in order to allow discrimination between one- and two-population models.

Using the whole data set (initial and second series of time-kill experiments), the two-subpopulation model best described experimental data, as illustrated in Fig. 5.

However, direct interpretation of this figure is difficult, since FOX degradation contributes to regrowth as well as the existence of an R subpopulation. In fact, time-kill experiments are frequently referred to as "static" conditions because they use several different antibiotic concentrations but are stable over time, as opposed to "dynamic" conditions, such as hollow-fiber experiments, in which the medium is replaced in order to let antibiotic concentration decay with time according to 1st-order kinetics, with an elimination half-life selected to mimic *in vivo* PK.

One point of interest in the PK/PD type model was that it allowed simulations of CFU versus time profiles, keeping FOX concentrations constant with time (Fig. 6). It was also possible to simulate the effect of FOX on each subpopulation. Due to the high γ value ($\gamma = 4.8$), the model suggests that a slight change in FOX concentrations around the IC_{50S} (16.2 mg/liter) has dramatic consequences on FOX antimicrobial effect on the S subpopulation. Accordingly, no effect would be expected at a FOX concentration equal to 10 mg/liter, but a marked initial decay of CFU with time with no regrowth is predicted at a FOX concentration equal to 20 mg/liter (Fig. 6). Thus, as far as FOX concentrations remain low compared with the IC_{50R} (252 mg/liter), regrowth of the R subpopulation should be observed at later times (Fig. 6).

Interestingly, after systemic administration at the usual dose (2 g) in patients, FOX total plasma concentrations reach values of up to 200 mg/liter (23), which, considering that the unbound fraction is close to 25% (24), corresponds to maximum unbound plasma concentrations on the order of 50 mg/liter. In this range of values, unbound FOX concentrations should demonstrate antimicrobial efficacy only against the susceptible *M. abscessus* population. Therefore, the possibility of achieving much higher FOX concentrations at the infection site (lung ELF) after nebulization, as suggested in this study using noninfected rats, may offer an opportunity to provide antimicrobial efficacy against the R subpopulation as well.

However, extrapolation of these new data to the clinical setting must be done extremely carefully. First, from a PK standpoint, nebulization with the Penn-Century microsprayer allows good control of the dose, which is of interest for the biopharmaceutical characterization of nebulized antibiotics (8–12, 25) but which does not reflect the clinical setting. Furthermore, on top of potential between-species differences, *M. abscessus* produces biofilm (21), and lung infection induces changes in lung physiology. These phenomena may have an effect on FOX membrane permeability and therefore on lung PK that is not reflected using healthy rats. Second, from a PD point of view, most of our findings rely on a model with a simple two-subpopulation model, which, as previously stated, may be too simplistic. Another limitation of these *in vitro* experiments is that they do not take into consideration the distribution of *M. abscessus* within macrophages or the limited FOX intracellular distribution (19). Finally, in clinical practice *M. abscessus* infections are treated by several antibiotics in combination. This obviously has major consequences in terms of antimicrobial efficacy, which was not addressed here.

In conclusion, the PK/PD type modeling approach developed in this study enabled correction for FOX degradation and, therefore, characterization of the effect-concentration relationship, as is usually done by time-kill experiments. Moreover, combined with the possibility of reaching much higher FOX lung ELF concentrations after nebulization than traditional parenteral administration, it provides evidence to support a potential therapeutic advantage of this route of administration. Furthermore, as far as these high FOX ELF concentrations would not be responsible for undesirable effects, combined with the slow elimination half-life of FOX after NEB, they would allow us to maintain the effect maximum for a long period of time postnebulization. In other words, PK/PD characteristics of FOX may allow spaced nebulization. However, numerous complementary experiments would be necessary to confirm the potential therapeutic advantage of FOX NEB for the treatment of *M. abscessus* infections.

MATERIALS AND METHODS

Antibiotics. FOX sodium salt was obtained from Panpharma (Luitré, France) for *in vivo* and *in vitro* experiments and from Sigma (Saint-Quentin-Fallavier, France) for analytical purposes. Cefuroxime (CXM) was obtained from Aprokam (Clermont-Ferrand, France).

Pharmacokinetics in healthy rats. (i) Administration and sampling. Animal experiments were conducted in compliance with EC Directive 2010/63/EU after approval by the local ethics committee (COMETHEA) and were registered by the French Ministry of Higher Education and Research under authorization number 2015070211159865. Male Sprague Dawley rats ($n = 59$; mean weight of rats, 300 g) from Charles River Laboratories (Saint Germain Nuelles, France) were used for experiments. All rats were divided in two groups corresponding to route of administration (i.v. or NEB) (11). On day 1 of the experiment, FOX sodium salt solutions were prepared in 0.9% NaCl at a concentration of 300 mg/ml for NEB and 30 mg/ml for i.v. administrations. As previously described (9), FOX was administered under isoflurane anesthesia either by i.v. bolus in the tail vein (1 ml) or by intratracheal NEB (100 μl) using a 1A-1B Penn-Century microsprayer (Wyndmoor, USA) at doses commonly used in clinical practices after correction for body weight, close to 90 mg/kg of body weight (23). Bronchoalveolar lavage (BAL) fluid and blood sampling was performed as previously described (8) at various times until 1.25 h after i.v. and 3 h and NEB administration (0.08, 0.25, 0.5, 0.75, and 1.25 h for i.v. and 0.08, 0.25, 0.5, 0.75, 1.25, 2, and 3 h for NEB; 4 to 5 rats were included per time point).

(ii) FOX analytical assay. The FOX analytical assay was conducted by liquid chromatography-tandem mass spectroscopy (LC-MS/MS). The system included a Shimadzu high-performance liquid chromatography (HPLC) module coupled with an API 3500 mass spectrometer (Sciex, Les Ulis, France). An XBridge amide column (3.5 μm; 50- by 2.1-mm inside diameter; Waters, Saint-Quentin en Yvelines, France) was used, and a gradient mobile phase composed of 5 mM ammonium formate and acetonitrile (70:30 [vol/vol]) with 0.01% of formic acid was delivered at 0.4 ml/min. The mass spectrometer was operated in the negative mode. Ions were analyzed by multiple-reaction monitoring (MRM). CXM was used as an internal standard. The transitions were *m/z* 426/156 for FOX and 423/207 for CXM. The standard curve of 0, 0.05, 0.1, 0.5, 1, 5, 15, and 20 mg/liter was performed for BAL fluid and plasma samples. Three levels of concentrations (0.1, 1, and 15 mg/liter) were tested for intraday variability with precision and accuracy of <15% ($n = 18$ per medium). The between-day variability was studied at 0.1, 1, and 15 mg/liter with a precision and bias of <15% ($n = 6$). The urea concentrations in plasma and BAL fluid samples were measured as previously described (9).

(iii) Data analysis. Noncompartmental PK analysis was conducted from time-averaged unbound FOX concentrations. FOX protein binding was fixed at 25% in plasma (24) and considered to be negligible within ELF, in which protein concentration is 10 times lower than that in plasma (26). Mean areas under unbound concentrations versus time from time zero to infinity were estimated using a trapezoidal method with extrapolation to infinity in plasma ($AUC_{u,plasma}$) and ELF ($AUC_{u,ELF}$) using Phoenix WinNonlin 7.0 software (Certara, St. Louis, MO). Elimination rate constants, ke, in plasma and ELF were estimated by least-squares fit of data points (log concentration-time) in the terminal phase of decline. Corresponding apparent elimination half-lives ($t_{1/2}$) were estimated as 0.693/ke. The $AUC_{u,ELF}/AUC_{u,plasma}$ ratios were compared after NEB and i.v. administration, and the TA of NEB compared to that of i.v. was estimated from the ratio of $AUC_{u,ELF}$ after NEB versus i.v. administration (27). Results are presented as means ± standard deviations (SD).

***In vitro* FOX degradation.** For FOX degradation in 7H9 broth, a 10-mg/ml stock solution of FOX sodium salt in water was prepared and stored at −80°C until being thawed for preparing working solutions after appropriate dilutions in 7H9 broth. To evaluate the degradation of FOX in 7H9 broth, individual tubes of 20 ml of 7H9 broth containing 2, 8, 32, 64, 128, and 512 mg/liter of FOX as an initial concentration were inoculated with the bacterial suspension (~1×10^6 CFU/ml) and incubated at 35°C ± 2°C. Samples were collected daily for up to 8 days. FOX concentrations then were measured by the LC-MS/MS analytical method as explained above.

***In vitro* pharmacodynamics. (i) Bacterial strain and suspension preparation.** *M. abscessus* subsp. *abscessus* reference strain CIP 104536 (Collection of Institute Pasteur, Paris, France) was used. Stock vials were conserved at −80°C in Middlebrook 7H9 broth (referred to as 7H9 broth; BD, BBL, Sparks, MD, USA) with 10% oleic acid-bovine albumin-dextrose-catalase (OADC) growth supplement (BD, BBL, Sparks, MD, USA) and 20% glycerol (Carl Roth GmbH Co. KG, Karlsruhe, Germany). *M. abscessus* was grown on Middlebrook 7H11 agar plates (referred to as 7H11 agar plates) with 10% OADC growth supplement and 0.5% glycerol at 30°C for 3 to 5 days. For each experiment, the mycobacterial inoculum was prepared freshly according to CLSI guidelines (28). Briefly, colonies from agar plates were transferred into a hemodialysis tube with 5 to 6 sterile glass beads of 3 nm and then vortexed for 1 min. One ml of sterile water then was added and the mixture incubated for 15 min at room temperature. The bacterial suspension was adjusted to an optical density at 600 nm of 0.10 to 0.15 (~10^8 CFU/ml). Finally, the suspension was diluted to 1/100 to obtain an ~1×10^6 CFU/ml final concentration in appropriate media.

(ii) Time-kill kinetics assay. Individual tubes of 20 ml of 7H9 broth containing 2, 4, 8, 16, 32, 64, 128, 256, 512, and 1,024 mg/liter of FOX as an initial concentration and growth control (CTL) were inoculated with the bacterial suspension (~1×10^6 CFU/ml) and incubated at 35°C ± 2°C under shaking conditions (150 rpm) for up to 8 days. To quantify bacteria at defined time intervals (0, 2, 4, 6, and 8 days), 100-μl samples were taken and diluted serially when appropriate in phosphate-buffered saline (PBS; pH 7.4; Gibco by Life Technologies, France). Samples were then plated on 7H11 agar plates for further CFU counting after 3 to 5 days of incubation at 35°C ± 2°C. The theoretical detection limit was set to 200 CFU/ml, i.e., 2.3 $\log_{10}$ CFU/ml. A second series of experiments was carried out using FOX initial

concentrations of 12, 20, 30, 45, 75, 115, and 175 mg/liter and a growth control using a protocol similar to that explained above. Numbers of CFU were determined daily for up to 11 days.

(iii) Time-kill modeling. CFU counts and FOX concentrations over time were analyzed separately using a nonlinear fixed-effects PK/PD type modeling approach. Parameters were estimated using the first-order conditional estimation (FOCE) method and Laplacian option available in NONMEM version 7.4.1 (Icon Development Solutions Ellicott City, MD, USA). NONMEM project management was made easier using Pirana (29), and CFU counts below the limit of quantification (200 CFU/ml) were handled using Beal's M3 method (30). The degradation of FOX (C) during the experiment was modelled as a first-order process:

$$C = C_0 e^{-K_e \times t} \quad (1)$$

Where C_0 is the initial concentration of FOX (mg/liter) spiked in the tube at time zero, K_e is the first-order degradation rate constant (days^{-1}), and t is the corresponding elimination half-life, equal to 0.693/K_e (days). Two bacterial subpopulations were considered: susceptible (S) and resistant (R) bacteria. In the absence of FOX, they were assumed to grow until reaching a plateau, and this was described by a logistic growth function. The effect of FOX on *M. abscessus* CIP 104536 was modelled as an inhibition of bacterial growth, with an I_{max} model and different IC_{50} for each subpopulation. The structure of the PD model is presented in Fig. 5. The differential equations describing variations of susceptible bacterial counts (S) and resistant bacterial counts (R) over time are presented below:

$$\frac{dS}{dt} = K_g \times \left(1 - \frac{B}{10^{B_{max}}}\right) \times \left(1 - \frac{I_{max} \times C^{\gamma}}{IC_{50S}^{\gamma} + C^{\gamma}}\right) \times S - K_d \times S \quad (2)$$

$$\frac{dR}{dt} = K_g \times \left(1 - \frac{B}{10^{B_{max}}}\right) \times \left(1 - \frac{I_{max} \times C^{\gamma}}{IC_{50R}^{\gamma} + C^{\gamma}}\right) \times R - K_d \times R \quad (3)$$

where $B = S + R$ is the total bacterial count (CFU/ml), K_g (day^{-1}) is the bacterial growth rate, K_d (day^{-1}) is the bacterial natural death rate, B_{max} ($\log_{10}$ CFU/ml) is the maximum population size supported by the environment, I_{max} is the maximal inhibition, which was supposed to be total inhibition (I_{max} fixed to 1), and IC_{50S} and IC_{50R} (mg/liter) are the concentrations of FOX for which the effect was 50% of I_{max} for susceptible and resistant bacteria, respectively. The residual variability was described by an additive error model on a $\log_{10}$ scale for bacterial count data and by a proportional error model for concentrations of FOX data. No interexperimental variability was estimated on the parameters because we assumed that it would not be distinguishable from residual variability. Model performance was assessed by the evaluation of the goodness-of-fit plots (e.g., observation versus predictions) and objective function value (OFV). The model was evaluated by performing VPCs with stratification on the type of experiments and FOX concentration. All observations were plotted and overlaid with the median, and 80% prediction intervals were obtained by performing 1,000 simulations of the final model with the original data set as the input.

(iv) Simulations of CFU versus time profiles without FOX degradation. In order to evaluate the effect of FOX on *M. abscessus* at constant concentration, the developed PK/PD type model with two subpopulations was used along with PD parameter estimates to simulate the variation in CFU count over time at different concentrations. R package mrgsolve (31) was used to simulate CFU versus time profiles. The final parameter estimates from the current FOX PK/PD type model with two subpopulations were used to simulate the CFU versus time profiles without considering FOX degradation.

SUPPLEMENTAL MATERIAL

Supplemental material for this article may be found at https://doi.org/10.1128/AAC.02651-18.

SUPPLEMENTAL FILE 1, PDF file, 0.2 MB.

ACKNOWLEDGMENTS

We acknowledge F. Mougari and E. Cambau for their helpful discussion and technical expertise at the initial phase of this project. We thank program Nouvelle Aquitaine CPER 2015-2020 and FEDER 2014-2020 for their participation in LC-MS/MS funding. This work has benefited from the facilities and expertise of the PREBIOS platform (University of Poitiers).

REFERENCES

1. Roux A-L, Catherinot E, Ripoll F, Soismier N, Macheras E, Ravilly S, Bellis G, Vibet M-A, Le Roux E, Lemonnier L, Gutierrez C, Vincent V, Fauroux B, Rottman M, Guillemot D, Gaillard J-L. 2009. Multicenter study of prevalence of nontuberculous mycobacteria in patients with cystic fibrosis in France. J Clin Microbiol 47:4124–4128. https://doi.org/10.1128/JCM.01257-09.
2. Nessar R, Cambau E, Reyrat JM, Murray A, Gicquel B. 2012. Mycobacterium abscessus: a new antibiotic nightmare. J Antimicrob Chemother 67:810–818. https://doi.org/10.1093/jac/dkr578.
3. Jarand J, Levin A, Zhang L, Huitt G, Mitchell JD, Daley CL. 2011. Clinical and microbiologic outcomes in patients receiving treatment for Mycobacterium abscessus pulmonary disease. Clin Infect Dis 52:565–571. https://doi.org/10.1093/cid/ciq237.
4. Griffith DE, Aksamit T, Brown-Elliott BA, Catanzaro A, Daley C, Gordin F, Holland SM, Horsburgh R, Huitt G, Iademarco MF, Iseman M, Olivier K, Ruoss S, von Reyn CF, Wallace RJ, Winthrop K, ATS Mycobacterial Diseases Subcommittee, American Thoracic Society, Infectious Disease Society of America. 2007. An official ATS/IDSA statement: diagnosis, treat-

ment, and prevention of nontuberculous mycobacterial diseases. Am J Respir Crit Care Med 175:367–416. https://doi.org/10.1164/rccm.200604-571ST.
5. van Ingen J, Ferro BE, Hoefsloot W, Boeree MJ, van Soolingen D. 2013. Drug treatment of pulmonary nontuberculous mycobacterial disease in HIV-negative patients: the evidence. Expert Rev Anti Infect Ther 11:1065–1077. https://doi.org/10.1586/14787210.2013.830413.
6. Sfeir M, Walsh M, Rosa R, Aragon L, Liu SY, Cleary T, Worley M, Frederick C, Abbo LM. 2018. Mycobacterium abscessus complex infections: a retrospective cohort study. Open Forum Infect Dis 5:ofy022. https://doi.org/10.1093/ofid/ofy022.
7. Flume PA, VanDevanter DR. 2015. Clinical applications of pulmonary delivery of antibiotics. Adv Drug Deliv Rev 85:1–6. https://doi.org/10.1016/j.addr.2014.10.009.
8. Gontijo AVL, Brillault J, Grégoire N, Lamarche I, Gobin P, Couet W, Marchand S. 2014. Biopharmaceutical characterization of nebulized antimicrobial agents in rats. 1. Ciprofloxacin, moxifloxacin, and grepafloxacin. Antimicrob Agents Chemother 58:3942–3949. https://doi.org/10.1128/AAC.02818-14.
9. Gontijo AVL, Grégoire N, Lamarche I, Gobin P, Couet W, Marchand S. 2014. Biopharmaceutical characterization of nebulized antimicrobial agents in rats. 2. Colistin. Antimicrob Agents Chemother 58:3950–3956. https://doi.org/10.1128/AAC.02819-14.
10. Marchand S, Grégoire N, Brillault J, Lamarche I, Gobin P, Couet W. 2016. Biopharmaceutical characterization of nebulized antimicrobial agents in rats. 4. Aztreonam. Antimicrob Agents Chemother 60:3196–3198. https://doi.org/10.1128/AAC.00165-16.
11. Marchand S, Grégoire N, Brillault J, Lamarche I, Gobin P, Couet W. 2015. Biopharmaceutical characterization of nebulized antimicrobial agents in rats. 3. Tobramycin. Antimicrob Agents Chemother 59:6646–6647. https://doi.org/10.1128/AAC.01647-15.
12. Marchand S, Boisson M, Mehta S, Adier C, Mimoz O, Grégoire N, Couet W. 2018. Biopharmaceutical characterization of nebulized antimicrobial agents in rats. 6. Aminoglycosides. Antimicrob Agents Chemother 62:e01261-18. https://doi.org/10.1128/AAC.01261-18.
13. Boisson M, Mimoz O, Hadzic M, Marchand S, Adier C, Couet W, Grégoire N. 2018. Pharmacokinetics of intravenous and nebulized gentamicin in critically ill patients. J Antimicrob Chemother 73:2830–2837. https://doi.org/10.1093/jac/dky239.
14. Levison ME, Levison JH. 2009. Pharmacokinetics and pharmacodynamics of antibacterial agents. Infect Dis Clin North Am 23:791–797. https://doi.org/10.1016/j.idc.2009.06.008.
15. Rominski A, Schulthess B, Müller DM, Keller PM, Sander P. 2017. Effect of β-lactamase production and β-lactam instability on MIC testing results for Mycobacterium abscessus. J Antimicrob Chemother 72:3070–3078. https://doi.org/10.1093/jac/dkx284.
16. Schoutrop ELM, Brouwer MAE, Jenniskens JCA, Ferro BE, Mouton JW, Aarnoutse RE, van Ingen J. 2018. The stability of antimycobacterial drugs in media used for drug susceptibility testing. Diagn Microbiol Infect Dis 92:305–308. https://doi.org/10.1016/j.diagmicrobio.2018.06.015.
17. Lavollay M, Dubée V, Heym B, Herrmann J-L, Gaillard J-L, Gutmann L, Arthur M, Mainardi J-L. 2014. In vitro activity of cefoxitin and imipenem against Mycobacterium abscessus complex. Clin Microbiol Infect 20:O297–O300. https://doi.org/10.1111/1469-0691.12405.
18. Ferro BE, van Ingen J, Wattenberg M, van Soolingen D, Mouton JW. 2015. Time-kill kinetics of antibiotics active against rapidly growing mycobacteria. J Antimicrob Chemother 70:811–817. https://doi.org/10.1093/jac/dku431.
19. Lefebvre A-L, Dubée V, Cortes M, Dorchêne D, Arthur M, Mainardi J-L. 2016. Bactericidal and intracellular activity of β-lactams against Mycobacterium abscessus. J Antimicrob Chemother 71:1556–1563. https://doi.org/10.1093/jac/dkw022.
20. Oberholtzer ER, Brenner GS. 1979. Cefoxitin sodium: solution and solid-state chemical stability studies. J Pharm Sci 68:863–866. https://doi.org/10.1002/jps.2600680720.
21. Greendyke R, Byrd TF. 2008. Differential antibiotic susceptibility of Mycobacterium abscessus variants in biofilms and macrophages compared to that of planktonic bacteria. Antimicrob Agents Chemother 52:2019–2026. https://doi.org/10.1128/AAC.00986-07.
22. Ferro BE, Srivastava S, Deshpande D, Pasipanodya JG, van Soolingen D, Mouton JW, van Ingen J, Gumbo T. 2016. Failure of the amikacin, cefoxitin, and clarithromycin combination regimen for treating pulmonary Mycobacterium abscessus infection. Antimicrob Agents Chemother 60:6374–6376. https://doi.org/10.1128/AAC.00990-16.
23. Brunetti L, Kagan L, Forrester G, Aleksunes LM, Lin H, Buyske S, Nahass RG. 2016. Cefoxitin plasma and subcutaneous adipose tissue concentration in patients undergoing sleeve gastrectomy. Clin Ther 38:204–210. https://doi.org/10.1016/j.clinthera.2015.11.009.
24. Schrogie JJ, Rogers JD, Yeh KC, Davies RO, Holmes GI, Skeggs H, Martin CM. 1979. Pharmacokinetics and comparative pharmacology of cefoxitin and cephalosporins. Rev Infect Dis 1:90–98. https://doi.org/10.1093/clinids/1.1.90.
25. Galindo Bedor DC, Marchand S, Lamarche I, Laroche J, Pereira de Santana D, Couet W. 2016. Biopharmaceutical characterization of nebulized antimicrobial agents in rats. 5. Oseltamivir carboxylate. Antimicrob Agents Chemother 60:5085–5087. https://doi.org/10.1128/AAC.00909-16.
26. Zhang R, Ghosh SN, Zhu D, North PE, Fish BL, Morrow NV, Lowry T, Nanchal R, Jacobs ER, Moulder JE, Medhora M. 2008. Structural and functional alterations in the rat lung following whole thoracic irradiation with moderate doses: injury and recovery. Int J Radiat Biol 84:487–497. https://doi.org/10.1080/09553000802078396.
27. Yapa S, Li J, Patel K, Wilson JW, Dooley MJ, George J, Clark D, Poole S, Williams E, Porter CJH, Nation RL, McIntosh MP. 2014. Pulmonary and systemic pharmacokinetics of inhaled and intravenous colistin methanesulfonate in cystic fibrosis patients: targeting advantage of inhalational administration. Antimicrob Agents Chemother 58:2570–2579. https://doi.org/10.1128/AAC.01705-13.
28. National Committee for Clinical Laboratory Standards. 2003. Susceptibility testing of mycobacteria, nocardiae, and other aerobic actinomycetes; approved standard. NCCLS document M24-A. National Committee for Clinical Laboratory Standards, Wayne, PA.
29. Keizer RJ, van Benten M, Beijnen JH, Schellens JHM, Huitema A. 2011. Piraña and PCluster: a modeling environment and cluster infrastructure for NONMEM. Comput Methods Programs Biomed 101:72–79. https://doi.org/10.1016/j.cmpb.2010.04.018.
30. Beal SL. 2001. Ways to fit a PK model with some data below the quantification limit. J Pharmacokinet Pharmacodyn 28:481–504. https://doi.org/10.1023/A:1012299115260.
31. Baron KT. 2019. mrgsolve: simulate from ODE-based population PK/PD and systems pharmacology models. https://mrgsolve.github.io/.

Supplementary material:

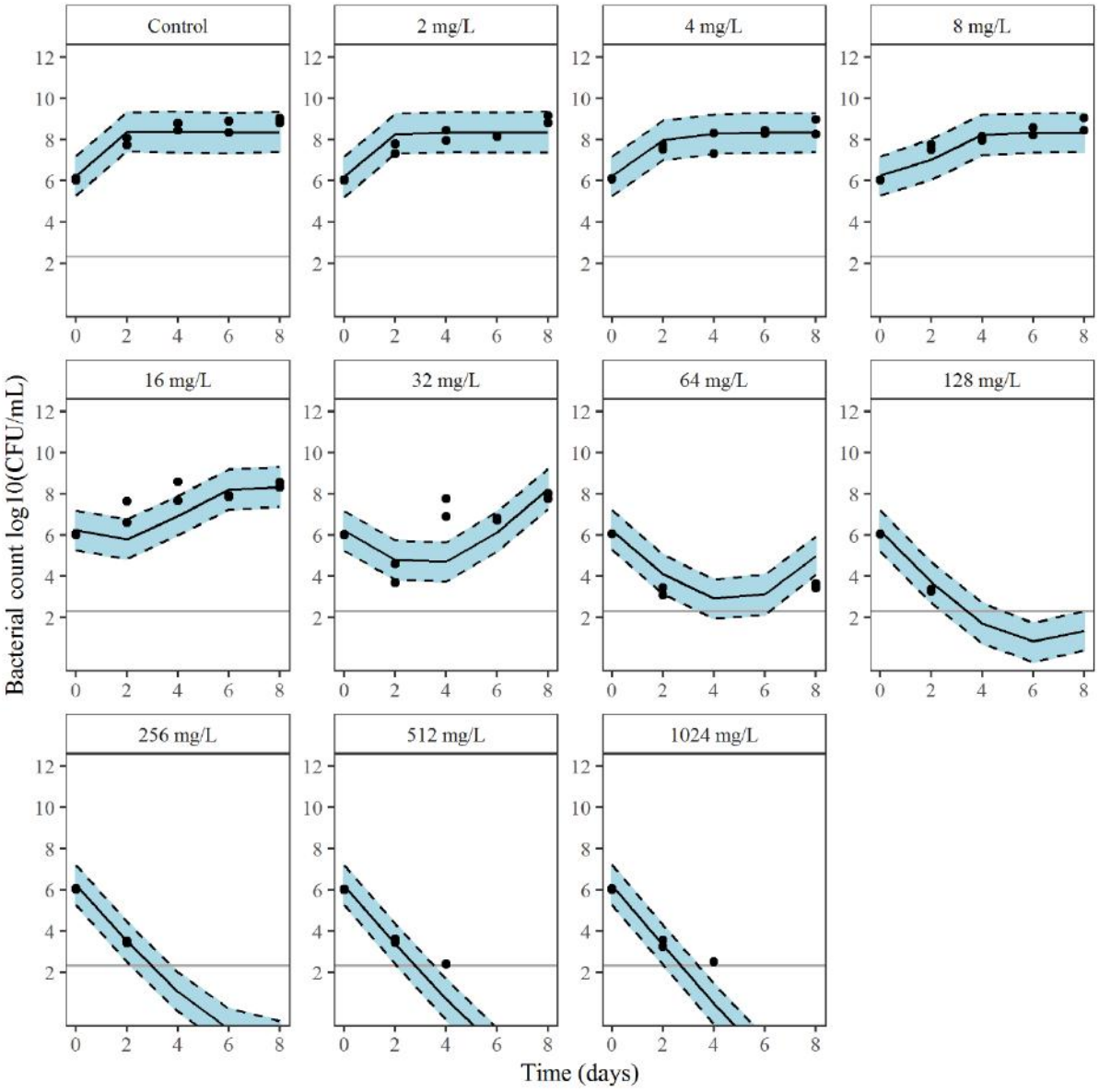

Figure S1: Visual predictive checks (VPCs) for one homogenous population PK/PD type model of cefoxitin against *M. abscessus* CIP 104536 with observed bacterial counts (circles), median (black continuous line) and 80% prediction interval (black dotted line) of simulated data. Plots include growth control and experimental data by time-kill kinetics. The indicated concentration are the initial FOX concentrations. Line shows the limit of quantification (200 CFU/mL).

X. 3e JPIAMR : CO ACTION

En 2014 le rapport O'Neill[4] prévoyait qu'en absence de mesures prises, les bactéries multirésistantes seraient responsables de plus de morts que le cancer d'ici 2050. En réponse à ce constat, de multiples organisations internationales ont mis en place des programmes pour lutter contre l'antibiorésistance (OMS[110], G7[111], G20[112]…). Une des réponses de l'Union Européenne a été la mise en place du programme JPIAMR (Joint Program Initiative on Antimicrobial Resistance) [113], qui a pour but de coordonner la lutte contre l'antibiorésistance en associant les agences nationales de la recherche de 27 pays dans le financement de projets internationaux[114].

Le projet CO-ACTION est un projet qui a été sélectionné dans le cadre du second appel à projets JPIAMR, ayant pour point focal l'étude des antibiotiques oubliés et non utilisés (ND-AB) et l'évaluation de combinaisons de ND-AB avec une autre molécule (antibiotique ou non)[115].

Parmi les ND-AB on retrouve une classe d'antibiotiques, les polymyxines considérés comme des antibiotiques de la dernière chance. La colistine (seule polymyxine autorisée par voie systémique en France) a fait l'objet d'une revue de la littérature en amont du projet CO-ACTION, présentée ci-après.

X.A. Article 2: Clinical Pharmacokinetics and Pharmacodynamics of Colistin.

Clin Pharmacokinet
DOI 10.1007/s40262-017-0561-1

REVIEW ARTICLE

Clinical Pharmacokinetics and Pharmacodynamics of Colistin

Nicolas Grégoire[1,2] · Vincent Aranzana-Climent[1,2] · Sophie Magréault[1,2] · Sandrine Marchand[1,2,3] · William Couet[1,2,3]

Abstract In this review, we provide an updated summary on colistin pharmacokinetics and pharmacodynamics. Colistin is an old molecule that is frequently used as last-line treatment for infections caused by multidrug-resistant Gram-negative bacteria. Colistin is a decapeptide administered either as a prodrug, colistin methanesulfonate (CMS), when used intravenously, or as colistin sulfate when used orally. Because colistin binds to laboratory materials, many experimental issues are raised and studies on colistin can be tricky. Due to its large molecular weight and its cationic properties at physiological pH, colistin passes through physiological membranes poorly and is mainly distributed within the extracellular space. Renal clearance of colistin is very low, but the dosing regimen should be adapted to the renal function of the patient because CMS is partly eliminated by the kidney. Therapeutic drug monitoring of colistin is warranted because the pharmacokinetics of colistin are very variable, and because its therapeutic window is narrow. Resistance of bacteria to colistin is increasing worldwide in parallel to its clinical and veterinary uses and a plasmid-mediated resistance mechanism (MCR-1) was recently described in animals and humans. In vitro, bacteria develop various resistance mechanisms rapidly when exposed to colistin. The use of a loading dose might reduce the emergence of resistance but the use of colistin in combination also seems necessary.

Key Points

Because colistin binds to laboratory materials, many experimental issues are raised.

The dosing regimen of colistin methanesulfonate should be adapted to the renal function of patients, and the use of a loading dose is recommended.

Therapeutic drug monitoring of colistin is warranted.

Because the resistance of bacteria to colistin is increasing, its use in combination seems necessary.

1 Introduction

Colistin, also called polymyxin E, belongs to the group of polymyxin antibiotics (antibacterials). It is an old antibiotic discovered in the 1940s but its clinical use was largely abandoned in the 1970s mainly due to its nephrotoxicity. However, the increase of multidrug resistance (MDR) in Gram-negative bacteria (GNB), particularly *Pseudomonas aeruginosa*, *Acinetobacter baumannii* and *Klebsiella pneumoniae*, led to the re-emergence of its use during the last few years [1]. Parenteral and nebulisation formulations for colistin contain the sodium salt of colistin methanesulfonate (CMS), also called colistimethate, which is an inactive prodrug. The aim of this review is to give an updated summary on colistin with respect to its complex pharmacokinetics and pharmacodynamics. A literature search was conducted using PubMed where colistin or colistin methanesulfonate were combined with key words such as "chemistry", "bioanalysis", "pharmacokinetics"

✉ Nicolas Grégoire
nicolas.gregoire@univ-poitiers.fr

[1] INSERM U1070, Poitiers, France

[2] Université de Poitiers, UFR Médecine-Pharmacie, Poitiers, France

[3] CHU Poitiers, Poitiers, France

Published online: 26 May 2017

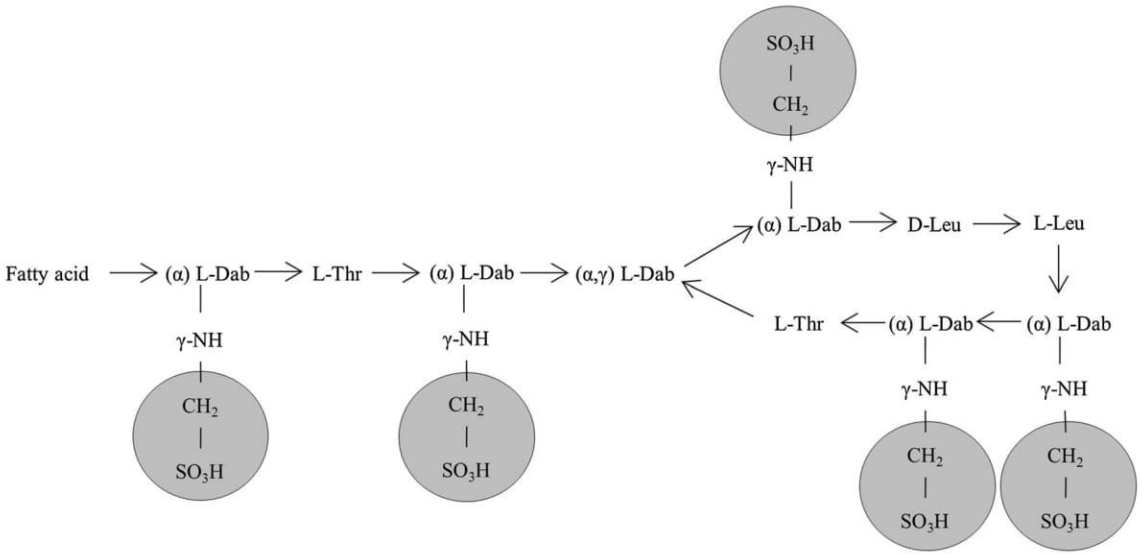

Fig. 1 Structure of colistin methanesulfonate and colistin. Sulfomethyl groups of colistin methanesulfonate are highlighted with *grey circles*. Fatty acyl: 6-methyloctanyl for colistin A and 6-methylheptanyl for colistin B; α and γ indicate the respective $-NH_2$ involved in the peptide linkage. *Dab* α ,γ-diaminobutyric acid, *Leu* leucine, *Thr* threonine

or "pharmacodynamics" to identify relevant literature. Additional references were identified from the references lists of published articles.

2 Conventions Used to Describe Doses of Colistin

At the first International Conference of Polymyxins in Prato, Italy, in 2013, it was stated that colistin doses should be referred to using international units (IU) or mg of colistin base activity (CBA) in order to avoid medication errors [2]. In Europe, India and few other countries, doses of CMS are expressed in million international units (MIU), but also in mg of CMS. By contrast, in North and South America, Southeast Asia and Australia, doses are expressed in mg CBA. In order to convert these different units, it should be known that 1 MIU is equivalent to about 30 mg of CBA, which corresponds to about 80 mg of CMS [2].

3 Chemistry

Colistin (commercially available as the sulfate salt) is a decapeptide compound, corresponding to a complex mixture of about 30 different compounds with two main components, colistin A and colistin B, the proportion of which can vary from batch to batch [3]. Colistin A and B are large molecules with molecular weights of 1169 and 1155 g/mol, respectively. They are composed of a hydrophilic cycloheptapeptide ring, a tail tripeptide moiety and a hydrophobic acyl chain tail, being one carbon shorter for colistin B than for colistin A (Fig. 1) [4]. Colistin is a hydrophilic drug ($\log P = -2.4$ [5]) but with an amphipathic property due to the presence of both lipophilic and hydrophilic groups [6]. Colistin exhibits basic properties (acid dissociation constant [p*K*a] of about 10) due to the unmasked γ-amino groups of the five L-α,γ-diaminobutyric acid (Dab) residues present in the cyclopeptide ring and tripeptide moiety (Fig. 1) [7]. Therefore, colistin is polycationic at pH 7.4 [8].

Colistin is administered parenterally as a prodrug, CMS. CMS differs from colistin by additional sulfomethyl groups on each of the five Dab residues (Fig. 1). In vivo, CMS undergoes hydrolysis to form a mixture of partially sulfomethylated derivatives that can eventually convert to colistin [9]. CMS A and B molecular weights are higher than for colistin (1635 and 1621 g/mol, respectively) due to the five additional sulfomethyl groups. CMS is more hydrophilic ($\log P = -12.1$ [10]), and is supposed to be less basic than colistin, but to our knowledge its p*K*a has not been reported yet [11, 12]. At a physiological pH of 7.4, CMS is a polyanion [1].

CMS and colistin were shown to aggregate into micelles at high concentrations in aqueous solution: their critical micelle concentrations (CMCs) were 3.5 mmol/L (5.7 g/L) and 1.5 mmol/L (1.8 g/L), respectively [13]. The conversion of CMS into colistin was much faster when the concentration of CMS was below the CMC (60% over 48 h) than when it was above the CMC (1% over 48 h) [13]. The instability of CMS at low concentrations in pharmaceutical formulations is of concern, particularly because active colistin is much more toxic than CMS [14].

4 Bioanalysis

It is important that bioanalytical methods discriminate between colistin and CMS. Yet in old studies (overall before the start of the twenty-first century), colistin concentrations were measured by microbiological assays that could not discriminate between the two components because CMS was converted into colistin during the experimental time-course. By contrast, recent methods use high-performance liquid chromatography (HPLC) or liquid chromatography–tandem mass spectrometry (LC–MS/MS) that separate CMS and colistin. Colistin concentrations are generally calculated by summing the peak areas of the major components, i.e. colistin A and B. The internal standard is generally polymyxin B [15]. The measurement of CMS concentrations implies a two-step method with firstly the quantitation of colistin alone and secondly the hydrolysis of CMS into colistin by sulphuric acid, and the quantitation of the total colistin formed [15, 16]. CMS concentration is then obtained by subtracting the concentration of colistin measured before hydrolysis to that measured after hydrolysis. This method does not allow the discrimination of the different sulfomethyl derivatives and therefore the reported CMS concentrations should be interpreted as the summed concentrations of all these derivatives. Therefore, the reported pharmacokinetic parameters for CMS may best be considered as hybrid parameters for CMS and partially sulfomethylated derivatives [17].

For measuring plasma concentration, sample preparation can include a simple protein precipitation using trichloroacetic acid and methanol [18–21] and/or a solid-phase extraction [15, 18–21]. After separation by chromatography, detection is carried out either by LC–MS/MS [15, 21] or fluorimetry after derivatisation of colistin [18, 19]. The reported limits of quantification for colistin concentration in plasma are 0.03–0.04 mg/L with LC–MS/MS [15, 21] and 0.1–0.3 mg/L by HPLC-fluorimetry [18, 19]. It is of note that for measuring colistin concentrations in broth culture medium, urine, broncho-alveolar liquid and other biological fluids (cerebrospinal fluid [CSF], peritoneal, etc.) it has been recommended to spike the samples with blank plasma in order to avoid matrix effect and colistin binding to experimental materials [15, 21, 22].

5 Mechanism of Action

Most investigations on the mechanisms of action of polymyxins were carried out with polymyxin B, but the similarities between the chemical structures of polymyxin B and colistin suggest that their mechanisms of action are identical [23]. The lipopolysaccharide (LPS) present at the surface of the outer membrane of GNB prevents the penetration of hydrophobic and/or large antibiotics (antibacterials) [24]. Due to its positive charge, colistin interacts electrostatically with the negatively charged outer membrane of GNB and competitively displaces calcium (Ca^{2+}) and magnesium (Mg^{2+}) ions from the phosphate groups of LPS [7, 25]. Binding of colistin on the outer membrane is antagonised by divalent cations [26–28], resulting in a decreased antibacterial activity. It is of note that CMS, which differs from colistin by the addition of sulfomethyl groups masking the amines responsible for the positive charge, has a very weak antibacterial activity. Moreover, as the outer leaflet of mammalian cell membranes is charged neutral at physiological pH, colistin interacts less with mammalian cells [29]. Destabilisation of LPS leads to the disruption of the outer membrane, the loss of periplasmic and cytoplasmic contents and eventually bacterial death [24, 25, 30].

The endotoxin of GNB consists of the lipid A portion of the LPS, which can be shed by bacteria during antimicrobial therapy and can be responsible for endotoxic shock [31]. Colistin has an anti-endotoxin activity by binding to and neutralising the LPS [31–35].

Colistin also acts by several other mechanisms [36], such as an inhibition of vital respiratory enzymes (nicotinamide adenine dinucleotide [NADH]-quinone oxidoreductase) in the bacterial inner membrane [37].

6 Minimum Inhibitory Concentration Determination

For the European Committee on Antimicrobial Susceptibility Testing (EUCAST) and the Clinical and Laboratory Standards Institute (CLSI), the reference method for minimum inhibitory concentration (MIC) determination of Enterobacteriaceae, *P. aeruginosa* and *Acinetobacter* spp. is the ISO (International Organization for Standardization)-standard broth microdilution [38, 39]. Cation-adjusted Mueller-Hinton broth (CAMHB) is used as the broth medium, with no additives included (in particular no polysorbate-80 or surfactants), the tray must be of plain polystyrene and not treated before use, and sulfate salt of colistin must be used [38, 39]. Addition of polysorbate-80 reduces the adsorption of colistin to polystyrene wells (see Sect. 12.1.1), but is currently not recommended by EUCAST and CLSI [40, 41]. The disc diffusion method should be avoided because colistin poorly diffuses in agar [42]. Moreover, the E-test method should be used with caution because about 50% of the results were reported to

be false when compared with the results of the broth microdilution method [41, 43].

7 Antibacterial Activity

Susceptibility breakpoints for colistin published by EUCAST are 2 mg/L for *P. aeruginosa*, *Acinetobacter* spp. and Enterobacteriaceae [44]. For now, the susceptibility breakpoint published by CLSI is 2 mg/L for both *P. aeruginosa* and *Acinetobacter* spp. (resistance if MIC $\geq$8 and 4 mg/L, respectively) [38], but this breakpoint should be revised in 2017.

Colistin is active against several GNB including *Acinetobacter* spp., *P. aeruginosa*, *Klebsiella* spp., *Enterobacter* spp., *Escherichia coli*, *Salmonella* spp., *Shigella* spp., *Yersinia* spp. and *Citrobacter* spp. [40, 45]. By contrast, colistin is inactive on Gram-positive bacteria, anaerobes and some GNB (*Proteus* spp., *Providencia* spp., *Morganella morganii*, *Serratia* spp. and *Burkholderia cepacia*) [40, 45].

8 Resistance

Increasing use of colistin has led to the emergence of colistin resistance worldwide and although resistance to colistin is generally less than 10%, colistin resistance rates are continually increasing [24]. Resistance to colistin has been described in many GNB species such as *A. baumannii*, *K. pneumoniae* and *P. aeruginosa* [24, 46].

Colistin resistance in GNB is most commonly related to LPS modifications via diverse routes, of which several involve two-component regulatory systems (TCSs) [24]. PhoPQ and PmrAB are two TCSs whose functions and regulations overlap [47]. PhoPQ and PmrAB both include a sensor kinase (PhoQ and PmrB, respectively), which senses environmental signals such as low Mg^{2+}, low pH or the presence of antimicrobial peptides. Moreover, exposure to colistin might also change the expression patterns of these TCSs [48, 49]. Activation of these sensor kinases lead to the phosphorylation of a response regulator (PhoP and PmrA, respectively), which, once phosphorylated, typically enhances their binding to promoters of regulated genes. Hence, phosphorylation of PhoP enhances the transcription of several genes, including *pmr*D, whose product binds to and stabilises PmrA in its phosphorylated state. Phosphorylation of PmrA upregulates the transcription of enzymes that are required for the addition of 4-aminoarabinose (L-ara4N) and/or ethanolamine to the lipid A component of LPS [6, 49–51]. These additions contribute to colistin resistance by reducing the negative charge of the bacterial membrane, and thereby decreasing the binding of positively charged colistin [50, 52, 53]. These adaptive mechanisms of resistance were generally of moderate level [52].

Recently, a plasmid-mediated colistin resistance mechanism MCR-1 was described for an *E. coli* strain in animals and human [54]. MCR-1 is a member of the phosphoethanolamine transferase enzyme family, with expression resulting in the addition of an ethanolamine moiety to the lipid A. Despite its relatively low level (MICs about 4–8 mg/L), this plasmid-mediated mechanism of resistance causes concern about a possible spread of colistin resistance into a range of enteric bacteria in humans and animals [55].

The phenomenon of colistin heteroresistance due to mutations in the chromosomal genes, involved in mechanisms such as lipid A biosynthesis (*lpxA*, *lpxC*, *lpxD*) or addition of L-ara4N, have also been described in *A. baumannii* and *P. aeruginosa* [53, 56–58]. This mechanism of resistance was shown to be of high level (MIC >128 mg/L) and was associated with a fitness cost for the bacteria [53, 56, 58]. Mutant strains were stable but in some patients the original susceptible isolate was able to re-emerge [53]. The reasons of this re-emergence were unclear, and could be due to the presence of a dormant persister population [59] or to the bacterial presence in locations inaccessible to colistin. Moreover, resistance was lost in one patient via the acquisition of a secondary mutation, which compensated for the fitness cost of drug resistance [53].

9 Clinical Pharmacokinetics

9.1 Plasma Concentrations in Healthy Volunteers

After a 1 h intravenous (IV) infusion of 1 MIU of CMS to healthy volunteers the CMS plasma concentrations reached a mean maximal value of 4.8 mg/L at the end of administration [60]. Thereafter, CMS concentrations declined biexponentially with a distribution half-life ($t_{½\alpha}$) of 0.5 h and a terminal half-life ($t_{½\beta}$) of 2.0 h (Fig. 2).

The time to maximal plasma concentrations (C_{max}) of the active compound colistin was 2 h after the start of the infusion (1 h after the infusion stop), and the mean colistin C_{max} was 0.83 mg/L. Colistin plasma concentrations declined monoexponentially with a $t_{½\beta}$ of 3.0 h. It is of note that as the $t_{½\beta}$ of colistin was longer than that of CMS, meaning that colistin elimination is not rate-limited by its formation.

9.2 Clearance and Metabolism

CMS was two-thirds cleared by renal excretion in healthy volunteers [60]. The renal clearance of CMS in healthy volunteers was about 100 mL/min, which was close to the

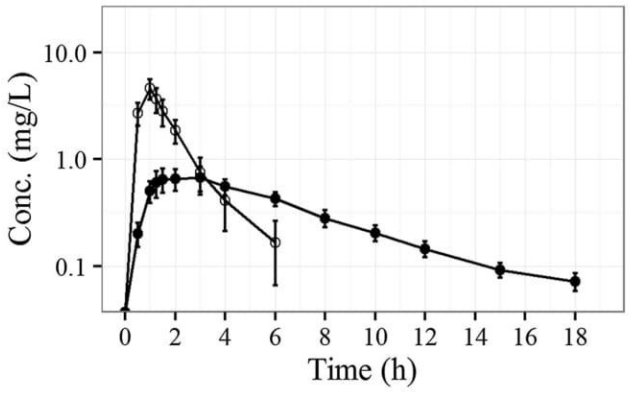

Fig. 2 Colistin methanesulfonate (*open circles*) and colistin (*filled circles*) mean (±standard deviation) plasma concentrations observed in 12 healthy volunteers after a single 1 h infusion of colistin methanesulfonate 1 MIU (million international units) (data from Couet et al. [60]). *Conc.* concentrations

glomerular filtration rate (GFR; around 120 mL/min) [60]. However, as the unbound fraction (f_u) of CMS in plasma is unknown, tubular reabsorption and secretion of CMS were not able to be estimated.

The non-renal clearance of CMS in healthy volunteers was about 50 mL/min [60]. One of the non-renal pathways for CMS clearance is its conversion into colistin by hydrolysis and removal of the five sulfomethyl groups from Dab residues. This hydrolysis leads to the formation of a series of different sulfomethylated derivatives ($2^5 = 32$ possible different derivatives) and to colistin. Other non-renal pathways, such as hydrolysis of peptide bonds, are possible for CMS but have not yet been assessed (Fig. 3).

The colistin average concentration at steady state ($C_{ss,avg}$) depends on both the fraction of CMS that is converted into colistin and the colistin clearance (adapted from Couet et al. [61]) (Eq. 1):

$$C_{ss,avg} = \frac{CL_{conv}}{CL_R + CL_{NR}} \times \frac{Dose}{\tau \times CL_{coli}}, \quad (1)$$

where CL_{conv} is the conversion clearance of CMS into colistin, CL_R is the renal clearance of CMS, CL_{NR} is the non-renal clearance of CMS (=CL_{conv} + clearance due to other non-renal pathways), τ is the dosing interval and CL_{coli} is the total clearance of colistin. As the fraction of CMS eventually converted into colistin is unknown, clearance and volume of distribution parameters for colistin are apparent parameters.

Colistin renal clearance was very low in healthy volunteers (1.9 mL/min) due to extensive tubular reabsorption [60]. The renal reabsorption of colistin may involve organic cation transporters (OCTN1), peptide transporters (PEPT2) and megalin, which is a low-density lipoprotein receptor. The renal reabsorption process is sensitive to the pH of urine [62–64]. Although renal excretion of colistin is very low, urine concentrations of colistin after administration of CMS can be high because of post-excretion hydrolysis of CMS into colistin within the urinary tract.

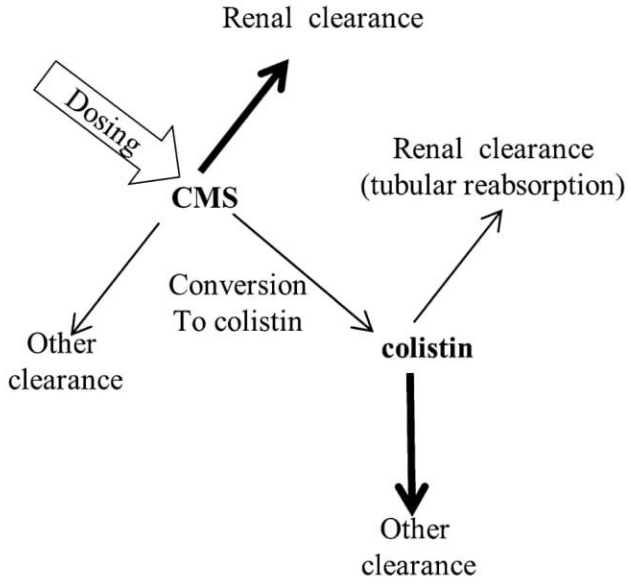

Fig. 3 Overview of the elimination pathways for colistin methanesulfonate and colistin. The *thickness* of the *arrows* indicates the relative magnitude of the respective clearance pathways when kidney function is normal. Colistin methanesulfonate includes fully and partially sulfomethylated derivatives of colistin (adapted from Nation et al. [23]). *CMS* colistin methanesulfonate

Elimination pathways of colistin are for the most part unknown. Considering its peptidic structure, colistin should be eliminated through hydrolysis but the enzymes involved and their localisation are still unknown. Blood, liver and kidneys are likely important sites for colistin elimination because they contain large amounts of proteases and peptidases; however, due to the ubiquitous availability of these enzymes throughout the body, proteolytic degradation of colistin should not be limited to classic elimination organs [65]. It is of note that the cyclic structure of colistin helps to protect colistin from proteolytic endopeptidases and the hydrophobic acyl chain helps to protect against exopeptidases, thus explaining that the colistin half-life ($t_{½}$) is longer than that of many peptides [65].

9.3 Distribution After Systemic Administration

Due to their large molecular weights and electric charge (polyanionic for CMS and polycationic for colistin) at physiologic pH, CMS and colistin cross cellular membranes and physiological barriers poorly. Indeed, volumes of distribution of CMS and colistin in healthy volunteers (14.0 and 12.4 L, respectively, apparent volume for colistin) have been shown to be consistent with a distribution restricted to the extracellular space [60].

9.3.1 Protein Binding

Colistin has been reported to bind to α-1-acid glycoprotein (AGP), whereas the binding to other plasma components such as albumin, lipoproteins or globulins remains to be elucidated [66]. Colistin is a large molecule that cannot enter the cavity of AGP to form a tight complex and instead a two-step process of binding has been proposed [66]. An initial electrostatic attraction occurs between the positive Dab residues of colistin and the negative sialyloligosaccharides proximal to the binding cavity of AGP. The second step consists of a stabilisation of the liaison by insertion of the lipophilic tail of colistin into the hydrophobic ligand binding cavity of AGP and/or binding to lipidic substances, such as phospholipid, bound to AGP. Therefore, both the positive charge and the amphipathic properties of colistin seem necessary for its binding to AGP in plasma. The importance of the charge is exemplified by the fact that CMS, for which Dab moieties are masked, does not bind to AGP [66]. It has been shown that colistin binds to AGP with less affinity than for bacterial LPS, thus suggesting that in vivo the affinity for LPS is strong enough to dissociate and sequester the colistin from AGP [66].

Protein binding can be determined either by ultrafiltration or equilibrium dialysis [67]. However, the extensive non-specific binding (>99%) of colistin to commonly used membranes [68] requires these experiments to be implemented with specific dialysis cells and membranes [67]. The assessment of colistin protein binding using a microdialysis method raises the same problem of colistin adhesion to experimental equipment [69].

In animals, plasma protein binding of 55% ($f_u = 45\%$) has been reported for colistin in rats, dogs and calves [68, 70]. In mice, the average percentage bound was around 91% ($f_u = 9\%$) in the total concentration range of 2–50 mg/L [67].

In critically ill patients, colistin binding to plasma components was about 59–74% [71]. Across the 0.01–15 mg/L range of total concentrations, at 37 °C, the bound fraction of colistin B was constant (average 57%), whereas the bound fraction of colistin A was dependent on the concentration. At 0.1 mg/L the average binding of colistin A was 84% against 69% at 10 mg/L, meaning that the f_u of colistin A varied greatly as a function of the concentration (average 16% at 0.1 mg/L and 31% at 10 mg/L). This greater binding of colistin A, also demonstrated in rats [68], is most probably due to its longer fatty acid chain, since it is the only difference with colistin B. Whereas there is a difference in protein binding between colistin A and colistin B, to our knowledge, no difference in potency has been reported.

The level of plasma AGP can increase, depending on the disease condition, particularly bacterial infection [72]. Therefore, protein binding of colistin is expected to be higher in critically ill patients than in healthy volunteers. This has not been reported yet; however, protein binding of colistin was greater in infected mice than in healthy mice [66]. Moreover, protein binding of polymyxin B, which is chemically close to colistin, is greater in critically ill patients than in healthy volunteers [73].

In airways, colistin binds to mucin, which may reduce its antibacterial efficacy as illustrated by the >100-fold increase of MICs when mucin is added to growth medium [74].

9.3.2 Distribution Within Lung

Concentrations of CMS and colistin in epithelial lining fluid (ELF) are generally determined from concentrations measured in bronchoalveolar lavage (BAL) fluid after correction for dilution. The dilution factor is estimated based on the assumption that urea concentration is identical in plasma and ELF, by measurement of urea concentrations in plasma and BAL [22]. The determination of colistin concentration in BAL fluid should take into account the non-specific binding to the BAL material, which can be particularly high at low concentrations (80% for colistin concentrations <1 mg/L; unpublished data).

Intravenous (IV) Administration After repeated IV administrations of 2 MIU CMS every 8 h to critically ill patients, Imberti et al. [75] could not measure colistin in BAL (limit of quantification = 0.1 mg/L). By contrast, Boisson et al. [76] reported colistin concentrations in the ELF at steady state ranging between 0.1 and 29 mg/L. For their part, Yapa et al. [77] reported colistin concentrations in sputum lower than 1 mg/L after a single IV administration of CMS 5 MIU. No active transport has been reported yet for the passage of the pulmonary barrier by colistin. However, OCTN1 and PEPT2, which are involved in the renal reabsorption of colistin, are also present in the lung [78]. Moreover, the involvement of these proteins in the pulmonary transport of active substances has already been suggested: the uptake of anti-cholinergic drugs for OCTN [79] and transport of bacterial peptides for PEPT2 [80]. In addition to their capability to pass through pulmonary barrier, CMS and colistin distribution into lung also depends on their binding to lung components. This issue is not yet elucidated but it has been shown that colistin binds to mucin [74].

Inhalation Aerosolised colistin, administered as CMS, is used to treat nosocomial pneumonia caused by MDR GNB [76, 80–84]. After pulmonary administration of CMS, the presence of colistin in plasma can either result from the absorption of CMS followed by systemic conversion into colistin or from the pre-systemic conversion of CMS into colistin followed by its absorption [22]. When nebulised

directly as colistin, the absolute bioavailability was shown to be high (69%) in rats [85]. However, after nebulisation of CMS to critically ill or cystic fibrosis (CF) patients, colistin plasma concentrations were either below the limit of quantification [77] or low (<0.73 mg/L) [76, 86], except for one study for which concentrations up to 2 mg/L were reported [87]. In critically ill patients, when nebulised as CMS, only 9% of the dose reached the systemic circulation: 1.4% as colistin converted presystemically and 7.6% as CMS [76].

After aerosol delivery of CMS to critically ill patients ELF colistin concentrations were much higher than those in plasma (5- to 1000-fold) but varied considerably, from 1 to 1100 mg/L, depending on dose (1 or 2 MIU single dose or every 8 h), time (1–8 h post-dose) and the study [76, 87].

In CF patients, CMS and colistin concentrations are generally determined in sputum. In these patients, after nebulisation of single 2 or 4 MIU doses of CMS, systemic exposure to colistin was very low, whereas colistin concentrations measured in sputum ranged from 1 to 45 mg/L [77, 86]. However, a conversion of CMS to colistin during the preparation of sputum samples before bioanalytical assay cannot be ruled out in one of these studies, due to a relatively high concentration of trifluoroacetic acid used for sample preparation [86].

Overall, these studies show that colistin systemic exposure is low after CMS nebulisation, whereas colistin concentrations in lung are high.

9.3.3 Distribution Within the Central Nervous System

IV Administration The passage across the blood–brain barrier (BBB) by CMS and colistin is limited. Colistin penetration into the CSF after repeated IV administrations of CMS was demonstrated to be low (5%) in critically ill patients [88]. The presence of meningeal inflammation enhanced penetration in CSF (11%) [89]. In paediatric patients the CSF/serum ratios were reported to be 34–67% in the presence of meningitis (measurement before and after IV CMS administration), whereas it was minimal in the absence of meningeal inflammation [90]. Moreover, it has been shown in mice that LPS can induce BBB disruption by decreasing the tight junction function; this effect depends on the bacterial species and can increase colistin uptake into the brain [91]. For now, the effect of transporters on the passage of BBB by CMS or colistin has not been reported.

Intrathecal–Intraventricular Administrations Colistin concentrations in CSF are higher when patients are treated by intraventricular or intrathecal CMS administration than when they are treated intravenously. Imberti et al. [92] reported CSF concentrations continuously above 2 mg/L if the intraventricular CMS dose was greater than 0.06 MIU every 24 h. Ziaka et al. [89] reported CSF concentrations ranging between 0.6 and 1.5 mg/L when patients were treated with combined IV CMS 3 MIU every 8 h and intraventricular CMS 0.125 MIU every 24 h.

9.3.4 Distribution in Peritoneal Fluid

In one case report, after multiple administrations of CMS 2 MIU every 8 h, colistin distributed slowly into the peritoneal fluid of a patient with severe peritonitis, but colistin concentrations in peritoneal fluid were close to that in plasma at steady state [93].

9.4 Oral Route of Administration

Colistin absorption from the gastrointestinal tract is slight or absent [94]. In simulated gastric fluid it has been shown that colistin was rapidly degraded by rupture of peptide bonds in the tail tripeptide moiety under the action of pepsin [4], the formed metabolites keeping an antimicrobial activity. Colistin sulfate is sometimes used for perioperative decontamination of the digestive tract, particularly for the suppression of extended-spectrum β-lactamase-producing Enterobacteriaceae (ESBL-E). In this indication, colistin sulfate is generally administered orally following a dosing regimen of 100 mg every 6 h, in combination with other anti-infective agents (e.g., amphotericin B, tobramycin) [94–99]. However, this practice has been shown to select colistin-resistant bacteria and its use is controversial [99–103].

9.5 Pharmacokinetics in Special Populations

9.5.1 Pharmacokinetics in Critically Ill Patients

Maintenance Dose After IV administration of CMS to critically ill patients, the pharmacokinetics of CMS was very variable (Fig. 4). The C_{max} values were observed at the end of infusion; thereafter, CMS concentrations decreased in a mono- or bi-exponential manner, with a mean $t_{½β}$ ranging from 1.9 to 4.5 h depending on the study [103–106]. The mean plasma profile was comparable to that observed in healthy volunteers, except when the renal function of the patient was altered. Indeed, concentrations of colistin are related to the renal clearance of CMS (Eq. 1), which correlates with creatinine clearance [104, 105]. For illustration, for patients with creatinine clearance values of 120, 50 and 25 mL/min, the typical renal clearances of CMS were about 100, 50 and 25 mL/min, respectively. The main impact of this decrease of CMS renal clearance when the renal function was impaired was that the fraction of CMS converted into colistin increased, e.g. 33, 50 and 67% for the three different values

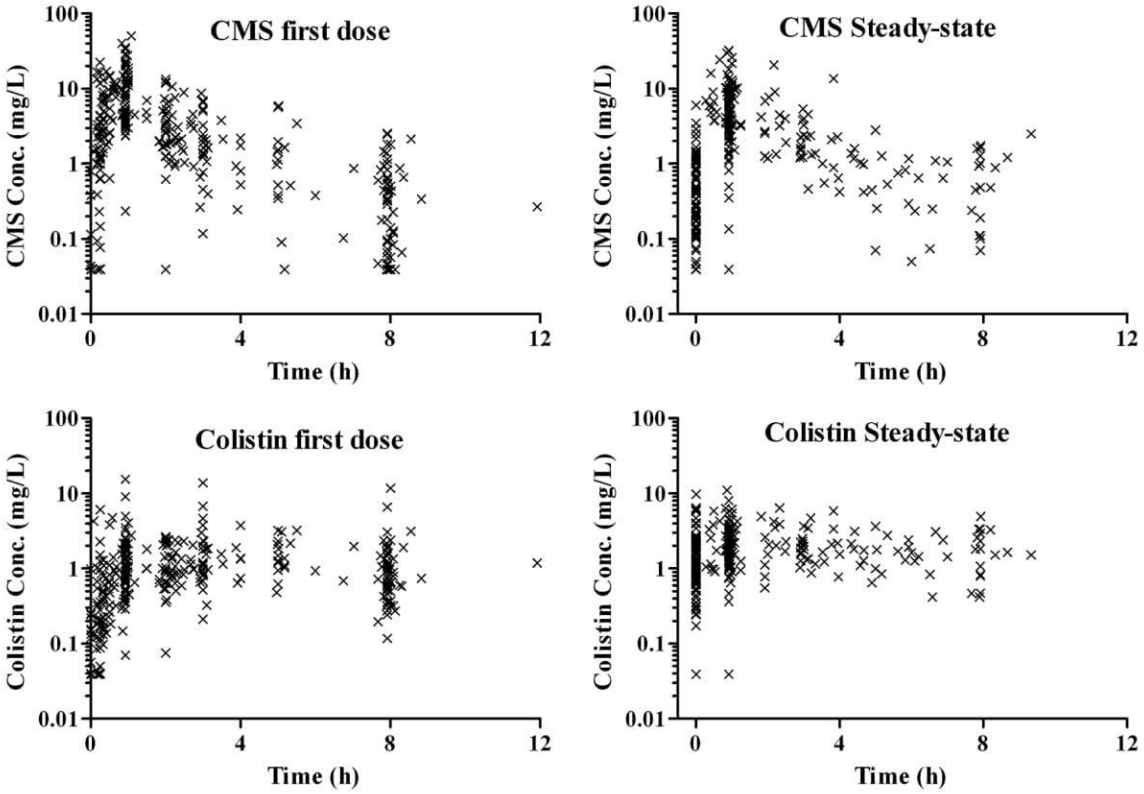

Fig. 4 Colistin methanesulfonate and colistin plasma concentrations observed (×) in 73 critically ill patients after first colistin methanesulfonate dose and at steady state. Reproduced from Grégoire et al. [105] with permission of the American Society of Microbiology. *CMS* colistin methanesulfonate, *Conc*. concentrations

of creatinine clearance of 120, 50 and 25 mL/min, thus resulting in greater colistin concentrations for patients with altered renal function. Moreover, the volume of distribution of CMS was shown to be proportional to the body weight, which after a single dose impacts on the C_{max} of CMS and colistin (to a lesser extent) and after repeated administrations impacts on the fluctuation of concentrations, i.e. the larger the volume of distribution is, the lower the concentrations fluctuate [104, 105]. However, even when considering individual renal function and body weight, the pharmacokinetics of CMS were very variable between patients after IV administration of CMS [104, 105].

Concerning the pharmacokinetics of colistin after administration of CMS to critically ill patients, some discrepancies were observed between studies. Indeed, after a first dose of 2 MIU of CMS, Grégoire et al. [105] observed typical colistin C_{max} values of about 2 mg/L, whereas after a first dose of 3 MIU of CMS Plachouras et al. [106] observed a colistin C_{max} of 0.6 mg/L [106] (Fig. 5). Moreover, the C_{max} values were reached sooner for Grégoire et al. [105] (about 3 h) than for Plachouras et al. [106] (maximum not reached at next administration, i.e. 8 h). These different time to C_{max} values were related to greater apparent volumes of distribution, resulting in longer

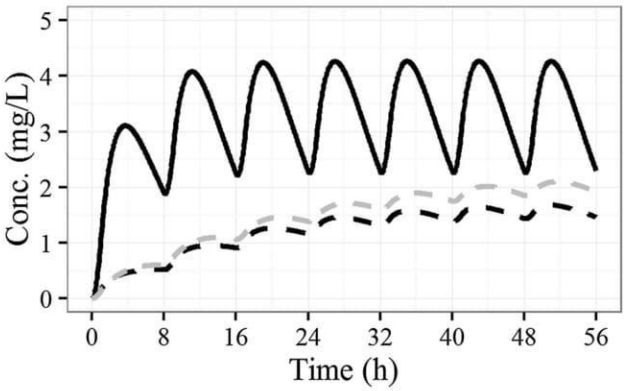

Fig. 5 Colistin concentrations following a 3 MIU (million international units) dose of colistin methanesulfonate infused over 60 min every 8 h in a critically ill patient with a creatinine clearance of 82 mL/min and a body weight of 80 kg, predicted from Grégoire et al. [105] (*solid black line*), Plachouras et al. [106] (*dashed grey line*) and Garonzik et al. [104] (*dashed black line*). Reproduced from Grégoire et al. [105] with permission of the American Society of Microbiology. *Conc*. concentrations

typical $t_{½}$ values for colistin (9–14 vs. 3 h) [103–106]. One major consequence of a longer $t_{½}$is that from Plachouras et al. [106] at least 48 h is necessary to reach steady state, whereas from Grégoire et al. [105] steady state should be reached after as soon as 12 h. At steady state there were

fewer discrepancies between studies: for a patient with a clearance of creatinine of 82 mL/min, treated with CMS 3 MIU every 8 h, the typical colistin $C_{ss,avg}$ was predicted to be between 1.5 and 3.5 mg/L depending on the study (Fig. 5) [103–106]. Plachouras et al. [106] were the first to point out the difficulties in attaining a $C_{ss,avg}$ of 2 mg/L for patients with a creatinine clearance ≥80 mL/min [106]. Recently, Nation et al. [107] suggested the use of an algorithm to calculate the CMS dose to administer according to the creatinine clearance, and demonstrated that less than 40% of the patients with creatinine clearance above 80 mL/min attained a $C_{ss,avg}$ >2 mg/L, even with a maximal 12 MIU daily dose.

Loading Dose Plachouras et al. [106] suggested that administration of a loading dose is necessary to achieve effective colistin concentrations as soon as the first CMS administration; two subsequent studies have assessed this suggestion [71, 108]. In the first study, after administration of 6 MIU of CMS to ten critically ill patients, colistin C_{max} values were on average 1.3 mg/L (range 0.3–2.6 mg/L) at 8 h following dosing and the mean colistin $t_{½}$ was 18.5 h [71]. In the second study, following administration of a 9 MIU loading dose to 19 critically ill patients the C_{max} values of colistin were also very variable (mean 2.65 mg/L, range 0.9–5.1 mg/L) and the mean colistin $t_{½}$ was 11.2 h [108]. Colistin concentrations observed in this latter study were therefore higher than expected from previous studies performed by the same team [71, 106] but lower than those predicted by Grégoire et al. [105]. Overall, these discrepancies of colistin pharmacokinetics between studies were attributed either to (1) a higher proportion of the A and B forms in the more recent CMS formulations [108]; (2) the use of different CMS brands; (3) the inclusion of patients with different renal function; (4) CMS solutions for infusions at concentrations below or above the CMCs of 5.7 g/L (71,250 IU/mL); (5) in vitro conversion of CMS to colistin after blood collection [109]; or (6) potential discrepancies in the analytical methods (e.g. in the quantification of partly sulfomethylated compounds and potential hydrolysis during work-up) [108].

Dosing Suggestions Considering the pharmacokinetics of both CMS and colistin, the CMS dose has to be adapted to each patient's renal function. In case of normal renal function, all of the previous cited studies recommend a maintenance dose of 9 MIU of CMS per day in two or three injections [105, 106], which corresponds to the calculated maintenance dose suggested by the algorithm of Garonzik et al. [104]. It is of note that the most recent publications all agree that CMS should be administered twice daily [105–108]. The maintenance dose should be adapted to the renal function of the patient. The European Medicines Agency (EMA) suggests that for patients with a creatinine clearance above 50 mL/min the daily dose should be 9 MIU (up to 12 MIU in some cases, for patients with good renal function), for patients with a creatinine clearance between 30 and 50 mL/min the daily dose should be between 5.5 and 7.5 MIU, and for patients with a creatinine clearance between 10 and 30 mL/min the daily dose should be 5 MIU [110, 111].

Concerning the loading dose, Garonzik et al. [104] suggest it should be adapted to the patient's body weight without exceeding 10 MIU, whatever their renal function, and to begin maintenance doses 24 h later. Karaiskos et al. [108] demonstrated that a loading dose of 9 MIU followed by the beginning of a maintenance dose 24 h later was safe for their 19 critically ill patients with normal renal function. The Committee for Medicinal Products for Human Use (CHMP) of the EMA proposed a loading dose of 9 MIU for patients above 60 kg and 6 MIU for patients below 60 kg; doses up to 12 MIU may be required for patients but the clinical experience with such doses is limited [110]. The loading dose should apply to all patients regardless of renal function. Recently, it was suggested that the first maintenance dose be administered 12 h after the loading dose [107].

9.5.2 Pharmacokinetics in Patients with Haemodialysis

In patients with highly impaired renal function, CMS is poorly excreted in urine and therefore the fraction of dose available for conversion to colistin is higher. As a consequence, on days without a haemodialysis session, colistin exposure was threefold greater in critically ill patients requiring haemodialysis than in patients with preserved renal function and treated with the same dosage [112].

Considering their molecular weights, CMS and colistin fractions unbound in plasma can freely pass through dialysis membranes. Moreover, colistin might also adsorb on dialysis membranes, notably those used for continuous renal replacement therapy, which could contribute to the removal mechanism [113]. Indeed, during intermittent haemodialysis sessions, CMS and colistin are efficiently cleared [104, 113–116]. Mean clearance of CMS during haemodialysis session was reported to be between 71 and 95 mL/min [104, 114, 116], and associated estimation of inter-individual variability was sometimes low (26% coefficient of variation) [114] but sometimes high (96%) [104]. Mean clearance of colistin during haemodialysis session was reported to be between 57 and 134 mL/min [104, 114, 116]; inter-individual variability was estimated to be moderate (15 and 44%) [104, 114].

Dosing Suggestions for Intermittent Renal Replacement Therapy Previous data suggested that during a non-haemodialysis day, the CMS daily dose should not exceed 3 MIU [104, 112], but recently Nation et al. [107] suggested administration of 3.95 MIU per day to achieve the

average steady-state colistin concentration of 2 mg/L. During a haemodialysis day, it is suggested that a supplemental dose be administered at the end of the haemodialysis session (30–50% of the daily dose) [104]. In each study, CMS was administered twice daily [104, 107, 112].

During continuous venovenous haemofiltration (CVVH) Garonzik et al. [104] reported mean CMS and colistin removal clearances slightly lower than those measured during intermittent haemodialysis (64 vs. 95 mL/min and 34 vs. 57 mL/min for CMS and colistin, respectively). During continuous venovenous haemodiafiltration (CVVHDF) Markou et al. [117] reported that extracorporeal clearance contributed to about 50% of total colistin clearance; however, the total colistin clearance was lower than that in patients with normal renal function, suggesting that a dose reduction may be needed in critically ill patients with CVVHDF. By contrast, Karvanen et al. [118] reported that colistin concentrations obtained under CVVHDF and receiving 2 MIU CMS every 8 h were lower than those for corresponding patients without CVVHDF, and consequently that CMS dosage should not be reduced for patients undergoing CVVHDF. More strongly, Karaiskos et al. [119] recommended an increased dose for patients under CVVH with a loading dose of 12 MIU of CMS followed by 13–15 MIU daily maintenance doses.

Dosing Suggestions for Patients Under Continuous Venovenous Haemofiltration The last recommendations published by Nation et al. [107] correspond with those published by Karaiskos et al. [119] and suggest a maintenance dose of 13 MIU daily divided into two doses. Concerning the loading dose, even if a loading dose of 12 MIU has been found more appropriate, clinical data of safety are limited and it is recommended not to exceed 9 MIU [107, 119]. Considering the large inter-individual variability, therapeutic drug monitoring (TDM) is advised for patients undergoing CVVHDF [120].

9.5.3 Pharmacokinetics in Cystic Fibrosis (CF) Patients

The pharmacokinetics of colistin in CF patients have been described after IV administration [77, 121] and after nebulisation of CMS. Following IV infusion of CMS, plasmatic pharmacokinetics for CMS were consistent between studies [77, 121] and with healthy volunteers [60], i.e. the reported values for clearance were about 100 mL/min, volume of distribution about 18 L and $t_{½}$ about 2.5 h. Colistin pharmacokinetics in plasma after infusion of CMS were also characterised by a $t_{½}$ close to that in healthy volunteers (4–7 h) [77, 121]. However, it should be noted that after a single IV infusion with the same CMS brand (Colimycin®), colistin (the active compound) exposure was 39% lower in CF patients than in healthy volunteers, suggesting that colistin clearance could be higher in CF patients [122].

After single nebulisation of CMS 2 or 4 MIU to CF patients, Yapa et al. [77] reported CMS and colistin concentrations in sputum that were higher (C_{max} for colistin in sputum ranging from 2.09 to 21.2 mg/L) than those resulting from IV administration ($C_{max} < 1.0$ mg/L) [77]. Moreover, the systemic availability of CMS was low (about 6%) and systemic exposures to CMS and colistin were minimal. Ratjen et al. [86] reported colistin concentrations that were significantly higher (mean C_{max} about 40 mg/L) than those reported by Yapa et al. [77] in sputum following nebulisation of a single dose of 2 MIU of CMS, but their bioanalytical method for quantitating colistin might have promoted the conversion of CMS into colistin and thus overestimate colistin concentrations in sputum.

Dosing Suggestion for CF Patients Local administration of CMS by nebulization with or without IV administration is suggested for this population. CF centres worldwide have adopted different inhaled CMS dosing regimens (dose and dosing interval), with current therapies ranging from 1 MIU of CMS twice daily to 2 MIU of CMS three times daily [122–125].

9.5.4 Pharmacokinetics in Burn Patients

In burn patients, after IV administration of CMS 5 MIU every 12 h, the typical $t_{½}$ of colistin was reported to be 6.6 h [126] and the clearance of colistin was comparable to that of critically ill patients [103–106] and healthy volunteers [60, 127], suggesting that it was not affected by the hypermetabolism in burn patients. The volume of distribution of colistin was slightly greater than that reported in healthy volunteers and either greater [105] or lower [104, 106] than those reported in critically ill patients.

10 Adverse Events

Two main types of toxicity, nephrotoxicity and neurotoxicity, are reported with the use of colistin. However, recent studies have reported that the incidence of nephrotoxicity is less common and severe than that reported in studies and case reports published until 1983 [128]. The observed nephrotoxicity was as high as 50% in old studies versus 15–25% in recent studies, although the definition of nephrotoxicity was not standardised between the studies [128]. However, in a recent study in patients with severe sepsis or septic shock, there was an incidence rate of acute kidney injury (AKI) of 44% following colistin administration [129]. Risk factors for nephrotoxicity include baseline renal impairment, age, severity of illness, nephrotoxic agents, duration of therapy and daily dose by ideal body weight [129, 130]. A residual concentration of colistin >2.42 mg/L was also reported as a predictor for

AKI [131]. In contrast, CF might be protective against the development of nephrotoxicity [130].

Colistin-associated nephrotoxicity usually occurs within the first 5 days of treatment and is reversible upon cessation of treatment [132, 133]. Renal insufficiency generally manifests as a decrease in creatinine clearance but haematuria, proteinuria, cylindruria or oliguria can also occur [128]. The nephrotoxicity of colistin is certainly related to its extensive renal tubular reabsorption due to the numerous transporters located in the proximal tubules, particularly the megalin (see Sect. 9.2) [64, 134]. Colistin toxicity could be due to its accumulation in the endoplasmic reticulum and mitochondria of renal tubular cells, resulting in a modification of the cell fate under oxidative stress [135]. Coadministration of ascorbic acid at a daily dose of 2–4 g in patients with severe sepsis was shown to reduce the AKI risk to four times lower than that in patients who did not receive ascorbic acid [129]. This effect could be explained by a double kidney-protective effect toward both colistin-induced and septic renal damage [129]. However, in another study with moderately ill patients the ascorbic acid did not offer a nephroprotective effect [134].

The incidence of neurotoxicity related to the use of colistin is lower than that of nephrotoxicity [128]. The most frequent neurological adverse effect is paraesthesia, which in old studies was reported to occur in 27 and 7.3% of patients receiving IV and intramuscular CMS, respectively. Other neurological adverse events include mental confusion, vertigo, ataxia and seizure, but the most dreaded complication is neuromuscular blockade presenting as respiratory muscle paralysis and apnoea [128, 136]. Like renal toxicity, neurological toxicity is considered to be dose dependent and is usually reversible after early discontinuation of the treatment [128].

Colistin aerosol therapy is generally well-tolerated, with few reported adverse events such as throat irritation, cough and bronchospasm [137, 138].

Intrathecal/intraventricular administration is also well-tolerated. One of the adverse effects reported is chemical meningitis (5/153 cases reported between 1972 and 2016) with complete resolution after the discontinuation of the intrathecal administrations, and there is no mention of nephrotoxicity [139].

11 Therapeutic Drug Monitoring

Because the pharmacokinetics of colistin is very variable between patients (Fig. 4), and because its therapeutic window is narrow, TDM of colistin is warranted after IV administration [140]. TDM of colistin requires a validated bioanalytical method (see Sect. 4). Because CMS can hydrolyse into colistin after sampling, it is recommended that blood specimens be drawn just before the next dose (trough), i.e. when the CMS concentrations are the lowest, and to handle the samples quickly.

It has been reported that colistin $C_{ss,avg}$ values should be higher than 2 mg/L to be effective [107]. These plasma concentrations of colistin should allow the pharmacokinetic/pharmacodynamic indices to reach target values determined in the mouse thigh infection model (ratio of the area under the unbound concentration–time curve to the MIC [*f*AUC/MIC] of about 12) for bacteria with an MIC lower than 2–4 mg/L [111], which correspond to the EUCAST breakpoint for susceptibility [44]. However, minimum plasma concentrations (C_{min}) of colistin higher than 2.5 mg/L have been associated with an increased risk of nephrotoxicity [131, 141]. Therefore, to be effective and avoid adverse events, $C_{ss,avg}$ should ideally be between 2 and 2.5 mg/L. In practice, the clinically desirable range of $C_{ss,avg}$ is rather from 2 to 4 mg/L [107], but renal function has to be monitored. Because it is preferable to draw the samples just before the next dose and because the fluctuations of plasma concentrations are relatively weak, this therapeutic window can also apply to residual concentrations. CMS dosing regimen has to be individualised according to concomitant medications and to the risk/benefit ratio for each patient.

12 Pharmacodynamics

12.1 In Vitro Pharmacodynamics

12.1.1 Experimental Issues

As the presence of Ca^{2+} and Mg^{2+} ions modifies the susceptibility of bacteria to colistin, their concentration into broth should be controlled and CAMHB is generally used for in vitro pharmacodynamic experiments with colistin [41]. From an experimental point of view, the fraction of colistin bound to CAMHB with initial colistin concentrations of 10 and 30 mg/L was 5% [142]. Therefore, the growth medium seems to not affect unbound concentrations of colistin used for in vitro experiments.

The in vitro determination of bacterial susceptibility to colistin poses numerous experimental problems. Several studies reported potential non-specific binding of colistin to experimental material [142–145]. Karvanen [146] characterised the extent of the colistin loss in different types of laboratory materials during simulated time-kill experiments without bacteria. The type of material and the concentration of colistin were the two main factors contributing to non-specific binding of colistin: out of four tested materials (glass, polypropylene, polystyrene and low protein-binding polypropylene), none performed well enough to enable to

ignore binding to material at concentrations between 0.125 and 8 mg/L. The best performing material was low protein-binding polypropylene with colistin loss between 45 and 10%. The relative loss due to binding increased when the concentration decreased; for instance in CAMHB, when using large polypropylene tubes, at 24 h the measured colistin concentration represented 13 and 62% of the 0 h concentrations of 0.125 and 4 mg/L, respectively. In polystyrene microplates the colistin losses were even larger, e.g. the measured concentration represented 4% of the expected 8 mg/L concentrations [146]. The impact of this non-specific binding on in vitro pharmacodynamic results is unclear. However, it is recommended, when possible, that low protein-binding polypropylene be used and colistin concentrations are measured during the time course of the experiments.

12.1.2 *Pharmacokinetics/Pharmacodynamics of Colistin Alone*

For colistin, in vitro pharmacokinetic/pharmacodynamic studies mainly focused on three Gram-negative pathogens: *P. aeruginosa*, *A. baumannii* and *K. pneumoniae*.

Determination of the pharmacokinetic/pharmacodynamic index that best predicted colistin efficacy on *P. aeruginosa* was performed using a dynamic in vitro pharmacokinetic model. *f*AUC/MIC was shown to be the pharmacokinetic/pharmacodynamic index that most closely correlated with the killing of *P. aeruginosa*, with target values for 2 $\log_{10}$ kill at 24 h of between 27.2 and 41.7 for reference strains (ATCC27853 and PAO1) [147].

In time-kill experiments, with a constant concentration of colistin over time, colistin was shown to be bactericidal on 21 *P. aeruginosa* strains at concentrations higher than 0.5 × MIC, with complete killing happening very quickly and bacteria becoming undetectable 4 h after treatment initiation. At concentrations equal to 0.5 × MIC, a small initial decrease in the concentration of colony forming units (cfu) was observed, followed by regrowth at 24 h [148] (Fig. 6). Time-kill experiments were also performed on the *A. baumannii* ATCC19606 reference strain and on 16 clinical isolates. Similar to what was observed with *P. aeruginosa*, low concentrations of colistin produced an initial decrease in cfu/mL followed by regrowth at 24 h [149]. In time-kill experiments on reference and clinical strains of *K. pneumoniae*, a regrowth was also observed after an initial rapid killing, even at a high colistin concentration (i.e. 64 × MIC) [150].

Dynamic in vitro models allow mimicking of human clinical regimens and evaluation of antimicrobial efficacy at concentrations varying over time. In this way, the efficacy of four different clinical dosing regimens of colistin against *A. baumannii* were compared, but none were able to eradicate the bacterial strain [151].

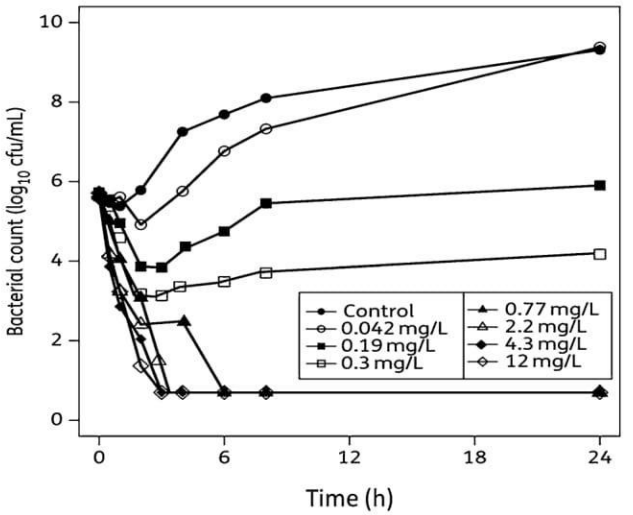

Fig. 6 Typical observed profile from one experiment for static time-kill curves for *Pseudomonas aeruginosa* exposed to colistin. Time-kill curve experiments for wild-type (ATCC27853) *P. aeruginosa* with concentrations ranging between 0.042 and 12 mg/L (minimum inhibitory concentration [MIC] = 1 mg/L). Reproduced from Mohamed et al. [155] with permission of the American Society of Microbiology. *cfu* colony-forming units

Population analysis profiles (PAPs) can be performed during time-kill or dynamic experiments in order to explore the heteroresistance phenomenon, characterised by the presence of several subpopulations of bacteria with different susceptibilities to colistin. A dynamic in vitro pharmacokinetic model was used to compare the efficacy of colistin regimens with 8, 12 or 24 h dosing intervals against *P. aeruginosa* [152]. No difference in bacterial kill was observed between regimens, but PAPs suggested that the 8 h dosing interval minimised the emergence of resistance [152]. PAPs on *A. baumannii* strains showed that 15 of 16 clinical isolates contained a resistant subpopulation, representing a small fraction of bacteria, at the start of the experiment. This so-called 'heteroresistance' was observed even though all strains were classified as colistin sensitive according to their MIC values [149]. Heteroresistance was also observed with reference and clinical *K. pneumoniae* strains, even in strains categorised as colistin sensitive based on their MIC [150].

Semi-Mechanistic Modelling Traditional analysis of pharmacokinetic/pharmacodynamic experiments are mostly qualitative, based on the variations of bacteria counts at a given time. Analysis data with semi-mechanistic mathematical models are useful to quantify the phenomenon observed during time-kill or dynamic experiments, such as bacterial resistance, antimicrobial efficacy or inoculum effect. Moreover, once a model has been developed it can be used to simulate different dosing regimens.

Table 1 Chequerboard results

Drug class	Bacteria species			References
	Klebsiella pneumoniae	*Pseudomonas aeruginosa*	*Acinetobacter baumannii*	
β-Lactam	–	18/125	63/245	[161, 164, 165, 183, 184]
Carbapenem	3/8	1/1	63/124	[156, 158, 161, 167]
Ciprofloxacin	–	14/26	–	[183]
Fosfomycin	–	19/87	–	[157]
Glycopeptide	1/12	0/4	38/111	[157–160, 162, 169, 171, 172, 174]
Linezolid	–	–	6/40	[162]
Daptomycin	–	–	2/2	[170]
Rifampicin	8/8	–	10/45	[158, 172, 184]
Tigecycline	6/8	–	18/95	[158, 166, 184]
Trimethoprim	2/8	0/8	8/8	[174]

Fractions are given as the number of strains with a Fractional Inhibitory Concentration Index (FICI) $\leq$0.5/total number of strains tested

These pharmacokinetic/pharmacodynamic models have to describe the bacterial resistance to colistin. Resistance of *P. aeruginosa* and *A. baumannii* has been modelled either by splitting the bacterial population into several growing subpopulations with different susceptibility to colistin [153, 154], or with one sensitive subpopulation that adapts itself in the presence of colistin and gradually becomes resistant to it, but that can also switch to a non-growing 'persistent' form [155].

Mechanistic models can take into account some other aspects of the colistin mechanism of action, such as the inoculum effect and the competitive binding between cations (i.e. Ca^{2+} and Mg^{2+}) and colistin on the bacterial LPS [153, 154].

These models enable characterisation of the susceptibility of a specific strain to colistin (e.g. concentration of drug producing 50% of maximum effect [EC_{50}] = 1.16 mg/L for *P. aeruginosa* ATCC27853 [155]), the bacterial growth rate (e.g. mean turnover time of 75 min for *A. baumannii* ATCC19606 [154]) or the adaptation development rate (first-order adaptation rate constant of 7.2 h^{-1} for *A. baumannii* ATCC19606 [154]).

Based on a pharmacokinetic/pharmacodynamic model, recommendation of a flat fixed loading dose followed by 8- or 12-hourly maintenance doses with an infusion duration of up to 2 h was made for patients infected with *P. aeruginosa* [155]. In *A. baumannii* infection, these simulations suggested that with current regimens used in the clinical setting, polymyxin B administration was better than colistin administered as CMS because of more rapid target concentration attainment [154].

12.1.3 Pharmacokinetics/Pharmacodynamics of Colistin in Combination

In order to counteract the growing number of colistin-resistant strains, recent studies have shifted from studying colistin monotherapy to studying colistin activity in combination. Multiple methods have been used to evaluate the efficacy of combinations. Chequerboards and E-tests have been used for initial screening but, given the problems encountered with colistin E-tests (see Sect. 12.1.1), results obtained with this method are not covered in this review. Interesting combinations have been more thoroughly studied using time-kill experiments, with data resulting from these experiments being analysed with traditional methods or mathematical modelling.

Chequerboards Chequerboard results reported in the literature are summarised in Table 1. Chequerboard studies were interpreted by calculating the Fractional Inhibitory Concentration Index (FICI). Thresholds for FICI were usually as follows: FICI $\leq$0.5 indicated synergy, FICI between 0.5 and <4 indicated indifference/additivity and FICI $\geq$4 indicated antagonism [23, 155–171].

The most studied species was *A. baumannii* ($n = 670$) and the most tested antibiotic family were β-lactams ($n = 370$). From this review of the literature, the global rate of synergy between colistin and various antibiotics was 29% (280/965). When synergy was not elicited, the different combinations were at least additive or indifferent, except for some very rare cases of antagonism. Therefore, these chequerboard results support the use of colistin in combination, even if no particular antibiotic class seems to be synergistic with colistin.

Time-Kill Experiments In time-kill experiments, combinations were considered synergistic when they led at least to a 2 $\log_{10}$ cfu/mL decrease compared to the most active monotherapy at 24 h.

Colistin was shown to be synergistic with imipenem, doripenem, vancomycin, rifampicin (rifampin), trimethoprim and trimethoprim/sulfamethoxazole against *A. baumannii* strains [167, 171–174]. The addition of sulbactam improved the efficacy of the doripenem–colistin combination [173].

Against *K. pneumoniae* strains, colistin was shown to be synergistic with aztreonam, fosfomycin, meropenem, rifampicin, trimethoprim, trimethoprim/sulfamethoxazole and vancomycin [168, 174]. The same was true for aztreonam, fosfomycin and rifampicin in triple-antibiotic combinations with meropenem and colistin [168].

Colistin was shown to be synergistic with trimethoprim, trimethoprim/sulfamethoxazole and vancomycin against one colistin-resistant strain of *P. aeruginosa* [174].

Traditional time-kill criteria for evaluating synergy (e.g. $\Delta\log_{10}$ cfu/mL at 24 h) have the same limitations as FICI to show a synergy when one of the tested drugs is already effective against the studied strain, because it is hard to improve an already important effect. This could explain why synergy was more often observed against strains that were resistant to one antibiotic of the combination than against sensitive strains. Moreover, time-kill studies found synergistic combinations more often than chequerboards. This could be either because the time-kill experiments are a more powerful tool to demonstrate synergy or because time-kill experiments focused on more resistant strains. Indeed, the number of strains tested by chequerboards was generally greater than that tested by time-kill experiments because chequerboards are quicker and cheaper.

Semi-Mechanistic Modelling Built on a previously developed pharmacokinetic/pharmacodynamic model for colistin against *P. aeruginosa* [153], a model for the colistin–doripenem combination effect on *P. aeruginosa* was developed from time-kill and PAPs data [163]. In this study, multiple dosing regimens and inocula were tested. Results suggested that colistin monotherapy, even at a high dose, should be avoided due to rapid amplification of resistant subpopulations. In contrast, the results suggest that the colistin–doripenem combination would be efficient. The impact of the combination on the different subpopulations characterised by the PAPs was also assessed.

Based on another previously developed pharmacokinetic/pharmacodynamic model of colistin on *P. aeruginosa* [155], a model of the colistin–meropenem combination effect on *P. aeruginosa* was developed from time-kill data [175]. This pharmacokinetic/pharmacodynamic model suggested that the combination at clinically achievable concentrations would be efficient to treat infections with meropenem-resistant *P. aeruginosa*.

12.2 In Vivo Pharmacodynamics

Only a few in vivo pharmacodynamic studies have been performed with colistin alone or in combination. Studies of colistin monotherapy focused on the determination of the best pharmacokinetic/pharmacodynamic index and its target value. Studies of colistin combination therapy used $\Delta\log_{10}$ cfu/mL at different timepoints to assess synergism.

12.2.1 Colistin Alone

The pharmacokinetic/pharmacodynamic index that best predicted in vivo colistin efficacy was determined in mice thigh and lung infection models with three *P. aeruginosa* strains and three *A. baumannii* strains. Initially, two studies reported in vivo pharmacokinetic/pharmacodynamic index target values [176, 177], but errors in the determination of the in vivo f_u of colistin led the experiments to be repeated [67]. In this next study, *f*AUC/MIC was the pharmacokinetic/pharmacodynamic index that most closely correlated with the killing of bacteria. In the thigh infection model, target values for 2 $\log_{10}$ kill were between 7.4 and 13.7 for *P. aeruginosa* strains and between 7.4 and 17.6 for *A. baumannii* strains. In the lung infection model the target values for efficacy were much higher. It was possible to achieve 2 $\log_{10}$ kill in lung for only two-thirds of *P. aeruginosa* and one-third of *A. baumannii* strains (target values of *f*AUC/MIC between 36.8 and 105) [178].

12.2.2 Colistin in Combination

A murine thigh infection model was used to evaluate combinations of colistin and several antibiotics against extensively drug-resistant (XDR) *A. baumannii* [179] and against *K. pneumoniae* and *E. coli* [180]. Efficacy was evaluated with bacterial counts in thigh at 24 h. Rifampicin, fusidic acid and meropenem combined with colistin were synergistic against XDR *A. baumannii* [179]. By contrast, colistin and tigecycline in association were antagonist against several strains of *K. pneumoniae* and *E. coli* [180].

Colistin monotherapy and its combination with tigecycline were compared in a mice sepsis model infected by carbapenem-resistant *K. pneumoniae* [181]. Colistin and tigecycline monotherapies significantly reduced bacterial counts in liver and lung tissues, but the combination therapy was not superior to these monotherapies.

Readers especially interested in clinical combinations of polymyxins are referred to Lenhard et al. [182] for a more detailed review.

13 Conclusion

Pharmacokinetic and pharmacodynamic studies on colistin are difficult to carry out because it binds to many types of laboratory materials. Colistin renal clearance is very low due to intensive tubular reabsorption. However, the dosing regimen of colistin should be adapted to the renal function of the patient because CMS is partly eliminated by the kidney. Moreover, because the pharmacokinetics of colistin are very variable, and because its therapeutic window

is narrow, TDM of colistin is warranted. Resistance of bacteria to colistin is increasing worldwide in parallel to its clinical and veterinary uses. In vitro, when exposed to colistin, bacteria develop resistance mechanisms rapidly. In these cases, pharmacokinetic/pharmacodynamic models can be used to quantify the loss of colistin efficacy and determine optimal dosing regimens. The use of a loading dose might reduce the emergence of resistance but the use of colistin in combination also seems necessary. Some pharmacokinetic/pharmacodynamic studies of colistin in combination have already been conducted, but further investigations are necessary.

Compliance with Ethical Standards

Funding No support was received for the preparation of this manuscript.

Conflicts of interest Nicolas Grégoire, Vincent Aranzana-Climent, Sophie Magréault, Sandrine Marchand and William Couet declare that they have no conflicts of interest.

References

1. Li J, Nation RL, Turnidge JD, Milne RW, Coulthard K, Rayner CR, et al. Colistin: the re-emerging antibiotic for multidrug-resistant Gram-negative bacterial infections. Lancet Infect Dis. 2006;6(9):589–601.
2. Nation RL, Li J, Cars O, Couet W, Dudley MN, Kaye KS, et al. Framework for optimisation of the clinical use of colistin and polymyxin B: the Prato polymyxin consensus. Lancet Infect Dis. 2015;15(2):225–34.
3. He H, Li JC, Nation RL, Jacob J, Chen G, Lee HJ, et al. Pharmacokinetics of four different brands of colistimethate and formed colistin in rats. J Antimicrob Chemother. 2013;68(10):2311–7.
4. Rhouma M, Beaudry F, Theriault W, Bergeron N, Laurent-Lewandowski S, Fairbrother JM, et al. Gastric stability and oral bioavailability of colistin sulfate in pigs challenged or not with *Escherichia coli* O149: F4 (K88). Res Vet Sci. 2015;102:173–81.
5. Shah SR, Henslee AM, Spicer PP, Yokota S, Petrichenko S, Allahabadi S, et al. Effects of antibiotic physicochemical properties on their release kinetics from biodegradable polymer microparticles. Pharm Res. 2014;31(12):3379–89.
6. Velkov T, Roberts KD, Nation RL, Thompson PE, Li J. Pharmacology of polymyxins: new insights into an 'old' class of antibiotics. Future Microbiol. 2013;8(6):711–24.
7. Li J, Nation RL, Milne RW, Turnidge JD, Coulthard K. Evaluation of colistin as an agent against multi-resistant Gram-negative bacteria. Int J Antimicrob Agents. 2005;25(1):11–25.
8. Bergen PJ, Landersdorfer CB, Zhang J, Zhao M, Lee HJ, Nation RL, et al. Pharmacokinetics and pharmacodynamics of 'old' polymyxins: what is new? Diagn Microbiol Infect Dis. 2012;74(3):213–23.
9. Bergen PJ, Landersdorfer CB, Lee HJ, Li J, Nation RL. 'Old' antibiotics for emerging multidrug-resistant bacteria. Curr Opin Infect Dis. 2012;25(6):626–33.
10. Yapa SWS, Li J, Porter CJ, Nation RL, Patel K, McIntosh MP. Population pharmacokinetics of colistin methanesulfonate in rats: achieving sustained lung concentrations of colistin for targeting respiratory infections. Antimicrob Agents Chemother. 2013;57(10):5087–95.
11. DrugBank. Colistimethate. https://www.drugbank.ca/drugs/DB01111. Accessed 30 Oct 2016.
12. DrugBank. Colistin. https://www.drugbank.ca/drugs/DB00803. Accessed 30 Oct 2016.
13. Wallace SJ, Li J, Nation RL, Prankerd RJ, Velkov T, Boyd BJ. Self-assembly behavior of colistin and its prodrug colistin methanesulfonate: implications for solution stability and solubilization. J Phys Chem B. 2010;114(14):4836–40.
14. Wallace SJ, Li J, Rayner CR, Coulthard K, Nation RL. Stability of colistin methanesulfonate in pharmaceutical products and solutions for administration to patients. Antimicrob Agents Chemother. 2008;52(9):3047–51.
15. Gobin P, Lemaitre F, Marchand S, Couet W, Olivier JC. Assay of colistin and colistin methanesulfonate in plasma and urine by liquid chromatography tandem mass spectrometry (LC–MS/MS). Antimicrob Agents Chemother. 2010;22(54):1941–8.
16. Li J, Milne RW, Nation RL, Turnidge JD, Coulthard K, Valentine J. Simple method for assaying colistin methanesulfonate in plasma and urine using high-performance liquid chromatography. Antimicrob Agents Chemother. 2002;46(10):3304–7.
17. Li J, Milne RW, Nation RL, Turnidge JD, Smeaton TC, Coulthard K. Pharmacokinetics of colistin methanesulphonate and colistin in rats following an intravenous dose of colistin methanesulphonate. J Antimicrob Chemother. 2004;53(5):837–40.
18. Chepyala D, Tsai IL, Sun HY, Lin SW, Kuo CH. Development and validation of a high-performance liquid chromatography-fluorescence detection method for the accurate quantification of colistin in human plasma. J Chromatogr B Anal Technol Biomed Life Sci. 2015;1(980):48–54.
19. Li J, Milne RW, Nation RL, Turnidge JD, Coulthard K, Johnson DW. A simple method for the assay of colistin in human plasma, using pre-column derivatization with 9-fluorenylmethyl chloroformate in solid-phase extraction cartridges and reversed-phase high-performance liquid chromatography. J Chromatogr B Biomed Sci Appl. 2001;761(2):167–75.
20. Van den Meersche T, Pamel EV, Poucke CV, Herman L, Heyndrickx M, Rasschaert G, et al. Development, validation and application of an ultra high performance liquid chromatographic-tandem mass spectrometric method for the simultaneous detection and quantification of five different classes of veterinary antibiotics in swine manure. J Chromatogr A. 2016;15(1429):248–57.
21. Jansson B, Karvanen M, Cars O, Plachouras D, Friberg LE. Quantitative analysis of colistin A and colistin B in plasma and culture medium using a simple precipitation step followed by LC/MS/MS. J Pharm Biomed Anal. 2009;49(3):760–7.
22. Marchand S, Gobin P, Brillault J, Baptista S, Adier C, Olivier JC, et al. Aerosol therapy with colistin methanesulfonate: a biopharmaceutical issue illustrated in rats. Antimicrob Agents Chemother. 2010;54(9):3702–7.
23. Nation RL, Velkov T, Li J. Colistin and polymyxin B: peas in a pod, or chalk and cheese? Clin Infect Dis. 2014;59(1):88–94.
24. Bialvaei AZ, Samadi Kafil H. Colistin, mechanisms and prevalence of resistance. Curr Med Res Opin. 2015;31(4):707–21.
25. Dixon RA, Chopra I. Leakage of periplasmic proteins from *Escherichia coli* mediated by polymyxin B nonapeptide. Antimicrob Agents Chemother. 1986;29(5):781–8.
26. Chen CC, Feingold DS. Locus of divalent cation inhibition of the bactericidal action of polymyxin B. Antimicrob Agents Chemother. 1972;2(5):331–5.
27. Schindler M, Osborn MJ. Interaction of divalent cations and polymyxin B with lipopolysaccharide. Biochemistry. 1979;18(20):4425–30.

28. Davis SD, Iannetta A, Wedgwood RJ. Activity of colistin against *Pseudomonas aeruginosa*: inhibition by calcium. J Infect Dis. 1971;124(6):610–2.
29. Clausell A, Garcia-Subirats M, Pujol M, Busquets MA, Rabanal F, Cajal Y. Gram-negative outer and inner membrane models: insertion of cyclic cationic lipopeptides. J Phys Chem B. 2007;111(3):551–63.
30. Peterson AA, Hancock RE, McGroarty EJ. Binding of polycationic antibiotics and polyamines to lipopolysaccharides of *Pseudomonas aeruginosa*. J Bacteriol. 1985;164(3):1256–61.
31. Gough M, Hancock RE, Kelly NM. Antiendotoxin activity of cationic peptide antimicrobial agents. Infect Immun. 1996;64(12):4922–7.
32. Martis N, Leroy S, Blanc V. Colistin in multi-drug resistant *Pseudomonas aeruginosa* blood-stream infections: a narrative review for the clinician. J Infect. 2014;69(1):1–12.
33. Gardiner KR, Erwin PJ, Anderson NH, McCaigue MD, Halliday MI, Rowlands BJ. Lactulose as an antiendotoxin in experimental colitis. Br J Surg. 1995;82(4):469–72.
34. Escartin P, Rodriguez-Montes JA, Cuervas-Mons V, Rossi I, Alvarez-Cienfuegos J, Maganto P, et al. Effect of colistin on reduction of biliary flow induced by endotoxin in *E. coli*. Dig Dis Sci. 1982;27(10):875–9.
35. Lopes J, Inniss WE. Electron microscopy of effect of polymyxin on *Escherichia coli* lipopolysaccharide. J Bacteriol. 1969;100(2):1128–9.
36. Storm DR, Rosenthal KS, Swanson PE. Polymyxin and related peptide antibiotics. Annu Rev Biochem. 1977;46:723–63.
37. Deris ZZ, Akter J, Sivanesan S, Roberts KD, Thompson PE, Nation RL, et al. A secondary mode of action of polymyxins against Gram-negative bacteria involves the inhibition of NADH-quinone oxidoreductase activity. J Antibiot (Tokyo). 2014;67(2):147–51.
38. Clinical and Laboratory Standards Institute (CLSI). M100-S25. Performance standards for antimicrobial susceptibility testing; twenty-fifth informational supplement. Wayne: Clinical and Laboratory Standards Institute; 2015.
39. EUCAST. Recommendations for MIC determination of colistin (polymyxin E). As recommended by the joint CLSI-EUCAST Polymyxin Breakpoints Working Group. European Committee on Antimicrobial Susceptibility Testing; 2016. http://www.eucast.org/fileadmin/src/media/PDFs/EUCAST_files/General_documents/Recommendations_for_MIC_determination_of_colistin_March_2016.pdf. Accessed 24 May 2017.
40. Cai Y, Lee W, Kwa AL. Polymyxin B versus colistin: an update. Expert Rev Anti Infect Ther. 2015;13(12):1481–97.
41. Hindler JA, Humphries RM. Colistin MIC variability by method for contemporary clinical isolates of multidrug-resistant Gram-negative bacilli. J Clin Microbiol. 2013;51(6):1678–84.
42. Lo-Ten-Foe JR, de Smet AM, Diederen BM, Kluytmans JA, van Keulen PH. Comparative evaluation of the VITEK 2, disk diffusion, etest, broth microdilution, and agar dilution susceptibility testing methods for colistin in clinical isolates, including heteroresistant Enterobacter cloacae and *Acinetobacter baumannii* strains. Antimicrob Agents Chemother. 2007;51(10):3726–30.
43. Dafopoulou K, Zarkotou O, Dimitroulia E, Hadjichristodoulou C, Gennimata V, Pournaras S, et al. Comparative evaluation of colistin susceptibility testing methods among carbapenem-non-susceptible *Klebsiella pneumoniae* and *Acinetobacter baumannii* clinical isolates. Antimicrob Agents Chemother. 2015;59(8):4625–30.
44. European Committee on Antimicrobial Susceptibility Testing. Version 7.1, 2017. Breakpoint tables for interpretation of MICs and zone diameters. Available from: http://www.eucast.org/fileadmin/src/media/PDFs/EUCAST_files/Breakpoint_tables/v_7.1_Breakpoint_Tables.pdf. Accessed 24 May 2017.
45. Kwa AL, Tam VH, Falagas ME. Polymyxins: a review of the current status including recent developments. Ann Acad Med Singap. 2008;37(10):870–83.
46. Park YK, Choi JY, Shin D, Ko KS. Correlation between overexpression and amino acid substitution of the PmrAB locus and colistin resistance in *Acinetobacter baumannii*. Int J Antimicrob Agents. 2011;37(6):525–30.
47. Gunn JS. The Salmonella PmrAB regulon: lipopolysaccharide modifications, antimicrobial peptide resistance and more. Trends Microbiol. 2008;16(6):284–90.
48. Kim SY, Choi HJ, Ko KS. Differential expression of two-component systems, pmrAB and phoPQ, with different growth phases of *Klebsiella pneumoniae* in the presence or absence of colistin. Curr Microbiol. 2014;69(1):37–41.
49. Raetz CR, Guan Z, Ingram BO, Six DA, Song F, Wang X, et al. Discovery of new biosynthetic pathways: the lipid A story. J Lipid Res. 2009;50(Suppl):S103–8.
50. Fernandez L, Jenssen H, Bains M, Wiegand I, Gooderham WJ, Hancock RE. The two-component system CprRS senses cationic peptides and triggers adaptive resistance in *Pseudomonas aeruginosa* independently of ParRS. Antimicrob Agents Chemother. 2012;56(12):6212–22.
51. McPhee JB, Bains M, Winsor G, Lewenza S, Kwasnicka A, Brazas MD, et al. Contribution of the PhoP-PhoQ and PmrA-PmrB two-component regulatory systems to Mg^{2+}-induced gene regulation in *Pseudomonas aeruginosa*. J Bacteriol. 2006;188(11):3995–4006.
52. Beceiro A, Llobet E, Aranda J, Bengoechea JA, Doumith M, Hornsey M, et al. Phosphoethanolamine modification of lipid A in colistin-resistant variants of *Acinetobacter baumannii* mediated by the pmrAB two-component regulatory system. Antimicrob Agents Chemother. 2011;55(7):3370–9.
53. Snitkin ES, Zelazny AM, Gupta J, Palmore TN, Murray PR, Segre JA. Genomic insights into the fate of colistin resistance and *Acinetobacter baumannii* during patient treatment. Genome Res. 2013;23(7):1155–62.
54. Liu YY, Wang Y, Walsh TR, Yi LX, Zhang R, Spencer J, et al. Emergence of plasmid-mediated colistin resistance mechanism MCR-1 in animals and human beings in China: a microbiological and molecular biological study. Lancet Infect Dis. 2016;16(2):161–8.
55. Schwarz S, Johnson AP. Transferable resistance to colistin: a new but old threat. J Antimicrob Chemother. 2016;71(8):2066–70.
56. Moffatt JH, Harper M, Harrison P, Hale JD, Vinogradov E, Seemann T, et al. Colistin resistance in *Acinetobacter baumannii* is mediated by complete loss of lipopolysaccharide production. Antimicrob Agents Chemother. 2010;54(12):4971–7.
57. Li J, Rayner CR, Nation RL, Owen RJ, Spelman D, Tan KE, et al. Heteroresistance to colistin in multidrug-resistant *Acinetobacter baumannii*. Antimicrob Agents Chemother. 2006;50(9):2946–50.
58. Lee JY, Park YK, Chung ES, Na IY, Ko KS. Evolved resistance to colistin and its loss due to genetic reversion in *Pseudomonas aeruginosa*. Sci Rep. 2016;06(6):25543.
59. Lewis K. Persister cells, dormancy and infectious disease. Nat Rev Microbiol. 2007;5(1):48–56.
60. Couet W, Gregoire N, Gobin P, Saulnier PJ, Frasca D, Marchand S, et al. Pharmacokinetics of colistin and colistimethate sodium after a single 80-mg intravenous dose of CMS in young healthy volunteers. Clin Pharmacol Ther. 2011;89(6):875–9.
61. Couet W, Gregoire N, Marchand S, Mimoz O. Colistin pharmacokinetics: the fog is lifting. Clin Microbiol Infect. 2012;18(1):30–9.
62. Ma Z, Wang J, Nation RL, Li J, Turnidge JD, Coulthard K, et al. Renal disposition of colistin in the isolated perfused rat kidney. Antimicrob Agents Chemother. 2009;53(7):2857–64.

63. Lu X, Chan T, Xu C, Zhu L, Zhou QT, Roberts KD, et al. Human oligopeptide transporter 2 (PEPT2) mediates cellular uptake of polymyxins. J Antimicrob Chemother. 2016;71(2):403–12.
64. Suzuki T, Yamaguchi H, Ogura J, Kobayashi M, Yamada T, Iseki K. Megalin contributes to kidney accumulation and nephrotoxicity of colistin. Antimicrob Agents Chemother. 2013;57(12):6319–24.
65. Diao L, Meibohm B. Pharmacokinetics and pharmacokinetic–pharmacodynamic correlations of therapeutic peptides. Clin Pharmacokinet. 2013;52(10):855–68.
66. Azad MA, Huang JX, Cooper MA, Roberts KD, Thompson PE, Nation RL, et al. Structure-activity relationships for the binding of polymyxins with human alpha-1-acid glycoprotein. Biochem Pharmacol. 2012;84(3):278–91.
67. Cheah SE, Wang J, Nguyen VT, Turnidge JD, Li J, Nation RL. New pharmacokinetic/pharmacodynamic studies of systemically administered colistin against *Pseudomonas aeruginosa* and *Acinetobacter baumannii* in mouse thigh and lung infection models: smaller response in lung infection. J Antimicrob Chemother. 2015;70(12):3291–7.
68. Li J, Milne RW, Nation RL, Turnidge JD, Smeaton TC, Coulthard K. Use of high-performance liquid chromatography to study the pharmacokinetics of colistin sulfate in rats following intravenous administration. Antimicrob Agents Chemother. 2003;47(5):1766–70.
69. Matzneller P, Gobin P, Lackner E, Zeitlinger M. Feasibility of microdialysis for determination of protein binding and target site pharmacokinetics of colistin in vivo. J Clin Pharmacol. 2015;55(4):431–7.
70. al-Khayyat AA, Aronson AL. Pharmacologic and toxicologic studies with the polymyxins. 3. Consideration regarding clinical use in dogs. Chemotherapy. 1973;19(2):98–108.
71. Mohamed AF, Karaiskos I, Plachouras D, Karvanen M, Pontikis K, Jansson B, et al. Application of a loading dose of colistin methanesulphonate in critically ill patients: population pharmacokinetics, protein binding, and prediction of bacterial kill. Antimicrob Agents Chemother. 2012;56(8):4241–9.
72. Kremer JM, Wilting J, Janssen LH. Drug binding to human alpha-1-acid glycoprotein in health and disease. Pharmacol Rev. 1988;40(1):1–47.
73. Zavascki AP, Goldani LZ, Cao G, Superti SV, Lutz L, Barth AL, et al. Pharmacokinetics of intravenous polymyxin B in critically ill patients. Clin Infect Dis. 2008;47(10):1298–304.
74. Huang JX, Blaskovich MA, Pelingon R, Ramu S, Kavanagh A, Elliott AG, et al. Mucin binding reduces colistin antimicrobial activity. Antimicrob Agents Chemother. 2015;59(10):5925–31.
75. Imberti R, Cusato M, Villani P, Carnevale L, Iotti GA, Langer M, et al. Steady-state pharmacokinetics and BAL concentration of colistin in critically Ill patients after IV colistin methanesulfonate administration. Chest. 2010;138(6):1333–9.
76. Boisson M, Jacobs M, Gregoire N, Gobin P, Marchand S, Couet W, et al. Comparison of intrapulmonary and systemic pharmacokinetics of colistin methanesulfonate (CMS) and colistin after aerosol delivery and intravenous administration of cms in critically ill patients. Antimicrob Agents Chemother. 2014;58(12):7331–9.
77. Yapa SWS, Li J, Patel K, Wilson JW, Dooley MJ, George J, et al. Pulmonary and systemic pharmacokinetics of inhaled and intravenous colistin methanesulfonate in cystic fibrosis patients: targeting advantage of inhalational administration. Antimicrob Agents Chemother. 2014;58(5):2570–9.
78. Nickel S, Clerkin CG, Selo MA, Ehrhardt C. Transport mechanisms at the pulmonary mucosa: implications for drug delivery. Expert Opin Drug Deliv. 2016;13(5):667–90.
79. Nakamura T, Nakanishi T, Haruta T, Shirasaka Y, Keogh JP, Tamai I. Transport of ipratropium, an anti-chronic obstructive pulmonary disease drug, is mediated by organic cation/carnitine transporters in human bronchial epithelial cells: implications for carrier-mediated pulmonary absorption. Mol Pharm. 2010;7(1):187–95.
80. Swaan PW, Bensman T, Bahadduri PM, Hall MW, Sarkar A, Bao S, et al. Bacterial peptide recognition and immune activation facilitated by human peptide transporter PEPT2. Am J Respir Cell Mol Biol. 2008;39(5):536–42.
81. Kofteridis DP, Alexopoulou C, Valachis A, Maraki S, Dimopoulou D, Georgopoulos D, et al. Aerosolized plus intravenous colistin versus intravenous colistin alone for the treatment of ventilator-associated pneumonia: a matched case–control study. Clin Infect Dis. 2010;51(11):1238–44.
82. Korbila IP, Michalopoulos A, Rafailidis PI, Nikita D, Samonis G, Falagas ME. Inhaled colistin as adjunctive therapy to intravenous colistin for the treatment of microbiologically documented ventilator-associated pneumonia: a comparative cohort study. Clin Microbiol Infect. 2010;16(8):1230–6.
83. Michalopoulos A, Fotakis D, Virtzili S, Vletsas C, Raftopoulou S, Mastora Z, et al. Aerosolized colistin as adjunctive treatment of ventilator-associated pneumonia due to multidrug-resistant Gram-negative bacteria: a prospective study. Respir Med. 2008;102(3):407–12.
84. Tumbarello M, De Pascale G, Trecarichi EM, De Martino S, Bello G, Maviglia R, et al. Effect of aerosolized colistin as adjunctive treatment on the outcomes of microbiologically documented ventilator-associated pneumonia caused by colistin-only susceptible gram-negative bacteria. Chest. 2013;144(6):1768–75.
85. Gontijo AV, Gregoire N, Lamarche I, Gobin P, Couet W, Marchand S. Biopharmaceutical characterization of nebulized antimicrobial agents in rats: 2. Colistin. Antimicrob Agents Chemother. 2014;58(7):3950–6.
86. Ratjen F, Rietschel E, Kasel D, Schwiertz R, Starke K, Beier H, et al. Pharmacokinetics of inhaled colistin in patients with cystic fibrosis. J Antimicrob Chemother. 2006;57(2):306–11.
87. Athanassa ZE, Markantonis SL, Fousteri MZ, Myrianthefs PM, Boutzouka EG, Tsakris A, et al. Pharmacokinetics of inhaled colistimethate sodium (CMS) in mechanically ventilated critically ill patients. Intensive Care Med. 2012;38(11):1779–86.
88. Markantonis SL, Markou N, Fousteri M, Sakellaridis N, Karatzas S, Alamanos I, et al. Penetration of colistin into cerebrospinal fluid. Antimicrob Agents Chemother. 2009;53(11):4907–10.
89. Ziaka M, Markantonis SL, Fousteri M, Zygoulis P, Panidis D, Karvouniaris M, et al. Combined intravenous and intraventricular administration of colistin methanesulfonate in critically ill patients with central nervous system infection. Antimicrob Agents Chemother. 2013;57(4):1938–40.
90. Antachopoulos C, Karvanen M, Iosifidis E, Jansson B, Plachouras D, Cars O, et al. Serum and cerebrospinal fluid levels of colistin in pediatric patients. Antimicrob Agents Chemother. 2010;54(9):3985–7.
91. Jin L, Nation RL, Li J, Nicolazzo JA. Species-dependent blood–brain barrier disruption of lipopolysaccharide: amelioration by colistin in vitro and in vivo. Antimicrob Agents Chemother. 2013;57(9):4336–42.
92. Imberti R, Cusato M, Accetta G, Marino V, Procaccio F, Del Gaudio A, et al. Pharmacokinetics of colistin in cerebrospinal fluid after intraventricular administration of colistin methanesulfonate. Antimicrob Agents Chemother. 2012;56(8):4416–21.
93. Mimoz O, Petitpas F, Gregoire N, Gobin P, Marchand S, Couet W. Colistin distribution into the peritoneal fluid of a patient with

severe peritonitis. Antimicrob Agents Chemother. 2012;56(7):4035–6.
94. Guyonnet J, Manco B, Baduel L, Kaltsatos V, Aliabadi MH, Lees P. Determination of a dosage regimen of colistin by pharmacokinetic/pharmacodynamic integration and modeling for treatment of G.I.T. disease in pigs. Res Vet Sci. 2010;88(2):307–14.
95. Abis GS, Oosterling SJ, Stockmann HB, van der Bij GJ, van Egmond M, Vandenbroucke-Grauls CM, et al. Perioperative selective decontamination of the digestive tract and standard antibiotic prophylaxis versus standard antibiotic prophylaxis alone in elective colorectal cancer patients. Dan Med J. 2014;61(4):A4695.
96. Huttner B, Haustein T, Uckay I, Renzi G, Stewardson A, Schaerrer D, et al. Decolonization of intestinal carriage of extended-spectrum beta-lactamase-producing Enterobacteriaceae with oral colistin and neomycin: a randomized, double-blind, placebo-controlled trial. J Antimicrob Chemother. 2013;68(10):2375–82.
97. Melsen WG, de Smet AM, Kluytmans JA, Bonten MJ. Selective decontamination of the oral and digestive tract in surgical versus non-surgical patients in intensive care in a cluster-randomized trial. Br J Surg. 2012;99(2):232–7.
98. Oren I, Sprecher H, Finkelstein R, Hadad S, Neuberger A, Hussein K, et al. Eradication of carbapenem-resistant Enterobacteriaceae gastrointestinal colonization with nonabsorbable oral antibiotic treatment: a prospective controlled trial. Am J Infect Control. 2013;41(12):1167–72.
99. Saidel-Odes L, Polachek H, Peled N, Riesenberg K, Schlaeffer F, Trabelsi Y, et al. A randomized, double-blind, placebo-controlled trial of selective digestive decontamination using oral gentamicin and oral polymyxin E for eradication of carbapenem-resistant *Klebsiella pneumoniae* carriage. Infect Control Hosp Epidemiol. 2012;33(1):14–9.
100. Brink AJ, Coetzee J, Corcoran C, Clay CG, Hari-Makkan D, Jacobson RK, et al. Emergence of OXA-48 and OXA-181 carbapenemases among Enterobacteriaceae in South Africa and evidence of in vivo selection of colistin resistance as a consequence of selective decontamination of the gastrointestinal tract. J Clin Microbiol. 2013;51(1):369–72.
101. Halaby T, Al Naiemi N, Kluytmans J, van der Palen J, Vandenbroucke-Grauls CM. Emergence of colistin resistance in Enterobacteriaceae after the introduction of selective digestive tract decontamination in an intensive care unit. Antimicrob Agents Chemother. 2013;57(7):3224–9.
102. Lubbert C, Faucheux S, Becker-Rux D, Laudi S, Durrbeck A, Busch T, et al. Rapid emergence of secondary resistance to gentamicin and colistin following selective digestive decontamination in patients with KPC-2-producing *Klebsiella pneumoniae*: a single-centre experience. Int J Antimicrob Agents. 2013;42(6):565–70.
103. Strenger V, Gschliesser T, Grisold A, Zarfel G, Feierl G, Masoud L, et al. Orally administered colistin leads to colistin-resistant intestinal flora and fails to prevent faecal colonisation with extended-spectrum beta-lactamase-producing enterobacteria in hospitalised newborns. Int J Antimicrob Agents. 2011;37(1):67–9.
104. Garonzik SM, Li J, Thamlikitkul V, Paterson DL, Shoham S, Jacob J, et al. Population pharmacokinetics of colistin methanesulfonate and formed colistin in critically ill patients from a multicenter study provide dosing suggestions for various categories of patients. Antimicrob Agents Chemother. 2011;55(7):3284–94.
105. Grégoire N, Mimoz O, Mégarbane B, Comets E, Chatelier D, Lasocki S, et al. New colistin population pharmacokinetic data in critically ill patients suggesting an alternative loading dose rationale. Antimicrob Agents Chemother. 2014;58(12):7324–30.
106. Plachouras D, Karvanen M, Friberg LE, Papadomichelakis E, Antoniadou A, Tsangaris I, et al. Population pharmacokinetic analysis of colistin methanesulfonate and colistin after intravenous administration in critically ill patients with infections caused by Gram-negative bacteria. Antimicrob Agents Chemother. 2009;53(8):3430–6.
107. Nation RL, Garonzik SM, Thamlikitkul V, Giamarellos-Bourboulis EJ, Forrest A, Paterson DL, et al. Dosing guidance for intravenous colistin in critically-ill patients. Clin Infect Dis. 2016. doi:10.1093/cid/ciw839.
108. Karaiskos I, Friberg LE, Pontikis K, Ioannidis K, Tsagkari V, Galani L, et al. Colistin population pharmacokinetics after application of a loading dose of 9 MU colistin methanesulfonate in critically ill patients. Antimicrob Agents Chemother. 2015;59(12):7240–8.
109. Vardakas KZ, Rellos K, Triarides NA, Falagas ME. Colistin loading dose: evaluation of the published pharmacokinetic and clinical data. Int J Antimicrob Agents. 2016;48(5):475–84.
110. European Medicines Agency, Committee for Medicinal Products for Human Use (CHMP). Assessment report. Polymyxin-based products. 2014. http://www.ema.europa.eu/docs/en_GB/document_library/Referrals_document/Polymyxin_31/WC500179664.pdf. Accessed 23 March 2017.
111. Nation RL, Garonzik SM, Li J, Thamlikitkul V, Giamarellos-Bourboulis EJ, Paterson DL, et al. Updated US and European dose recommendations for intravenous colistin: how do they perform? Clin Infect Dis. 2016;62(5):552–8.
112. Jacobs M, Gregoire N, Megarbane B, Gobin P, Balayn D, Marchand S, et al. Population pharmacokinetics of colistin methanesulphonate (CMS) and colistin in critically ill patients with acute renal failure requiring intermittent haemodialysis. Antimicrob Agents Chemother. 2016;60(3):1788–93.
113. Honore PM, Jacobs R, Lochy S, De Waele E, Van Gorp V, De Regt J, et al. Acute respiratory muscle weakness and apnea in a critically ill patient induced by colistin neurotoxicity: key potential role of hemoadsorption elimination during continuous venovenous hemofiltration. Int J Nephrol Renovasc Dis. 2013;6:107–11.
114. Jitmuang A, Nation RL, Koomanachai P, Chen G, Lee HJ, Wasuwattakul S, et al. Extracorporeal clearance of colistin methanesulphonate and formed colistin in end-stage renal disease patients receiving intermittent haemodialysis: implications for dosing. J Antimicrob Chemother. 2015;70(6):1804–11.
115. Luque S, Sorli L, Li J, Collado S, Barbosa F, Berenguer N, et al. Effective removal of colistin methanesulphonate and formed colistin during intermittent haemodialysis in a patient infected by polymyxin-only-susceptible *Pseudomonas aeruginosa*. J Chemother. 2014;26(2):122–4.
116. Marchand S, Frat JP, Petitpas F, Lemaitre F, Gobin P, Robert R, et al. Removal of colistin during intermittent haemodialysis in two critically ill patients. J Antimicrob Chemother. 2010;65(8):1836–7.
117. Markou N, Fousteri M, Markantonis SL, Zidianakis B, Hroni D, Boutzouka E, et al. Colistin pharmacokinetics in intensive care unit patients on continuous venovenous haemodiafiltration: an observational study. J Antimicrob Chemother. 2012;67(10):2459–62.
118. Karvanen M, Plachouras D, Friberg LE, Paramythiotou E, Papadomichelakis E, Karaiskos I, et al. Colistin methanesulfonate and colistin pharmacokinetics in critically ill patients receiving continuous venovenous hemodiafiltration. Antimicrob Agents Chemother. 2013;57(1):668–71.
119. Karaiskos I, Friberg LE, Galani L, Ioannidis K, Katsouda E, Athanassa Z, et al. Challenge for higher colistin dosage in critically ill patients receiving continuous venovenous haemodiafiltration. Int J Antimicrob Agents. 2016;48(3):337–41.

120. Fiaccadori E, Antonucci E, Morabito S, d'Avolio A, Maggiore U, Regolisti G. Colistin use in patients with reduced kidney function. Am J Kidney Dis. 2016;68(2):296–306.
121. Li J, Coulthard K, Milne R, Nation RL, Conway S, Peckham D, et al. Steady-state pharmacokinetics of intravenous colistin methanesulphonate in patients with cystic fibrosis. J Antimicrob Chemother. 2003;52(6):987–92.
122. Marchand S, Diot P, Gregoire N, Henriet A, Gobin P, Couet W. Plasma pharmacokinetics and sputum concentrations of colistin after nebulization or intravenous administration of colistin methansulphonate (CMS) to ambulatories cystic fibrosis patients. In: 52nd international conference on antimicrobial agents and chemotherapy (ICAAC), 9–12 Sep 2012, San Francisco (Poster A-036).
123. Banerjee D, Stableforth D. The treatment of respiratory pseudomonas infection in cystic fibrosis: what drug and which way? Drugs. 2000;60(5):1053–64.
124. Hansen CR, Pressler T, Hoiby N. Early aggressive eradication therapy for intermittent *Pseudomonas aeruginosa* airway colonization in cystic fibrosis patients: 15 years experience. J Cyst Fibros. 2008;7(6):523–30.
125. Schuster A, Haliburn C, Doring G, Goldman MH. Safety, efficacy and convenience of colistimethate sodium dry powder for inhalation (Colobreathe DPI) in patients with cystic fibrosis: a randomised study. Thorax. 2013;68(4):344–50.
126. Lee J, Han S, Jeon S, Hong T, Song W, Woo H, et al. Population pharmacokinetic analysis of colistin in burn patients. Antimicrob Agents Chemother. 2013;57(5):2141–6.
127. Mizuyachi K, Hara K, Wakamatsu A, Nohda S, Hirama T. Safety and pharmacokinetic evaluation of intravenous colistin methanesulfonate sodium in Japanese healthy male subjects. Curr Med Res Opin. 2011;27(12):2261–70.
128. Falagas ME, Kasiakou SK. Toxicity of polymyxins: a systematic review of the evidence from old and recent studies. Crit Care. 2006;10(1):R27.
129. Dalfino L, Puntillo F, Ondok MJ, Mosca A, Monno R, Coppolecchia S, et al. Colistin-associated acute kidney injury in severely ill patients: a step toward a better renal care? A prospective cohort study. Clin Infect Dis. 2015;61(12):1771–7.
130. Phe K, Johnson ML, Palmer HR, Tam VH. Validation of a model to predict the risk of nephrotoxicity in patients receiving colistin. Antimicrob Agents Chemother. 2014;58(11):6946–8.
131. Sorli L, Luque S, Grau S, Berenguer N, Segura C, Montero MM, et al. Trough colistin plasma level is an independent risk factor for nephrotoxicity: a prospective observational cohort study. BMC Infect Dis. 2013;13:380.
132. Deryke CA, Crawford AJ, Uddin N, Wallace MR. Colistin dosing and nephrotoxicity in a large community teaching hospital. Antimicrob Agents Chemother. 2010;54(10):4503–5.
133. Kelesidis T, Falagas ME. The safety of polymyxin antibiotics. Expert Opin Drug Saf. 2015;14(11):1687–701.
134. Sirijatuphat R, Limmahakhun S, Sirivatanauksorn V, Nation RL, Li J, Thamlikitkul V. Preliminary clinical study of the effect of ascorbic acid on colistin-associated nephrotoxicity. Antimicrob Agents Chemother. 2015;59(6):3224–32.
135. Yun B, Azad MA, Nowell CJ, Nation RL, Thompson PE, Roberts KD, et al. Cellular uptake and localization of polymyxins in renal tubular cells using rationally designed fluorescent probes. Antimicrob Agents Chemother. 2015;59(12):7489–96.
136. Spapen HD, Honore PM, Gregoire N, Gobin P, de Regt J, Martens GA, et al. Convulsions and apnoea in a patient infected with New Delhi metallo-beta-lactamase-1 *Escherichia coli* treated with colistin. J Infect. 2011;63(6):468–70.
137. Antoniu SA, Cojocaru I. Inhaled colistin for lower respiratory tract infections. Expert Opin Drug Deliv. 2012;9(3):333–42.
138. Gurjar M. Colistin for lung infection: an update. J Intensive Care. 2015;3(1):3.
139. Bargiacchi O, De Rosa FG. Intrathecal or intraventricular colistin: a review. Infez Med. 2016;24(1):3–11.
140. Landersdorfer CB, Nation RL. Colistin: how should it be dosed for the critically ill? Semin Respir Crit Care Med. 2015;36(1):126–35.
141. Horcajada JP, Sorli L, Luque S, Benito N, Segura C, Campillo N, et al. Validation of a colistin plasma concentration breakpoint as a predictor of nephrotoxicity in patients treated with colistin methanesulfonate. Int J Antimicrob Agents. 2016;48(6):725–7.
142. Bergen PJ, Bulitta JB, Forrest A, Tsuji BT, Li J, Nation RL. Pharmacokinetic/pharmacodynamic investigation of colistin against *Pseudomonas aeruginosa* using an in vitro model. Antimicrob Agents Chemother. 2010;54(9):3783–9.
143. Dudhani RV, Turnidge JD, Coulthard K, Milne RW, Rayner CR, Li J, et al. Elucidation of pharmacokinetic/pharmacodynamic determinant of colistin activity against *Pseudomonas aeruginosa* in murine thigh and lung infection models. Antimicrob Agents Chemother. 2010;54(3):1117–24.
144. Mohamed AF, Cars O, Friberg LE. A pharmacokinetic/pharmacodynamic model developed for the effect of colistin on *Pseudomonas aeruginosa* in vitro with evaluation of population pharmacokinetic variability on simulated bacterial killing. J Antimicrob Chemother. 2014;69(5):1350–61.
145. Wiegand I, Hilpert K, Hancock RE. Agar and broth dilution methods to determine the minimal inhibitory concentration (MIC) of antimicrobial substances. Nat Protoc. 2008;3(2):163–75.
146. Karvanen M. Optimisation of colistin dosage in the treatment of multiresistant gram-negative infections. Uppsala: Uppsala Universitet; 2013.
147. Bergen PJ, Bulitta JB, Forrest A, Tsuji BT, Li J, Nation RL. Pharmacokinetic/pharmacodynamic investigation of colistin against *Pseudomonas aeruginosa* using an in vitro model. Antimicrob Agents Chemother. 2010;54:3783–9.
148. Li J, Turnidge J, Milne R, Nation RL, Coulthard K. In vitro pharmacodynamic properties of colistin and colistin methanesulfonate against *Pseudomonas aeruginosa* isolates from patients with cystic fibrosis. Antimicrob Agents Chemother. 2001;45:781–5.
149. Li J, Rayner CR, Nation RL, Owen RJ, Spelman D, Tan KE, et al. Heteroresistance to colistin in multidrug-resistant *Acinetobacter baumannii*. Antimicrob Agents Chemother. 2006;50:2946–50.
150. Poudyal A, Howden BP, Bell JM, Gao W, Owen RJ, Turnidge JD, et al. In vitro pharmacodynamics of colistin against multidrug-resistant *Klebsiella pneumoniae*. J Antimicrob Chemother. 2008;62:1311–8.
151. Tan C-H, Li J, Nation RL. Activity of colistin against heteroresistant *Acinetobacter baumannii* and emergence of resistance in an in vitro pharmacokinetic/pharmacodynamic model. Antimicrob Agents Chemother. 2007;51:3413–5.
152. Bergen PJ, Li J, Nation RL, Turnidge JD, Coulthard K, Milne RW. Comparison of once-, twice- and thrice-daily dosing of colistin on antibacterial effect and emergence of resistance: studies with *Pseudomonas aeruginosa* in an in vitro pharmacodynamic model. J Antimicrob Chemother. 2008;61:636–42.
153. Bulitta JB, Yang JC, Yohonn L, Ly NS, Brown SV, D'Hondt RE, et al. Attenuation of colistin bactericidal activity by high inoculum of *Pseudomonas aeruginosa* characterized by a new mechanism-based population pharmacodynamic model. Antimicrob Agents Chemother. 2010;54:2051–62.
154. Cheah S-E, Li J, Tsuji BT, Forrest A, Bulitta JB, Nation RL. Colistin and polymyxin B dosage regimens against *Acinetobacter baumannii*: differences in activity and the emergence of resistance. Antimicrob Agents Chemother. 2016;60:3921–33.
155. Mohamed AF, Cars O, Friberg LE. A pharmacokinetic/pharmacodynamic model developed for the effect of colistin on

Pseudomonas aeruginosa in vitro with evaluation of population pharmacokinetic variability on simulated bacterial killing. J Antimicrob Chemother. 2014;69:1350–61.
156. Cirioni O, Ghiselli R, Silvestri C, Kamysz W, Orlando F, Mocchegiani F, et al. Efficacy of tachyplesin III, colistin, and imipenem against a multiresistant *Pseudomonas aeruginosa* strain. Antimicrob Agents Chemother. 2007;51:2005–10.
157. Di X, Wang R, Liu B, Zhang X, Ni W, Wang J, et al. In vitro activity of fosfomycin in combination with colistin against clinical isolates of carbapenem-resistant Pseudomas aeruginosa. J Antibiot. 2015;68:551–5.
158. Gaibani P, Lombardo D, Lewis RE, Mercuri M, Bonora S, Landini MP, et al. In vitro activity and post-antibiotic effects of colistin in combination with other antimicrobials against colistin-resistant KPC-producing *Klebsiella pneumoniae* bloodstream isolates. J Antimicrob Chemother. 2014;69:1856–65.
159. Gordon NC, Png K, Wareham DW. Potent synergy and sustained bactericidal activity of a vancomycin-colistin combination versus multidrug-resistant strains of *Acinetobacter baumannii*. Antimicrob Agents Chemother. 2010;54:5316–22.
160. Hornsey M, Wareham DW. In vivo efficacy of glycopeptide-colistin combination therapies in a *Galleria mellonella* model of *Acinetobacter baumannii* Infection. Antimicrob Agents Chemother. 2011;55:3534–7.
161. Le Minh V, Thi Khanh Nhu N, Vinh Phat V, Thompson C, Huong Lan NP, Thieu Nga TV, et al. In vitro activity of colistin in antimicrobial combination against carbapenem-resistant *Acinetobacter baumannii* isolated from patients with ventilator-associated pneumonia in Vietnam. J Med Microbiol. 2015;64:1162–9.
162. Liu B, Liu Y, Di X, Zhang X, Wang R, Bai Y, et al. Colistin and anti-Gram-positive bacterial agents against *Acinetobacter baumannii*. Rev Soc Bras Med Trop. 2014;47:451–6.
163. Ly NS, Bulitta JB, Rao GG, Landersdorfer CB, Holden PN, Forrest A, et al. Colistin and doripenem combinations against *Pseudomonas aeruginosa*: profiling the time course of synergistic killing and prevention of resistance. J Antimicrob Chemother. 2015;70:1434–42.
164. Marie MAM, Krishnappa LG, Alzahrani AJ, Mubaraki MA, Alyousef AA. A prospective evaluation of synergistic effect of sulbactam and tazobactam combination with meropenem or colistin against multidrug resistant *Acinetobacter baumannii*. Bosn J Basic Med Sci. 2015;15:24–9.
165. Mitsugui CS, Tognim MCB, Cardoso CL, Carrara-Marroni FE, Garcia LB. In vitro activity of polymyxins in combination with β-lactams against clinical strains of *Pseudomonas aeruginosa*. Int J Antimicrob Agents. 2011;38:447–50.
166. Ni W, Cui J, Liang B, Cai Y, Bai N, Cai X, et al. In vitro effects of tigecycline in combination with colistin (polymyxin E) and sulbactam against multidrug-resistant *Acinetobacter baumannii*. J Antibiot. 2013;66:705–8.
167. Sheng W-H, Wang J-T, Li S-Y, Lin Y-C, Cheng A, Chen Y-C, et al. Comparative in vitro antimicrobial susceptibilities and synergistic activities of antimicrobial combinations against carbapenem-resistant Acinetobacter species: *Acinetobacter baumannii* versus Acinetobacter genospecies 3 and 13TU. Diagn Microbiol Infect Dis. 2011;70:380–6.
168. Tangden T, Hickman RA, Forsberg P, Lagerback P, Giske CG, Cars O. Evaluation of double- and triple-antibiotic combinations for VIM- and NDM-producing *Klebsiella pneumoniae* by in vitro time-kill experiments. Antimicrob Agents Chemother. 2014;58:1757–62.
169. Wareham DW, Gordon NC, Hornsey M. In vitro activity of teicoplanin combined with colistin versus multidrug-resistant strains of *Acinetobacter baumannii*. J Antimicrob Chemother. 2011;66:1047–51.
170. Yang H, Chen G, Hu L, Liu Y, Cheng J, Li H, et al. In vivo activity of daptomycin/colistin combination therapy in a *Galleria mellonella* model of *Acinetobacter baumannii* infection. Int J Antimicrob Agents. 2015;45:188–91.
171. Yang H, Lv N, Hu L, Liu Y, Cheng J, Ye Y, et al. In vivo activity of vancomycin combined with colistin against multidrug-resistant strains of *Acinetobacter baumannii* in a *Galleria mellonella* model. Infect Dis. 2016;48:189–94.
172. Leite GC, Oliveira MS, Perdigão-Neto LV, Rocha CKD, Guimarães T, Rizek C, et al. Antimicrobial combinations against pan-resistant *Acinetobacter baumannii* isolates with different resistance mechanisms. PloS One. 2016;11:e0151270.
173. Oleksiuk LM, Nguyen MH, Press EG, Updike CL, O'Hara JA, Doi Y, et al. In vitro responses of *Acinetobacter baumannii* to two- and three-drug combinations following exposure to colistin and doripenem. Antimicrob Agents Chemother. 2014;58:1195–9.
174. Vidaillac C, Benichou L, Duval RE. In vitro synergy of colistin combinations against colistin-resistant *Acinetobacter baumannii*, *Pseudomonas aeruginosa*, and *Klebsiella pneumoniae* isolates. Antimicrob Agents Chemother. 2012;56:4856–61.
175. Mohamed AF, Kristoffersson AN, Karvanen M, Nielsen EI, Cars O, Friberg LE. Dynamic interaction of colistin and meropenem on a WT and a resistant strain of *Pseudomonas aeruginosa* as quantified in a PK/PD model. J Antimicrob Chemother. 2016;71(5):1279–90.
176. Dudhani RV, Turnidge JD, Coulthard K, Milne RW, Rayner CR, Li J, et al. Elucidation of the pharmacokinetic/pharmacodynamic determinant of colistin activity against *Pseudomonas aeruginosa* in murine thigh and lung infection models. Antimicrob Agents Chemother. 2010;54:1117–24.
177. Dudhani RV, Turnidge JD, Nation RL, Li J. fAUC/MIC is the most predictive pharmacokinetic/pharmacodynamic index of colistin against *Acinetobacter baumannii* in murine thigh and lung infection models. J Antimicrob Chemother. 2010;65:1984–90.
178. Cheah S-E, Wang J, Nguyen VTT, Turnidge JD, Li J, Nation RL. New pharmacokinetic/pharmacodynamic studies of systemically administered colistin against *Pseudomonas aeruginosa* and *Acinetobacter baumannii* in mouse thigh and lung infection models: smaller response in lung infection. J Antimicrob Chemother. 2015;70:3291–7.
179. Fan B, Guan J, Wang X, Cong Y. Activity of colistin in combination with meropenem, tigecycline, fosfomycin, fusidic acid, rifampin or sulbactam against extensively drug-resistant *Acinetobacter baumannii* in a murine thigh-infection model. PLoS One. 2016;11:e0157757.
180. Michail G, Labrou M, Pitiriga V, Manousaka S, Sakellaridis N, Tsakris A, et al. Activity of tigecycline in combination with colistin, meropenem, rifampin, or gentamicin against KPC-producing Enterobacteriaceae in a murine thigh infection model. Antimicrob Agents Chemother. 2013;57:6028–33.
181. Demiraslan H, Dinc G, Ahmed SS, Elmali F, Metan G, Alp E, et al. Carbapenem-resistant *Klebsiella pneumoniae* sepsis in corticosteroid receipt mice: tigecycline or colistin monotherapy versus tigecycline/colistin combination. J Chemother. 2014;26:276–81.
182. Lenhard JR, Nation RL, Tsuji BT. Synergistic combinations of polymyxins. Int J Antimicrob Agents. 2016;48:607–13.
183. D'Souza BB, Padmaraj SR, Rekha PD, Tellis RC, Prabhu S, Pothen P. In vitro synergistic activity of colistin and ceftazidime or ciprofloxacin against multidrug-resistant clinical strains of *Pseudomonas aeruginosa*. Microb Drug Resist. 2014;20:550–4.
184. Dong X, Chen F, Zhang Y, Liu H, Liu Y, Ma L. In vitro activities of rifampin, colistin, sulbactam and tigecycline tested alone and in combination against extensively drug-resistant *Acinetobacter baumannii*. J Antibiot. 2014;67:677–80.

X.B. Projet CO-ACTION

Dans le projet CO-ACTION, c'est l'autre polymyxine, la polymyxine B qui a été sélectionnée comme ND-AB de base à combiner avec les autres molécules[116]. La polymyxine B partage de nombreuses caractéristiques avec la colistine, mais quelques différences subsistent, qui vont être évoquées dans cette partie.

X.B.1. Polymyxine B

Chimiquement, la polymyxine B est comme la colistine un mélange de plus de 30 composants, la différence entre la polymyxine B et la colistine étant la substitution d'une D-Leucine par une D-phénylalanine dans le cycle peptidique[117] (Voir figure 17).

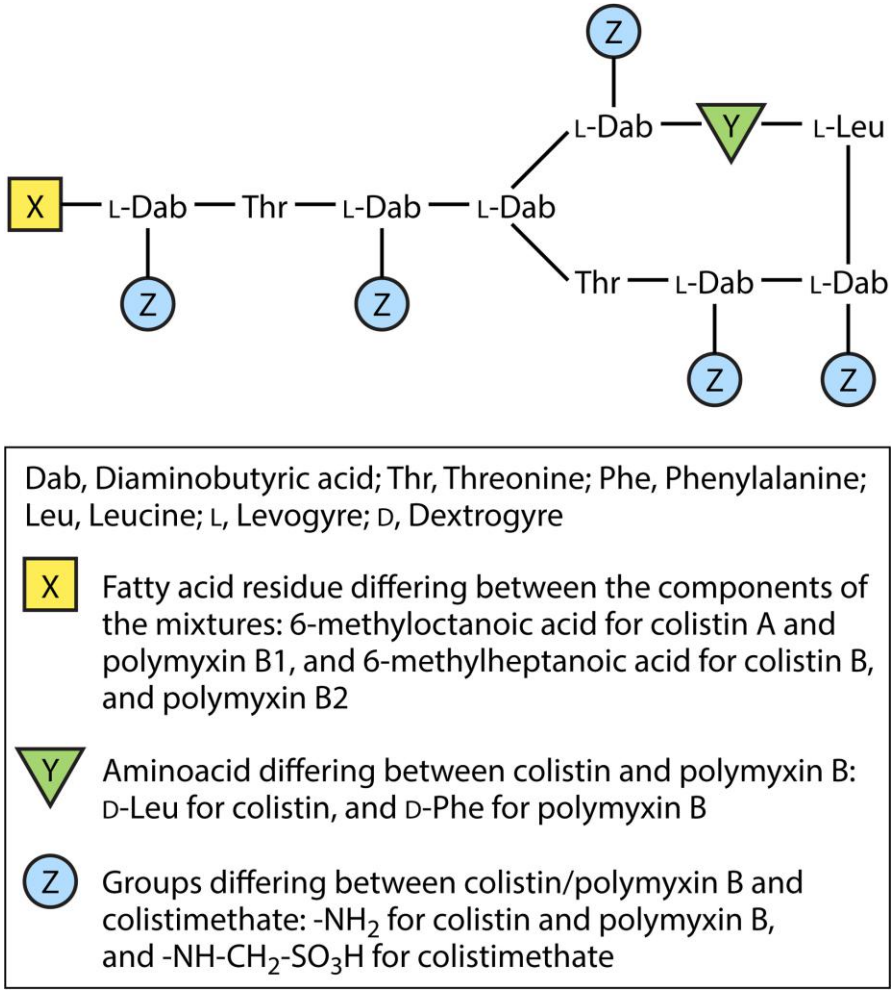

Figure 17. Structures de la colistine A et B, du colistimethate A et B, ainsi que de la polymyxine B1 et B2 (d'après [118])

Cette modification ne semble pas entrainer de variation majeure de la pharmacodynamie et les deux molécules sont considérées comme équivalentes *in vitro*[119]. La principale différence entre les deux molécules vient de l'usage clinique qui en est fait. En effet la colistine est administrée sous la forme d'une pro-drogue inactive, le méthanesulfonate de colistine sodique (CMS) moins toxique que la forme active le sulfate de colistine[120], qui est ensuite converti *in vivo* en sa forme active. La polymyxine B en revanche est administrée directement dans sa forme active, rendant sa pharmacocinétique moins variable. De plus, de plus faibles taux de nephrotoxicité ont été reportés après traitement par la polymyxine B [119,121–123]. En revanche, il faut noter que dans le cas d'infections urinaires le traitement par la polymyxine B n'est pas appropriée, car elle est peu excrétée par le rein[124], contrairement au CMS qui peut ensuite être converti en colistine dans le tractus urinaire.

Le projet CO-ACTION s'intéresse particulièrement aux bactéries à Gram négatif multirésistantes, et plus précisément à *Pseudomonas aeruginosa*, *Klebsiella pneumoniae*, et *Acinetobacter baumannii*. Notre laboratoire s'est vu confier les études *in vitro* vis-à-vis d'*A. baumannii*.

X.B.2. Acinetobacter baumannii

X.2.a. Epidemiologie clinique

A. baumannii est un cocobacille Gram négatif qui pose de plus en plus de problèmes en clinique de par la variété d'infections qu'il provoque et à cause de l'émergence de souches multirésistantes[125]. Ce pathogène est responsable notamment de pneumopathies acquises sous ventilation dans les services de soins intensifs[126]. La mortalité globale des pneumopathies acquises sous ventilation varie selon les rapports entre 40% et 70%[127,128] et il a été montré que l'infection par *A. baumannii* était associée à une augmentation de la mortalité[129–132]. Cette bactérie est aussi responsable de sepsis dans les services de soins intensifs[133]. Parmi les facteurs de risques associés à l'infection il y a l'immunodépression, la ventilation associée à une défaillance respiratoire, le traitement par les antibiotiques et les procédures invasives[134–136]. La mortalité associée à ces infections varie selon les rapports entre 28% et 43% [133,137]. Plus rarement *A. baumannii* peut être responsable d'infections des zones de brûlures, des tissus mous ou de méningites[125].

X.2.b. Résistance aux antibiotiques

Le « succès » des infections dues à *A. baumannii* peut être en partie attribué à la variété des mécanismes de résistances pouvant être développés par ce pathogène. Le tableau 2 en présente les principaux.

Tableau 2. Mécanismes de résistance aux antibiotiques d'Acinetobacter baumannii (d'après [125])

Classe antibioitique	**Mécanisme de résistance**	**Exemples**
β-lactamines	Enzymes d'inactivation	β-lactamases (AmpC, TEM, VEB*, PER, CTX-M,SHV)
		Carbapénémases (OXA-23,-40,-51,-58,143-like, VIM, IMP,NDM-1,-2)
	Reduction de l'expression des proteins de la membrane externe	CarO, 33-36 kDa protein, OprD-like protein
	Expression de protéine liant les pénicillines altérée	PBP2
	Pompes d'efflux	AdeABC
Fluoroquinolones	Modification de la cible	Mutations dans *gyrA* et *parC*
	Pompes d'efflux	AdeABC, AdeM
Aminoglycosides	Enzymes modifiant les aminoglycosides	AAC*,**, ANT, APH*,**
	Pompes d'efflux	AdeABC,AdeM
	Méthylation ribosomale	ArmA
Tétracyclines	Pompes d'efflux	AdeABC, TetA*, TetB
	Protection ribosomale	TetM
Glycylcyclines	Pompes d'efflux	AdeABC
Polymyxines (colistine)	Modification de la cible	Mutations dans le système PmrA/B (modification du LPS), mutation des gènes de biosynthèse du LPS

*Retrouvé dans AbaR1 de la souche *A. baumannii* AYE[138]

**Retrouvé dans AbaR2 de la souche *A. baumannii* ACICU[139]

Une étude rétrospective étudiant les souches isolées au Royaume-Uni entre 1998 et 2006 a montré une augmentation du pourcentage de souches résistantes aux carbapénèmes qui est passé de 0% à 55% des isolats d'*A. baumannii* ayant causé une bactériémie[140]. Cette résistance possède aussi un coût économique, une

étude des bactériémies causées par *A. baumannii* dans un hôpital de Taiwan a montré que les souches multirésistantes étaient responsable d'une augmentation des coûts de 3758$ par patients ainsi qu'une augmentation de la durée d'hospitalisation de 13.4 jours par patient, en moyenne, par rapport aux bactériémie causées par des souches d'*A. baumannii* non résistantes[132] .

En conséquence, et face à l'absence de nouveaux traitements, les souches d'*A. baumannii* résistantes aux carbapénèmes font partie des bactéries de priorité critique, sur lesquelles l'OMS demande que les acteurs de la recherche et du développement concentrent leurs efforts[5].

La première partie du projet a consisté à la réalisation d'expériences de checkerboards afin de pouvoir tester rapidement plusieurs combinaisons sur de multiples souches d'*A. baumannii*. 5 couples de souches cliniques obtenues avant et après traitement du patient par la colistine. 6 molécules ont été testées en combinaison avec la polymyxine B, la fosfomycine, le chloramphénicol, l'aztréonam, le méropénème, la minocycline et la rifampicine. L'étude est présentée dans l'article 3.

X.C. Article 3 In Vitro Activity of Polymyxin B Alone and in Combination Against Colistin-Resistant Acinetobacter Baumannii.

In Vitro Activity of Polymyxin B Alone and in Combination Against Colistin-Resistant *Acinetobacter Baumannii*

Vincent Aranzana-Climent[a,b], Alexia Chauzy[a,b], Nicolas Grégoire[a,b] , Sandrine Marchand[a,b,c], William Couet[a,b,c], Julien M. Buyck[a,b]#

#Address correspondence to Julien M. Buyck, julien.buyck@univ-poitiers.fr, tel : +33549454928

Running Title: Polymyxin B activity versus colistin-resistant *A. baumannii*

[a]INSERM, U1070, Pôle Biologie Santé, 1 rue Georges Bonnet, TSA 51106, 86073 Poitiers Cedex 9, France

[b]Université de Poitiers, UFR de Médecine Pharmacie, 6 rue de la Milétrie, 86000 Poitiers, France

[c]Laboratoire de Toxicologie-Pharmacocinétique, CHU de Poitiers, 2 rue de la Milétrie, 86000 Poitiers, France

In Manuscript.

1. Abstract

1.1 Introduction

In the fight against multi-drug resistant *Acinetobacter baumannii*, antibiotics like polymyxins are the last line of defence. As polymyxin-resistance is emerging worldwide, solutions are needed. Combining a polymyxin with another antibiotic could be an option. Colistin resistant strains could be more susceptible to polymyxin B, being naïve to it. Also, colistin is administered as a prodrug while polymyxin B is administered as an active moiety to patients, making its pharmacokinetics easier to predict, making polymyxin B interesting to study.

1.2 Objectives

Identify promising polymyxin B-based antibiotic combinations to use against colistin resistant *A. baumannii*.

1.3 Methods

Eleven *A. Baumannii* strains were tested including 5 colistin resistant clinical isolates. MICs of colistin, polymyxin B, minocycline, rifampicin, aztreonam, chloramphenicol, fosfomycin and meropenem were

determined for all strains then, checkerboards evaluating the effect of minocycline, rifampicin, aztreonam, chloramphenicol, fosfomycin and meropenem combined with polymyxin B were performed on all strains.

1.4 Results

All strains showed high MICs for aztreonam, chloramphenicol and fosfomycin and 7/11 of the studied strains were resistant to meropenem. All strains were susceptible to minocycline, and 8/11 of the studied strains showed low rifampicin MICs. On all colistin resistant strains, using clinical concentrations of minocycline restored their sensitivity to polymyxin B. Using clinical concentrations of rifampicin restored sensitivity to polymyxin B of 4 out of 5 colistin resistant strains.

1.5 Conclusions

A. baumannii strains resistant to colistin can be susceptible to polymyxin B and combining polymyxin B with minocycline or rifampicin can be effective at clinically achievable concentrations of both antibiotics.

2. Keywords

Antibiotic combination, checkerboard, bacterial resistance, polymyxins, rifampicin, minocycline

3. Introduction

Acinetobacter baumannii is one of the most difficult to treat multi-drug resistant (MDR) pathogens responsible for opportunistic nosocomial infections all over the world [1]. It can cause a broad range of infections, the deadliest being ventilator associated pneumonia and bloodstream infections [2], and has the ability to become resistant to a wide variety of drugs [3]. In face of these resistances, neglected and disused antibiotics like polymyxins (colistin and polymyxin B) may be used as the last line of defence against MDR *A. baumannii* [4]. While chemically similar, the two polymyxin have their differences, colistin is administered as a prodrug, colistin methanosulphate (CMS) while polymyxin B is administered as an active moiety to patients, making its pharmacokinetics less variable thus easier to predict. Also lower nephrotoxicity rates were reported with polymyxin B [5–8]. As resistance to polymyxin is emerging worldwide [9], there is an increasing demand for new therapeutic strategies to overcome such resistance. Since only colistin is available in Europe, colistin resistant strains could still be susceptible to polymyxin B. Also, using combinations of existing antibiotics with polymyxins could help overcoming resistance. Hence, in this work, polymyxin B was used with the aim to identify promising polymyxin B-based antibiotic combinations to use against colistin resistant *A. baumannii*.

4. Materials and Methods

Eleven *A. Baumannii* strains were tested: ATCC19606 reference strain and 5 colistin susceptible/resistant clinical isolates couples, before and after treatment by colistin. Strain description can be found in **Table 1**.

MICs of colistin, polymyxin B, minocycline, rifampicin, aztreonam, chloramphenicol, fosfomycin and meropenem were determined for all strains in duplicate by broth microdilution according to CLSI standard procedure [14].

Checkerboards evaluating the effect of minocycline, rifampicin, aztreonam, chloramphenicol, fosfomycin and meropenem combined with polymyxin B were performed. For each well without bacterial growth, fractional inhibitory concentration index (FICI) values were calculated as follows: $FICI = FIC_A + FIC_{PMB} = [A]/MIC_A + [PMB]/MIC_{PMB}$ (where [A] is the concentration of the antibiotic associated with polymyxin B and MIC_A its MIC, [PMB] is the concentration of polymyxin B and MIC_{PMB} its MIC).

For each checkerboard plate, the minimum FICI ($FICI_{min}$) was determined and the $FICI_{min}$ values were averaged over the replicates. These $FICI_{min}$ were interpreted as follows: $FICI_{min} \leq 0.5$ synergy, $FICI_{min} > 4$ antagonism, $0.5 < FICI_{min} \leq 4$ no interaction. Checkerboards were replicated 2 to 4 times.

5. Results and discussion

MIC values are presented in **Table 1.** colistin MICs were in accordance with previously published data [10–13]. Polymyxin B and colistin had similar MIC values against colistin susceptible strains, but against colistin resistant strains polymyxin B had much lower MIC values (16 to 128-fold difference). This difference is unexplained though and warrants further investigation. All strains showed high MICs for aztreonam, chloramphenicol and fosfomycin and most of the studied strains (7/11) were resistant to meropenem according to EUCAST with the exception of ATCC19606, 248, 249 and 347 [15]. All strains were susceptible to minocycline according to CLSI [16], and all but 3 (CS01, CR17, ABIsac_ColiR) showed low rifampicin MICs. Although minocycline and rifampicin are not usually recommended against *A. baumannii* [17,18], our results indicated that they could still be used alone or as part of combinations against this bacteria as already suggested by other studies [19,20].

Checkerboard results are presented in **Table 2.** To further improve polymyxin B efficacy on CST_R strains, the two most promising candidates were minocycline and rifampicin. In addition to being synergistic with polymyxin B, minocycline exhibits low MIC against colistin resistant strains, and could therefore be a good candidate for being combined with polymyxin B to treat colistin resistant strains. On all colistin resistant strains using clinical concentrations of minocycline restored their susceptibility to polymyxin B, i.e. in presence of minocycline, the polymyxin B MIC was below the CLSI breakpoint for resistance (2 mg/L). rifampicin was another good candidate for combination with polymyxin B based on MIC results.

Using clinical concentrations of rifampicin restored sensitivity to polymyxin B of 4 out of 5 colistin resistant strains, including strain CR17 which had a rifampicin MIC >512 mg/L when used alone. Indeed, when polymyxin B and rifampicin were used in combination on CR17, a concentration of 8 mg/L of rifampicin brought the polymyxin B MIC to 1 mg/L which is below the CLSI breakpoint for resistance (2 mg/L).

The first major result of this study was that polymyxin B exhibited much better activity than CST against the colistin resistant strains used in this paper. Also combining polymyxin B with minocycline or rifampicin show promising results, especially on colistin resistant strains, now these promising results have to be confirmed.

6. Acknowledgments.

We thank Emma Marquizeau for her excellent technical support. We thank G. Bou for the kind gift of the A. baumannii 248, 249 pmrB, 299, and 347 pmrB strains. We also thank E. Dé for the kind gift of the A. baumannii S 1025 and R 30890 strains. We also thank Y. Smani for the kind gift of the A. baumannii CS01 and CR17 strains. We also thank T. Naas for the kind gift of the A. baumannii 062 D6 and 062 D7 strains.

7. Funding.

This study was jointly supported by the Joint Programming Initiative on Antimicrobial Resistance (JPIAMR) and Agence Nationale de la Recherche (ANR) under the research grant “CO-ACTION”.

8. References.

[1] Antunes LCS, Visca P, Towner KJ. Acinetobacter baumannii: evolution of a global pathogen. Pathog Dis 2014;71:292–301. doi:10.1111/2049-632X.12125.

[2] Dijkshoorn L, Nemec A, Seifert H. An increasing threat in hospitals: multidrug-resistant *Acinetobacter baumannii*. Nat Rev Microbiol 2007;5:939–51. doi:10.1038/nrmicro1789.

[3] Fournier P-E, Vallenet D, Barbe V, Audic S, Ogata H, Poirel L, et al. Comparative Genomics of Multidrug Resistance in Acinetobacter baumannii. PLOS Genet 2006;2:e7. doi:10.1371/journal.pgen.0020007.

[4] Nation RL, Li J, Cars O, Couet W, Dudley MN, Kaye KS, et al. Framework for optimisation of the clinical use of colistin and polymyxin B: the Prato polymyxin consensus. Lancet Infect Dis 2015;15:225–34. doi:10.1016/S1473-3099(14)70850-3.

[5] Aggarwal R, Dewan A. Comparison of nephrotoxicity of Colistin with Polymyxin B administered in currently recommended doses: a prospective study. Ann Clin Microbiol Antimicrob 2018;17:15. doi:10.1186/s12941-018-0262-0.

[6] Zavascki AP, Nation RL. Nephrotoxicity of Polymyxins: Is There Any Difference between Colistimethate and Polymyxin B? Antimicrob Agents Chemother 2017;61. doi:10.1128/AAC.02319-16.

[7] Rigatto MH, Oliveira MS, Perdigão-Neto LV, Levin AS, Carrilho CM, Tanita MT, et al. Multicenter Prospective Cohort Study of Renal Failure in Patients Treated with Colistin versus Polymyxin B. Antimicrob Agents Chemother 2016;60:2443–9. doi:10.1128/AAC.02634-15.

[8] Nation RL, Velkov T, Li J. Colistin and Polymyxin B: Peas in a Pod, or Chalk and Cheese? Clin Infect Dis Off Publ Infect Dis Soc Am 2014;59:88–94. doi:10.1093/cid/ciu213.

[9] Cai Y, Chai D, Wang R, Liang B, Bai N. Colistin resistance of Acinetobacter baumannii: clinical reports, mechanisms and antimicrobial strategies. J Antimicrob Chemother 2012;67:1607–15. doi:10.1093/jac/dks084.

[10] López-Rojas R, McConnell MJ, Jiménez-Mejías ME, Domínguez-Herrera J, Fernández-Cuenca F, Pachón J. Colistin Resistance in a Clinical Acinetobacter baumannii Strain Appearing after Colistin Treatment: Effect on Virulence and Bacterial Fitness. Antimicrob Agents Chemother 2013;57:4587–9. doi:10.1128/AAC.00543-13.

[11] Jaidane N, Naas T, Mansour W, Radhia BB, Jerbi S, Boujaafar N, et al. Genomic analysis of in vivo acquired resistance to colistin and rifampicin in Acinetobacter baumannii. Int J Antimicrob Agents 2018;51:266–9. doi:10.1016/j.ijantimicag.2017.10.016.

[12] Pournaras S, Poulou A, Dafopoulou K, Chabane YN, Kristo I, Makris D, et al. Growth Retardation, Reduced Invasiveness, and Impaired Colistin-Mediated Cell Death Associated with Colistin Resistance Development in Acinetobacter baumannii. Antimicrob Agents Chemother 2014;58:828–32. doi:10.1128/AAC.01439-13.

[13] Rolain J-M, Diene SM, Kempf M, Gimenez G, Robert C, Raoult D. Real-Time Sequencing To Decipher the Molecular Mechanism of Resistance of a Clinical Pan-Drug-Resistant Acinetobacter baumannii Isolate from Marseille, France. Antimicrob Agents Chemother 2013;57:592–6. doi:10.1128/AAC.01314-12.

[14] Clinical and Laboratory Standards Institute. M07-A10: Methods for Dilution Antimicrobial Susceptibility Tests for Bacteria That Grow Aerobically; Approved Standard—Tenth Edition n.d.:110.

[15] The European Committee on Antimicrobial Susceptibility Testing. Breakpoint tables for interpretation of MICs and zone diameters. Version 8.1, 2018 n.d.

[16] Clinical and Laboratory Standards Institute. Performance standards for antimicrobial susceptibility testing: 24th informational supplement M100-S24 n.d.:110.

[17] European Committee on Antimicrobial Susceptibility Testing. Minocycline: Rationale for the clinical breakpoints, version 1.0, 2009. n.d.

[18] European Committee on Antimicrobial Susceptibility Testing. Rifampicin: Rationale for the clinical breakpoints, version 1.0, 2010. n.d.

[19] Greig SL, Scott LJ. Intravenous Minocycline: A Review in Acinetobacter Infections. Drugs 2016;76:1467–76. doi:10.1007/s40265-016-0636-6.
[20] Hong DJ, Kim JO, Lee H, Yoon E-J, Jeong SH, Yong D, et al. In vitro antimicrobial synergy of colistin with rifampicin and carbapenems against colistin-resistant Acinetobacter baumannii clinical isolates. Diagn Microbiol Infect Dis 2016;86:184–9. doi:10.1016/j.diagmicrobio.2016.07.017.

Table 1. Description of *A. baumannii* isolates and MIC results

			CST (>2[+])	PMB (>2[*])	FOF (n.d.)	CHL (n.d.)	ATM (n.d.)	MEM (>4[+])	MIN (>8[*])	RIF (n.d.)
Strain	**Ref.**	**Description**								
ATCC19606		Reference strain	0.25	0.5	128	64	16	0.5	0.06	1
CS01	[141]	Clinical isolate recovered from CSF of a patient treated for meningitis	0.5	0.25	512	128	32	64	4	>512
CR17	[141]	Isogenic derivative mutant of CR17; single amino acid substitution (Met16Lys) in PmrA	128	8	512	32	32	64	4	>512
062 D6	[142]	Clinical isolate recovered from bronchoscopy of a febrile patient	0.25	0.25	512	8	64	16	0.06	0.25
062 D7	[142]	Isogenic derivative mutant of 062 D6; with duplication of 30 nucleotides in PmrB	256	4	64	16	32	32	0.03	4
248	[143]	Clinical isolate recovered from pus of an ICU patient	0.5	0.5	256	64	128	8	0.25	2
249 pmrB	[143]	Isogenic derivative mutant of 248; single amino acid substitution (Pro233Ser) in PmrB	128	4	256	128	128	4	0.5	2
299	[143]	Clinical isolate recovered from bronchial secretion of an ICU patient	0.5	0.5	512	64	64	16	0.125	2
347 pmrB	[143]	Isogenic derivative mutant of 299; single amino acid substitution (Pro170Leu) in PmrB	64	4	512	32	128	8	0.25	2
ABIsac_ColiS	[144]	Clinical isolate recovered from pulmonary secretions of a pneumonic patient	0.5	0.5	256	64	32	32	0.25	0.125
ABIsac_ColiR	[144]	Isogenic derivative mutant of ABIsac_ColiS; single amino acid substitution in (Glu5Asp) PmrA	128	1	128	128	16	32	0.25	>512

[*] Clinical breakpoint for resistance according to CLSI [13], [+] Clinical breakpoint for resistance according to EUCAST [12], n.d.: not determined. CST : colistin, PMB : polymyxin B, FOF : fosfomycin, CHL : chloramphenicol, ATM :aztreonam, MEM, meropenem, MIN : minocycline, RIF :rifampicin

Table 2: FICI from checkerboard synergy testing. FICIs were determined by checkerboard; the values correspond to the mean of the minimal FICI values for each plate. S: $FICI_{min,avg} \leq 0.5$ = Synergy, NI: $0.5 < FICI_{min,avg} \leq 4$ = No interaction. Grey cells are indicating synergy.

Strain	**Means of $FICI_{min}$**					
	FOF	**CHL**	**ATM**	**MEM**	**MIN**	**RIF**
ATCC19606	0.50 (S)	0.61 (NI)	0.73 (NI)	0.88 (NI)	0.56 (NI)	0.50 (S)
CS01	0.88(NI)	0.52 (NI)	0.69 (NI)	0.79 (NI)	0.81 (NI)	1.00 (NI)
CR17	0.22 (S)	0.63 (NI)	0.31 (S)	0.31 (S)	0.27 (S)	0.10 (S)
062 D6	0.71 (NI)	0.77 (NI)	0.70 (NI)	0.77 (NI)	0.67 (NI)	0.41 (S)
062 D7	0.64 (NI)	0.33 (S)	0.42 (S)	0.50 (S)	0.79 (NI)	0.12 (S)
248	0.69 (NI)	0.69 (NI)	0.52 (NI)	0.55 (NI)	0.55 (NI)	0.39 (S)
249 pmrB	0.45 (S)	0.44 (S)	0.43 (S)	0.38 (S)	0.40 (S)	0.08 (S)
299	0.31 (S)	0.63 (NI)	0.69 (NI)	0.50 (S)	0.53 (NI)	0.69 (NI)
347 pmrB	0.46 (S)	0.59 (NI)	0.31 (S)	0.28 (S)	0.44 (S)	0.09 (S)
ABIsac_ColiS	0.34 (S)	0.56 (NI)	0.66 (NI)	0.50 (S)	0.31 (S)	0.38 (S)
ABIsac_ColiR	0.41 (S)	0.52 (NI)	0.44 (S)	0.44 (S)	0.50 (S)	0.53 (NI)

CST : colistin, PMB : polymyxin B, FOF : fosfomycin, CHL : chloramphenicol, ATM :aztreonam, MEM, meropenem, MIN : minocycline, RIF :rifampicin

Les résultats de cette étude préliminaire ont mis en évidence un intérêt supplémentaire de la polymyxine B vis-à-vis de la colistine, qui contre les souches testées, a montré une efficacité plus grande que la colistine. Aussi elle nous a permis d'identifier des combinaisons intéressantes à des concentrations atteignables en clinique, qu'il nous fallait maintenant étudier plus en détail.

Le choix s'est porté sur la combinaison polymyxine B + minocycline contre la souche CR17 pour plusieurs raisons. Tout d'abord cette combinaison a été identifiée comme étant aussi synergique contre les souches de *K. pneumoniae* et de *P. aeruginosa* étudiées par les autres membres du consortium CO-ACTION. De plus la souche CR17 était la seule souche parmi celles testées à être considérée comme résistante à la polymyxine B vis-à-vis des critères définis par le CLSI[13] et aussi à la limite d'être résistante vis-à-vis de la minocycline selon ces mêmes critères.

X.C.1. Minocycline

La minocycline est une tétracycline de seconde génération mise sur le marché dans les années 60[145,146].

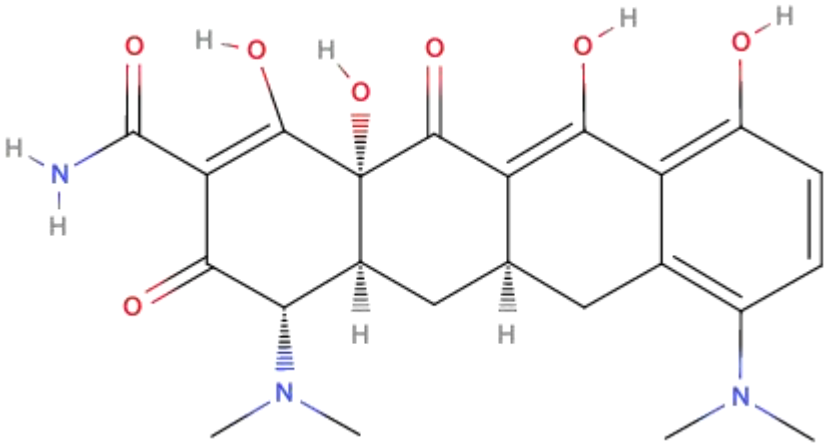

Figure 18 Formule chimique de la minocycline (d'après[147])

X.1.a. Mécanisme d'action

La minocycline agit en se liant à la sous unité 30S du ribosome bactérien, inhibant par ce biais la synthèse protéique[145]

X.1.b. Spectre antibactérien et indications

Cet antibiotique est lipophile à pH physiologique[106] ce qui lui permet une bonne pénétration dans les cellules de l'hôte et dans les bactéries. Cette molécule est disponible en voie orale et intraveineuse et

est aujourd'hui utilisée principalement contre les organismes multirésistants, y compris *A. baumannii* après avoir établi que la souche y était sensible[148,149]

X.1.c. Mécanismes de résistance

La minocycline n'est pas affectée par les mécanismes classiques de résistances aux tétracyclines, les pompes d'efflux AdeABC, TetA ou la protection ribosomale conférée par une mutation de *tetM*. La principale forme de résistance d'*A. baumannii* à la minocycline est associée au gène *tetB* qui code pour une pompe d'efflux et il a été montré lors d'une étude sur 258 souches que le gène était absent chez les 93 souches classées comme sensibles par leur CMI et qu'il était présent chez 154 des 165 (93.3%) souches classées comme résistantes par leur CMI[150].

Pour aller au-delà des études de checkerboards de l'article 3, une étude de la PK/PD de l'association polymyxine B et minocycline contre la souche CR17 est présentée dans l'article 4. Cette étude *in vitro* comprend des données de bactéricidie avec suivi de la densité de bactéries résistantes à la polymyxine B, enrichies d'expériences complémentaires servant à préciser les caractéristiques de cette sous-population résistante. Ces données ont toutes été analysées par modélisation PK/PD semi-mécanistique afin d'en extraire un maximum d'information.

X.D. Article 4. Semi-mechanistic PK-PD modelling of combined polymyxin B and minocycline against a polymyxin-resistant strain of *Acinetobacter baumannii*

Submitted to Clinical Microbiology and Infection

Intended category: Original article

Title: *Semi-mechanistic PK-PD modelling of combined polymyxin B and minocycline against a polymyxin-resistant strain of Acinetobacter baumannii*

Authors: Vincent Aranzana-Climent (1,2), Julien M. Buyck (1,2), Younes Smani (3,4), Jerónimo Pachón-Diaz (3), Sandrine Marchand (1,2,5), William Couet (1,2,5), Nicolas Grégoire* (1,2,5)

Institutions:
(1) Université de Poitiers, Pharmacologie des anti-infectieux, Poitiers, France,
(2) INSERM U1070 - Pharmacologie des anti-infectieux, Poitiers, France,
(3) Institut of Biomedicine of Seville (IBiS), Seville, Spain,
(4) University Hospital Virgen del Rocio/CSIC/University of Seville, Seville, Spain,
(5) CHU de Poitiers, Service de Pharmacologie-Toxicologie, Poitiers, France

* Corresponding author,

Address : Université de Poitiers - Pole Biologie Sante
Bâtiment B36/B37 - 1 Rue Georges Bonnet

TSA 51106 -86073 POITIERS Cedex 9 – France

Email: nicolas.gregoire@univ-poitiers.fr

tel: +33549366436, fax: +33549454378

Keywords: PK/PD modelling, combinations, GPDI, polymyxin B, minocycline, *Acinetobacter baumannii*

Abstract

Objectives

The goal of this study was to expand on previous reports of synergy between polymyxin B and minocycline against *Acinetobacter baumannii* and gain insights on the qualitative and quantitative determinants of the synergy.

Methods

A semi-mechanistic PK/PD model was developed based on *in vitro* time-kill experiments data with determination of resistant bacterial count to describe the effects of polymyxin B and minocycline alone and in combination. The model was enriched by complementary experiments providing information on the characteristics of the resistant sub-population.

Results

The model successfully described the data and made possible quantification of the strength of interaction between the two drugs and to formulation of hypotheses about the mechanisms of the observed interaction. Synergy between polymyxin B and minocycline is confirmed on a polymyxin B resistant *A. baumannii* strain. The effect of the combination is driven by minocycline and concentrations above 1 mg/L prevent selection of the polymyxin B resistant subpopulation.

Conclusions

Synergy observed in checkerboards between polymyxin B and minocycline is confirmed on a polymyxin B resistant *A. baumannii* strain. The main effect of the combination is driven by minocycline and concentrations above 1 mg/L prevent selection of the polymyxin B resistant subpopulation in addition to reduce adaptive resistance to polymyxin B, in addition low concentrations (0.1 mg/L) of polymyxin B are sufficient to significantly enhance minocycline efficacy.

Introduction

Acinetobacter baumannii is one of the most difficult to treat multi-drug resistant (MDR) pathogens responsible for opportunistic nosocomial infections worldwide [1]. It can cause a broad range of infections, the deadliest being ventilator-associated pneumonia and bloodstream infections [2] and has the ability to become resistant to a wide variety of drugs [3]. In face of these resistances, interest in using neglected and disused antibiotics like polymyxins (colistin and polymyxin B (PMB)) has surged, especially in combination with other antibiotics, as the last line of defence against MDR *A. baumannii* [4].

Semi-mechanistic PK/PD modelling is a valuable tool that can be used to quantify concentration-effect curves and describe bacterial resistance [5], and is especially useful in the context of drug combination when both drugs concentrations are linked with the effect [6].

Previous works studied polymyxin-based combinations against *A. baumannii*, mainly with carbapenems [7–9], rifampicin [7,10,11], tigecycline [12–15], and minocycline (MIN) [16,17]. While semi-mechanistic PK/PD modelling was applied to the other combinations, for the PMB and MIN combination, analysis was limited to qualitative assessment of synergy.

The goal of this study was to expand on previous reports of synergy between PMB and MIN against *A. baumannii* by developing a semi-mechanistic PK/PD model based on extensive *in vitro* time-kill experiments with determination of resistant bacterial count, thus gaining insights on the qualitative and quantitative determinants of the interaction between PMB and MIN.

Methods

Antibiotics

MIN sulphate and PMB sulphate were obtained from Merck (Germany).

Strain

A previously described colistin-resistant *A. baumannii* clinical isolate (CR17) [18], collected from patient cerebro-spinal-fluid after treatment by colistin was used with PMB and MIN MICs of 8 mg/L and 4 mg/L, respectively.

Heteroresistance to PMB and MIN

One microliter of frozen bacteria were taken from -80°C storage and put in 50 mL of cation-adjusted Mueller-Hinton broth (Ca-MHB) then incubated overnight at 37°C with shaking at 150 rpm. The resulting culture was centrifuged at 4000 *g* for 15 min, broth was removed, then bacteria were resuspended in 5 mL of Ca-MHB. Serially diluted samples were plated using a easySpiral automatic plater (Interscience, France) on drug-free Mueller-Hinton E plates (MHE) (Biomérieux, France) and on Mueller-Hinton Agar II plates (MHA-II) (Merck, Germany) containing 8 to 256 mg/L of PMB or 4 to 128 mg/L of MIN. Plates were incubated at 37°C for 24 h then colonies were counted using a SCAN 300 colony counter (Interscience, France). The experiment was repeated 6 times.

Growth rate determination

Following the heteroresistance fraction determination, colonies that grew on drug-free MHE plates and drug-containing MHA-II plates were harvested and suspended in Ca-MHB. An initial inoculum of 10^6 CFU/mL (0.1 OD at 600 nm diluted 100 fold) was prepared in Ca-MHB, and 200 µL were added in 11 wells per colony type in a polypropylene 96 well plate. The 12^{th} well contained 200 µL of bacteria-free, drug-free media and was used as negative control. Plates were incubated at 37°C in a Tecan Infinite 200 PRO plate reader (Tecan, Switzerland). OD at 600 nm was measured every 5 min over 24 h. The maximum growth rate (MGR) of bacteria was calculated as described in [20]. The experiment was repeated 4 times.

Kill curve + population analysis profiles

Static time-kill experiments (TKE) were performed. An initial inoculum of 10^6 CFU/mL was prepared in Ca-MHB and PMB, MIN or a combination of both were added to the media. A drug-free control was also prepared. PMB concentrations ranged from 0.0625 to 8 mg/L and MIN concentrations ranged from 0.25 to 16 mg/L. Limit of quantification was 200 CFU/mL. The preparation was incubated at 37°C with shaking at 150 rpm for 30 h. Samples were taken at t = 0, 3, 8, 24 and 30 h, diluted serially and each dilution was plated on a MHE plate and a MHA-II plate containing 64 mg/L of PMB, using an easySpiral automatic plater (Interscience, France). Plates were incubated for 24 h at 37°C and counted as previously described

pmrA, pmrB, lpxA, lpxC, lpxD genes amplification and sequencing

In order to investigate the possible contribution of *pmrAB* and *lpxACD* operons modifications to polymyxin resistance in *A. baumannii* after 30 h of growth in drug-free media, in presence of 1 mg/L MIN + 0.0625 mg/L PMB or in presence of 1 mg/L MIN + 0.125 mg/L PMB, genes were sequenced and analysed to detect any genetic alteration. DNA samples were obtained from bacteria that grew on drug-free and on drug-containing plates at t = 0 and 30 h, by heating the colonies in water at 96°C. The genes were amplified and the obtained bands were purified with the kit MEGAquick-spin plus (iNtRON Biotechnology, WA) and sequenced at the Institute of Biomedicine of Seville (Spain). The nucleotide and deduced protein sequences were analysed using the Serial Cloner program (http://serialbasics.free.fr/Serial_Cloner.html).

Semi-mechanistic PK/PD modelling

Semi-mechanistic PK/PD modelling was performed to quantify the exposure-effect relationships of both drugs given alone or in combination. Model building is detailed in **Text S1**. The number of

subpopulations was determined from the results of the heteroresistance fraction determination experiment. Interaction between the two drugs and their effects on bacterial growth was modelled using the GPDI model developed by Wicha et al. [21], under the simple effect addition hypothesis. PMB was assumed to be stable *in vitro* as shown previously [22]. MIN was shown to be stable over 24 h in separate experiments (data not shown). Dataset preparation was performed using R, parameter estimation was performed using NONMEM (ICON, Ireland) version 7.4.2.

Influence of interaction effect on total effect

To evaluate the contribution of each model component to the global effect of the combination, simulations of expected typical bacterial counts over time with the final model were performed under various scenarios: Then for each simulated curve, area under the curve of $\log_{10}$(CFU/mL) *versus* time (AUBC), was calculated. From these AUCs a percentage of effect imputable to the component removed from model was calculated according to the following equation:

$$\%\ Imputable\ Effect = 1 - \frac{AUBC_{Control} - AUBC_{reduced\ model}}{AUBC_{Control} - AUBC_{final\ model}}$$

R code is given in **Code S2**.

Results

Heteroresistance to PMB and MIN

Bacterial growth was seen on plates containing up to 64 mg/L (8*MIC) of PMB. At 64 mg/L of PMB the mean frequency of highly resistant bacteria was 5.07 $*10^{-6}$ (range [$1.22*10^{-5}$ - $7.68*10^{-7}$], n = 6), however bacteria were not able to grow on plates containing MIN at concentrations higher than 8 mg/L (2*MIC).

Growth rate determination

Mean MGR of bacteria that grew on drug-free plates was 1.12 h^{-1} (sd: 0.0372 h^{-1}, n = 44), was almost identical to the mean MGR of bacteria that grew on plates containing 64 mg/L of PMB which was 1.08 h^{-1} (sd: 0.0241 h^{-1}, n = 43), demonstrating a very limited if any fitness cost.

Kill curve + population analysis profiles

Mean CFU counts for total and highly resistant bacteria for selected concentrations are shown on **Figure 1** and plots of all individual data points are given in **Figure S1**.

In single drug TKE, using MIN concentrations of lower than 4 mg/L resulted in regrowth and an amplification of highly resistant bacteria at 30 h with a median fraction of $10^{-1.79}$ with 2 mg/L of MIN compared to $10^{-4.13}$ for the drug-free control. Using PMB concentration of 8 mg/L and below resulted in regrowth and amplification of highly resistant bacteria at 30 h with a median fraction of $10^{-0.54}$ with 8 mg/L of PMB compared to $10^{-4.13}$ for the drug-free control.

When combining MIN and PMB, increasing the MIN concentration to 1 mg/L and above had an important impact on the initial decrease and regrowth over 30 h whereas increasing PMB concentration did not improve the effect as much; e.g. combining 1 mg/L of MIN with 0.5 mg/L of PMB prevented regrowth at 30 h for 2 out of 3 replicates. When regrowth was not prevented by the combination, highly resistant bacteria were selected with a fraction of $10^{-0.29}$ compared to $10^{-4.13}$ for the drug-free control.

pmrA, pmrB, lpxA, lpxC, lpxD genes amplification and sequencing

On top of a M12K mutation in *pmrA* [18], no additional change in *pmrB*, *lpxA*, *lpxC*, *lpxD* sequenced genes was found after 30 h of growth in drug-free or drug-containing media in DNA extracted from total (mostly R) and from highly resistant (HR) CR17 bacteria.

Mathematical modelling

A schematic representation of the final model is shown in **Figure 2.** The final differential equations for the model are given in **Text S2**. Final parameter estimates are given in **Table 1.** VPCs of the final model are shown in **Figure S2**. NPDE of the final model are shown in **Figure S3.** Final model code is given in **Code S1.**

The final model had two subpopulations: resistant (R) bacteria to PMB, growing on drug-free plates only and highly resistant (HR) bacteria to PMB, able to grow on drug-free plates and plates containing 64 mg/L of PMB with the same natural growth rate (k_{net} = 1.11 h^{-1}), the initial fraction of HR bacteria (mutf) was estimated to be $10^{-5.10}$.

Both drugs increased the bacterial death rate, with a concentration-effect relationship following a linear-power model for PMB and a sigmoidal E_{max} model for MIN. The kill rate constant due to PMB was reduced by 41% for the HR subpopulation when compared with the R subpopulation ($k_{slope,PMB-R}$ = 4.94 mg/L/h > $k_{slope,PMB-HR}$ = 3.00 mg/L/h) and the EC_{50} of MIN was 64% higher for the HR subpopulation when compared with the R subpopulation ($EC_{50,MIN-R}$ = 1.02 mg/L < $EC_{50,MIN-HR}$ = 1.67 mg/L).

Both subpopulations were able to develop adaptive resistance to PMB with the same rate constant $k_{on0,PMB}$ =0.646 h^{-1}, but no adaptive resistance to MIN was identified.

No potentiation of PMB killing by MIN was identified. Interaction between PMB and MIN was integrated in the final model as a reduction of the rate of adaptation to PMB by MIN by a maximum of 29% in presence of 0.1 mg/L and more of PMB (INT_{ADA} = - 29.2 %), and potentiation of MIN killing effect by PMB with a maximum reduction of MIN EC_{50} by 49% in presence of 1 mg/L and more of MIN (INT_{PMB} = - 49.3 %).

Influence of interaction effect on total effect

Four scenarios were simulated: control without antibiotics, final model, inhibition of adaptation to PMB by MIN removed from the model (INT_{ADA}=0) and potentiation of MIN killing effect by PMB removed from the model (INT_{PMB}=0).

For all tested concentrations, increase of MIN kill rate by PMB is a significant contributor while inhibition of adaptation to PMB by MIN becomes significant when MIN concentration is above 1 mg/L. Inhibition of adaptation to PMB by MIN, accounted for at most 20% (median:7% range: [0%-20%]) of the total effect. For most concentrations it was responsible for a smaller part of the total effect than the potentiation effect of MIN by PMB which accounted for as much as 52% (median:30% range: [15%-52%]) of the total effect

Simulations for selected concentrations are presented on **Figure 3** and simulations for all tested concentrations are presented in **Figure S4**.

Discussion

To our knowledge there are only two other studies about the combination of PMB and MIN against *A. baumannii* [16,17]. Zhang *et al.* performed checkerboards on 25 strains having PMB and MIN MIC around breakpoints (PMB = 4 mg/L, MIN = 8 mg/L [23]) and found synergy 44% of the time and no antagonism. Bowers *et al.* performed *in vitro* TKE and *in vivo* lung infection experiments against 4 strains, *in vitro* and *in vivo* synergy was observed on a strain with PMB and MIN MIC 4-fold lower than CR17 strain MICs. The synergy observed in the current study is in accordance with these previous works with the added value of testing a wide range of concentrations, performing mechanistic experiments (fitness cost, heteroresistance) and developing a semi-mechanistic PK/PD model integrating all produced data to gain quantitative insight.

In this study, PMB combined with MIN was shown to be synergistic against a polymyxin-resistant *A. baumannii* clinical isolate. Using clinically achievable concentrations of both antibiotic individually

resulted in bacterial killing or, when MIN concentration was lower than 1 mg/L in selection of HR bacteria. This HR subpopulation was present before treatment and did not exhibit *in vitro* fitness cost.

The final PK/PD model included heteroresistance and adaptive resistance to PMB. These two approaches to model antibiotic resistance are usually not used together in a final model due to identifiability problems [24]. But, in this work the typical experimental protocol was expanded by first determining the fraction of bacteria that could grow on plates containing PMB and also improving TKE by adding counts on drug-containing plates, to enable direct counting of highly resistant bacteria over time. This enabled making parameters for both resistance mechanisms identifiable. In a similar vein, model selection was guided by fitness cost experiments which determined that no change in growth was observed in the highly resistant subpopulation, enabling reduction of the model based on mechanistic information.

Interaction between PMB and MIN was integrated in the final model as a reduction of the rate of adaptation to PMB by MIN and potentiation of MIN killing effect by PMB. The fraction of the total effect imputable to interaction between the two molecules was calculated for each pair of concentrations tested. It was shown that maintaining MIN concentrations at least 1 mg/L maximized the contribution of both interactions to the total effect.

The HR subpopulation was less susceptible to PMB but also to MIN which was not expected given that the drugs have different sites of action and that no other study reported it. One potential explanation could be that a change of membrane charge in the highly resistant subpopulation, making it harder for PMB to bind to Lipid A of LPS as described previously [25], would also make it harder for MIN to get into the cell, because of its basicity, as it would bind to the cell membrane instead.

Yet, it was not possible to identify a genetic specificity of the highly resistant subpopulation by amplification the usual resistance genes. It could be interesting to sequence the whole genome using NGS or WGS techniques to find the determinants of this resistance in order to fight them more efficiently, especially given that this specific resistance does not seem to come with diminished fitness. Alternatively, or in addition, analysis of gene expression by RT-qPCR could help explain the difference between the two subpopulations.

Potentiation of MIN by PMB is observed on both resistant and highly resistant subpopulations and a low concentration of PMB is sufficient to reach maximum synergy with a 49% reduction of MIN EC_{50} on both subpopulations for 0.1 mg/L of PMB. Mechanistically this could be explained by PMB opening up the bacterial membrane to increase MIN uptake into the cell, and Bowers *et al.* showed an increase of intracellular MIN concentration when bacteria were treated by PMB at a low concentration (0.5 mg/L) and MIN in combination [17].

Usually, adaptive resistance is seen as a change in expression of resistance genes when the bacteria is in presence of antibiotic [26,27]. Hence, inhibition of adaptation to PMB by MIN could be explained by the mechanism of action of MIN. Indeed, MIN acts by inhibiting the 30S subunit of ribosomes [28], therefore reducing overall expression of bacterial genes.

In conclusion, PMB and MIN were synergistic against a PMB resistant *A. baumannii* strain. The main effect of the combination is driven by MIN and concentrations above 1 mg/L prevent selection of the highly resistant subpopulation in addition to reduce adaptive resistance to PMB. Low concentrations (0.1 mg/L) of PMB are sufficient to significantly enhance MIN efficacy.

Conflict of interest statement: None to declare

Funding information: This study was jointly supported by the Joint Programming Initiative on Antimicrobial Resistance (JPIAMR) and Agence Nationale de la Recherche (ANR) under the research grant "CO-ACTION".

Acknowledgements

We would like to thank Lena Friberg for her input related to the model building. We would also like to thank Emma Marquizeau for her excellent technical support. We would also like to thank Helene Mirfendereski for performing minocycline assays.

Author Contributions

Vincent Aranzana-Climent: Wrote Manuscript, Designed Research, Performed Microbiology and Pharmacodynamic Experiments and Performed modelling.

Julien Buyck: Wrote Manuscript, Designed Research, Analysed Data

Younes Smani: Performed Genetic Experiments, Reviewed Manuscript

Jerónimo Pachón-Diaz: Performed Genetic Experiments, Reviewed Manuscript

Sandrine Marchand: Reviewed Manuscript, Designed Research

William Couet: Reviewed Manuscript, Designed Research

Nicolas Grégoire: Wrote Manuscript, Designed Research, Analysed Data

References

[1] Antunes LCS, Visca P, Towner KJ. Acinetobacter baumannii: evolution of a global pathogen. Pathog Dis 2014;71:292–301. doi:10.1111/2049-632X.12125.

[2] Dijkshoorn L, Nemec A, Seifert H. An increasing threat in hospitals: multidrug-resistant *Acinetobacter baumannii*. Nat Rev Microbiol 2007;5:939–51. doi:10.1038/nrmicro1789.

[3] Fournier P-E, Vallenet D, Barbe V, Audic S, Ogata H, Poirel L, et al. Comparative Genomics of Multidrug Resistance in Acinetobacter baumannii. PLOS Genet 2006;2:e7. doi:10.1371/journal.pgen.0020007.

[4] Nation RL, Li J, Cars O, Couet W, Dudley MN, Kaye KS, et al. Framework for optimisation of the clinical use of colistin and polymyxin B: the Prato polymyxin consensus. Lancet Infect Dis 2015;15:225–34. doi:10.1016/S1473-3099(14)70850-3.

[5] Nielsen EI, Friberg LE. Pharmacokinetic-pharmacodynamic modeling of antibacterial drugs. Pharmacol Rev 2013;65:1053–90. doi:10.1124/pr.111.005769.

[6] Brill MJE, Kristoffersson AN, Zhao C, Nielsen EI, Friberg LE. Semi-mechanistic pharmacokinetic–pharmacodynamic modelling of antibiotic drug combinations. Clin Microbiol Infect 2017;0. doi:10.1016/j.cmi.2017.11.023.

[7] Hong DJ, Kim JO, Lee H, Yoon E-J, Jeong SH, Yong D, et al. In vitro antimicrobial synergy of colistin with rifampicin and carbapenems against colistin-resistant Acinetobacter baumannii clinical isolates. Diagn Microbiol Infect Dis 2016;86:184–9. doi:10.1016/j.diagmicrobio.2016.07.017.

[8] Lenhard JR, Bulitta JB, Connell TD, King-Lyons N, Landersdorfer CB, Cheah S-E, et al. High-intensity meropenem combinations with polymyxin B: new strategies to overcome carbapenem resistance in Acinetobacter baumannii. J Antimicrob Chemother 2017;72:153–65. doi:10.1093/jac/dkw355.

[9] Rao GG, Ly NS, Bulitta JB, Soon RL, San Roman MD, Holden PN, et al. Polymyxin B in combination with doripenem against heteroresistant Acinetobacter baumannii: pharmacodynamics of new dosing strategies. J Antimicrob Chemother 2016;71:3148–56. doi:10.1093/jac/dkw293.

[10] Lim T-P, Tan T-Y, Lee W, Sasikala S, Tan T-T, Hsu L-Y, et al. In-Vitro Activity of Polymyxin B, Rifampicin, Tigecycline Alone and in Combination against Carbapenem-Resistant Acinetobacter baumannii in Singapore. PLOS ONE 2011;6:e18485. doi:10.1371/journal.pone.0018485.

[11] Song JY, Kee SY, Hwang IS, Seo YB, Jeong HW, Kim WJ, et al. In vitro activities of carbapenem/sulbactam combination, colistin, colistin/rifampicin combination and tigecycline against carbapenem-resistant Acinetobacter baumannii. J Antimicrob Chemother 2007;60:317–22. doi:10.1093/jac/dkm136.

[12] Bae S, Kim M-C, Park S-J, Kim HS, Sung H, Kim M-N, et al. In Vitro Synergistic Activity of Antimicrobial Agents in Combination against Clinical Isolates of Colistin-Resistant Acinetobacter baumannii. Antimicrob Agents Chemother 2016;60:6774–9. doi:10.1128/AAC.00839-16.

[13] Cai X, Yang Z, Dai J, Chen K, Zhang L, Ni W, et al. Pharmacodynamics of tigecycline alone and in combination with colistin against clinical isolates of multidrug-resistant Acinetobacter baumannii in an in vitro pharmacodynamic model. Int J Antimicrob Agents 2017;49:609–16. doi:10.1016/j.ijantimicag.2017.01.007.

[14] Dizbay M, Tozlu DK, Cirak MY, Isik Y, Ozdemir K, Arman D. In vitro synergistic activity of tigecycline and colistin against XDR-Acinetobacter baumannii. J Antibiot (Tokyo) 2009;63:51–3. doi:10.1038/ja.2009.117.

[15] Rao GG, Ly NS, Diep J, Forrest A, Bulitta JB, Holden PN, et al. Combinatorial pharmacodynamics of polymyxin B and tigecycline against heteroresistant Acinetobacter baumannii. Int J Antimicrob Agents 2016;48:331–6. doi:10.1016/j.ijantimicag.2016.06.006.

[16] Zhang Y, Chen F, Sun E, Ma R, Qu C, Ma L. In vitro antibacterial activity of combinations of fosfomycin, minocycline and polymyxin B on pan-drug-resistant Acinetobacter baumannii. Exp Ther Med 2013;5:1737–9. doi:10.3892/etm.2013.1039.

[17] Bowers DR, Cao H, Zhou J, Ledesma KR, Sun D, Lomovskaya O, et al. Assessment of Minocycline and Polymyxin B Combination against Acinetobacter baumannii. Antimicrob Agents Chemother 2015;59:2720. doi:10.1128/AAC.04110-14.
[18] López-Rojas R, McConnell MJ, Jiménez-Mejías ME, Domínguez-Herrera J, Fernández-Cuenca F, Pachón J. Colistin Resistance in a Clinical Acinetobacter baumannii Strain Appearing after Colistin Treatment: Effect on Virulence and Bacterial Fitness. Antimicrob Agents Chemother 2013;57:4587–9. doi:10.1128/AAC.00543-13.
[19] Aranzana-Climent V, Chauzy A, Grégoire N, Marchand S, Couet W, Buyck J. In vitro activity of polymyxin B alone and in combination against colistin-resistant Acinetobacter baumannii, ECCMID, Amsterdam: 2019.
[20] Bleibtreu A, Gros P-A, Laouénan C, Clermont O, Le Nagard H, Picard B, et al. Fitness, Stress Resistance, and Extraintestinal Virulence in Escherichia coli. Infect Immun 2013;81:2733–42. doi:10.1128/IAI.01329-12.
[21] Wicha SG, Chen C, Clewe O, Simonsson USH. A general pharmacodynamic interaction model identifies perpetrators and victims in drug interactions. Nat Commun 2017;8:2129. doi:10.1038/s41467-017-01929-y.
[22] Orwa JA, Govaerts C, Gevers K, Roets E, Van Schepdael A, Hoogmartens J. Study of the stability of polymyxins B1, E1 and E2 in aqueous solution using liquid chromatography and mass spectrometry. J Pharm Biomed Anal 2002;29:203–12. doi:10.1016/S0731-7085(02)00016-X.
[23] Clinical and Laboratory Standards Institute. Methods for Dilution Antimicrobial Susceptibility Tests for Bacteria That Grow Aerobically; Approved Standard—Ninth Edition. CLSI document M07-A9. Wayne, PA: Clinical and Laboratory Standards Institute: 2012.
[24] Jacobs M, Grégoire N, Couet W, Bulitta JB. Distinguishing Antimicrobial Models with Different Resistance Mechanisms via Population Pharmacodynamic Modeling. PLoS Comput Biol 2016;12. doi:10.1371/journal.pcbi.1004782.
[25] Beceiro A, Llobet E, Aranda J, Bengoechea JA, Doumith M, Hornsey M, et al. Phosphoethanolamine Modification of Lipid A in Colistin-Resistant Variants of Acinetobacter baumannii Mediated by the pmrAB Two-Component Regulatory System. Antimicrob Agents Chemother 2011;55:3370–9. doi:10.1128/AAC.00079-11.
[26] Barin J, Martins AF, Heineck BL, Barth AL, Zavascki AP. Hetero- and adaptive resistance to polymyxin B in OXA-23-producing carbapenem-resistant Acinetobacter baumannii isolates. Ann Clin Microbiol Antimicrob 2013;12:15. doi:10.1186/1476-0711-12-15.
[27] Skiada A, Markogiannakis A, Plachouras D, Daikos GL. Adaptive resistance to cationic compounds in Pseudomonas aeruginosa. Int J Antimicrob Agents 2011;37:187–93. doi:10.1016/j.ijantimicag.2010.11.019.
[28] Ritchie DJ, Garavaglia-Wilson A. A Review of Intravenous Minocycline for Treatment of Multidrug-Resistant Acinetobacter Infections. Clin Infect Dis 2014;59:S374–80. doi:10.1093/cid/ciu613.
[29] Comets E, Brendel K, Mentré F. Computing normalised prediction distribution errors to evaluate nonlinear mixed-effect models: the npde add-on package for R. Comput Methods Programs Biomed 2008;90:154–66. doi:10.1016/j.cmpb.2007.12.002.
[30] Beal SL. Ways to Fit a PK Model with Some Data Below the Quantification Limit. J Pharmacokinet Pharmacodyn 2001;28:481–504. doi:10.1023/A:1012299115260.

Table 1. Final model parameters

Parameter	Description	Value [CI95%]*
k_{net} (h^{-1})	Apparent growth rate constant	1.11 [1.03 -1.20]
B_{max} (CFU/mL)	Maximum capacity of the in vitro system	$10^{8.41}$ [$10^{8.34}$-$10^{8.48}$]
mutf	Fraction of resistant bacteria at time = 0	$10^{-5.10}$ [$10^{-5.28}$- $10^{-4.92}$]
Polymyxin B		
$k_{slope,PMB-R}$ (mg/L/h)	Kill rate constant due to polymyxin B on resistant subpopulation	4.94 [4.32 -5.59]
$k_{slope,PMB-HR}$ (mg/L/h)	Kill rate constant due to polymyxin B on highly resistant subpopulation	3.00 [2.57-3.51]
γ_{PMB}	Power parameter for polymyxin B effect on both subpopulations	0.292 [0.265-0.321]
$k_{on0,PMB}$ (h^{-1})	Rate constant for development of adaptive resistance to polymyxin B in absence of minocycline	0.646 [0.538 -0.760]
$k_{off,PMB}$ (h^{-1})	Rate constant for reversal of adaptive resistant to polymyxin B	0 (fixed)
Minocycline		
$E_{max,MIN}$ (h^{-1})	Maximum rate constant for minocycline effect on both subpopulations	1.41 [1.31 -1.51]
$EC_{50,MIN-R}$ (mg/L)	Minocycline concentration for which the effect is 50% on the resistant subpopulation	1.02 [0.90-1.13]
$EC_{50,MIN-HR}$ (mg/L)	Minocycline concentration for which the effect is 50% on the highly resistant subpopulation	1.67 [1.46-1.86]
γ_{MIN}	Power parameter for minocycline effect on both subpopulations	1.59 [1.40-1.79]
INTERACTION		
INT_{PMB} (%)	Maximal reduction of $EC_{50,MIN-S}$ and $EC_{50,MIN-R}$ due to potentiation by polymyxin B	-49.3 [-55.0- -42.6]

$EC_{50,INT\ PMB}$ (mg/L)	Polymyxin B concentration needed to achieve 50% of INT_{PMB}	0.0615 [0.0.570 – 0.0673]
$H_{INT\text{-}PMB}$	Power parameter for polymyxin B potentiation of minocycline effect	10 (fixed)
INT_{ADA} (%)	Maximal reduction of k_{on} due to inhibition by minocycline	-29.2 [-39.7 - -19.8]
$EC_{50,INT\text{-}ADA}$ (mg/L)	Minocycline concentration needed to reach 50% of INT_{ADA}	0.634 [0.547-0.801]
$H_{INT\ ADA}$	Power parameter for minocycline inhibition of k_{on}	10 (fixed)
RESIDUALS		
$\sigma_{total\ bacteria}$ (log_{10}CFU/mL)	Additive residual error on log_{10} scale for total bacteria count	0.474 [0.420 – 0.546]
$\sigma_{\ highly\ resistant\ bacteria}$ (log_{10}CFU/mL)	Additive residual error on log_{10} scale for highly resistant bacteria count	1.28 [1.07– 1.56]
Correlation	Correlation between $\sigma_{total\ bacteria}$ and $\sigma_{\ highly\ resistant\ bacteria}$	0.426 [0.317 - 0.537]

*CI obtained by SIR

Figures

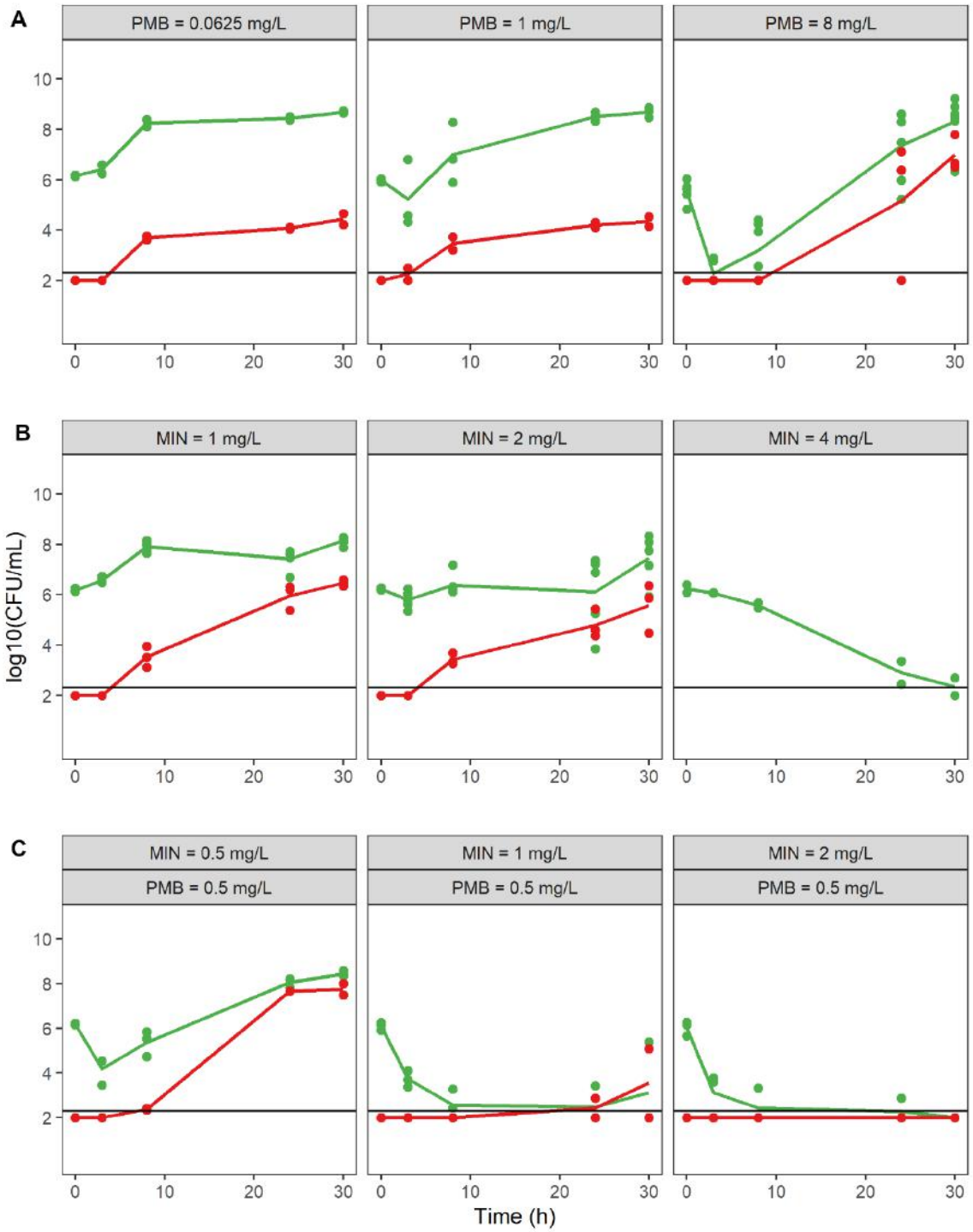

Figure 1. Time-kill experiment results for selected concentrations. Points represent experimental data. Lines represent geometrical means of the data. Green represents total bacteria (counted on drug-free plates) and red represents highly resistant bacteria (counted on plates containing 64 mg/L of polymyxin B). **A.** Polymyxin B alone; **B.** Minocycline alone; **C.** Polymyxin B + Minocycline combination. Full results are given in **Figure S1.** MIN: minocycline, PMB: polymyxin B.

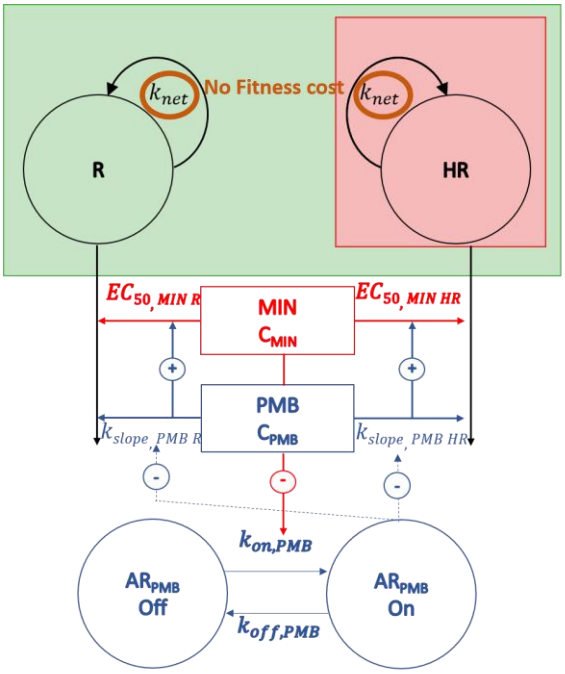

Figure 2. Schematic representation of the final model. R : resistant subpopulation; HR : highly resistant subpopulation; green area represents total bacteria (counted on drug-free plates) and red area represents highly resistant bacteria (counted on plates containing 64 mg/L of polymyxin B). k_{net} : apparent growth rate; C_{MIN} : minocycline concentration; $EC_{50,MIN\ R}$ and $EC_{50,MIN,HR}$: minoycline concentration for which the effect is 50% on R and HR subpopulations respectively; C_{PMB}: polymyxin B concentration; $k_{slope,PMB,R}$ and $k_{slope,PMB,HR}$: rate constant of polymyxin B effect on R and HR subpopulations respectively; $AR_{PMB,\ off}$ and $AR_{PMB,on}$ states of adaptive resistance to polymyxin B; $k_{on,PMB}$: rate constant for development of adaptive resistance to polymyxin B; $k_{off,PMB}$: rate constant for reversal of adaptive resistance to polymyxin B. The + and – symbols respectively represent an increase or a decrease of the parameter targeted by the arrow by the parameter at the base of it. Only the main parameters are illustrated, the model equations can be found in **text S2**. MIN: minocycline, PMB: polymyxin B

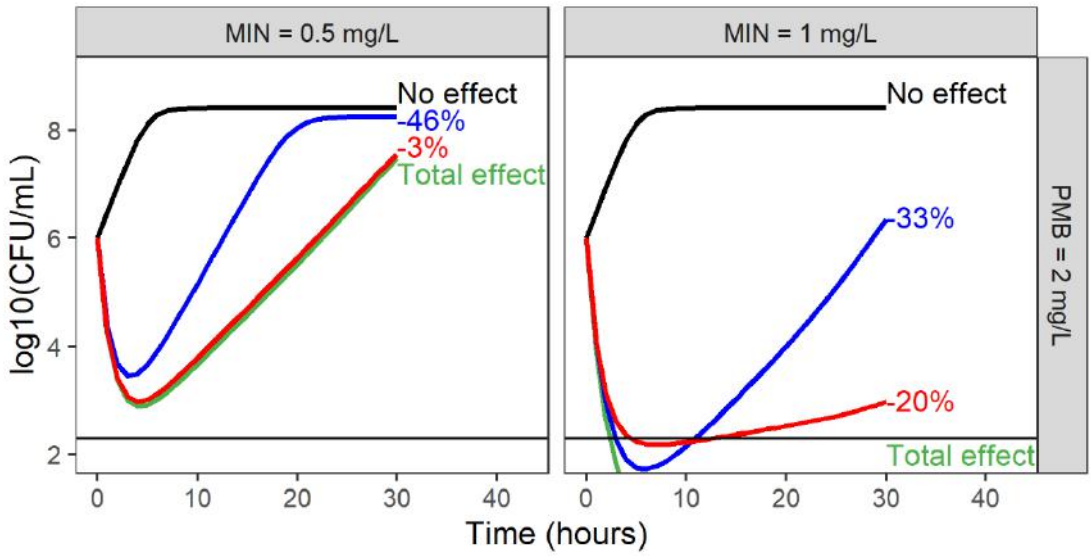

Figure 3. Simulations of expected log10(CFU/mL) versus time in presence of 2 mg/L of polymyxin B combined with 0.5 mg/L of minocycline (left column) or 1 mg/L of minocycline (right column) for different model parametrisations: black: absence of effect, green: under the final model; blue: under the final model with potentialization of minocycline by polymyxin B set to 0; red: under the final model with inhibition of adaptation to polymyxin B by minocycline set to 0. Percentages represent the part of the total effect imputable to the removed component. MIN: minocycline, PMB: polymyxin B

.

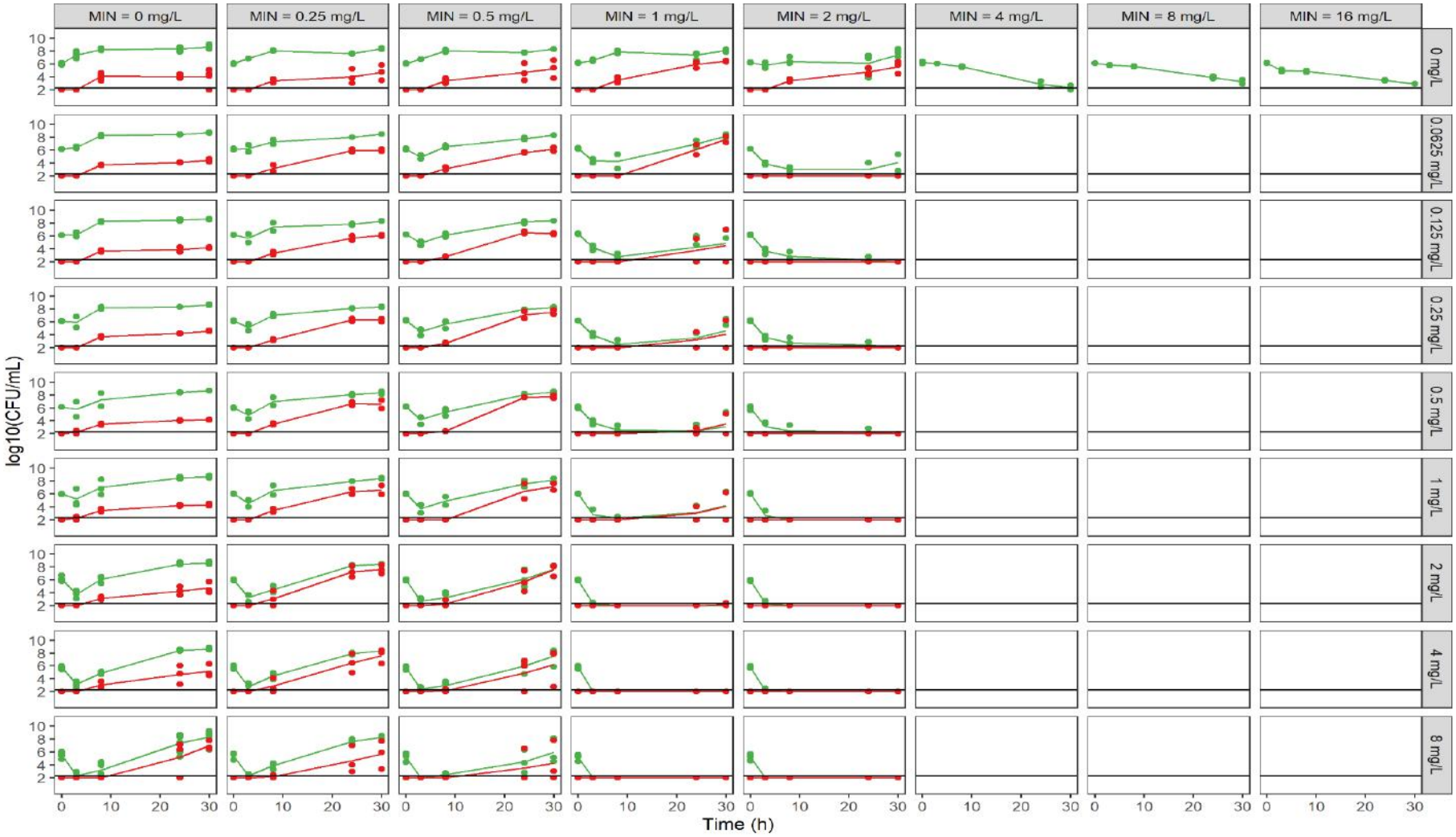

Figure S1. All experimental data. Points represent experimental data. Lines represent geometrical means of the data. Green represents total bacteria (counted on drug-free plates) and red represents highly resistant bacteria (counted on plates containing 64 mg/L of polymyxin B). Each column corresponds to a minocycline (MIN) concentration and each line is a polymyxin B (PMB) concentration.

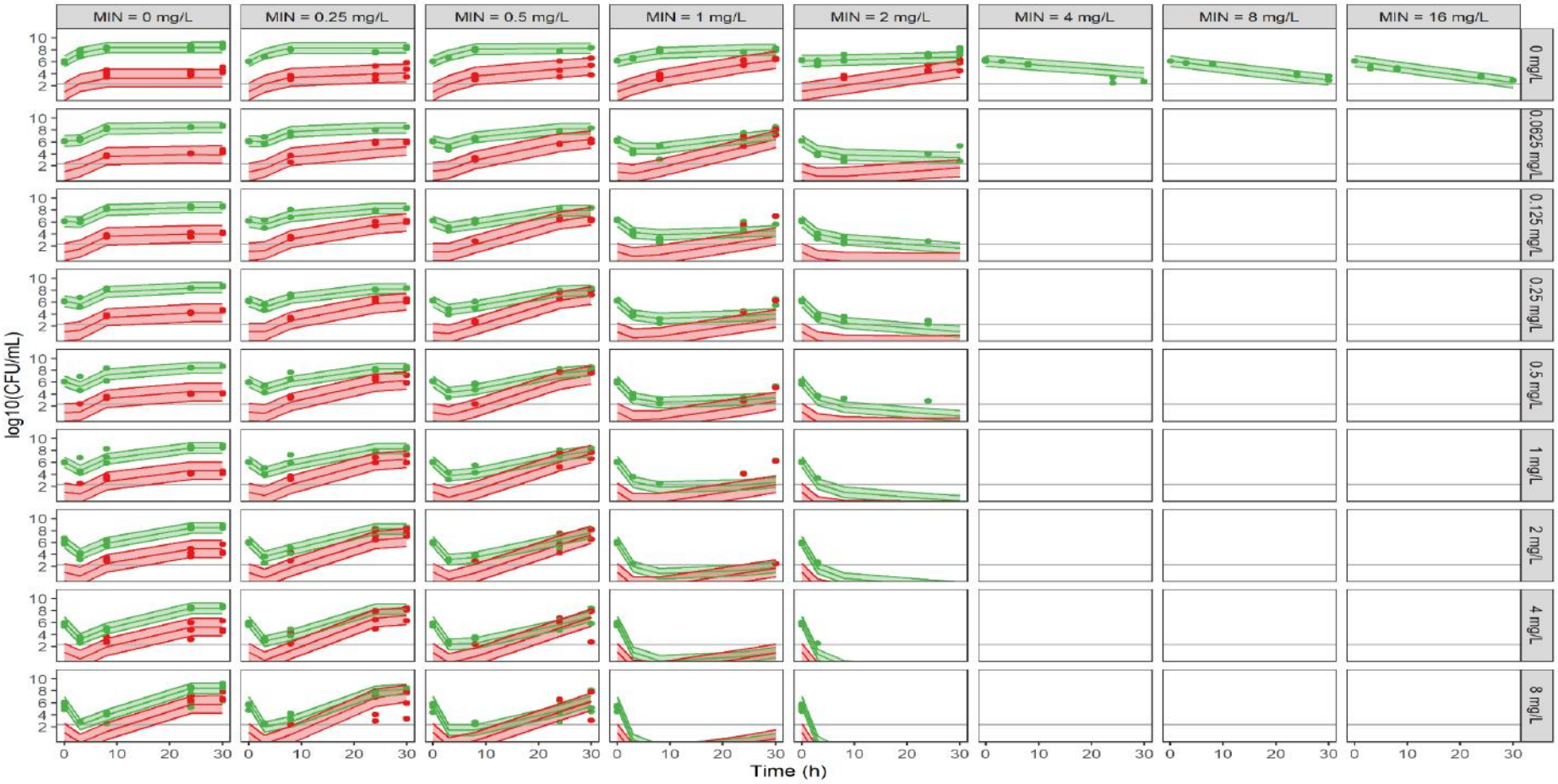

Figure S2. Visual predictive checks for the final model. Points represent experimental data. The shaded areas represent 80% prediction interval based on 1000 simulations under the final model for each tested concentration. Lines represent the 10th – 50th and 90th percentile of those simulations. Green represents total bacteria (counted on drug-free plates) and red represents highly resistant bacteria (counted on plates containing 64 mg/L of polymyxin B). Each column corresponds to a minocycline (MIN) concentration and each line is a polymyxin B (PMB) concentration.

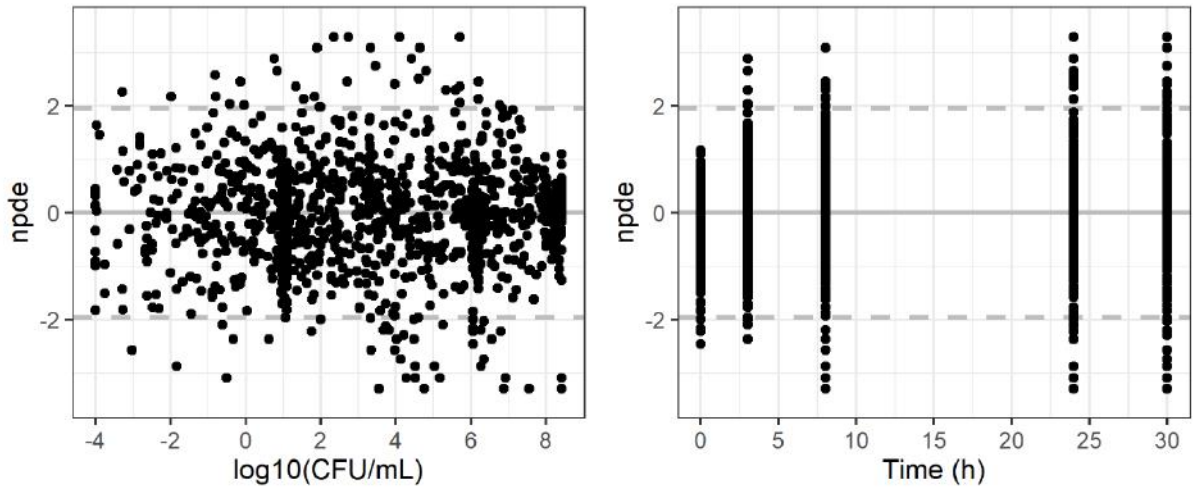

Figure S3. Normalized prediction distribution errors of the final model.

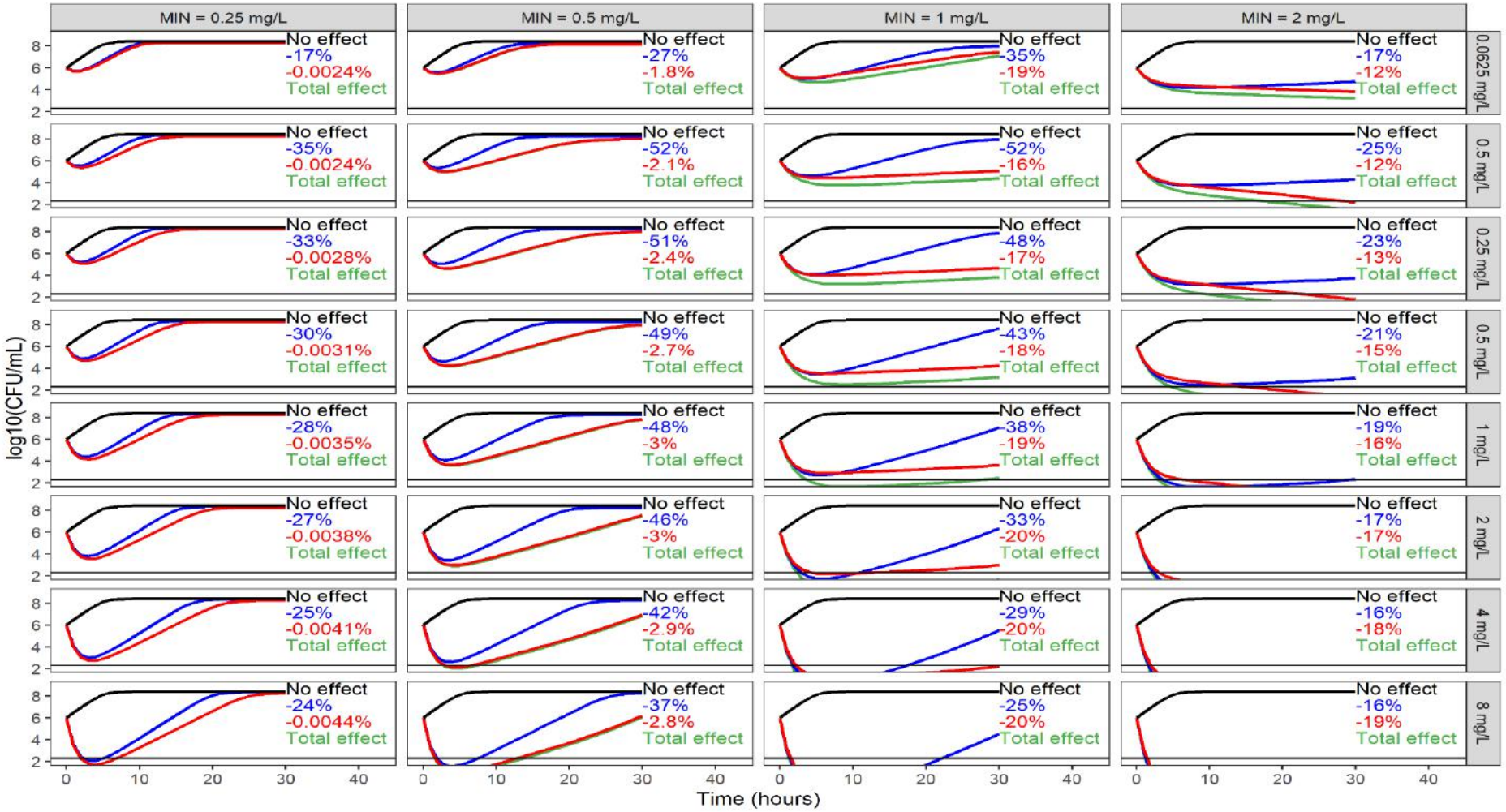

Figure S4. Simulations of CFU/mL for different model parametrisation. Simulations of expected log10(CFU/mL) versus time for different model parametrisations: black: absence of effect, green: under the final model; blue: under the final model with potentialization of minocycline by polymyxin B set to 0; red: under the final model with inhibition of adaptation to polymyxin B by minocycline set to 0. Percentages represent the part of the total effect imputable to the removed component. Each column corresponds to a minocycline (MIN) concentration and each line is a polymyxin B (PMB) concentration.

Text S1:

Model building

Bacterial growth model

A logistic growth model with one compartment for each bacterial subpopulation (Equations 1 and 2) and a model with two compartments for each bacterial subpopulation (Equations 3, 4 and 5) were tested.

$$\frac{dB_n}{dt} = k_{net} \times \left(1 - \frac{B_{tot}}{B_{max}}\right) \times B_n \text{ Equation 1}$$

$$B_{tot} = B_1 + B_2 + \cdots + B_n \text{ Equation 2}$$

Where n is the number of bacterial subpopulations, B_n (CFU/mL) is the n-th bacterial subpopulation, k_{net} (h^{-1}) is the apparent (net) growth constant and B_{max} (CFU/mL) the maximal capacity of the system.

$$\frac{dGrowing}{dt} = (k_g - k_d - k_{rest}) \times Growing \text{ Equation 3}$$

$$\frac{dResting}{dt} = k_{rest} \times Growing - k_d \times Resting \text{ Equation 4}$$

$$k_{rest} = \frac{Growing+Resting}{B_{max}} \times (k_g - k_d) \text{ Equation 5}$$

Where Growing (CFU/mL) is the bacterial density of bacteria in the growing state, Resting (CFU/mL) the bacterial density of bacteria in the resting state, k_g (h^{-1}) is the natural growth rate constant, k_d (h^{-1}) the natural death rate constant and B_{max} (CFU/mL) the maximal capacity of the system.

Models including 1 and 2 subpopulations with differing antibiotic susceptibilities were tested.

Drug effect model

Polymyxin B and minocycline were assumed to have an effect only on bacteria in a growing state, or on total bacteria if the logistic growth model was used.

$$\frac{dB_n}{dt} = \left(k_{net} \times \left(1 - \frac{B_{tot}}{B_{max}}\right) - k_{PMB} - k_{MIN} \right) \times B_n \text{ Equation 6}$$

$$\frac{dGrowing}{dt} = (k_g - k_d - k_{rest} - k_{PMB} - k_{MIN}) \times Growing \text{ Equation 7}$$

Where multiple functions for each k_{drug} (h^{-1}) were tested, a linear function ($k_{drug} = k_{slope,drug} \times [Drug]$) a power function ($k_{drug} = k_{slope,drug} \times [Drug]^{\gamma_{drug}}$), an Emax function ($k_{drug} = \frac{E_{max,drug} \times [Drug]}{EC_{50,drug} + [Drug]}$) or a sigmoidal Emax function ($k_{drug} = \frac{E_{max,drug} \times [Drug]^{\gamma_{drug}}}{EC_{50,drug}^{\gamma_{drug}} + [Drug]^{\gamma_{drug}}}$)

Adaptive resistance

A function representing adaptation of the bacteria to each drug was tested. Compartments $AR_{on,drug}$ and $AR_{off,drug}$ representing a virtual fraction of adapted and non-adapted bacteria respectively were added in the model and k_{drug} was reduced proportionally to $AR_{on,drug}$.

$$\frac{dAR_{on,PMB}}{dt} = k_{on,PMB} \times AR_{off,PMB} - k_{off,PMB} \times AR_{on,PMB}$$ Equation 8

$$\frac{dAR_{off,PMB}}{dt} = k_{off,PMB} \times AR_{on,PMB} - k_{on,PMB} \times AR_{off,PMB}$$ Equation 9

$$\frac{dAR_{on,MIN}}{dt} = k_{on,MIN} \times AR_{off,MIN} - k_{off,MIN} \times AR_{on,MIN}$$ Equation 10

$$\frac{dAR_{off,MIN}}{dt} = k_{off,MIN} \times AR_{on,MIN} - k_{on,MIN} \times AR_{off,MIN}$$ Equation 11

$$\frac{dB_n}{dt} = \left(k_{net} \times \left(1 - \frac{B_{tot}}{B_{max}}\right) - k_{PMB} \times \left(1 - AR_{on,PMB}\right) - k_{MIN} \times \left(1 - AR_{on,MIN}\right)\right) \times B_n$$ Equation 12

$$\frac{dGrowing}{dt} = (k_g - k_d - k_{rest} - k_{PMB} \times (1 - AR_{on,PMB}) - k_{MIN} \times (1 - AR_{on,MIN})) \times Growing$$

Equation 13

At the beginning of the experiment all bacetria are assumed to be non-adapted ($AR_{on,drug}$ = 0 and $AR_{off,drug}$ = 1). Multiple functions for $k_{on,drug}$ (h^{-1}) were tested, a linear function ($k_{on,drug} = k_{slope,drug} \times [Drug]$) a power function ($k_{on,drug} = k_{slope,drug} \times [Drug]^{\gamma_{drug}}$), an Emax function ($k_{on,drug} = \frac{E_{max,drug} \times [Drug]}{EC_{50,drug} + [Drug]}$) or a sigmoidal Emax function ($k_{on,drug} = \frac{E_{max,drug} \times [Drug]^{\gamma_{drug}}}{EC_{50,drug}^{\gamma_{drug}} + [Drug]^{\gamma_{drug}}}$)

Drug interaction:

Interaction between the two drugs and its effect on bacterial growth was modelled using the GPDI model under the simple effect addition hypothesis, developed by Wicha et al. [21] Using this approach, PD parameters describing the effect of (or resistance to) one drug are influenced by the presence of the other drug. For example, $EC_{50,MIN}$ could be modified in presence of polymyxin B following this equation :

$$EC_{50,MIN} = EC_{50,MIN\ alone} \times \left(1 + \frac{INTP_{PMB} \times [PMB]}{EC_{50,INT-PMB} + [PMB]}\right)$$ Equation 14

Where $EC_{50,MIN}$ (mg/L) alone is the EC_{50} of minocycline in absence of polymyxin B, $INT_{MIN\text{-}PMB}$ (no unit) is an interaction factor equal to 0 if there is no interaction, negative if there is synergy, positive if there is antagonism and $EC_{50,INT\ MIN\text{-}PMB}$ (mg/L) is the polymyxin B concentration needed to reach 50% of the interaction effect. Following the authors recommendations interactions were at first assumed to be without perpetrator and victim, then an individual set of parameters were estimated with each drug being perpetrator or victim. Potentiation of minocycline by polymyxin B, potentiation of polymyxin B by minocycline, and reduction of adaptive resistance rate to polymyxin B by minocycline were tested.

Estimation and evaluation methods

Bacterial count data were transformed into decimal logarithms before parameter estimation.

Model selection was based on objective function value (OFV) and goodness of fit plots. When two models were nested, a decrease in OFV of at least 10.84 (chi square 1df $p = 0.001$) was needed to select the most complex model. Visual predictive checks (VPCs) based on 1000 simulations were drawn to evaluate the fit to data and taken into account for model selection. Normalized Prediction Distribution Errors (NPDE) [29] were also calculated.

Residual error was split in two components one residual error for bacterial counts on drug-free plate and another for bacterial counts on drug-containing plates. For a given time-point, when bacteria density measurements on drug-free and drug-containing plates were both above LOQ, residual errors for these measurements were considered to be correlated and this correlation was estimated making use of NONMEM L2 data item.

Data below the LOQ were taken into account in the model estimation by applying Beal's M3 method [30]. Uncertainty around population parameter estimates was estimated using the sampling importance resampling (SIR) technique.

Dataset preparation was performed using R software, parameter estimation was performed using NONMEM software (ICON, Dublin, Ireland) version 7.4.2 using the LAPLACIAN algorithm.

Text S2: Final model

$$\frac{dR}{dt} = \left(k_{net} \times \left(\frac{R + HR}{B_{max}}\right) - k_{PMB,R} \times \left(1 - AR_{on,PMB}\right) - k_{MIN,R}\right) \times R$$

$$\frac{dHR}{dt} = \left(k_{net} \times \left(\frac{R + HR}{B_{max}}\right) - k_{PMB,HR} \times \left(1 - AR_{on,PMB}\right) - k_{MIN,HR}\right) \times HR$$

$$\frac{dAR_{on,PMB}}{dt} = k_{on,PMB} \times AR_{off,PMB} - k_{off,PMB} \times AR_{on,PMB}$$

$$\frac{dAR_{off,PMB}}{dt} = k_{off,PMB} \times AR_{on,PMB} - k_{on,PMB} \times AR_{off,PMB}$$

$$k_{PMB-R} = k_{slope,PMB-R} \times [PMB]^{\gamma_{PMB}}$$

$$k_{PMB-HR} = k_{slope,PMB-HR} \times [PMB]^{\gamma_{PMB}}$$

$$k_{MIN-R} = \frac{E_{max,MIN} \times [MIN]^{\gamma_{MIN}}}{\left(EC_{50,MIN-R} \times \left(1 + \frac{INT_{PMB} \times [PMB]^{H_{INT\ PMB}}}{EC_{50,INT\ PMB}^{H_{INT\ PMB}} + [PMB]^{H_{INT\ PMB}}}\right)\right)^{\gamma_{MIN}} + [MIN]^{\gamma_{MIN}}}$$

$$k_{MIN-HR} = \frac{E_{max,MIN} \times [MIN]^{\gamma_{MIN}}}{\left(EC_{50,MIN-HR} \times \left(1 + \frac{INT_{PMB} \times [PMB]^{H_{INT\ PMB}}}{EC_{50,INT\ PMB}^{H_{INT\ PMB}} + [PMB]^{H_{INT\ PMB}}}\right)\right)^{\gamma_{MIN}} + [MIN]^{\gamma_{MIN}}}$$

$$k_{on,PMB} = k_{on0,PMB} \times \left(1 + \frac{INT_{ADA} \times [MIN]^{H_{INT\ ADA}}}{EC_{50,INT\ ADA}^{H_{IND\ ADA}} + [MIN]^{H_{INT\ ADA}}}\right)$$

The bacterial growth model was selected based on heteroresistance and fitness cost results, so the final model had two subpopulations: resistant bacteria (R), growing on drug-free plates and highly resistant bacteria (HR), able to grow on drug-free plates and plates containing 64mg/L of polymyxin B, and their k_{net} was set to be identical.

Effect of polymyxin B on both subpopulations was best described by a power model with one slope parameter for each subpopulation and the same power parameter.

Effect of minocycline was best described by a sigmoidal E_{max} model, with the same E_{max} and gamma for both subpopulations but different EC_{50}.

Reduction of the rate of adaptation to polymyxin B due to minocycline was best described by a modification of k_{on} by a sigmoidal E_{max} function of minocycline concentration. Inclusion of potentiation of polymyxin B effect on bacteria by minocycline resulted in high correlation in parameter estimations ($r^2 > 0.9$) synonym of model over parametrization and thus was not kept in the final model.

Because of the experimental design, i.e. static polymyxin B concentrations, reversal of adaptive resistance was not expected thus k_{off} was fixed to 0 h^{-1}. Also only apparent growth (k_{net}) was identifiable.

Potentiation of minocycline effect on both subpopulations by polymyxin B was best described by a modification of $EC_{50\ MIN\text{-}R}$ and $EC_{50\ MIN\text{-}HR}$ by a sigmoidal E_{max} function of polymyxin B concentration. The interaction parameters were set to the same values for both subpopulations as having different values did not significantly improve the fit (delta OFV = -2.6).

Note pour la thèse : Les codes sont disponibles sur demande, les inclure dans le document papier semble peu approprié.

Code S1: Final model NONMEM file

Code S2 R files to perform the simulations for % effect

XI. Discussion/Perspectives

Les deux principales études présentées dans cette thèse proposent de développer des modèles PK/PD semi-mécanistiques afin d'étudier l'efficacité *in vitro* d'antibiotiques seuls ou en combinaison. Le développement de ces modèles est informé par des données mécanistiques provenant de la littérature ou d'expériences complémentaires réalisées en parallèle des études de bactéricidie ayant servi à construire les modèles. Ces modèles sont utiles pour extraire un maximum d'information de ces études *in vitro* et ainsi mieux comprendre la pharmacodynamie des antibiotiques étudiés. Ils nous ont notamment permis de prendre en compte la dégradation de la céfoxitine au cours du temps et ainsi d'estimer de façon plus fine l'apparition de résistance à la céfoxitine chez notre souche de *M. abscessus*. Aussi le modèle décrivant l'effet combiné de la polymyxine B et de la minocycline sur une souche d'*A. baumannii* nous a permis de quantifier la contribution des effets d'interaction à l'effet total et ainsi de déterminer les concentrations optimales de chacun des antibiotiques pour éliminer notre souche d'*A. baumannii* et pour éviter l'apparition de résistance.

Outre la quantification des effets, la modélisation PK/PD des antibiotiques peut permettre d'améliorer notre compréhension des mécanismes d'action des antibiotiques afin de pouvoir extrapoler les résultats souvent obtenus *in vitro* ou chez l'animal, pour mettre au point des études cliniques et améliorer le traitement des patients. C'est dans ce but que nous avons intégré à notre étude de la combinaison polymyxine B et minocycline un comptage de sous population très résistantes, une évaluation d'un éventuel coût métabolique dû à la résistance et une recherche de mutations sur certains gènes de résistance à la polymyxine B.

Cependant, cette division de la population bactérienne totale en deux sous populations reste purement phénotypique et grossière, et de nombreuses informations sont manquantes afin de pouvoir développer un modèle vraiment mécanistique.

Afin de construire un modèle mécanistique, il faudrait avoir à notre disposition des données qualitatives vis-à-vis des mécanismes de résistance existants d'un point de vue génétique. Mais il faut aussi des informations sur l'expression de ces gènes et le niveau de résistance résultant de leur expression. De plus, une connaissance des spécificités propres à chaque espèce bactérienne (Gram + ou - ...) ainsi que sur les différents états physiologiques se traduisant par des sensibilités différentes (e.g. bactéries viables non cultivables, bactéries persistantes …). Pour obtenir ces informations de multiples techniques sont à notre disposition. Le séquençage de génome entier (WGS) [171] permet d'obtenir la carte génétique d'une bactérie et donc de nous renseigner sur les mécanismes de résistance de ladite bactérie, et dans le cas de mécanismes connus d'intégrer ces informations dans nos modèles. Différents mécanismes de résistance vont se traduire par des différences de modèle, par exemple la présence d'une pompe d'efflux pourra être modélisée différemment de la présence d'une modification de la cible. Avec cette technique une information quantitative sur la proportion de bactéries portant les gènes de résistance est aussi

donnée. Plutôt que la division phénotypique grossière que nous avons présentée nous pourrions ainsi établir une division en sous populations homogènes d'un point de vue génotypique.

Le WGS peut être couplé à des techniques de mesure de l'expression génique telles que la transcriptomique (aussi appelée *RNAseq*) [172] qui nous permettrait d'obtenir une information quantitative vis-à-vis de l'expression des gènes. Cette information est d'autant plus importante parce que les mutations (détectées par le WGS) ne se traduisent pas nécessairement par des différences d'expression.

Cette expression génique va se traduire par la synthèse de protéines, et l'étude de ces protéines est appelée la protéomique. Ces techniques ont permis l'identification de nouvelles cibles [173], d'améliorer notre compréhension des mécanismes de résistance aux antibiotiques [174] ainsi que l'élucidation de mécanismes d'action d'antibiotiques [175]. Cependant certaines limitations persistent notamment dans les cas où les concentrations en protéines ne sont pas prédictives de l'activité métabolique [176].

Pour pallier ces défauts ,l'étude des produits du métabolisme s'est développée et les techniques mises en œuvre sont regroupées sous le terme de métabolomique [177] . La métabolomique va apporter des informations quantitatives vis-à-vis des changements en concentration de métabolites au cours de l'étude. Ces concentrations peuvent faire l'objet d'une modélisation où l'on envisagerait la bactérie comme le sont les organes dans les approches de *quantitative systems pharmacology*. Un modèle, décrivant la vie bactérienne à travers ses voies métaboliques pourrait s'avérer plus utile qu'un modèle empirique ou semi-mécanistique pour prédire l'efficacité d'un traitement, notamment dans les premières phases de développement, où l'on en sait peu sur les mécanismes d'action de la molécule [178].

Le comptage sur géloses ne permet pas de mettre en évidence tous les états physiologiques des bactéries, notamment les bactéries persistantes [49], ou les bactéries dites viables non cultivables [179]. Or les bactéries dans ces états physiologiques sont souvent décrites comme résistantes aux antibiotiques et présentent donc un intérêt pour la PK/PD des antibiotiques. Les techniques telles que l'oCelloScope [180] ou la cytométrie de flux [181] permettent toutes les deux le comptage de ces types de bactéries ainsi que la visualisation de l'évolution de leur forme (pour l'oCelloScope) ou de leur taille (pour la cytométrie de flux).

L'utilisation de toutes ces techniques, nous permettra de mieux identifier et catégoriser les différentes sous populations bactériennes présentes dans nos expériences. Un modèle décrivant l'évolution de ces différentes sous-populations au cours du temps et l'efficacité des antibiotiques sur chacune d'elle devrait améliorer les propriétés prédictives de l'efficacité *in vivo* de nos molécules. Mais pour améliorer d'autant plus ces prédictions il pourrait être intéressant d'obtenir des informations sur l'effet de l'environnement d'étude.

En effet, réaliser les expériences dans un milieu de culture plus proche du milieu d'infection *in vivo,* permettrait d'améliorer la qualité de nos prédictions. En règle générale, les expériences *in vitro* sont effectués avec des milieux riches et standardisés (*e.g.* milieu Mueller-Hinton supplémenté en cations pour les déterminations de CMI), ces milieux ne sont pas représentatifs des sites d'infection chez l'homme. Cette différence d'environnement peut se traduire par une différence de pharmacodynamie, par exemple Buyck *et al.* [182] ont montré que l'azithromycine utilisée contre une souche de *P. aeruginosa,* possédait une CMI 128 fois moins élevée dans un milieu représentatif du milieu pulmonaire par rapport à une CMI effectuée dans le milieu standard recommandé. Des différences d'ordre pharmacocinétique sont aussi attendues entre les milieu standard et les sites d'infection, par exemple l'albumine est une protéine retrouvée dans le sang qui lie certains antibiotiques, dans le milieu pulmonaire la mucine lie aussi certains antibiotiques [183,184]. L'utilisation *in vitro* de milieux dont la composition se rapprocherait des sites d'infections améliorerait les capacités prédictives de nos modèles, par exemple, si l'on s'intéresse aux infections pulmonaires un milieu mimant le *sputum* humain a été développé [185].

Aussi, dans ce travail les modèles ont été développés à partir de données *in vitro* où la pharmacocinétique humaine des molécules n'était pas simulée. Or, il est possible que certains phénomènes pharmacodynamiques n'apparaissent qu'avec une variation de la concentration en antibiotique, par exemple dans l'étude de la combinaison polymyxine B + minocycline, le fait d'être à concentration constante de polymyxine B a empêché l'estimation d'une constante de réversion de résistance adaptive. Afin de pouvoir simuler une pharmacocinétique humaine *in vitro* les expériences menées avec le système dit « hollow fibre » ont montré leur utilité et ont déjà fait l'objet de modélisation PK/PD dans le domaine des antibiotiques [186,187].

L'utilisation de toutes ces approches permettraient d'obtenir des modèles probablement complexes, mais avec une meilleure capacité prédictive. Cependant, un problème majeur de la mise en œuvre d'une approche aussi complète est la charge de travail que cela représenterait. Déjà, les données qui ont été modélisées dans les deux études présentées proviennent d'expériences avec une charge de travail importante à cause de leur durée (11 jours pour la céfoxitine) ou du nombre de conditions testées (notamment dans le cas de la combinaison polymyxine B + minocycline).

Cette charge de travail importante explique en partie pourquoi peu d'études de modélisation PK/PD à partir de données de bactéricidie *in vitro* sont disponibles dans la littérature, notamment par rapport aux études ayant pour critère d'efficacité la CMI ou le résultat de checkerboards (FICI) dans le cas de combinaisons d'antibiotique. Ces techniques (CMI et checkerboards) ont l'intérêt de permettre de tester de nombreuses souches en peu de temps tandis que les études de bactéricidie avec modélisation se limitent en général à quelques souches (une souche par étude dans ce travail). En ne construisant nos

modèles qu'à partir de données provenant d'un nombre limité de souches, nous limitons la portée des recommandations que nous pourrions faire à partir de ceux-ci.

Afin de remédier à ce problème, plusieurs pistes sont envisageables. Tout d'abord l'utilisation de techniques d'*optimal design* [188] pourrait nous permettre d'optimiser les plans d'expérience afin de réduire le nombre de prélèvements et de conditions de test, nous permettant ainsi de tester plus de souches. Aussi, certaines des techniques présentées auparavant, telles que l'oCelloScope [180] ou la cytométrie de flux [181] pour évaluer la charge bactérienne ont un fort potentiel d'automatisation, ce qui permettrait de tester plusieurs souches tout en apportant plus d'information que les CMI ou les *checkerboards*.

De plus, l'intégration des données issues des expériences de WGS, RNA-seq,de métabolomique et de protéomique à nos modèles PK/PD nécessiteront des développements dans nos méthodes de modélisation, notamment à cause l'importante quantité de données produites par ces techniques. Développer nos techniques de modélisation afin d'intégrer aussi les données issues d'expériences représentant une faible charge de travail telles que les CMI ou les checkerboards, pourrait améliorer les capacités prédictives de nos modèles sans alourdir le travail expérimental.

Au cours des dernières années, la modélisation PK/PD a pris de l'importance, notamment vis-à-vis des agences de sureté du médicament qui en encouragent activement l'utilisation. Dorénavant, il faut relever le défi posé par la difficulté d'extrapoler les résultats obtenus *in vitro* dans un contexte *in vivo*. Pour ce faire, l'intégration d'informations mécanistiques dans nos modèles semble une bonne piste et les travaux présentés dans cette thèse sont un premier pas dans cette direction. De nombreuses techniques expérimentales ont été développées afin de mieux comprendre les mécanismes en jeu lors d'un traitement antibiotique. Il appartient à la communauté des modélisateurs de faire évoluer les techniques de modélisation afin d'intégrer ces données aux modèles PK/PD et d'enfin pouvoir parler de modèles mécanistiques.

XII. Annexes

XII.A. Autorisations de reproduction des figures et tableaux

SPRINGER NATURE LICENSE
TERMS AND CONDITIONS

Aug 19, 2019

This Agreement between Mr. Vincent ARANZANA-CLIMENT ("You") and Springer Nature ("Springer Nature") consists of your license details and the terms and conditions provided by Springer Nature and Copyright Clearance Center.

License Number	4652460621748
License date	Aug 19, 2019
Licensed Content Publisher	Springer Nature
Licensed Content Publication	Pharmaceutical Research
Licensed Content Title	Simulation-Based Evaluation of PK/PD Indices for Meropenem Across Patient Groups and Experimental Designs
Licensed Content Author	Anders N. Kristoffersson, Pascale David-Pierson, Neil J. Parrott et al
Licensed Content Date	Jan 1, 2016
Licensed Content Volume	33
Licensed Content Issue	5
Type of Use	Thesis/Dissertation
Requestor type	academic/university or research institute
Format	print and electronic
Portion	figures/tables/illustrations
Number of figures/tables /illustrations	2
Will you be translating?	no
Circulation/distribution	<501
Author of this Springer Nature content	no
Title	Apport de la modélisation semi-mécanistique dans l'étude pharmacocinétique/pharmacodynamique des antibiotiques seuls et en combinaison dans la lutte contre les bactéries résistantes.
Institution name	Université de Poitiers
Expected presentation date	Oct 2019
Portions	Figure 3 and Figure 4
Requestor Location	Mr. Vincent ARANZANA-CLIMENT 120, côte de Montbernage Poitiers, Nouvelle-Aquitaine 86000 France Attn: Mr. Vincent ARANZANA-CLIMENT
Total	0.00 USD
Terms and Conditions	

Springer Nature Customer Service Centre GmbH
Terms and Conditions

SPRINGER NATURE LICENSE
TERMS AND CONDITIONS

Aug 19, 2019

This Agreement between Mr. Vincent ARANZANA-CLIMENT ("You") and Springer Nature ("Springer Nature") consists of your license details and the terms and conditions provided by Springer Nature and Copyright Clearance Center.

License Number	4652460211749
License date	Aug 19, 2019
Licensed Content Publisher	Springer Nature
Licensed Content Publication	Pharmaceutical Research
Licensed Content Title	Modeling of Pharmacokinetic/Pharmacodynamic (PK/PD) Relationships: Concepts and Perspectives
Licensed Content Author	Hartmut Derendorf, Bernd Meibohm
Licensed Content Date	Jan 1, 1999
Licensed Content Volume	16
Licensed Content Issue	2
Type of Use	Thesis/Dissertation
Requestor type	academic/university or research institute
Format	print and electronic
Portion	figures/tables/illustrations
Number of figures/tables /illustrations	1
Will you be translating?	no
Circulation/distribution	<501
Author of this Springer Nature content	no
Title	Apport de la modélisation semi-mécanistique dans l'étude pharmacocinétique/pharmacodynamique des antibiotiques seuls et en combinaison dans la lutte contre les bactéries résistantes.
Institution name	Université de Poitiers
Expected presentation date	Oct 2019
Portions	Figure 1
Requestor Location	Mr. Vincent ARANZANA-CLIMENT 120, côte de Montbernage Poitiers, Nouvelle-Aquitaine 86000 France Attn: Mr. Vincent ARANZANA-CLIMENT
Total	0.00 EUR
Terms and Conditions	

Springer Nature Customer Service Centre GmbH
Terms and Conditions

OXFORD UNIVERSITY PRESS LICENSE
TERMS AND CONDITIONS

Aug 20, 2019

This Agreement between Mr. Vincent ARANZANA-CLIMENT ("You") and Oxford University Press ("Oxford University Press") consists of your license details and the terms and conditions provided by Oxford University Press and Copyright Clearance Center.

License Number	4653000003255
License date	Aug 20, 2019
Licensed content publisher	Oxford University Press
Licensed content publication	FEMS Microbiology Reviews
Licensed content title	*Acinetobacter baumannii*: human infections, factors contributing to pathogenesis and animal models
Licensed content author	McConnell, Michael J.; Actis, Luis
Licensed content date	Mar 1, 2013
Type of Use	Thesis/Dissertation
Institution name	
Title of your work	Apport de la modélisation semi-mécanistique dans l'étude pharmacocinétique/pharmacodynamique des antibiotiques seuls et en combinaison dans la lutte contre les bactéries résistantes.
Publisher of your work	Université de Poitiers
Expected publication date	Oct 2019
Permissions cost	0.00 EUR
Value added tax	0.00 EUR
Total	0.00 EUR
Title	Apport de la modélisation semi-mécanistique dans l'étude pharmacocinétique/pharmacodynamique des antibiotiques seuls et en combinaison dans la lutte contre les bactéries résistantes.
Institution name	Université de Poitiers
Expected presentation date	Oct 2019
Portions	Table 1
Specific Languages	French
Requestor Location	Mr. Vincent ARANZANA-CLIMENT 120, côte de Montbernage Poitiers, Nouvelle-Aquitaine 86000 France Attn: Mr. Vincent ARANZANA-CLIMENT
Publisher Tax ID	GB125506730
Total	0.00 EUR
Terms and Conditions	

STANDARD TERMS AND CONDITIONS FOR REPRODUCTION OF MATERIAL FROM AN OXFORD UNIVERSITY PRESS JOURNAL

1. Use of the material is restricted to the type of use specified in your order details.
2. This permission covers the use of the material in the English language in the following

XIII. Références

[1] Courvalin P. Predictable and unpredictable evolution of antibiotic resistance. Journal of Internal Medicine 2008;264:4–16. doi:10.1111/j.1365-2796.2008.01940.x.

[2] European Centers for Disease Control and Prevention, editor. The bacterial challenge, time to react: a call to narrow the gap between multidrug-resistant bacteria in the EU and the development of new antibacterial agents. Stockholm: ECDC; 2009.

[3] Centers for Disease Control and Prevention. Antibiotic resistance threats in the United States, 2013. n.d.

[4] The Review on Antimicrobial Resistance, chaired by Jim O'Neill. Antimicrobial Resistance: Tackling a crisis for the health and wealth of nations 2014. https://amr-review.org/sites/default/files/AMR%20Review%20Paper%20-%20Tackling%20a%20crisis%20for%20the%20health%20and%20wealth%20of%20nations_1.pdf (accessed July 5, 2019).

[5] WHO | Global priority list of antibiotic-resistant bacteria to guide research, discovery, and development of new antibiotics. WHO n.d. http://www.who.int/medicines/publications/global-priority-list-antibiotic-resistant-bacteria/en/ (accessed July 16, 2019).

[6] Ventola CL. The Antibiotic Resistance Crisis. P T 2015;40:277–83.

[7] FDA Approved Drugs in Infections and Infectious Diseases | CenterWatch n.d. https://www.centerwatch.com/drug-information/fda-approved-drugs/therapeutic-area/25/infections-and-infectious-diseases (accessed July 16, 2019).

[8] Nation RL, Li J, Cars O, Couet W, Dudley MN, Kaye KS, et al. Framework for optimisation of the clinical use of colistin and polymyxin B: the Prato polymyxin consensus. The Lancet Infectious Diseases 2015;15:225–34. doi:10.1016/S1473-3099(14)70850-3.

[9] Derendorf H, Meibohm B. Modeling of pharmacokinetic/pharmacodynamic (PK/PD) relationships: concepts and perspectives. Pharm Res 1999;16:176–85.

[10] European Committee for Antimicrobial Susceptibility Testing (EUCAST). Determination of minimum inhibitory concentrations (MICs) of antibacterial agents by broth dilution. Clinical Microbiology and Infection 2003;9:ix–xv. doi:10.1046/j.1469-0691.2003.00790.x.

[11] Clinical and Laboratory Standards Institute. Methods for Dilution Antimicrobial Susceptibility Tests for Bacteria That Grow Aerobically; Approved Standard—Ninth Edition. CLSI document M07-A9. Wayne, PA: Clinical and Laboratory Standards Institute: 2012.

[12] The European Committee on Antimicrobial Susceptibility Testing. Breakpoint tables for interpretation of MICs and zone diameters. Version 8.1, 2018 n.d.

[13] Clinical and Laboratory Standards Institute. Performance standards for antimicrobial susceptibility testing: 24th informational supplement M100-S24 n.d.:110.

[14] Clinical and Laboratory Standards Institute. M07-A10: Methods for Dilution Antimicrobial Susceptibility Tests for Bacteria That Grow Aerobically; Approved Standard—Tenth Edition n.d.:110.

[15] Khan DD, Friberg LE, Nielsen EI. A pharmacokinetic-pharmacodynamic (PKPD) model based on in vitro time-kill data predicts the in vivo PK/PD index of colistin. J Antimicrob Chemother 2016. doi:10.1093/jac/dkw057.

[16] Mouton JW, Dudley MN, Cars O, Derendorf H, Drusano GL. Standardization of pharmacokinetic/pharmacodynamic (PK/PD) terminology for anti-infective drugs: an update. J Antimicrob Chemother 2005;55:601–7. doi:10.1093/jac/dki079.

[17] Andes D, Craig WA. In vivo pharmacodynamic activity of the glycopeptide dalbavancin. Antimicrob Agents Chemother 2007;51:1633–42. doi:10.1128/AAC.01264-06.

[18] Barbour A, Scaglione F, Derendorf H. Class-dependent relevance of tissue distribution in the interpretation of anti-infective pharmacokinetic/pharmacodynamic indices. Int J Antimicrob Agents 2010;35:431–8. doi:10.1016/j.ijantimicag.2010.01.023.

[19] Burgess DS, Frei CR. Comparison of beta-lactam regimens for the treatment of gram-negative pulmonary infections in the intensive care unit based on pharmacokinetics/pharmacodynamics. J Antimicrob Chemother 2005;56:893–8. doi:10.1093/jac/dki335.

[20] Kashuba ADM, Nafziger AN, Drusano GL, Bertino JS. Optimizing Aminoglycoside Therapy for Nosocomial Pneumonia Caused by Gram-Negative Bacteria. Antimicrobial Agents and Chemotherapy 1999;43:623–9. doi:10.1128/AAC.43.3.623.
[21] Turnidge J. Pharmacodynamics and dosing of aminoglycosides. Infect Dis Clin North Am 2003;17:503–28, v.
[22] Vogelman B, Gudmundsson S, Leggett J, Turnidge J, Ebert S, Craig WA. Correlation of antimicrobial pharmacokinetic parameters with therapeutic efficacy in an animal model. J Infect Dis 1988;158:831–47. doi:10.1093/infdis/158.4.831.
[23] Forrest A, Chodosh S, Amantea MA, Collins DA, Schentag JJ. Pharmacokinetics and pharmacodynamics of oral grepafloxacin in patients with acute bacterial exacerbations of chronic bronchitis. J Antimicrob Chemother 1997;40 Suppl A:45–57. doi:10.1093/jac/40.suppl_1.45.
[24] Forrest A, Nix DE, Ballow CH, Goss TF, Birmingham MC, Schentag JJ. Pharmacodynamics of intravenous ciprofloxacin in seriously ill patients. Antimicrobial Agents and Chemotherapy 1993;37:1073–81. doi:10.1128/AAC.37.5.1073.
[25] Drusano GL, Preston SL, Fowler C, Corrado M, Weisinger B, Kahn J. Relationship between fluoroquinolone area under the curve: minimum inhibitory concentration ratio and the probability of eradication of the infecting pathogen, in patients with nosocomial pneumonia. J Infect Dis 2004;189:1590–7. doi:10.1086/383320.
[26] Preston SL, Drusano GL, Berman AL, Fowler CL, Chow AT, Dornseif B, et al. Pharmacodynamics of levofloxacin: a new paradigm for early clinical trials. JAMA 1998;279:125–9. doi:10.1001/jama.279.2.125.
[27] Rayner CR, Forrest A, Meagher AK, Birmingham MC, Schentag JJ. Clinical pharmacodynamics of linezolid in seriously ill patients treated in a compassionate use programme. Clin Pharmacokinet 2003;42:1411–23. doi:10.2165/00003088-200342150-00007.
[28] Andes D, Ogtrop ML van, Peng J, Craig WA. In Vivo Pharmacodynamics of a New Oxazolidinone (Linezolid). Antimicrobial Agents and Chemotherapy 2002;46:3484–9. doi:10.1128/AAC.46.11.3484-3489.2002.
[29] Ogtrop ML van, Andes D, Stamstad TJ, Conklin B, Weiss WJ, Craig WA, et al. In Vivo Pharmacodynamic Activities of Two Glycylcyclines (GAR-936 and WAY 152,288) against Various Gram-Positive and Gram-Negative Bacteria. Antimicrobial Agents and Chemotherapy 2000;44:943–9. doi:10.1128/AAC.44.4.943-949.2000.
[30] Meagher AK, Passarell JA, Cirincione BB, Wart SAV, Liolios K, Babinchak T, et al. Exposure-Response Analyses of Tigecycline Efficacy in Patients with Complicated Skin and Skin-Structure Infections. Antimicrobial Agents and Chemotherapy 2007;51:1939–45. doi:10.1128/AAC.01084-06.
[31] Passarell JA, Meagher AK, Liolios K, Cirincione BB, Van Wart SA, Babinchak T, et al. Exposure-response analyses of tigecycline efficacy in patients with complicated intra-abdominal infections. Antimicrob Agents Chemother 2008;52:204–10. doi:10.1128/AAC.00813-07.
[32] Jain R, Danziger LH. The macrolide antibiotics: a pharmacokinetic and pharmacodynamic overview. Curr Pharm Des 2004;10:3045–53.
[33] Andes D, Anon J, Jacobs MR, Craig WA. Application of pharmacokinetics and pharmacodynamics to antimicrobial therapy of respiratory tract infections. Clin Lab Med 2004;24:477–502. doi:10.1016/j.cll.2004.03.009.
[34] Van Bambeke F, Tulkens PM. Macrolides: pharmacokinetics and pharmacodynamics. Int J Antimicrob Agents 2001;18 Suppl 1:S17-23.
[35] den Hollander JG, Knudsen JD, Mouton JW, Fuursted K, Frimodt-Møller N, Verbrugh HA, et al. Comparison of pharmacodynamics of azithromycin and erythromycin in vitro and in vivo. Antimicrob Agents Chemother 1998;42:377–82.
[36] Nightingale CH. Pharmacokinetics and pharmacodynamics of newer macrolides. Pediatr Infect Dis J 1997;16:438–43.
[37] Novelli A, Fallani S, Cassetta MI, Arrigucci S, Mazzei T. In vivo pharmacodynamic evaluation of clarithromycin in comparison to erythromycin. J Chemother 2002;14:584–90. doi:10.1179/joc.2002.14.6.584.

[38] Shi J, Montay G, Bhargava VO. Clinical pharmacokinetics of telithromycin, the first ketolide antibacterial. Clin Pharmacokinet 2005;44:915–34. doi:10.2165/00003088-200544090-00003.
[39] Knudsen JD, Fuursted K, Raber S, Espersen F, Frimodt-Moller N. Pharmacodynamics of glycopeptides in the mouse peritonitis model of Streptococcus pneumoniae or Staphylococcus aureus infection. Antimicrob Agents Chemother 2000;44:1247–54. doi:10.1128/aac.44.5.1247-1254.2000.
[40] Moise-Broder PA, Forrest A, Birmingham MC, Schentag JJ. Pharmacodynamics of vancomycin and other antimicrobials in patients with Staphylococcus aureus lower respiratory tract infections. Clin Pharmacokinet 2004;43:925–42. doi:10.2165/00003088-200443130-00005.
[41] Bhavnani SM, Passarell JA, Owen JS, Loutit JS, Porter SB, Ambrose PG. Pharmacokinetic-pharmacodynamic relationships describing the efficacy of oritavancin in patients with Staphylococcus aureus bacteremia. Antimicrob Agents Chemother 2006;50:994–1000. doi:10.1128/AAC.50.3.994-1000.2006.
[42] Boylan CJ, Campanale K, Iversen PW, Phillips DL, Zeckel ML, Parr TR. Pharmacodynamics of oritavancin (LY333328) in a neutropenic-mouse thigh model of Staphylococcus aureus infection. Antimicrob Agents Chemother 2003;47:1700–6. doi:10.1128/aac.47.5.1700-1706.2003.
[43] Li C, Kuti JL, Nightingale CH, Nicolau DP. Population pharmacokinetic analysis and dosing regimen optimization of meropenem in adult patients. J Clin Pharmacol 2006;46:1171–8. doi:10.1177/0091270006291035.
[44] Kristoffersson AN, David-Pierson P, Parrott NJ, Kuhlmann O, Lave T, Friberg LE, et al. Simulation-Based Evaluation of PK/PD Indices for Meropenem Across Patient Groups and Experimental Designs. Pharm Res 2016;33:1115–25. doi:10.1007/s11095-016-1856-x.
[45] Jusko WJ. Pharmacodynamics of chemotherapeutic effects: dose-time-response relationships for phase-nonspecific agents. J Pharm Sci 1971;60:892–5.
[46] Campion JJ, Chung P, McNamara PJ, Titlow WB, Evans ME. Pharmacodynamic modeling of the evolution of levofloxacin resistance in Staphylococcus aureus. Antimicrob Agents Chemother 2005;49:2189–99. doi:10.1128/AAC.49.6.2189-2199.2005.
[47] Meagher AK, Forrest A, Dalhoff A, Stass H, Schentag JJ. Novel pharmacokinetic-pharmacodynamic model for prediction of outcomes with an extended-release formulation of ciprofloxacin. Antimicrob Agents Chemother 2004;48:2061–8. doi:10.1128/AAC.48.6.2061-2068.2004.
[48] Nielsen EI, Viberg A, Löwdin E, Cars O, Karlsson MO, Sandström M. Semimechanistic Pharmacokinetic/Pharmacodynamic Model for Assessment of Activity of Antibacterial Agents from Time-Kill Curve Experiments. Antimicrob Agents Chemother 2007;51:128–36. doi:10.1128/AAC.00604-06.
[49] Balaban NQ, Merrin J, Chait R, Kowalik L, Leibler S. Bacterial Persistence as a Phenotypic Switch. Science 2004;305:1622–5. doi:10.1126/science.1099390.
[50] Bulitta JB, Yang JC, Yohonn L, Ly NS, Brown SV, D'Hondt RE, et al. Attenuation of Colistin Bactericidal Activity by High Inoculum of Pseudomonas aeruginosa Characterized by a New Mechanism-Based Population Pharmacodynamic Model. Antimicrob Agents Chemother 2010;54:2051–62. doi:10.1128/AAC.00881-09.
[51] Zhuang L, Sy SKB, Xia H, Singh RP, Mulder MB, Liu C, et al. Evaluation of in vitro synergy between vertilmicin and ceftazidime against Pseudomonas aeruginosa using a semi-mechanistic pharmacokinetic/pharmacodynamic model. Int J Antimicrob Agents 2015;45:151–60. doi:10.1016/j.ijantimicag.2014.09.017.
[52] Yano Y, Oguma T, Nagata H, Sasaki S. Application of logistic growth model to pharmacodynamic analysis of in vitro bactericidal kinetics. J Pharm Sci 1998;87:1177–83. doi:10.1021/js9801337.
[53] Tam VH, Schilling AN, Nikolaou M. Modelling time-kill studies to discern the pharmacodynamics of meropenem. J Antimicrob Chemother 2005;55:699–706. doi:10.1093/jac/dki086.
[54] Mohamed AF, Cars O, Friberg LE. A pharmacokinetic/pharmacodynamic model developed for the effect of colistin on Pseudomonas aeruginosa in vitro with evaluation of population

pharmacokinetic variability on simulated bacterial killing. J Antimicrob Chemother 2014;69:1350–61. doi:10.1093/jac/dkt520.
[55] Jacobs M, Gr?goire N, Couet W, Bulitta JB. Distinguishing Antimicrobial Models with Different Resistance Mechanisms via Population Pharmacodynamic Modeling. PLOS Computational Biology 2016;12:e1004782. doi:10.1371/journal.pcbi.1004782.
[56] Tamma PD, Cosgrove SE, Maragakis LL. Combination Therapy for Treatment of Infections with Gram-Negative Bacteria. Clinical Microbiology Reviews 2012;25:450–70. doi:10.1128/CMR.05041-11.
[57] Kumar A, Zarychanski R, Light B, Parrillo J, Maki D, Simon D, et al. Early combination antibiotic therapy yields improved survival compared with monotherapy in septic shock: a propensity-matched analysis. Crit Care Med 2010;38:1773–85. doi:10.1097/CCM.0b013e3181eb3ccd.
[58] Micek ST, Welch EC, Khan J, Pervez M, Doherty JA, Reichley RM, et al. Empiric Combination Antibiotic Therapy Is Associated with Improved Outcome against Sepsis Due to Gram-Negative Bacteria: a Retrospective Analysis. Antimicrob Agents Chemother 2010;54:1742–8. doi:10.1128/AAC.01365-09.
[59] Petrosillo N, Giannella M, Antonelli M, Antonini M, Barsic B, Belancic L, et al. Clinical Experience of Colistin-Glycopeptide Combination in Critically Ill Patients Infected with Gram-Negative Bacteria. Antimicrob Agents Chemother 2014;58:851–8. doi:10.1128/AAC.00871-13.
[60] Tängdén T. Combination antibiotic therapy for multidrug-resistant Gram-negative bacteria. Ups J Med Sci 2014;119:149–53. doi:10.3109/03009734.2014.899279.
[61] Berenbaum MC. What is synergy? Pharmacol Rev 1989;41:93–141.
[62] Greco WR, Bravo G, Parsons JC. The search for synergy: a critical review from a response surface perspective. Pharmacol Rev 1995;47:331–85.
[63] Geary N. Understanding synergy. Am J Physiol Endocrinol Metab 2013;304:E237-253. doi:10.1152/ajpendo.00308.2012.
[64] Foucquier J, Guedj M. Analysis of drug combinations: current methodological landscape. Pharmacol Res Perspect 2015;3. doi:10.1002/prp2.149.
[65] Käer E, Loewe S. Über Kombinationswirkungen. Archiv f experiment Pathol u Pharmakol 1928;127:308–18. doi:10.1007/BF01863639.
[66] Bliss CI. The Toxicity of Poisons Applied Jointly1. Annals of Applied Biology 1939;26:585–615. doi:10.1111/j.1744-7348.1939.tb06990.x.
[67] Grabovsky Y, Tallarida RJ. Isobolographic analysis for combinations of a full and partial agonist: curved isoboles. J Pharmacol Exp Ther 2004;310:981–6. doi:10.1124/jpet.104.067264.
[68] Tallarida RJ. An overview of drug combination analysis with isobolograms. J Pharmacol Exp Ther 2006;319:1–7. doi:10.1124/jpet.106.104117.
[69] Ezechiáš M, Cajthaml T. New insight into isobolographic analysis for combinations of a full and partial agonist: Curved isoboles. Toxicology 2018;402–403:9–16. doi:10.1016/j.tox.2018.04.004.
[70] Rao GG, Li J, Garonzik SM, Nation RL, Forrest A. Assessment and modelling of antibacterial combination regimens. Clin Microbiol Infect 2018;24:689–96. doi:10.1016/j.cmi.2017.12.004.
[71] Orhan G, Bayram A, Zer Y, Balci I. Synergy Tests by E Test and Checkerboard Methods of Antimicrobial Combinations against Brucella melitensis. Journal of Clinical Microbiology 2005;43:140. doi:10.1128/JCM.43.1.140-143.2005.
[72] Leber A, editor. Clinical Microbiology Procedures Handbook, Fourth Edition. American Society of Microbiology; 2016. doi:10.1128/9781555818814.
[73] Odds FC. Synergy, antagonism, and what the chequerboard puts between them. J Antimicrob Chemother 2003;52:1–1. doi:10.1093/jac/dkg301.
[74] Hsieh MH, Yu CM, Yu VL, Chow JW. Synergy assessed by checkerboard a critical analysis. Diagnostic Microbiology and Infectious Disease 1993;16:343–9. doi:10.1016/0732-8893(93)90087-N.
[75] Rand KH, Houck HJ, Brown P, Bennett D. Reproducibility of the microdilution checkerboard method for antibiotic synergy. Antimicrob Agents Chemother 1993;37:613–5. doi:10.1128/aac.37.3.613.

[76] Mouton JW, Ogtrop ML van, Andes D, Craig WA. Use of Pharmacodynamic Indices To Predict Efficacy of Combination Therapy In Vivo. Antimicrobial Agents and Chemotherapy 1999;43:2473–8. doi:10.1128/AAC.43.10.2473.
[77] Schentag JJ, Strenkoski-Nix LC, Nix DE, Forrest A. Pharmacodynamic Interactions of Antibiotics Alone and in Combination. Clin Infect Dis 1998;27:40–6. doi:10.1086/514621.
[78] Hollander JG den, Mouton JW, Verbrugh HA. Use of Pharmacodynamic Parameters To Predict Efficacy of Combination Therapy by Using Fractional Inhibitory Concentration Kinetics. Antimicrobial Agents and Chemotherapy 1998;42:744–8. doi:10.1128/AAC.42.4.744.
[79] Brill MJE, Kristoffersson AN, Zhao C, Nielsen EI, Friberg LE. Semi-mechanistic pharmacokinetic–pharmacodynamic modelling of antibiotic drug combinations. Clinical Microbiology and Infection 2017;0. doi:10.1016/j.cmi.2017.11.023.
[80] Greco WR, Park HS, Rustum YM. Application of a New Approach for the Quantitation of Drug Synergism to the Combination of cis-Diamminedichloroplatinum and 1-β-d-Arabinofuranosylcytosine. Cancer Res 1990;50:5318–27.
[81] Drusano GL, Neely M, Guilder MV, Schumitzky A, Brown D, Fikes S, et al. Analysis of Combination Drug Therapy to Develop Regimens with Shortened Duration of Treatment for Tuberculosis. PLOS ONE 2014;9:e101311. doi:10.1371/journal.pone.0101311.
[82] Wicha S, Huisinga W, Kloft C. Translational Pharmacometric Evaluation of Typical Antibiotic Broad-Spectrum Combination Therapies Against Staphylococcus Aureus Exploiting In Vitro Information. CPT Pharmacometrics Syst Pharmacol 2017;6:512–22. doi:10.1002/psp4.12197.
[83] Rao GG, Ly NS, Bulitta JB, Soon RL, San Roman MD, Holden PN, et al. Polymyxin B in combination with doripenem against heteroresistant Acinetobacter baumannii: pharmacodynamics of new dosing strategies. J Antimicrob Chemother 2016;71:3148–56. doi:10.1093/jac/dkw293.
[84] Yadav R, Landersdorfer CB, Nation RL, Boyce JD, Bulitta JB. Novel Approach To Optimize Synergistic Carbapenem-Aminoglycoside Combinations against Carbapenem-Resistant Acinetobacter baumannii. Antimicrob Agents Chemother 2015;59:2286–98. doi:10.1128/AAC.04379-14.
[85] Landersdorfer CB, Ly NS, Xu H, Tsuji BT, Bulitta JB. Quantifying Subpopulation Synergy for Antibiotic Combinations via Mechanism-Based Modeling and a Sequential Dosing Design. Antimicrobial Agents and Chemotherapy 2013;57:2343–51. doi:10.1128/AAC.00092-13.
[86] Ly NS, Bulitta JB, Rao GG, Landersdorfer CB, Holden PN, Forrest A, et al. Colistin and doripenem combinations against Pseudomonas aeruginosa: profiling the time course of synergistic killing and prevention of resistance. J Antimicrob Chemother 2015;70:1434–42. doi:10.1093/jac/dku567.
[87] Ly NS, Bulman ZP, Bulitta JB, Baron C, Rao GG, Holden PN, et al. Optimization of Polymyxin B in Combination with Doripenem To Combat Mutator Pseudomonas aeruginosa. Antimicrobial Agents and Chemotherapy 2016;60:2870–80. doi:10.1128/AAC.02377-15.
[88] Lenhard JR, Bulitta JB, Connell TD, King-Lyons N, Landersdorfer CB, Cheah S-E, et al. High-intensity meropenem combinations with polymyxin B: new strategies to overcome carbapenem resistance in Acinetobacter baumannii. J Antimicrob Chemother 2017;72:153–65. doi:10.1093/jac/dkw355.
[89] Sy SKB, Zhuang L, Xia H, Beaudoin M-E, Schuck VJ, Derendorf H. Prediction of in vivo and in vitro infection model results using a semimechanistic model of avibactam and aztreonam combination against multidrug resistant organisms. CPT: Pharmacometrics & Systems Pharmacology 2017;6:197–207. doi:10.1002/psp4.12159.
[90] Mohamed AF, Kristoffersson AN, Karvanen M, Nielsen EI, Cars O, Friberg LE. Dynamic interaction of colistin and meropenem on a WT and a resistant strain of Pseudomonas aeruginosa as quantified in a PK/PD model. J Antimicrob Chemother 2016. doi:10.1093/jac/dkv488.
[91] Wicha SG, Chen C, Clewe O, Simonsson USH. A general pharmacodynamic interaction model identifies perpetrators and victims in drug interactions. Nature Communications 2017;8:2129. doi:10.1038/s41467-017-01929-y.

[92] Lee M-R, Sheng W-H, Hung C-C, Yu C-J, Lee L-N, Hsueh P-R. Mycobacterium abscessus Complex Infections in Humans. Emerging Infect Dis 2015;21:1638–46. doi:10.3201/2109.141634.
[93] Teng S-H, Chen C-M, Lee M-R, Lee T-F, Chien K-Y, Teng L-J, et al. Matrix-Assisted Laser Desorption Ionization–Time of Flight Mass Spectrometry Can Accurately Differentiate between Mycobacterium masilliense (M. abscessus subspecies bolletti) and M. abscessus (Sensu Stricto). J Clin Microbiol 2013;51:3113–6. doi:10.1128/JCM.01239-13.
[94] Benwill J, Wallace R. Mycobacterium abscessus: challenges in diagnosis and treatment. Current Opinion in Infectious Diseases 2014;27:506–10. doi:10.1097/QCO.0000000000000104.
[95] Prevots DR, Shaw PA, Strickland D, Jackson LA, Raebel MA, Blosky MA, et al. Nontuberculous Mycobacterial Lung Disease Prevalence at Four Integrated Health Care Delivery Systems. Am J Respir Crit Care Med 2010;182:970–6. doi:10.1164/rccm.201002-0310OC.
[96] Lai C-C, Tan C-K, Chou C-H, Hsu H-L, Liao C-H, Huang Y-T, et al. Increasing Incidence of Nontuberculous Mycobacteria, Taiwan, 2000–2008. Emerg Infect Dis 2010;16:294–6. doi:10.3201/eid1602.090675.
[97] Lee M-R, Sheng W-H, Hung C-C, Yu C-J, Lee L-N, Hsueh P-R. Mycobacterium abscessus Complex Infections in Humans. Emerg Infect Dis 2015;21:1638–46. doi:10.3201/2109.141634.
[98] Mougari F, Guglielmetti L, Raskine L, Sermet-Gaudelus I, Veziris N, Cambau E. Infections caused by Mycobacterium abscessus: epidemiology, diagnostic tools and treatment. Expert Rev Anti Infect Ther 2016;14:1139–54. doi:10.1080/14787210.2016.1238304.
[99] Nessar R, Cambau E, Reyrat JM, Murray A, Gicquel B. Mycobacterium abscessus: a new antibiotic nightmare. J Antimicrob Chemother 2012;67:810–8. doi:10.1093/jac/dkr578.
[100] Sfeir M, Walsh M, Rosa R, Aragon L, Liu SY, Cleary T, et al. Mycobacterium abscessus Complex Infections: A Retrospective Cohort Study. Open Forum Infect Dis 2018;5:ofy022. doi:10.1093/ofid/ofy022.
[101] Ferro BE, van Ingen J, Wattenberg M, van Soolingen D, Mouton JW. Time-kill kinetics of antibiotics active against rapidly growing mycobacteria. J Antimicrob Chemother 2015;70:811–7. doi:10.1093/jac/dku431.
[102] Greendyke R, Byrd TF. Differential antibiotic susceptibility of Mycobacterium abscessus variants in biofilms and macrophages compared to that of planktonic bacteria. Antimicrob Agents Chemother 2008;52:2019–26. doi:10.1128/AAC.00986-07.
[103] Lefebvre A-L, Dubée V, Cortes M, Dorchêne D, Arthur M, Mainardi J-L. Bactericidal and intracellular activity of β-lactams against Mycobacterium abscessus. J Antimicrob Chemother 2016;71:1556–63. doi:10.1093/jac/dkw022.
[104] Cefoxitin. Wikipedia 2019.
[105] Story-Roller E, Maggioncalda EC, Cohen KA, Lamichhane G. Mycobacterium abscessus and β-Lactams: Emerging Insights and Potential Opportunities. Front Microbiol 2018;9. doi:10.3389/fmicb.2018.02273.
[106] Grayson ML, Cosgrove SE, Crowe S, Hope W, McCarthy JS, Mills J, et al. Kucers' The Use of Antibiotics : A Clinical Review of Antibacterial, Antifungal, Antiparasitic, and Antiviral Drugs, Seventh Edition - Three Volume Set. CRC Press; 2017. doi:10.1201/9781498747967.
[107] Jacoby GA, Archer GL. New Mechanisms of Bacterial Resistance to Antimicrobial Agents. New England Journal of Medicine 1991;324:601–12. doi:10.1056/NEJM199102283240906.
[108] Jacoby GA. AmpC beta-lactamases. Clin Microbiol Rev 2009;22:161–82, Table of Contents. doi:10.1128/CMR.00036-08.
[109] Sanders CC, Sanders WE. Emergence of resistance to cefamandole: possible role of cefoxitin-inducible beta-lactamases. Antimicrob Agents Chemother 1979;15:792–7. doi:10.1128/aac.15.6.792.
[110] WHO | Global action plan on AMR. WHO n.d. http://www.who.int/antimicrobial-resistance/global-action-plan/en/ (accessed July 5, 2019).
[111] G7 Health Ministers Declaration n.d. http://www.g7italy.it/sites/default/files/documents/FINAL_G7_Health_Communiqu%c3%a8_Milan_2017_0/index.pdf (accessed July 5, 2019).

[112] G20 Health Ministers Declaration n.d. https://www.bundesgesundheitsministerium.de/fileadmin/Dateien/3_Downloads/G/G20-Gesundheitsministertreffen/G20_Health_Ministers_Declaration_engl.pdf (accessed July 5, 2019).
[113] https://www.jpiamr.eu/ n.d. https://www.jpiamr.eu/ (accessed July 5, 2019).
[114] About JPIAMR :: n.d. https://www.jpiamr.eu/about/ (accessed July 5, 2019).
[115] Second JPIAMR Joint Call :: n.d. https://www.jpiamr.eu/supportedprojects/second-joint-call-result/ (accessed July 5, 2019).
[116] CO-ACTION : Developing combinations of CO-ACTIVE and non-antimicrobials n.d. https://www.jpiamr.eu/wp-content/uploads/2016/02/Developing-combinations-of-CO-ACTIVE.pdf (accessed July 5, 2019).
[117] Velkov T, Roberts KD, Nation RL, Thompson PE, Li J. Pharmacology of polymyxins: new insights into an 'old' class of antibiotics. Future Microbiol 2013;8. doi:10.2217/fmb.13.39.
[118] Poirel L, Jayol A, Nordmann P. Polymyxins: Antibacterial Activity, Susceptibility Testing, and Resistance Mechanisms Encoded by Plasmids or Chromosomes. Clin Microbiol Rev 2017;30:557–96. doi:10.1128/CMR.00064-16.
[119] Nation RL, Velkov T, Li J. Colistin and Polymyxin B: Peas in a Pod, or Chalk and Cheese? Clin Infect Dis 2014;59:88–94. doi:10.1093/cid/ciu213.
[120] Bergen PJ, Li J, Rayner CR, Nation RL. Colistin Methanesulfonate Is an Inactive Prodrug of Colistin against Pseudomonas aeruginosa. Antimicrob Agents Chemother 2006;50:1953–8. doi:10.1128/AAC.00035-06.
[121] Aggarwal R, Dewan A. Comparison of nephrotoxicity of Colistin with Polymyxin B administered in currently recommended doses: a prospective study. Annals of Clinical Microbiology and Antimicrobials 2018;17:15. doi:10.1186/s12941-018-0262-0.
[122] Zavascki AP, Nation RL. Nephrotoxicity of Polymyxins: Is There Any Difference between Colistimethate and Polymyxin B? Antimicrob Agents Chemother 2017;61. doi:10.1128/AAC.02319-16.
[123] Rigatto MH, Oliveira MS, Perdigão-Neto LV, Levin AS, Carrilho CM, Tanita MT, et al. Multicenter Prospective Cohort Study of Renal Failure in Patients Treated with Colistin versus Polymyxin B. Antimicrob Agents Chemother 2016;60:2443–9. doi:10.1128/AAC.02634-15.
[124] Sandri AM, Landersdorfer CB, Jacob J, Boniatti MM, Dalarosa MG, Falci DR, et al. Population Pharmacokinetics of Intravenous Polymyxin B in Critically Ill Patients: Implications for Selection of Dosage Regimens. Clin Infect Dis 2013;57:524–31. doi:10.1093/cid/cit334.
[125] McConnell MJ, Actis L, Pachón J. Acinetobacter baumannii: human infections, factors contributing to pathogenesis and animal models. FEMS Microbiol Rev 2013;37:130–55. doi:10.1111/j.1574-6976.2012.00344.x.
[126] Dijkshoorn L, Nemec A, Seifert H. An increasing threat in hospitals: multidrug-resistant *Acinetobacter baumannii*. Nature Reviews Microbiology 2007;5:939–51. doi:10.1038/nrmicro1789.
[127] Fagon JY, Chastre J, Domart Y, Trouillet JL, Gibert C. Mortality due to ventilator-associated pneumonia or colonization with Pseudomonas or Acinetobacter species: assessment by quantitative culture of samples obtained by a protected specimen brush. Clin Infect Dis 1996;23:538–42. doi:10.1093/clinids/23.3.538.
[128] Garnacho J, Sole-Violan J, Sa-Borges M, Diaz E, Rello J. Clinical impact of pneumonia caused by Acinetobacter baumannii in intubated patients: a matched cohort study. Crit Care Med 2003;31:2478–82. doi:10.1097/01.CCM.0000089936.09573.F3.
[129] Falagas ME, Kopterides P, Siempos II. Attributable mortality of Acinetobacter baumannii infection among critically ill patients. Clin Infect Dis 2006;43:389; author reply 389-390. doi:10.1086/505599.
[130] Abbo A, Carmeli Y, Navon-Venezia S, Siegman-Igra Y, Schwaber MJ. Impact of multi-drug-resistant Acinetobacter baumannii on clinical outcomes. Eur J Clin Microbiol Infect Dis 2007;26:793–800. doi:10.1007/s10096-007-0371-8.
[131] Falagas ME, Rafailidis PI. Attributable mortality of Acinetobacter baumannii: no longer a controversial issue. Crit Care 2007;11:134. doi:10.1186/cc5911.

[132] Lee N-Y, Lee H-C, Ko N-Y, Chang C-M, Shih H-I, Wu C-J, et al. Clinical and economic impact of multidrug resistance in nosocomial Acinetobacter baumannii bacteremia. Infect Control Hosp Epidemiol 2007;28:713–9. doi:10.1086/517954.
[133] Wisplinghoff H, Bischoff T, Tallent SM, Seifert H, Wenzel RP, Edmond MB. Nosocomial bloodstream infections in US hospitals: analysis of 24,179 cases from a prospective nationwide surveillance study. Clin Infect Dis 2004;39:309–17. doi:10.1086/421946.
[134] García-Garmendia JL, Ortiz-Leyba C, Garnacho-Montero J, Jiménez-Jiménez FJ, Monterrubio-Villar J, Gili-Miner M. Mortality and the increase in length of stay attributable to the acquisition of Acinetobacter in critically ill patients. Crit Care Med 1999;27:1794–9. doi:10.1097/00003246-199909000-00015.
[135] Jang T-N, Lee S-H, Huang C-H, Lee C-L, Chen W-Y. Risk factors and impact of nosocomial Acinetobacter baumannii bloodstream infections in the adult intensive care unit: a case-control study. J Hosp Infect 2009;73:143–50. doi:10.1016/j.jhin.2009.06.007.
[136] Jung JY, Park MS, Kim SE, Park BH, Son JY, Kim EY, et al. Risk factors for multi-drug resistant Acinetobacter baumannii bacteremia in patients with colonization in the intensive care unit. BMC Infect Dis 2010;10:228. doi:10.1186/1471-2334-10-228.
[137] Seifert H, Strate A, Pulverer G. Nosocomial bacteremia due to Acinetobacter baumannii. Clinical features, epidemiology, and predictors of mortality. Medicine (Baltimore) 1995;74:340–9. doi:10.1097/00005792-199511000-00004.
[138] Fournier P-E, Vallenet D, Barbe V, Audic S, Ogata H, Poirel L, et al. Comparative Genomics of Multidrug Resistance in Acinetobacter baumannii. PLOS Genetics 2006;2:e7. doi:10.1371/journal.pgen.0020007.
[139] Iacono M, Villa L, Fortini D, Bordoni R, Imperi F, Bonnal RJP, et al. Whole-genome pyrosequencing of an epidemic multidrug-resistant Acinetobacter baumannii strain belonging to the European clone II group. Antimicrob Agents Chemother 2008;52:2616–25. doi:10.1128/AAC.01643-07.
[140] Wareham DW, Bean DC, Khanna P, Hennessy EM, Krahe D, Ely A, et al. Bloodstream infection due to Acinetobacter spp: epidemiology, risk factors and impact of multi-drug resistance. Eur J Clin Microbiol Infect Dis 2008;27:607–12. doi:10.1007/s10096-008-0473-y.
[141] López-Rojas R, McConnell MJ, Jiménez-Mejías ME, Domínguez-Herrera J, Fernández-Cuenca F, Pachón J. Colistin Resistance in a Clinical Acinetobacter baumannii Strain Appearing after Colistin Treatment: Effect on Virulence and Bacterial Fitness. Antimicrob Agents Chemother 2013;57:4587–9. doi:10.1128/AAC.00543-13.
[142] Jaidane N, Naas T, Mansour W, Radhia BB, Jerbi S, Boujaafar N, et al. Genomic analysis of in vivo acquired resistance to colistin and rifampicin in Acinetobacter baumannii. Int J Antimicrob Agents 2018;51:266–9. doi:10.1016/j.ijantimicag.2017.10.016.
[143] Pournaras S, Poulou A, Dafopoulou K, Chabane YN, Kristo I, Makris D, et al. Growth Retardation, Reduced Invasiveness, and Impaired Colistin-Mediated Cell Death Associated with Colistin Resistance Development in Acinetobacter baumannii. Antimicrob Agents Chemother 2014;58:828–32. doi:10.1128/AAC.01439-13.
[144] Rolain J-M, Diene SM, Kempf M, Gimenez G, Robert C, Raoult D. Real-Time Sequencing To Decipher the Molecular Mechanism of Resistance of a Clinical Pan-Drug-Resistant Acinetobacter baumannii Isolate from Marseille, France. Antimicrobial Agents and Chemotherapy 2013;57:592–6. doi:10.1128/AAC.01314-12.
[145] Ritchie DJ, Garavaglia-Wilson A. A review of intravenous minocycline for treatment of multidrug-resistant Acinetobacter infections. Clin Infect Dis 2014;59 Suppl 6:S374-380. doi:10.1093/cid/ciu613.
[146] Bishburg E, Bishburg K. Minocycline--an old drug for a new century: emphasis on methicillin-resistant Staphylococcus aureus (MRSA) and Acinetobacter baumannii. Int J Antimicrob Agents 2009;34:395–401. doi:10.1016/j.ijantimicag.2009.06.021.
[147] Minocycline. Wikipedia 2019.
[148] Greig SL, Scott LJ. Intravenous Minocycline: A Review in Acinetobacter Infections. Drugs 2016;76:1467–76. doi:10.1007/s40265-016-0636-6.

[149] FDA. MINOCIN - Minocycline for injection n.d. https://www.accessdata.fda.gov/drugsatfda_docs/label/2010/050444s047lbl.pdf (accessed July 31, 2019).
[150] Lomovskaya O, Sun D, Rubio-Aparicio D, Nelson KJ, Thamlikitkul V, Dudley MN, et al. Absence of TetB Identifies Minocycline-Susceptible Isolates of Acinetobacter baumannii. International Journal of Antimicrobial Agents 2018;0. doi:10.1016/j.ijantimicag.2018.04.006.
[151] Antunes LCS, Visca P, Towner KJ. Acinetobacter baumannii: evolution of a global pathogen. Pathog Dis 2014;71:292–301. doi:10.1111/2049-632X.12125.
[152] Nielsen EI, Friberg LE. Pharmacokinetic-pharmacodynamic modeling of antibacterial drugs. Pharmacol Rev 2013;65:1053–90. doi:10.1124/pr.111.005769.
[153] Hong DJ, Kim JO, Lee H, Yoon E-J, Jeong SH, Yong D, et al. In vitro antimicrobial synergy of colistin with rifampicin and carbapenems against colistin-resistant Acinetobacter baumannii clinical isolates. Diagnostic Microbiology and Infectious Disease 2016;86:184–9. doi:10.1016/j.diagmicrobio.2016.07.017.
[154] Lim T-P, Tan T-Y, Lee W, Sasikala S, Tan T-T, Hsu L-Y, et al. In-Vitro Activity of Polymyxin B, Rifampicin, Tigecycline Alone and in Combination against Carbapenem-Resistant Acinetobacter baumannii in Singapore. PLOS ONE 2011;6:e18485. doi:10.1371/journal.pone.0018485.
[155] Song JY, Kee SY, Hwang IS, Seo YB, Jeong HW, Kim WJ, et al. In vitro activities of carbapenem/sulbactam combination, colistin, colistin/rifampicin combination and tigecycline against carbapenem-resistant Acinetobacter baumannii. J Antimicrob Chemother 2007;60:317–22. doi:10.1093/jac/dkm136.
[156] Bae S, Kim M-C, Park S-J, Kim HS, Sung H, Kim M-N, et al. In Vitro Synergistic Activity of Antimicrobial Agents in Combination against Clinical Isolates of Colistin-Resistant Acinetobacter baumannii. Antimicrob Agents Chemother 2016;60:6774–9. doi:10.1128/AAC.00839-16.
[157] Cai X, Yang Z, Dai J, Chen K, Zhang L, Ni W, et al. Pharmacodynamics of tigecycline alone and in combination with colistin against clinical isolates of multidrug-resistant Acinetobacter baumannii in an in vitro pharmacodynamic model. Int J Antimicrob Agents 2017;49:609–16. doi:10.1016/j.ijantimicag.2017.01.007.
[158] Dizbay M, Tozlu DK, Cirak MY, Isik Y, Ozdemir K, Arman D. In vitro synergistic activity of tigecycline and colistin against XDR-Acinetobacter baumannii. J Antibiot 2009;63:51–3. doi:10.1038/ja.2009.117.
[159] Rao GG, Ly NS, Diep J, Forrest A, Bulitta JB, Holden PN, et al. Combinatorial pharmacodynamics of polymyxin B and tigecycline against heteroresistant Acinetobacter baumannii. Int J Antimicrob Agents 2016;48:331–6. doi:10.1016/j.ijantimicag.2016.06.006.
[160] Zhang Y, Chen F, Sun E, Ma R, Qu C, Ma L. In vitro antibacterial activity of combinations of fosfomycin, minocycline and polymyxin B on pan-drug-resistant Acinetobacter baumannii. Exp Ther Med 2013;5:1737–9. doi:10.3892/etm.2013.1039.
[161] Bowers DR, Cao H, Zhou J, Ledesma KR, Sun D, Lomovskaya O, et al. Assessment of Minocycline and Polymyxin B Combination against Acinetobacter baumannii. Antimicrobial Agents and Chemotherapy 2015;59:2720. doi:10.1128/AAC.04110-14.
[162] Bleibtreu A, Gros P-A, Laouénan C, Clermont O, Le Nagard H, Picard B, et al. Fitness, Stress Resistance, and Extraintestinal Virulence in Escherichia coli. Infect Immun 2013;81:2733–42. doi:10.1128/IAI.01329-12.
[163] Orwa JA, Govaerts C, Gevers K, Roets E, Van Schepdael A, Hoogmartens J. Study of the stability of polymyxins B1, E1 and E2 in aqueous solution using liquid chromatography and mass spectrometry. Journal of Pharmaceutical and Biomedical Analysis 2002;29:203–12. doi:10.1016/S0731-7085(02)00016-X.
[164] Jacobs M, Grégoire N, Couet W, Bulitta JB. Distinguishing Antimicrobial Models with Different Resistance Mechanisms via Population Pharmacodynamic Modeling. PLoS Comput Biol 2016;12. doi:10.1371/journal.pcbi.1004782.
[165] Beceiro A, Llobet E, Aranda J, Bengoechea JA, Doumith M, Hornsey M, et al. Phosphoethanolamine Modification of Lipid A in Colistin-Resistant Variants of Acinetobacter

baumannii Mediated by the pmrAB Two-Component Regulatory System. Antimicrobial Agents and Chemotherapy 2011;55:3370–9. doi:10.1128/AAC.00079-11.
[166] Barin J, Martins AF, Heineck BL, Barth AL, Zavascki AP. Hetero- and adaptive resistance to polymyxin B in OXA-23-producing carbapenem-resistant Acinetobacter baumannii isolates. Ann Clin Microbiol Antimicrob 2013;12:15. doi:10.1186/1476-0711-12-15.
[167] Skiada A, Markogiannakis A, Plachouras D, Daikos GL. Adaptive resistance to cationic compounds in Pseudomonas aeruginosa. Int J Antimicrob Agents 2011;37:187–93. doi:10.1016/j.ijantimicag.2010.11.019.
[168] Ritchie DJ, Garavaglia-Wilson A. A Review of Intravenous Minocycline for Treatment of Multidrug-Resistant Acinetobacter Infections. Clin Infect Dis 2014;59:S374–80. doi:10.1093/cid/ciu613.
[169] Comets E, Brendel K, Mentré F. Computing normalised prediction distribution errors to evaluate nonlinear mixed-effect models: the npde add-on package for R. Comput Methods Programs Biomed 2008;90:154–66. doi:10.1016/j.cmpb.2007.12.002.
[170] Beal SL. Ways to Fit a PK Model with Some Data Below the Quantification Limit. J Pharmacokinet Pharmacodyn 2001;28:481–504. doi:10.1023/A:1012299115260.
[171] Deurenberg RH, Bathoorn E, Chlebowicz MA, Couto N, Ferdous M, García-Cobos S, et al. Application of next generation sequencing in clinical microbiology and infection prevention. Journal of Biotechnology 2017;243:16–24. doi:10.1016/j.jbiotec.2016.12.022.
[172] Wang Z, Gerstein M, Snyder M. RNA-Seq: a revolutionary tool for transcriptomics. Nat Rev Genet 2009;10:57–63. doi:10.1038/nrg2484.
[173] Pulido MR, García-Quintanilla M, Gil-Marqués ML, McConnell MJ. Identifying targets for antibiotic development using omics technologies. Drug Discov Today 2016;21:465–72. doi:10.1016/j.drudis.2015.11.014.
[174] Vranakis I, Goniotakis I, Psaroulaki A, Sandalakis V, Tselentis Y, Gevaert K, et al. Proteome studies of bacterial antibiotic resistance mechanisms. J Proteomics 2014;97:88–99. doi:10.1016/j.jprot.2013.10.027.
[175] Freiberg C, Brötz-Oesterhelt H, Labischinski H. The impact of transcriptome and proteome analyses on antibiotic drug discovery. Curr Opin Microbiol 2004;7:451–9. doi:10.1016/j.mib.2004.08.010.
[176] Ribeiro da Cunha B, Fonseca LP, Calado CRC. Antibiotic Discovery: Where Have We Come from, Where Do We Go? Antibiotics (Basel) 2019;8. doi:10.3390/antibiotics8020045.
[177] Zhu Y, Zhao J, Maifiah MHM, Velkov T, Schreiber F, Li J. Metabolic Responses to Polymyxin Treatment in Acinetobacter baumannii ATCC 19606: Integrating Transcriptomics and Metabolomics with Genome-Scale Metabolic Modeling. MSystems 2019;4:e00157-18. doi:10.1128/mSystems.00157-18.
[178] Benson N. Quantitative Systems Pharmacology and Empirical Models: Friends or Foes? CPT: Pharmacometrics & Systems Pharmacology 2019;8:135–7. doi:10.1002/psp4.12375.
[179] Ayrapetyan M, Williams TC, Oliver JD. Bridging the gap between viable but non-culturable and antibiotic persistent bacteria. Trends Microbiol 2015;23:7–13. doi:10.1016/j.tim.2014.09.004.
[180] Ungphakorn W, Lagerbäck P, Nielsen EI, Tängdén T. Automated time-lapse microscopy a novel method for screening of antibiotic combination effects against multidrug-resistant Gram-negative bacteria. Clin Microbiol Infect 2018;24:778.e7-778.e14. doi:10.1016/j.cmi.2017.10.029.
[181] Pharmacodynamics of polymyxin B against extensively drug-resistant Acinetobacter baumannii in a hollow fibre infection model - ECCMID Live n.d. https://www.eccmidlive.org/#!resources/pharmacodynamics-of-polymyxin-b-against-extensively-drug-resistant-acinetobacter-baumannii-in-a-hollow-fibre-infection-model-5d067995-cbc8-4600-9e81-d0015194006e (accessed August 11, 2019).
[182] Buyck JM, Plésiat P, Traore H, Vanderbist F, Tulkens PM, Van Bambeke F. Increased susceptibility of Pseudomonas aeruginosa to macrolides and ketolides in eukaryotic cell culture media and biological fluids due to decreased expression of oprM and increased outer-membrane permeability. Clin Infect Dis 2012;55:534–42. doi:10.1093/cid/cis473.

[183] Huang JX, Blaskovich MAT, Pelingon R, Ramu S, Kavanagh A, Elliott AG, et al. Mucin Binding Reduces Colistin Antimicrobial Activity. Antimicrob Agents Chemother 2015;59:5925–31. doi:10.1128/AAC.00808-15.
[184] Butnarasu C, Barbero N, Pacheco D, Petrini P, Visentin S. Mucin binding to therapeutic molecules: The case of antimicrobial agents used in cystic fibrosis. Int J Pharm 2019;564:136–44. doi:10.1016/j.ijpharm.2019.04.032.
[185] Kirchner S, Fothergill JL, Wright EA, James CE, Mowat E, Winstanley C. Use of Artificial Sputum Medium to Test Antibiotic Efficacy Against Pseudomonas aeruginosa in Conditions More Relevant to the Cystic Fibrosis Lung. Journal of Visualized Experiments : JoVE 2012. doi:10.3791/3857.
[186] Lenhard JR, Smith NM, Bulman ZP, Tao X, Thamlikitkul V, Shin BS, et al. High-Dose Ampicillin-Sulbactam Combinations Combat Polymyxin-Resistant Acinetobacter baumannii in a Hollow-Fiber Infection Model. Antimicrob Agents Chemother 2017;61:e01268-16. doi:10.1128/AAC.01268-16.
[187] Pichereau S, Pantrangi M, Couet W, Badiou C, Lina G, Shukla SK, et al. Simulated antibiotic exposures in an in vitro hollow-fiber infection model influence toxin gene expression and production in community-associated methicillin-resistant Staphylococcus aureus strain MW2. Antimicrob Agents Chemother 2012;56:140–7. doi:10.1128/AAC.05113-11.
[188] Aoki Y, Sundqvist M, Hooker AC, Gennemark P. PopED lite: An optimal design software for preclinical pharmacokinetic and pharmacodynamic studies. Computer Methods and Programs in Biomedicine 2016;127:126–43. doi:10.1016/j.cmpb.2016.02.001.

Résumé

La lutte contre les bactéries multirésistantes est une priorité majeure définie par l'Organisation Mondiale de la Santé, puisque les dernières prédictions estiment que les infections par des bactéries multirésistantes feront plus de morts que le cancer d'ici 2050. Dans le contexte actuel, avec un faible nombre de nouveaux antibiotiques mis sur le marché pour lutter contre les bactéries multirésistantes, il est important de d'optimiser l'utilisation des antibiotiques à notre disposition. C'est dans ce but que les modèles semi-mécanistiques servant à analyser les résultats d'études de PK/PD des antibiotiques peuvent être développés. Ces outils mathématiques permettent de quantifier les relations concentration-effet, de molécules seules ou de combinaisons de molécules afin d'optimiser leur efficacité, prévenir les résistances et donc prolonger la durée de vie des antibiotiques. Dans ce travail, après une présentation des méthodes d'étude de la PK/PD des antibiotiques seuls et en combinaison, les résultats de deux projets sont présentés :

3. Une étude de la PK/PD de la céfoxitine contre une souche de *Mycobacterium abscessus*. Dans une première partie, il a été montré que l'administration de la céfoxitine par nébulisation permet d'obtenir des concentrations pulmonaires 1000 fois plus importantes qu'après une administration intraveineuse, faisant de la céfoxitine un bon candidat à la nébulisation. Dans la seconde partie un modèle PK/PD semi-mécanistique a été développé à partir de données *in vitro*, ce qui permet d'identifier la relation concentration-effet pour deux sous-populations bactériennes tout en tenant compte de la dégradation de la molécule.
4. Une étude de la PK/PD de l'association polymyxine B et minocycline contre une souche d'*Acinetobacter baumannii* résistante à la polymyxine B. Cette étude *in vitro* comprend des données de bactéricidie avec suivi de la densité de bactéries résistantes à la polymyxine B, enrichies d'expériences complémentaires servant à préciser les caractéristiques de cette sous-population résistante. Ces données ont toutes été analysées par modélisation PK/PD semi-mécanistique, ce qui a notamment permis de quantifier l'importance de l'interaction entre les deux molécules et de formuler des hypothèses sur les mécanismes de cette interaction.

Mots-clés : céfoxitine, polymyxine B, minocycline, *Mycobacterium absscessus*, *Acinetobacter baumannii*, modélisation PK/PD, pharmacocinétique, pharmacodynamie, combinaison

Abstract

Fighting against multidrug-resistant bacteria is a major priority set by World Health Organisation, since it is forecasted that multi-drug-resistant bacteria will be responsible for more deaths than cancer by 2050. In the current context, with only a few new antibiotic drugs active against multidrug-resistant bacteria approved every year, it is of importance to optimize the use of already available antibiotics. It is with this goal in mind, that semi-mechanistic models used to analyse results from PK/PD studies of antibiotics, can be developed. These mathematical tools enable quantification of concentration-effect relationships of drugs, used alone or in combination, in order to optimize their efficacy, prevent bacterial resistance, thus lengthening the period of usability of antibiotics. In this work, after a presentation of the methods used to study PK/PD of antibiotics alone and in combination, results from two projects are presented:

1. A study of cefoxitin PK/PD against a *Mycobacterium abscessus* strain. Firstly, it was shown that after nebulisation of cefoxitin, pulmonary concentrations were 1000-fold higher than after intravenous administration, making cefoxitin a good candidate for nebulisation. In a second part, a semi-mechanistic PK/PD model was developed from *in vitro* data, enabling identification of concentration-effect relationships for two bacterial sub-populations while taking into account degradation of cefoxitin.
2. A study of the PK/PD of polymyxin B and minocycline association against a polymyxin B resistant *Acinetobacter baumannii* strain. This *in vitro* study incorporates data from time-kill experiments with quantification of a bacterial sub-population resistant to polymyxin B, enriched by complementary experiments providing information on the characteristics of this resistant sub-population. This data was analysed by semi-mechanistic PK/PD modelling, which made possible quantification of the strength of interaction between the two drugs and to form hypotheses about the mechanisms of the observed interaction.

Keywords: cefoxitin, polymyxin B, minocycline, *Mycobacterium abscessus*, *Acinetobacter baumannii*, PK/PD modelling, pharmacokinetics, pharmacodynamics, combination.